Synthesis and Characterization of Dyes and Macrocycles Derived from Dipyrrin and Modified Dipyrrins

A Thesis

Submitted in Partial Fulfillment of the Requirements

for the Degree of

Doctor of Philosophy

By

Santosh Chandrakant Gadekar

ID: 20103057

Indian Institute of Science Education and Research (IISER), Pune

2015

Dedicated to my Parents…

भारतीय विज्ञान शिक्षा एवं अनुसंधान संस्थान, पुणे
INDIAN INSTITUTE OF SCIENCE EDUCATION AND RESEARCH (IISER), PUNE
Mendeleeve Block, Dr. Homi Bhabha Road, Pune – 411 008, Maharashtra, India

Dr. V. G. Anand
Associate Professor

Certificate

Certified that the work described in this thesis entitled "***Synthesis and Characterization of Dyes and Macrocycles Derived from Dipyrrin and Modified Dipyrrins***" submitted by *Mr. Santosh Chandrakant Gadekar* was carried out by the candidate, under my supervision. The work presented here or any part of it has not been included in any other thesis submitted previously for the award of any degree or diploma from any other university or institution.

Date: - 24th December 2015

Dr. V. G. Anand

Research Supervisor

Ph: +91-20-25908091 | Fax: +91-20-25899790 *Email: vg.anand@iiserpune.ac.in*

Declaration

I declare that this written submission represents my ideas in my own words and wherever other's ideas have been included; I have adequately cited and referenced the original sources. I also declare that I have adhered to all principles of academic honesty and integrity and have not misrepresented or fabricated or falsified any idea/data/fact/source in this submission. I understand that violation of the above will result in disciplinary actions by the Institute and can also evoke penal action from the sources, which have thus not been properly cited or from whom appropriate permission has not been taken when needed.

Date: - 24th December 2015

S. C. Gadekar

ID: 20103057

Acknowledgement

I express my sincere gratitude and heartfelt thanks to my research supervisor Prof. V. G. Anand for his continuous support during my Ph.D. studies and research, for his patience, motivation, enthusiasm and immense knowledge. I thank him for believing in my abilities and giving work freedom during my Ph.D. It is difficult to compose appropriate sentence to express my gratefulness to him for his guidance and keen interest which made this work possible. I could not have imagined having a better advisor and mentor for my Ph.D. studies.

I am extremely thankful to Prof. K. N. Ganesh for providing excellent research facilities and an outstanding research ambiance.

I gratefully acknowledge Indian Institute of Science Education and Research (IISER) for financial support in the form of JRF and SRF fellowship.

I would like to express my sincere thanks to the Research Advisory Committee members Dr. Avinash S. Kumbhar (Savitribai Phule Pune University, Pune) and Dr. Manickam Jayakannan (IISER, Pune) for their invaluable suggestions and advices.

I take this opportunity to thank Dr. T. S. Mahesh, Dr. H. N. Gopi, Dr. R. Boomishankar, Dr. R. G. Bhat, Dr. Arun Venkatnathan and Dr. M. Musthafa for their assistance during my research period. In fact, I owe heartiest thank to every faculty of IISER Pune.

It gives me an immense pleasure to thank all of Lab members Dr. T. Y. Gopalakrishna, Dr. Neelam Shivran, Dr. Rashmi Prabhu, Kiran Reddy, Santosh Panchal, Rakesh Gaur, Ashok Kumar, Madan Ambhore, Prakhar, Rajkumar Yadav and Manish Kumar as good friends and creating friendly environment in the lab.

I am grateful to Dr. Rajesh G. Gonnade (*NCL, Pune*) for his excellent course on crystallography, Prof. M. Ravikanth (IIT Bombay) for his help in carrying out cyclic voltammetry experiment and Dr. Partha Hazra for helping me in carrying out fluorescence studies.

I thank Dr. V. S. Rao and Santosh Nevse for their precious support and timely help. I extend my heartfelt thank IISER Pune administrative staff members especially Mayuresh, Nayana, Tushar, Mahesh, Nitin, Yatish and Megha for their generous support.

I would like to thank Suresh Prajapat, Syed, Somnath and Pappu from UG lab IISER Pune. I thank Neeta Deo, Suresh and Sachin for IT support.

I acknowledge the help from Archana (SCXRD), Pooja Lunawat (NMR), Swati M. Dixit (MALDI), Swathi (HRMS) and Nayana (HRMS) for the instrumental support.

I thank my friends Dr. Prakash Sultane, Dr. Amar Mohite, Dr. Sachitanand Mali, Dr. Sandip Jadhav, Dr. Arvind Gupta, Dr. Anurag Sunda, Dr. Dnyaneshwar, Nitin Bansode, Vijay Kadam, Anantharaj, Bapurao Surnar, Anant Srivastava, Ashok Yadav, Mahesh Deshmukh, Barun Dhara and finally all dear friends from IISER Pune.

I am also thankful to all my friends outside IISER Pune Sandip Agalave, Kiran Dhawale, Bhusaheb Bulakhe and Nitin Thorat for their support and help.

My sincere thanks are due to my father Sri. Chandrakant G. Gadekar and mother Smt. Nanda C. Gadekar for their love, encouragement and motivation, without their support the entire journey would not have been possible. I am grateful to my beloved wife Mrs. Smita S. Gadekar and daughter Ishita S. Gadekar for their love, encouragement, support and sacrifice throughout this period. I thank my younger brothers Mr. Raju C. Gadekar and Mr. Vijay C. Gadekar for their love and support. I also thank my father-in-law Sri. Shrirang G. Kapse for his love and support.

I thank all my friends and colleagues in IISER Pune for making my stay comfortable and memorable.

Santosh

Contents

Synopsis

The thesis entitled ***"Synthesis and Characterization of Dyes and Macrocycles Derived from Dipyrrin and Modified Dipyrrins"*** describes synthesis and characterization of multiple BODIPY chromophores appended on benzene and biphenyl unit. It also describes the reactivity of N-confused dipyrrin, doubly N-confused dipyrrin and their benzo derivatives with various metal salts. In general, regular dipyrrins are known to form square planar, tetrahedral and octahedral metal complexes. Dipyrrin can be derived from dipyrromethane which contains two pyrrole rings are connected at their α-position to the *meso*-carbon atom. Regular dipyrrins having additional co-ordinating agents at α and *meso*-position leads to formation of complexes with diverse geometries. There are no reports known on reactivity of singly and doubly N-confused dipyrrin and their benzo derivatives with metal salts. This thesis describes the synthesis of multi-BODIPY appended dyes along with their structural and electronic properties. Subsequent chapters describe the results of the reactions between metal salts with modified dipyrrins that was aimed at the synthesis of metal complexes of N-confused dipyrrins. The first chapter describes the brief literature reports on synthesis, reactivity of regular dipyrrin and their derivatives with various metal salts leading to the formation of different types of metal complexes. It also describes the employability of these metal complexes in the synthesis of porphyrinoids. Overall, this thesis gives an account on the synthesis and characterization of BODIPY derivatives, expanded norroles, planar aza-heptalenes and couple of unusual dimers. Quantum mechanical calculations were also employed for the better understanding aromatic and anti-aromatic characteristics of these molecules.

The second chapter describes the detailed synthesis of multi-BODIPY units appended on benzene and biphenyl units. The single crystal X-ray diffraction analysis (SCXRD) of the 1,3-Bis BODIPY benzene confirmed the presence of two BODIPY moieties *meta* to each other on the benzene ring and in 1,4-Bis BODIPY benzene, *para* to each other on benzene ring. The location of the BODIPY directs the structural features and the intramolecular interactions of these molecules. This is justified by the two BODIPY moieties oriented in an orthogonal conformation in 1,3-Bis BODIPY and more planar in 1,4-Bis BODIPY. With the help of similar studies, the location of

three BODIPY moieties was confirmed at *meta* to each other in the 1,3,5-Tris BODIPY benzene. The packing diagram of this BODIPY displayed the formation of hydrogen bonded porous organic framework. The molecular structure of tetra BODIPY displayed a symmetrical link between the two 1,3-Bis BOIDPY through benzene rings and the two benzene rings were found to be co-planar suggesting the effective delocalization of π-electrons between them.

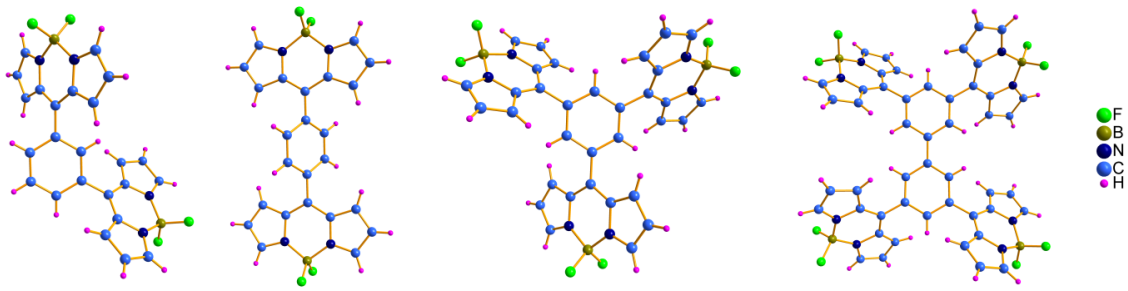

Chapter 3 consists of sections A and B. Section A starts with the description of the attempts at chelating various metals and non-metals by employing N-confused dipyrrin as a ligand as per the protocol employed for regular dipyrrins. N-confused dipyrromethane was synthesized as a precursor, which contains one pyrrole ring connected through their β-carbon to the *meso*-carbon atom. It was observed that only the confused pyrrole ring of the N-confused dipyrromethane gets oxidized upon oxidation by DDQ (2,3-dichloro-5,6-dicyano-1,4-benzoquinone). When N-confused dipyrrin reacted with boron trifluoride etherate, mass spectroscopy and SCXRD confirmed the formation of simple N-confused dipyrrin-boron trifluoride adduct instead of the expected boron difluoride complex. Surprisingly, N-confused dipyrrin reacts with copper(II) acetate to cyclomerize into macrocyclic products which are coined as expanded norroles. A similar cyclomerization was also observed with various other metal ions such as Zn^{2+}, Mn^{2+}, Fe^{2+}, Fe^{3+}, Ti^{4+} and Sn^{2+}. These expanded norroles with 24π and 32π are completely characterized by HMRS, NMR and SCXRD. The 24π anti-aromatic hexapyrrolic macrocycle represents the structural isomer of non-aromatic rosarin, while the 32π anti-aromatic octapyrrolic macrocycle is the apparent structural isomer of non-aromatic octaphyrin.

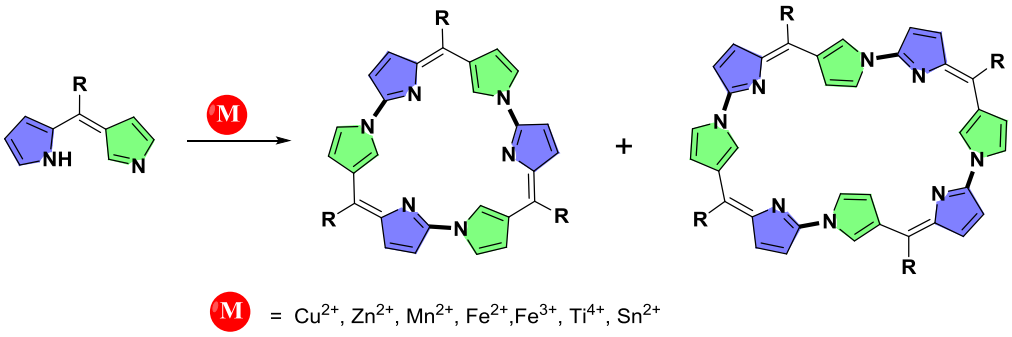

The section B of the third chapter describes the reactivity of doubly N-confused dipyrrins with metal salts. Doubly N-confused dipyrrin was derived from its dipyrromethane, which consists of two pyrrole rings linked to the *meso*-carbon through on of their β-carbon atoms. Doubly N-confused dipyrrin on reaction with copper(II) acetate undergoes cyclodimerization into pink colored symmerical aza-heptalene. The mode of dimerization depends on metal salt employed in the reaction. Under similar reaction conditions, this dipyrrin undergoes cyclodimerization with iron(III) acetylcetonoate into greenish yellow colored unsymmetrical aza-heptalene. Based on NMR studies, both the aza-heptalenes indicate diatropic ring current effect and hence characterized as aromatic in nature. The aromaticity of these molecules was also supported by calculating NICS(0) at the centre of seven membered rings. Furthermore, UV-Visible absorption spectroscopy and TD-DFT calculations provide evidence for heptalene kind of nature rather than macrocylic products.

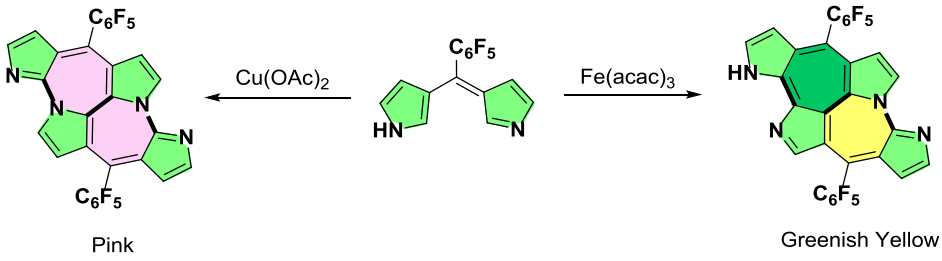

Chapter 4 describes the reactivity of monobenzo derivative of N-confused dipyrrin and monobenzo and dibenzo derivatives of doubly N-confused dipyrrin with metal salts. Monobenzo derivative of N-confused dipyrrin upon reaction with copper(II) acetate underwent cyclomerization into 24π oxidized expanded norrole. Under dilute reaction conditions, along with 24π oxidized expanded norrole an unexpected dimer was also obtained. This dimer has unsymmetrical connection between two confused dipyrrins leading to one seven membered ring between them.

Similar results were observed with other metal salts such as $Zn(OAc)_2$, $Co(OAc)_2$, $Mn(OAc)_2$, $Mn(acac)_3$, $Co(acac)_3$ and $Fe(acac)_3$.

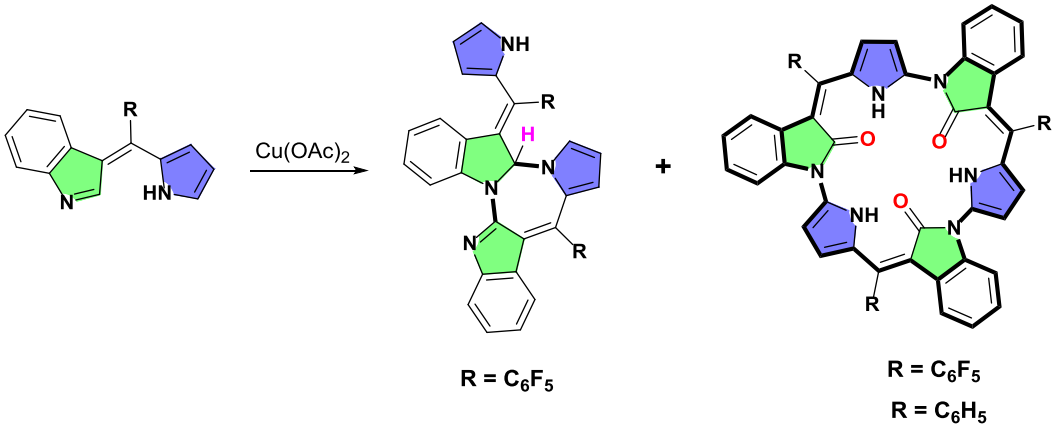

A similar synthetic process could be employed for the synthesis of aza-heptalenes. Monobenzo derivative of doubly N-confused dipyrrin on reaction with copper(II) acetate yielded a structural of the above described aromatic aza-heptalenes. A similar derivative of aza-heptalene was expected with dibenzo derivative of doubly N-confused dipyrrin but an unexpected dimer was obtained with copper(II) acetate. SCXRD has confirmed the formation of unusual dimer which was further well supported by NMR studies. This dimer also contains the unsymmetrical linkage of the two confused dipyrrin units leading to formation of one six and one seven membered ring between them.

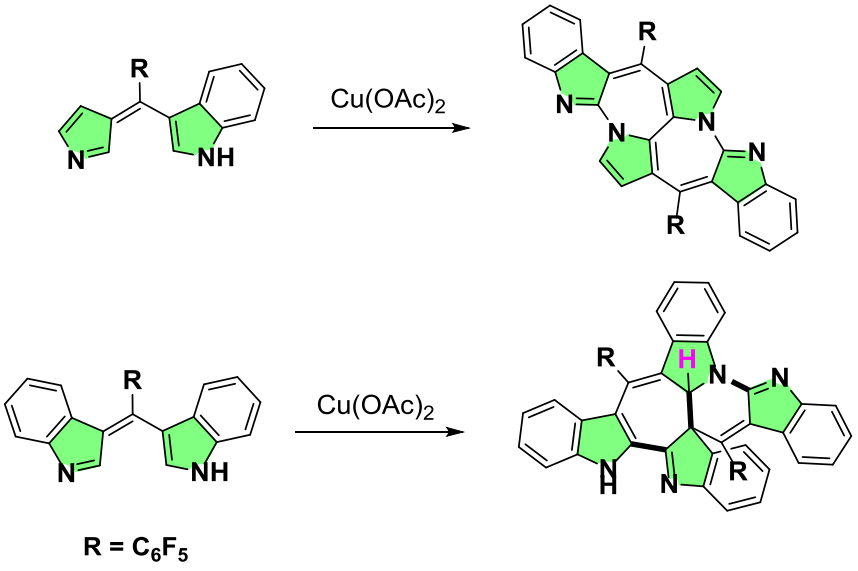

Chapter 1

Introduction

Dipyrrins versatility for metal complexation is well documented by its ability to bind a variety of metal ions and metalloids. The dipyrrin consists of two pyrrole rings connected through α carbon atom. The oxidation of diprromethane yields the completely conjugated dipyrrin. The time before the guideline given by IUPAC in 1987 for the dipyrrin nomenclature[1], these molecules were known by many names such as 4,6-dipyrrin[2], dipyrromethene[3], 4,6-dipyrromethene[4], dipyrrylmethene[5], pyrrylmethene[6], pyrromethene[7], 2,2' dipyrrolylmethene[8], dipyrrolemethene[9], diaza-*s*-indacene[10], 2-pyrrol-2-ylmethylene-*2H*-pyrrolenine[8] and 2-(*2H*-pyrrol-2-ylidenemethyl)-pyrrole.[2] The IUPAC recommended common numbering system for dipyrrins is shown in Figure I.1.

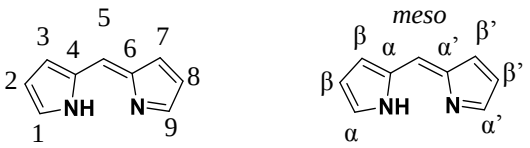

Figure I.1: IUPAC-recommended (left) and the common (right) numbering system of dipyrrin.

It has been observed that completely unsubtituted dipyrrin is prone to electrophilic and nucleophilic attack on the unsubstituted pyrrole rings and hence found to be unstable in solution above -40ºC.[11] However, alkyl substituents on 1,2,3,7,8,9-positions of dipyrrin is known to enhance its stability. Aryl substituents at the 5-position with no substitution on 1,2,3,7,8,9-positions of dipyrrin is also known to enhance its stability.

Synthesis of Dipyrrins:

(i) Synthesis by MacDonald Condensation:

The synthesis of 5-unsubstituted dipyrrin through acid catalysed condensation between 2-formyl pyrrole and pyrrole is generally known as the MacDonald condensation.[12] The catalyst used in this reaction is hydrobromic acid[3] and hence the dipyrrin obtained from this reaction is isolated as dipyrrin salts. This is a convenient synthetic strategy to generate the dipyrrin salts which are more stable than the free base 5-unsubstitued dipyrrins. MacDonald condensation is also useful for the synthesis of asymmetrical dipyrrins when complementary functionalities on the

pyrrolic precursor were reacted with each other. 5-substituted dipyrrin can also synthesized by condensing either carboxylic acid or acid halide with 2 equivalents of 2-unsubstituted pyrrole (Figure I.2).

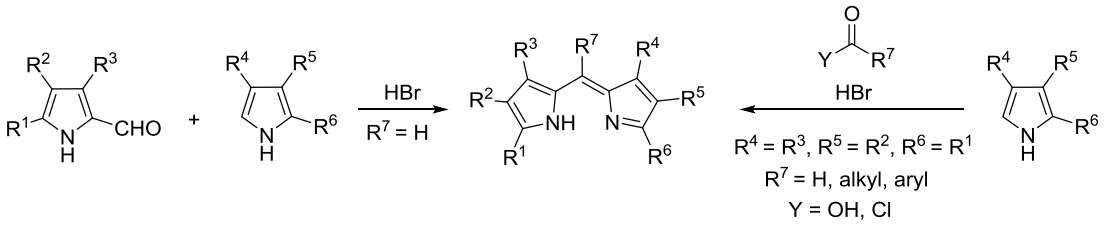

Figure I.2: Synthesis of dipyyrin by MacDonald condensation reaction

(ii) Synthesis by oxidation of Dipyrromethanes:

At room temperature, acid catalyzed condensation of aromatic aldehyde with large equivalents pyrrole under inert atmosphere, followed by crystallization yields more than 50% of dipyrromethane in high purity. Such reactions are also scalable[13] to synthesize large amounts of dipyrromethane. An important advantage about this procedure is the commercial availability of pyrrole and its purification by non-rigorous distillation. Dipyrromethane can be oxidized into dipyrrin with common reagents such as 2,3-dichloro-5,6-dicyano-1,4-benzoquinone (DDQ) or p-chloranil (Figure I.3).[14]

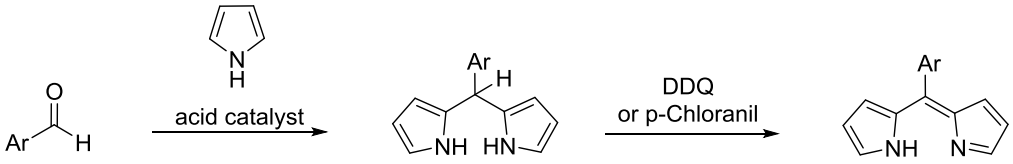

Figure I.3: Synthesis of 5-substituted dipyrromethane and its oxidation to dipyrrin

Reactivity of Dipyrrin

(i) Reactivity of Dipyrrin with Main Group Elements:

Dipyrrin acts as a chelating agent for various main group elements. In 1968, Treibs and Kreuzer discovered the highly fluorescent boron difluoride dipyrrin complex in their attempt to acylate 2,4-dimethylpyrrole with acetic anhydride in presence of boron trifluoride as the catalyst (Figure I.4).[15]

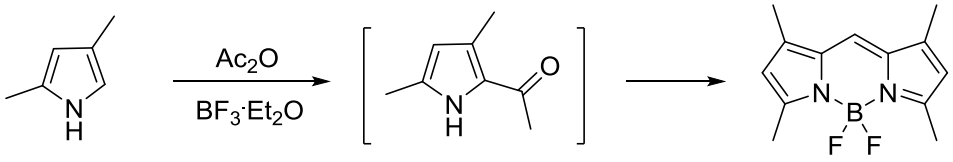

Figure I.4: First synthesis of a BODIPY dye by Treibs and Kreuzer

This fluorescent molecule, based on 4,4-difluoro-4-bora-3a,4a-diaza-*s*-indacene core (hereafter abbreviated as BODIPY) has IUPAC numbering system different than dipyrrin (Figure I.5). The term α-, β- and *meso*-position are similar for both molecules[1]. BODIPY's properties such as excellent thermal and photochemical stability, high fluorescence quantum yield, negligible triplet-state formation, intense absorption profile and good solubility has potential to be excellent probes for use in biological systems and for applications in opto-electronics.[16]

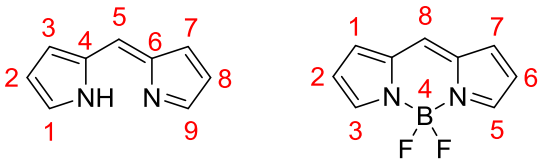

Figure I.5: Structure and IUPAC numbering system for dipyrrin and BODIPY

The free rotation around C-Phenyl bond in *meso*-phenyl BODIPY is involved in the major pathway for non-radiative decay to the ground state, which is responsible for a reduced quantum yield.[17] Two important functionalization strategies were designed in order to improve its fluorescence efficiency, (a) introduction of a sterically hindered group at the *meso*-position to prevent the free rotation of the phenyl group and hence to reduce the loss of energy from excited states via non-irradiative molecular motions, (b) functionalization of 1,9-positions by additional coordination units to provide pseudo-macrocyclic character in the resulting ligand (Figure I.6).[18] These two approaches have significantly increased the luminescence intensity of BODIPY due to the system rigidification of the organic backbone.

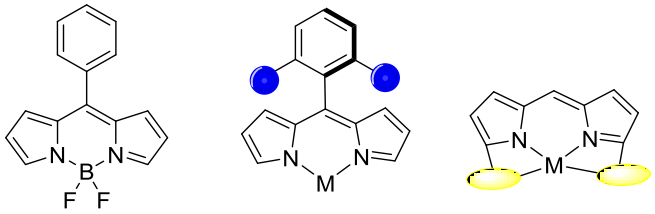

I.1

Figure I.6: BODIPY dye and two functionalization strategies

These functionalization strategies were implemented in N_2O_2 type dipyrrin tetradentate ligand. This was synthesized by an acid catalysed condensation of 2-(2-methoxyphenyl) pyrrole with mesitaldehyde followed by oxidation with DDQ and subsequent deprotection of phenol moiety by BBr_3. The boron and aluminium complexes were obtained by reaction with $B(OMe)_3$ and $Al(O^iPr)_3$ respectively (Figure I.7).[19] Boron complex displayed an absorption band at 626 nm while its emission was at 645 nm with a quantum yield of 72%. The aluminium analogue absorbed at 625 nm and emits at 647 nm with relatively same quantum yield. The choice of the aluminium as complexing ion with N_2O_2 type dipyrrin **I.2** was attributed to three important features (i) highly fluorescent nature of aluminium complexes, (ii) ligand has planar equatorial unit for formation of octahedral geometry around aluminium, (iii) in aluminium complex, the oxygen atoms are suitable for subsequent chelation since the oxygen atom of the Al-O bonds are more negatively charged than those of the B-O bond.[20] $ZnCl_2$ salt interacts strongly with the mononuclear aluminium complex leading to a decrease in the absorption at 625 nm and increased absorption at 608 nm. This binuclear heterometallic species can be obtained in 98% yield and has emission at 619 nm with increase in quantum yield to 83%. This enhancement in emission is probably due to increased rigidity of the dipyrrin framework caused by chelation which significantly hampers the non-radiative decay. Molecular structure of this complex displayed a distorted tetrahedral geometry at zinc centre and octahedral coordination for aluminium. The pyrrole rings and the phenol rings are planar enough to form the equatorial plane of N_2O_2 unit and two water molecules are present in the axial position. In contrast, boron complex did not exhibit any interaction with zinc salt due to the distorted N_2O_2 plane at the boron centre, caused by its tetrahedral geometry and lower negative charge on oxygen atoms.

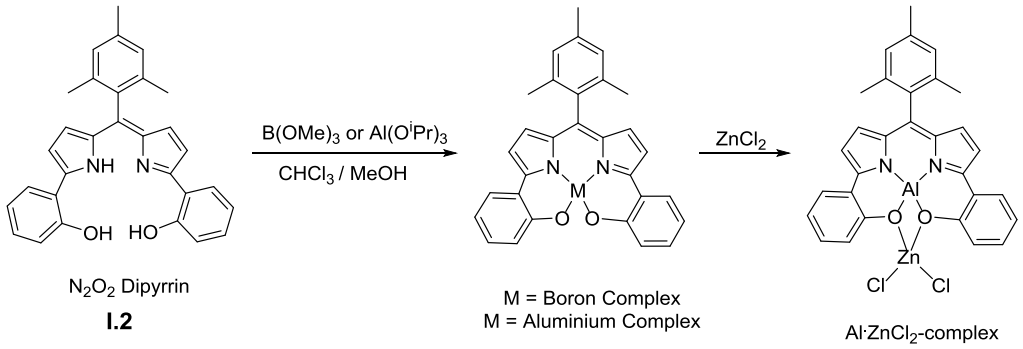

Figure I.7: Boron and Aluminium complex of N_2O_2 type dipyrrin

The N_2O_2-type dipyrrin **I.2** is known to form hypercoordinate silicon complexes which are known as silicon analogues of BODIPY (Figure I.8).[21] In presence of $N(Et)(^iPr)_2$ as a base, N_2O_2-type dipyrrin reacts with $MeSiCl_3$ and $PhSiCl_3$ to form silicon complexes **I.3-R** and **I.4-R** (R = Me, Ph) respectively bearing methyl and phenyl group on the silicon atom (Figure I.8). **I.3-Me** (Φ = 76%) and **I.3-Ph** (Φ = 72%) have higher quantum yields compared to **I.4-Me** and **I.4-Ph** due to the restricted rotation of mesityl group. This also led to red shifted absorption and emission for **I.3-Ph** and **I.4-Ph** to suggest that substituent on silicon centre also affects the optical properties of the complex. The monodipyrrin complex, silanol **I.3-OH** and disiloxane derivative **I.3$_2$-O** were obtained as major and minor products respectively upon reacting N_2O_2-type dipyrrin ligand with $SiCl_4$ and $N(Et)(^iPr)_2$. Single crystal studies of binuclear **I.3$_2$-O** confirmed the two silicon atoms were connected to each other through a μ-oxo bridge. The disiloxane **I.3$_2$-O** has absorption band at 573 and 601nm and its emission was observed at 671 and 664 nm. The silanol **I.3-OH** exhibited very sharp absorption and emission band with respect to **I.3$_2$-O** and its quantum yield of 81% was higher than **I.3$_2$-O** (4%). Disiloxane **I.3$_2$-O** was hydrolysed by refluxing in wet MeOH to **I.3-OH** and further dehydrated to **I.3$_2$-O** by refluxing in hexane. The reversible hydration/dehydration processes has been attributed to the on/off florescence property of these silicon complexes.

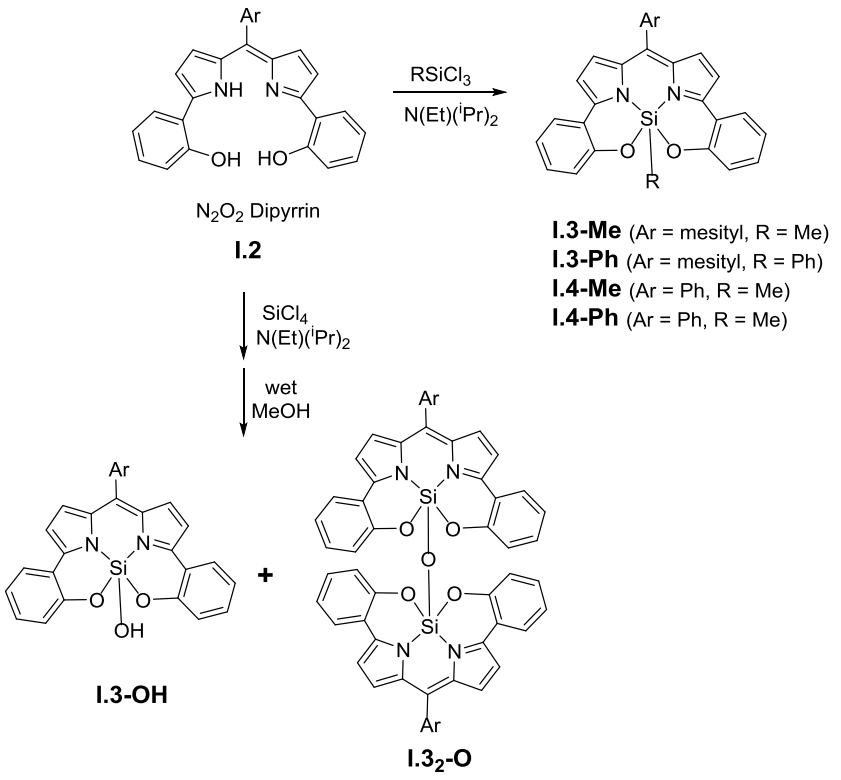

Figure I.8: Synthesis of silicon complexes

Apart from silicon, tin is also known to form a complex similar to BODIPY. SnClDIPY was synthesized in 74% yields by reacting the in-situ generated lithium dipyrranato, from dipyrrin **I.5**, with $SnCl_2$ (Figure I.9).[22] The molecular structure confirmed the pyramidal geometry at tin centre. Due to the intermolecular interactions between tin and chlorine atoms, the tin atom adopted pseudo-trigonal bipyramidal structure. SnClDIPY has a strong absorption at 509 nm and emission at 518 nm with a small stokes shift of 9 nm. But its quantum yield of only 4% is less than that of corresponding BODIPY (Φ = 89%). With AgOTf, SnClDIPY is easily converted into the cationic tin species [SnDIPY][OTf] which exhibits green emission. This cationic species has absorption maxima at 513 nm and emission at 524 nm. Its quantum yield was found to be 42%, almost 10 times more than SnClDIPY. Moreover, the cationic species was easily converted back to SnClDIPY upon treating with Bu_4NCl resulting in the quenching of its fluorescence. These complexes also represent examples of controlling on-off fluorescence by reversible dechlorination and chlorination reactions.

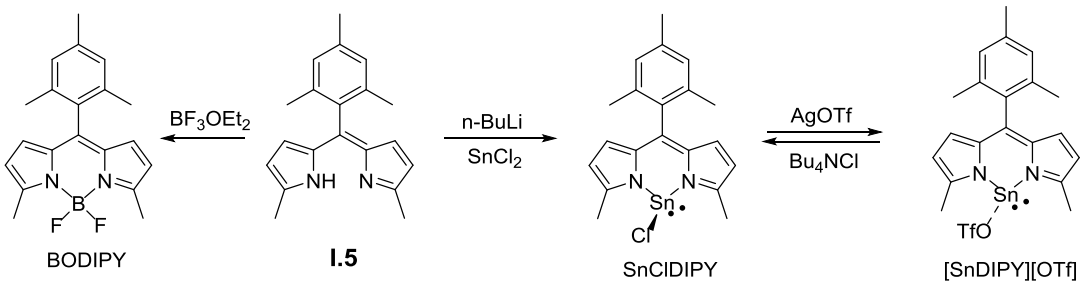

Figure I.9: Synthesis of BODIPY, SnClDIPY and [SnDIPY][OTf]

Tris(5-mesityldipyrrin) gallium(III) and tris(5-mesityldipyrrin) indium(III) (M[mesdpm]$_3$, M = Ga^{3+}, In^{3+}) were synthesized by mixing three equivalents of purified ligand 5-mesityldipyrrin (mesdpm) **I.6** with one equivalent of corresponding metal salt (Figure I.10).[23] These complexes displayed octahedrally coordinated metal to the pyrrole nitrogen atom of the chelating mesdpm ligand. These 13 Group complexes are less emissive than the Zn(mesdpm)$_2$.[17]

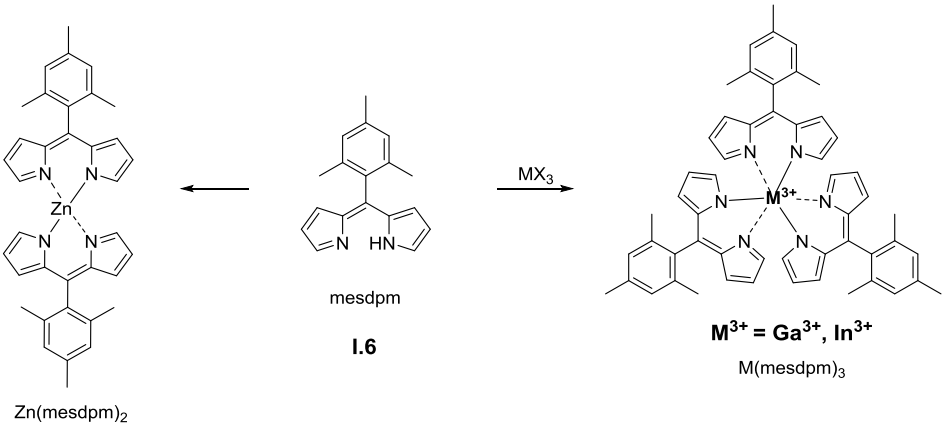

Figure I.10: Synthesis of Ga(mesdpm)$_3$ and In(mesdpm)$_3$ Complexes

(ii) Reactivity of Dipyrrin with Transition Metal Ion:

Employing Rothemund condensation reaction conditions, dipyrranato metal complexes were obtained as a side product during synthesis of strically hindered porphyrin. When mesitaldehyde was reacted with pyrrole in presence of zinc(II) acetate, zinc(II) dipyrranato complex was formed due to the steric hinderence provided by the ortho-substituent on the aldehyde which can hinder the cyclization to form a porphyrin (Figure I.11).[24] Similarly the 2-chlorobenzaldehyde[25], 2,6-dichlorobenzaldehyde[26], 2-acetoxybenzaldehyde[27] have yielded zinc(II) dipyrrinato complexs.

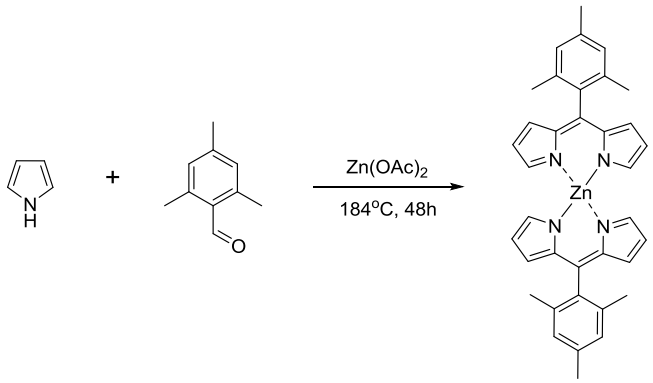

Figure I.11: Rothemund condensation reaction

Dipyrrins give monoanionic resonance stabilised ligand which easily can co-ordinate to variety of transition metal ions to form neutral square planar, tetrahedral or octahedral complexes (Figure I.12).[28] They can be homoleptic (metal centre has two or more identical ligands) or heteroleptic (bearing two or more different ligands on a metal centre). Many metal ions such as magnesium(II), calcium(II), chromium(III), manganese(II), manganese(III), iron(II), iron(III), cobalt(II), cobalt(III), nickel(II), copper(II), zinc(II), gallium(III), rhodium(II), palladium(II), cadmium(II), indium(III), mercury(II), thallium(I), and thallium(III) are known to form homoleptic complexes.[28]

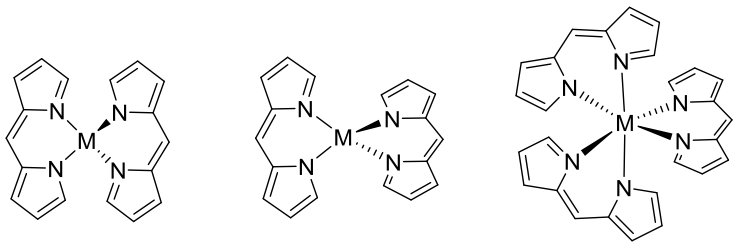

Figure I.12: Possible geometries for dipyrrin metal complexes.

The structural characterization of these metal complexes is predominantly done by Single Crystal X-Ray Diffraction (SCXRD). However, it is also possible to identify square planar, tetrahedral or octahedral complexes by NMR studies. In octahedral complex of dipyrrin, 1,9-hydrogen substituents in ^{1}H-NMR spectrum are deshielded by two aryl dipyrrinato systems. Octahedral geometry around metal ion push the α-proton towards the face of a neighbouring aromatic unit leading to the observation of relatively shielded chemical shift (α-protons δ = 6.43 ppm). In square planar geometry of dipyrrin metal complexes, α-proton overlap with two aromatic

dipyrrinato systems and hence increased deshielding was observed (α-proton δ = 10.83) in the ^{1}H-NMR spectrum. In tetrahedral arrangement, the α-protons of the dipyrrinato unit are far away from the opposing pyrrole rings (α-proton δ = 7.59). The steric interaction between the 1,9-substituent of the multiple dipyrrins brought together by complexation is also known to affect the coordination geometry of the metal centre[29]. 1,9-substituent such as hydrogen, results in the formation of non-square planar metal complex. For example, copper(II) complexes of 5-phenyldipyrrin adopts a distorted tetrahedral coordination geometry.

On the other hand, *meso*-substituted dipyrrin is a rigid ligand and can be easily derivatized at the *meso*-position. This makes the dipyrrin an attractive ligand for the synthesis of co-ordination polymer with various transition metal ions.

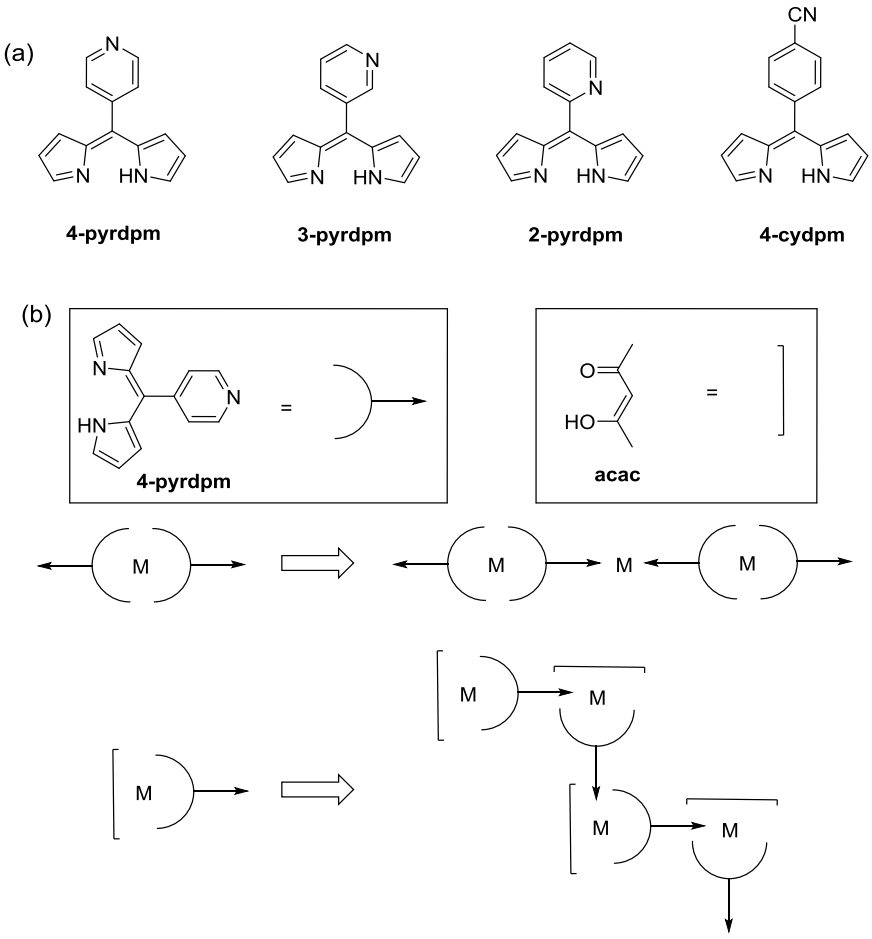

Figure I.13: (a) Structure of dipyrrin ligands (pyrdpm = pyridyldipyrromethene) (b) some plausible schemes for the formation of homo- and heterometallic coordination solids. Heterometallic (top) and homometallic 1-dimensional (bottom) coordination polymers may be accessible.

A variety of *meso*-substituted dipyrrins bearing two different binding sites have been synthesized with the aid of functionalized aromatic aldehyde. Several dipyrrin compounds have been synthesized in order to explore their coordination chemistry and to study the role of dipyrrin in the formation of coordination solid (Figure I.13a)[30]. These dipyrrins are also excellent precursors for the synthesis of metal complexes with 2-fold and 3-fold symmetry which can be explored as homoleptic and heteroleptic co-ordination polymers. It has been observed that asymmetric dipyrrin metal complexes can also form co-ordination polymers with lower dimensionality (Figure I.13b).

In general, a 1:1 ratio of dipyrrin and metal salt [$Cu(acac)_2$] yields the heteroleptic [Cu(dpm)(acac)], while a ratio of 1: 0.4 of dipyrrin with metal salt force the formation of homoleptic [$Cu(dpm)_2$] complex.[30]

The single crystal X-ray diffraction studies of the complexes [$Cu(4\text{-pyrdpm})_2$] and [$Cu(4\text{-cydpm})_2$] confirmed the distorted square planar geometry with Cu-N bond distance of 1.95Å.[30] The heteroleptic [Cu(4-pyrdpm)(acac)] complex displayed square pyramidal geometry because of acac and dipyrrin ligands with Cu-O and Cu-N bond lengths of 1.96 and 1.98 Å respectively. The axial position of the complex was occupied by the nitrogen atom of pyridine ring from neighbouring molecule of the [Cu(4-pyrdpm)(acac)] complex with a Cu-N bond length 2.32 Å (Figure I.14). The copper(II) ion is puckered out of square planar geometry towards the axial pyridine donor, while the pyridine ring of the 4-pyrdpm was orthogonal to the plane of the complex with a dihedral angle of 88º. This co-ordination of nitrogen atom from the pyridine ring leads to formation of extended one-dimentional zigzag coordination polymer. The [Cu(3-pyrdpm)(acac)] complex also exhibited similar one-dimentional coordination polymer but the structure of the complex and resulting coordination polymer were noticeably different. This complex also adopted square pyramidal coordination geometry around copper(II) ion but the axially coordinated nitrogen atom of the pyridine ring from neighbouring [Cu(3-pyrdpm)(acac)] complex was twisted perpendicular relative to the dipyrrin plane with dihedral angle 73º.

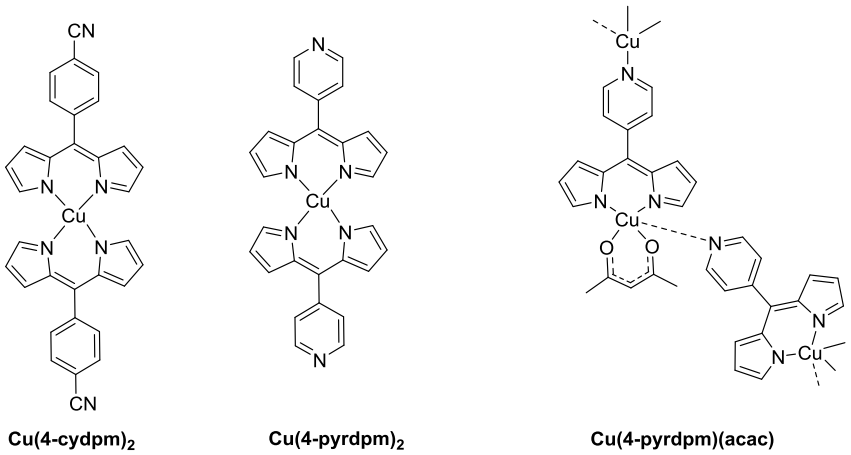

Cu(4-cydpm)$_2$ **Cu(4-pyrdpm)$_2$** **Cu(4-pyrdpm)(acac)**

Figure I.14: Structure of Metal dipyrrin complexes

The [Cu(2-pyrdpm)(acac)] complex was found to be mononuclear heteroleptic metal complex with a square planar geometry unlike [Cu(4-pyrdpm)(acac)] and [Cu(3-pyrdpm)(acac)][30]. This complex did not form coordination polymer due to lack of intermolecular interactions supported by the long Cu-N distance between pyridine ring nitrogen atom of the dipyrrin and [Cu(2-pyrdpm)(acac)]. Similarly, the [Cu(4-cydpm)(acac)] complex did not favour formation of the coordination polymer because of the sufficiently strong donor cyano group. But the complex is simple and similar to [Cu(2-pyrdpm)(acac)]. [Cu(4-pyrdpm)2], [Cu(3-pyrdpm)2] and [Cu(4-cydpm)2] which are mononuclear complexes with highly distorted square planar complexes because of steric hindrance between the α-protons of the opposing ligands. This distorted square planar geometry at the metal center avoids the coordination of fifth nitrogen of the pyridine ring and hence unable to form coordination polymer.

Even weakly co-ordinating ligands were also employed as ligands for heteroleptic complexes toward co-ordination polymers. The ligand (4-mtdpm) was synthesized to evaluate its role in the synthesis of co-ordination polymers. The complexation of Cu(hfacac)$_2$ (hfacac = hexafluoroacetylacetonato) with the ligand gave the desired coordination polymer with square pyramidal [Cu(4-mtdpm)(hfacac)] complex similar to [Cu(4-pyrdpm)-(acac)]. Surprisingly, the [Cu(3-mtdpm)(hfacac)] complex (3-mtdpm =5-(3-methylthiophenyl)dipyrromethene) obtained in a similar fashion displayed a cyclic dimer instead of the expected co-ordination polymers (Figure I.15).[31] The coordination geometry is the same as observed for [Cu(4-mtdpm)(hfacac)] complex and dimer was held together by thioether groups with a Cu-S distance of 2.86 Å in the axial position of the coordination sphere. Recently, a

similar rigid binuclear complex was reported from 2,8-diethyl-1,3,7,9-tetramethyl-5-(2-pyridyl) dipyrromethene and zinc(II) ions (Figure I.15).[32]

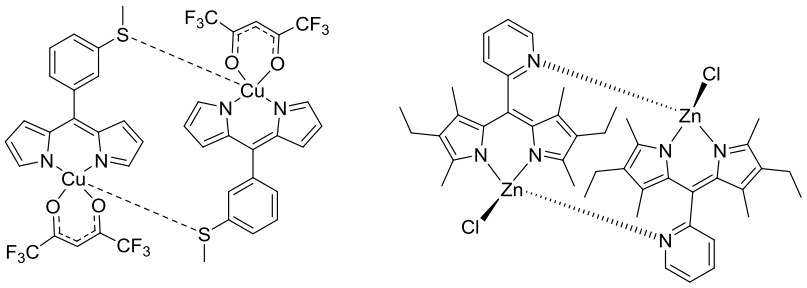

Figure I.15: Dimeric structures of copper(II) and zinc(II) dipyrrin complexes

Employing $Cu(hfacac)_2$ as copper(II) ion source, instead of $Cu(acac)_2$, also provided the heteroleptic metal complex with a blocking hfacac ligand. When dipyrrin (4-pyrdpm=5-(4-pyridyl)dipyrromethene) ligand was mixed with excess of $Cu(hfacac)_2$, a trinuclear species was isolated (Figure I.16)[33].

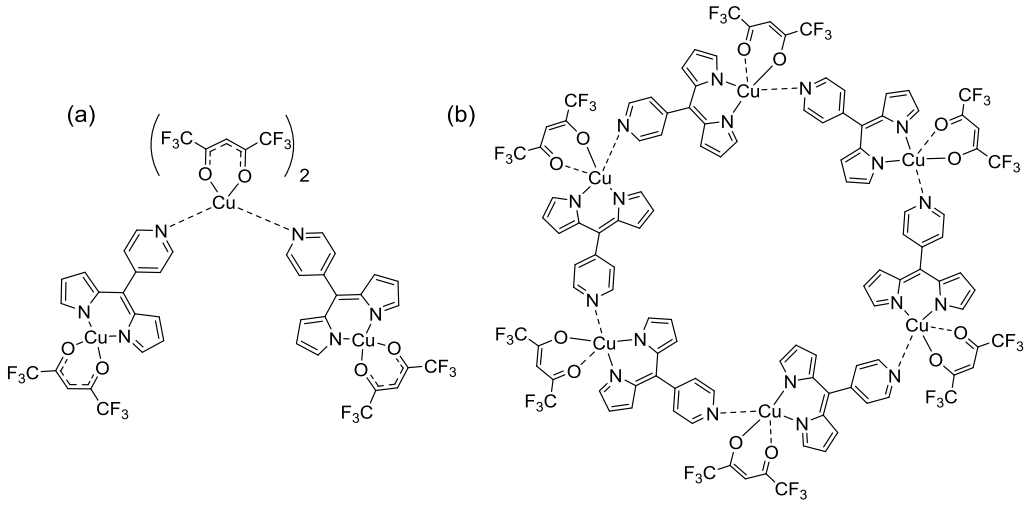

Figure I.16: Heteroleptic copper(II) complexes (a) Trinuclear metal complex, (b) Hexagonal metal complex

This species has two distorted square planar copper(II) complexes coordinated to a octahedral copper(II) centre through the pyridine nitrogen atom at *meso* position. This complex could not be synthesized under similar reaction conditions with $Cu(acac)_2$ as the metal ion. A serendipitous discovery revealed that reacting an equimolar ratio of $Cu(hfacac)_2$ with 4-pyrdpm leads to the discrete self-organized hexagonal structure instead of the expected heteroleptic co-ordination polymer (Figure I.16).[33] This hexagon ring contains six molecules of [Cu(4-pyrdpm)(hfacac)] connected to each

other by axial coordination of pyridine nitrogen atom at *meso*-position and estimated ring diameter was 19.24 Å.

(iii) Functionalization of Dipyrrin Complexes:

Some of these boron and metal complexes are well known starting materials for synthesis of anti-aromatic porphyrinoids. Porphyrinoids are generally synthesized through an acid catalysed condensation reaction between pyrrole and aldehyde. Even though metal mediated processes are well known in recent synthetic organic chemistry, only couple of protocols were established for synthesis of porphyrinoids framework.[34] Very recently, BODIPY dyes have gained much attention for applications such as labelling experiments, chemosensors, light-harvesting systems and dye-sensitized solar cells.[35] In 2011, Shinokubo and co-workers have exhibited incorporation of BODIPY unit into stable anti-aromatic porphyrinoids by transition metal catalysed coupling reaction (Figure I.17)[34a]. In this synthesis, trimethylsilylethynyl groups were introduced into α,α'-dichloro BODIPY under Stille coupling conditions followed by sila-Glaser coupling using CuCl in DMSO to afford the target molecules **I.9** and **I.10**. The macrocycle **I.9** contains 24π electron in conjugation hence anti-aromatic in nature. The single-crystal X-ray diffraction analysis of **I.9** unambiguously confirmed the planar and rectangular conformation because of rigid butadiyne linkage and co-ordinated BF_2 moiety. The 36π electron porphyrinoid **I.10** is anti-aromatic molecule and displayed distorted planar conformation in solid state. These molecules do not display fluorescence due to the small HOMO-LUMO gap expected of anti-aromatic compounds which increases the rate of nonradiative decay. However, molecule **I.9** undergoes selective hydrogenation in presence of Pd/C at butylene unit to form the butylene bridged BODIPY dimer **I.11** (Figure I.18). This conversion displayed blue shifted absorption band at 488 nm with respect to the precursor BODIPY and regains its bright green fluorescence at 543 nm. The molecular structure obtained indicates that **I.11** has a step-like structure with two BODIPY units.

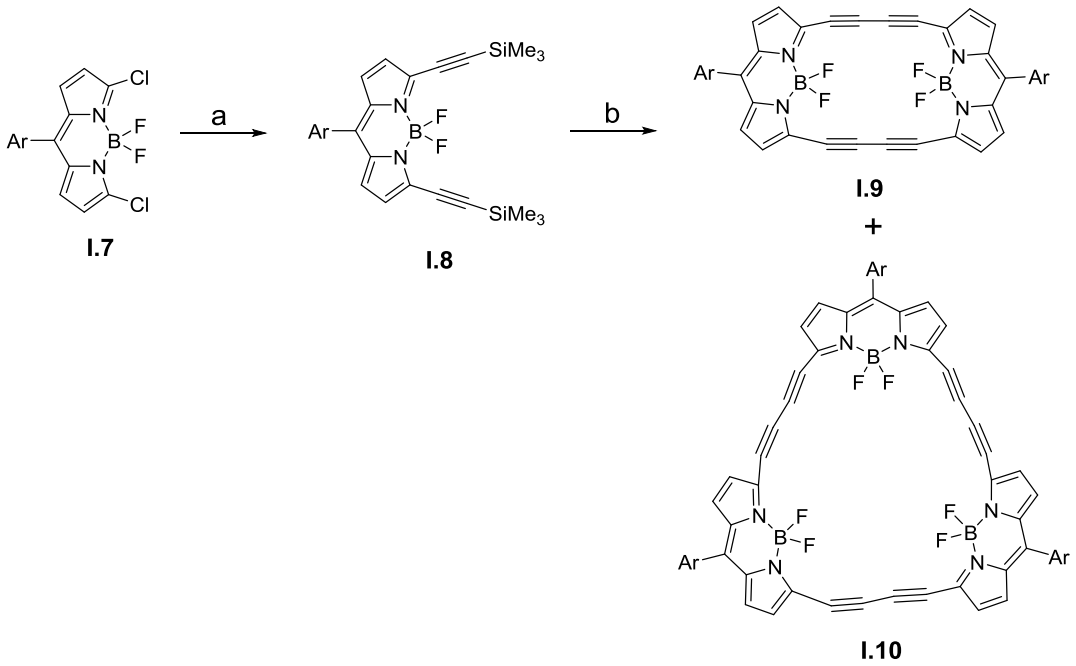

Figure I.17: Synthesis of butadiyne-bridged BODIPY oligomers.

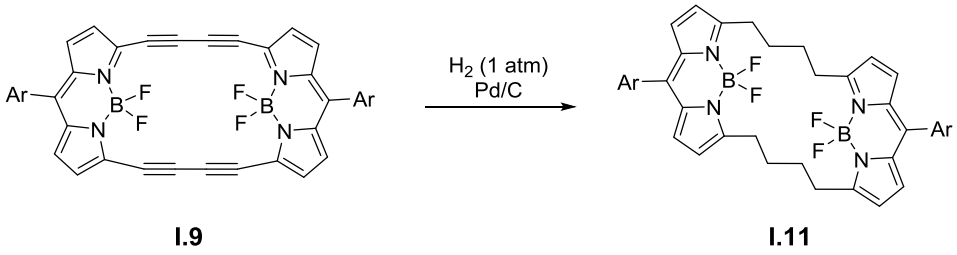

Figure I.18: Hydrogenation of BODIPY dimer.

In 2012, Shinokubo et al synthesized air stable 16π anti-aromatic Ni(II) norcorrole, **I.13** in 90% yields by Ni(0) mediated intramolecular reductive homocoupling of precursor bis(α,α'-dibromodipyrrinato) nickel complex, **I.12** (Figure I.19)[34b]. This is a simple and efficient route for metal mediated synthesis of contracted porphyrinoid at room temperature. The Norcorrole contains two *meso*-carbon atoms less than the regular porphyrin but still adopts a perfect planar geometry in the solid state. It undergoes oxidation at high temperature (100ºC) in presence of molecular O_2 in 5 days to the 18π aromatic Ni(II) 10-oxacorrole, **I.14**. *m*-chloroperoxybenzoic acid was used as a oxidizing agent in order to observe similar changes at low temperature (-30ºC) for 3 h. Apart from highly planar nature of **I.14**, the presence of lone pair of electron on oxygen at the *meso*-position is responsible for

aromaticity. This indicates the norcorrole has ability to act as precursor for synthesis of different heteroatom-substituted porphyrinoid.

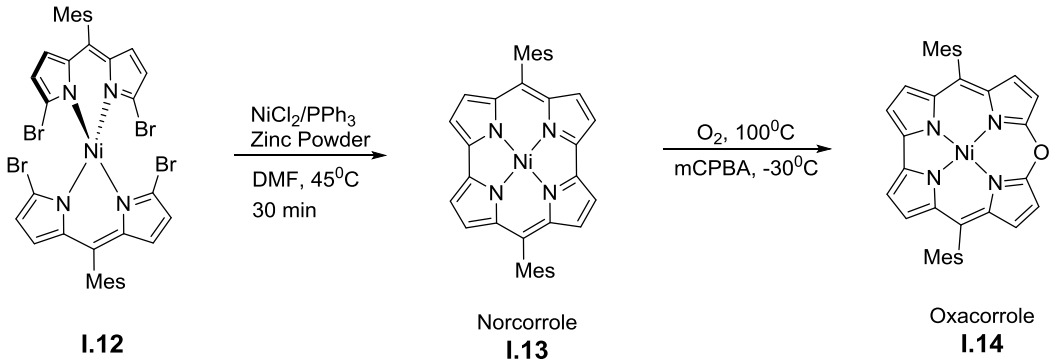

Figure I.19: Synthesis of Ni(II) norcorrole, **I.13** and its oxidation to Ni(II) oxacorrole **I.14**.

Objectives of the Work:

Dipyrrins are known to form very common homoletptic and heteroleptic metal complexes with square planar, tetrahedral and octahedral geometries. Changing the substituents on *meso*-position and availing extra coordination at 1,9-position of dipyrrins, provide molecules with tuneable fluorescence efficiency. Co-ordination polymers were also obtained by adding the extra coordination sites on *meso*-substituted aromatic ring of dipyrrin. In light of all these well-established strategies, this thesis describes the efforts to synthesize metal complexes derived from singly and doubly N-confused dipyrrins as well their benzo-derivatives. It can be expected that such molecules can also have properties similar to the dipyrrin based complexes and hence this thesis will also describe the structural and electronic properties of the aimed synthetic targets.

Chapter 2

Synthesis and Characterization of Bis, Tris and Tetra-BODIPY

II.1: Introduction:

BODIPY dimer has gained significant focus for its interesting properties such as charge delocalization and exciton coupling leading to unusual fluorescence properties. There are several types of directly linked BODIPY dimers such as α-α linked dimers **A**[36], β-β linked dimers **B**[37], *meso-meso* linked dimers **C**[38], and *meso*-β linked dimers **D**[38a, 39] (Figure II.1).

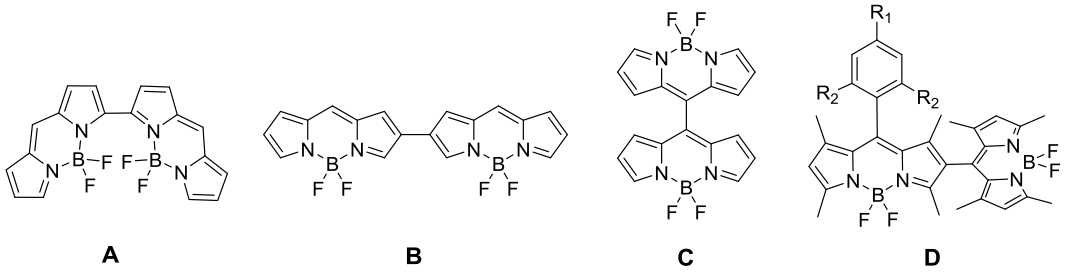

Figure II.1: Structures of α-α (**A**), β-β (**B**), *meso-meso* (**C**) and *meso*-β (**D**) directly linked BODIPY dimers

The dipyrrin backbone (C9BN2 framework) of the monomer **II.1** does not exhibit significant difference between single and double bond lengths to justify its symmetric π-system and flat nature suggestive of strong delocalization π-electrons. The α-α linked dimer synthesized by Broring et al exibits two-fold boron difluoride complexation of 2,2'-dipyrrin, **II.2** as shown in scheme II.1.[36] This dimer shows less pronounced planarity (twisted conformation) of the two different C9BN2 subunits than the monomer, **II.1**. The BODIPY monomer, **II.1** displayed absorption at 535 nm and emission 540 nm with unit quantum yield whereas dimer, **II.3b** displayed a characteristic two strong bathochromically shifted absorption bands at 490 and 559 nm clearly suggesting the presence of exciton splitting. The luminescence spectra were characterized by 79 nm Stokes shifted intense and broad emission band with respect to the lowest energy absorption band and quantum yield of 76%.

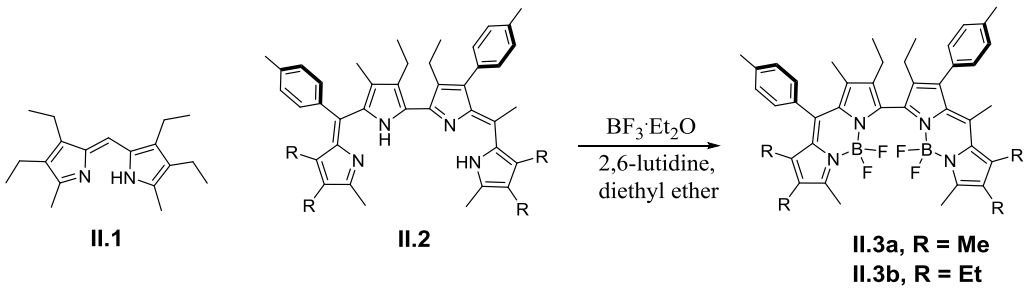

Scheme II.1: Synthesis of α-α directly linked BODIPY dimer (**II.3**)

Ziessel et al reported the oxidative β-β coupling of BODIPY monomer by employing PIFA (Phenyliodine(III) bis(trifluoroacetate) in presence of Lewis acid such as $BF_3{\cdot}Et_2O$ at -78ºC to yield the β-β linked dimers, **II.5** and trimer, **II.6** as shown in scheme II.2.[37] The dihedral angle between the two planes of the planar BODIPY subunits was found to be 64º as determined from the molecular structure through single-crystal X-ray diffraction. The absorption spectra of β-β linked dimers and trimer were found to be redshifted by 30 nm and 58 nm respectively with respect to the BODIPY monomer **II.4**. The emission spectra displayed a 51 nm shift for the dimer and 79 nm shift for the trimer with respect to the BODIPY monomer, **II.4**.

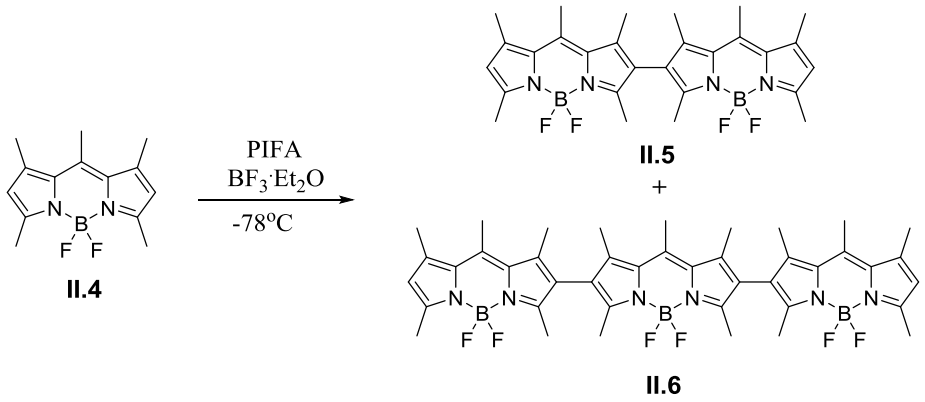

Scheme II.2: Synthesis of non-planar β-β directly linked BODIPY dimer (**II.5**) and trimer (**II.6**)

Hiroshi Shinokubo and co-workers report indicated monobromo BODIPY, **II.8** undergoes homocoupling to directly β-β linked dimer, **II.1**, through a Palladium-catalyzed borylation with bis(pinacolato)diboron (pin2B2) and in situ cross-coupling with the use of Cs_2CO_3 as a base[40]. However, Suzuki Miyaura cross-coupling of monobromo BODIPY yielded the trimer, **II.12** (Scheme II.3.). Unambiguous determination of the molecular structure of dimer from SCXRD indicated a flat conformation due to the absence of substitution on the 1,3,5,7-postions in both the BODIPY core which aids effective conjugation between the two chromophores. The highly planar conformation aids the effective extension of conjugation and hence, the electronic absorption profile of dimer and trimer is red-shifted by 108 nm and 177 nm respectively in comparison with BODIPY monomer, **II.7**. The fluorescence spectra of the dimer and trimer displayed a 141 nm stoke shift with a quantum yield of 15% and

217 nm stoke shift with quantum yield of 25% in comparison to the BODIPY monomer, **II.7** respectively.

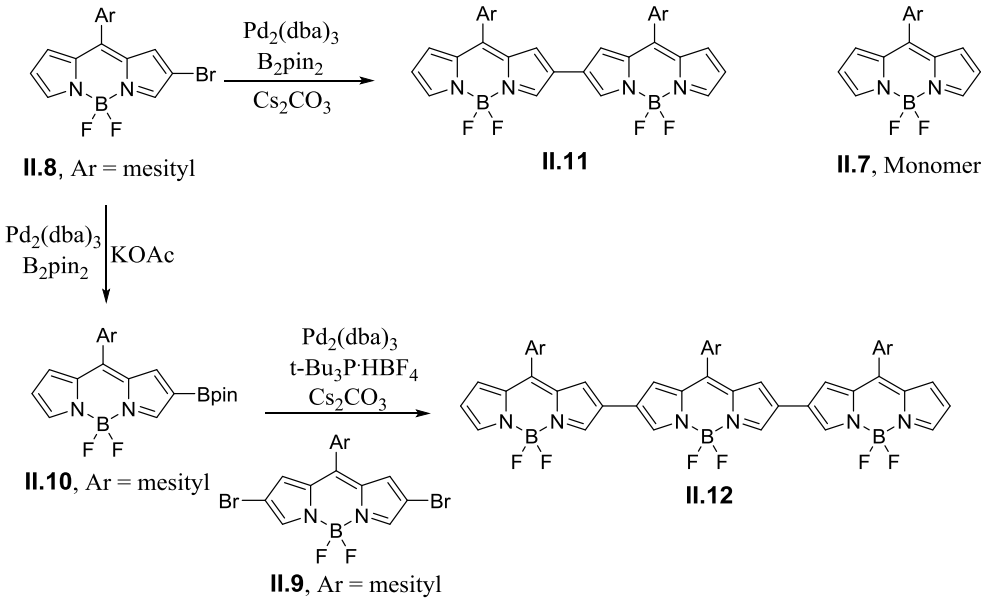

Scheme II.3: Synthesis of planar β-β directly linked BODIPY dimer (**II.11**) and trimer (**II.12**)

Apart from the above mentioned intermolecular bonds between the two BODIPY units, Akkaya et al reported the orthogonally linked dimeric Bodipys such as *meso*-β linked dimer (Scheme II.4)[38a, 39b]. The *meso*-β linked dimer, **II.15** was synthesized from 2-formyl BODIPY, **II.14** and the *meso-meso* linked dimer was obtained from 8-formyl BODIPY. Interestingly, the *meso*-β linked dimer, **II.15** was found to absorb similar to the parent BODIPY monomer, **II.13** while it lacked characteristic fluorescence expected from the dye. As per the elucidated molecular structure of *meso*-β linked dimer, the dihedral angle between the two BODIPY units was found to be 90º. When they attempted to detect singlet-oxygen phosphorescence, this dimer, **II.15** gave the strongest singlet-oxygen phosphorescence emission with quantum yield of 51% for singlet-oxygen generation in dichloromethane which is higher than any other non-halogenated BODIPY.

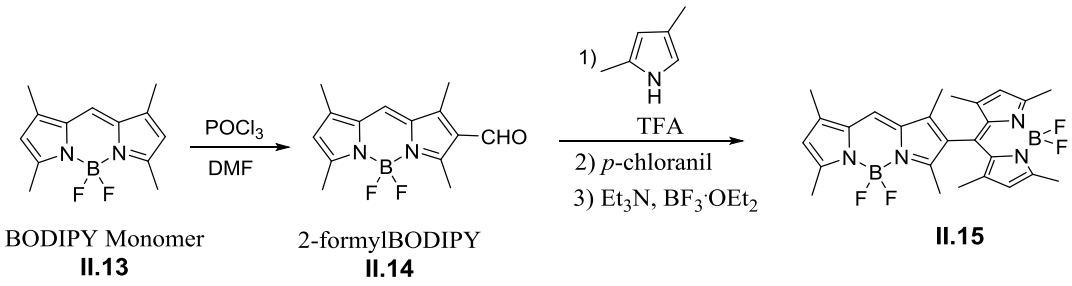

BODIPY Monomer
II.13

2-formylBODIPY
II.14

II.15

Scheme II.4: Synthesis of *meso*-β directly linked BODIPY dimer (**II.15**)

The *meso*-β linked dimer, **II.17** was synthesised by Jiao et al under acidic conditions from β-formyl BODIPY, **II.16** in good yield (Scheme II.5)[39a]. As compared to the Akkaya's *meso*-β linked dimer, the substituent on the *meso*-aryl and newly formed BODIPY core restricted the free rotation with respect to main BODIPY core in a more efficient way. The orthogonal geometry of the BODIPY dimers, **II.17**, is found to be the cause for their modified photophysical properties. With respect to starting BODIPY monomer **II.16**, a 30 nm red-shifted broadened and additional absorption band was observed for dimers, **II.17a** and **II.17c** because of formation of ground-state charge-transfer complex through exciton coupling between two BODIPY subunits. These dimers, **II.17** displayed weak fluorescence emission than the corresponding BODIPY monomer, **II.16** similar to the Akkaya's *meso*-β directly linked BODIPY dimers[38a]. It was also observed that the orthogonal *meso*-β BODIPY dimers, **II.17b** and **II.17d** have very high efficiency for generating singlet oxygen than their non-orthogonal *meso*-β BODIPY dimers, **II.17a** and **II.17c**.

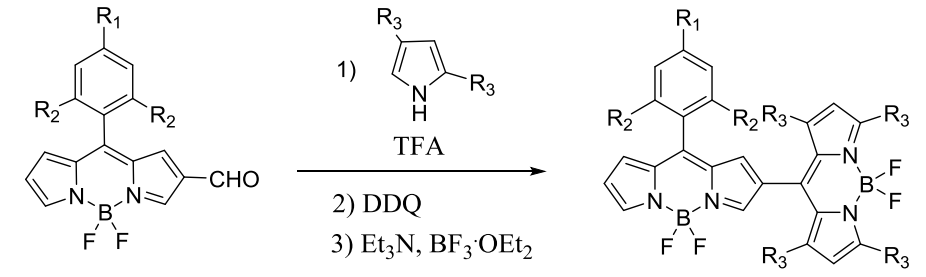

BODIPY monomer
II.16

II.17a, R_1 = OMe, R_2 = H, R_3 = H
II.17b, R_1 = OMe, R_2 = H, R_3 = Me
II.17c, R_1 = H, R_2 = Cl, R_3 = Me
II.17d, R_1 = H, R_2 = Cl, R_3 = Me

Scheme II.5: Synthesis of *meso*-β directly linked BODIPY dimer (**II.17**)

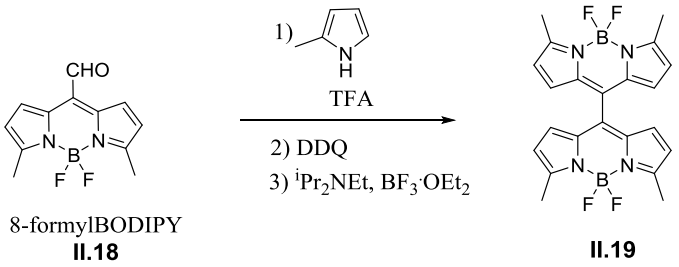

Scheme II.6: Synthesis of *meso-meso* directly linked BODIPY dimer (**II.19**)

Thompson et al accounted the synthesis of orthogonal *meso-meso* directly linked dimer, **II.19** from 8-formyl BODIPY, **II.18** derivative using standard protocol (Scheme II.6)[38b]. This dimer also did not exhibit exciton coupling between the BODIPY units with absorbance at 530 nm and emission at 651 nm in dichloromethane.

Recently Kursunlu et. al. synthesized the new fluorescent conjugated molecules such as single **II.20**, dual **II.21** and triple-BODIPY **II.22** by a condensation reaction of 2,4-dimethyl-3-ethylpyrrole with 1,3,5-benzenetricarbonyl chloride to study effect of number of BODIPY moieties on photophysical properties (Scheme II.7)[41]. It was discovered that the number of BODIPY moieties is directly proportional to the absorption and emission wavelength and intensity and also to the quantum yield.

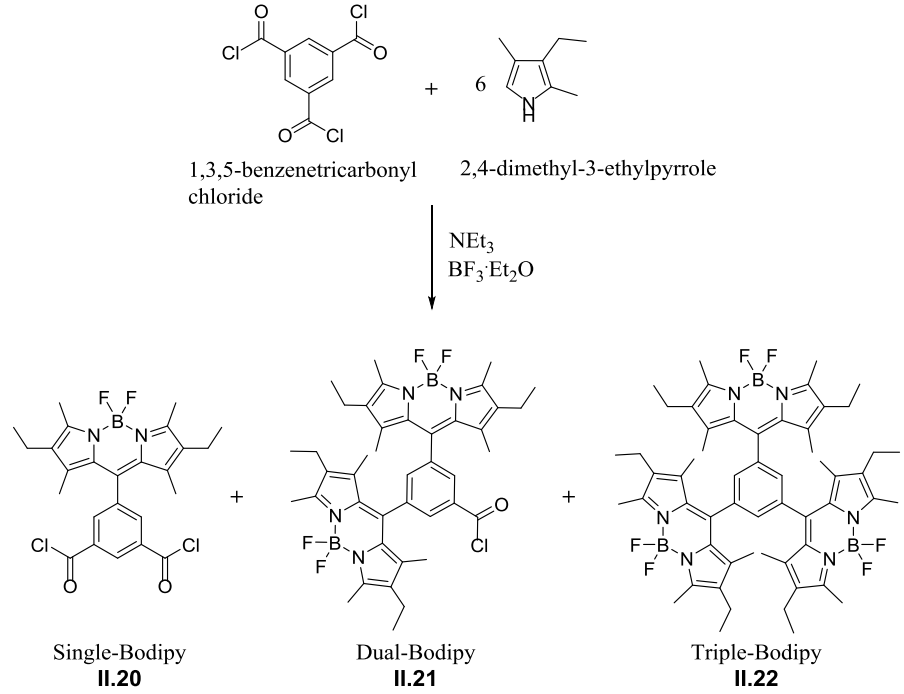

Scheme II.7: Synthesis of Single (**II.20**), Dual (**II.21**) and Triple-BODIPY (**II.22**)

II.2: Objectives:

With respect to mono-BODIPY dyes, only limited reports are available on the synthesis of multi-BODIPY dyes their structure elucidation and optical properties. Therefore, it was decided to employ BOIDPY as a substituent at various positions on benzene and biphenyl unit and to study their photophysical properties.

II.3: Synthesis BODIPY Derivatives:

1,3 and 1,4-bis dipyrromethane benzene **II.23**[42] and **II.25**[43] were synthesized as per reported procedure and converted them into 1,3 and 1,4-bis BODIPY benzene **II.24** and **II.26** respectively as per regular protocol used for BODIPY synthesis (Scheme II.8 and II.9). The attempt to synthesize 1,2-bis dipyrromethane from o-phthaldehyde was unsuccessful, probably due to the steric hindrance between two neighbouring dipyrromethane unit (Scheme II.10). The 1,3,5-benzene tricarboxaldehyde[44] was condensed with excess pyrrole under acidic conditions to yield 1,3,5-tris dipyrromethane benzene **II.27** which was further converted into 1,3,5-tris BODIPY benzene **II.28** (Scheme II.11). The tetra-BODIPY was synthesized starting from 5-bromoisophthaldehyde[45]. It was protected with ethylene glycol in quantitative yield. The protected dialdehyde **II.29** was converted into its lithiated salt using n-BuLi at -78ºC followed by coupling reaction with 1,2-Bis(diphenylphosphino)ethane nickel(II) chloride [$NiCl_2$(dppe)] to yield the protected tetraldehyde **II.30**. We deprotected **II.30** to obtain 1,1'-biphenyl 3,3'5,5'-tetraldehyde **II.31** using 6N HCl. The 1,1'-biphenyl 3,3'5,5'-tetra dipyrromethane **II.32** was obtained by condensation reaction between the tetraldehyde **II.31** and pyrrole. Finally **II.32** was further converted into its boron complex 1,1'-biphenyl 3,3'5,5'-tetra-BODIPY **II.33** (Scheme II.12).

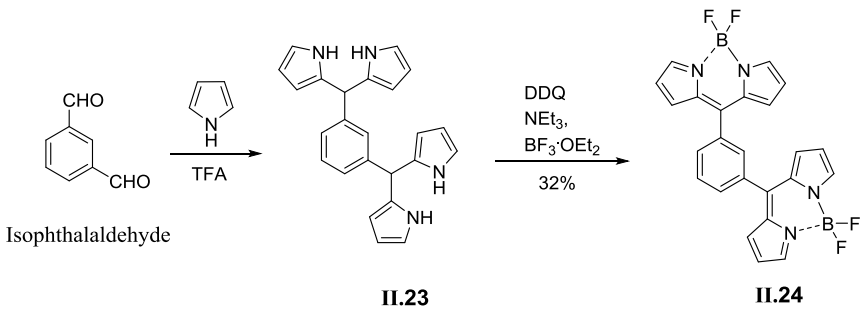

Scheme II.8: Synthesis of 1,3-Bis BODIPY Benzene (**II.24**)

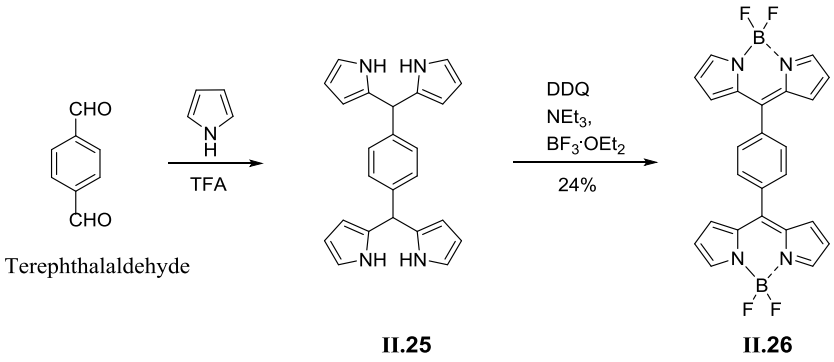

II.25 II.26

Scheme II.9: Synthesis of 1,4-Bis BODIPY Benzene (**II.26**).

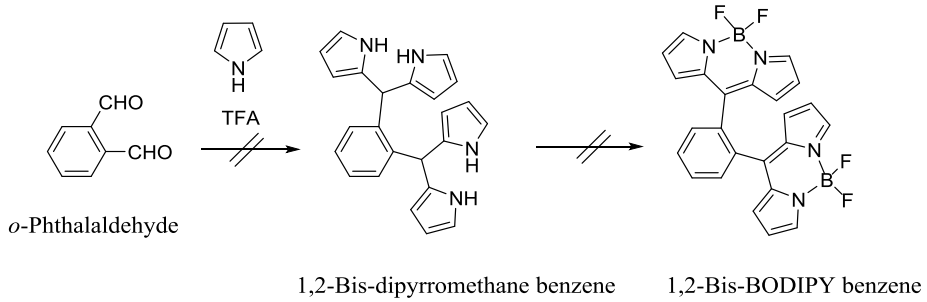

1,2-Bis-dipyrromethane benzene 1,2-Bis-BODIPY benzene

Scheme II.10: Synthesis of 1,2-Bis BODIPY Benzene.

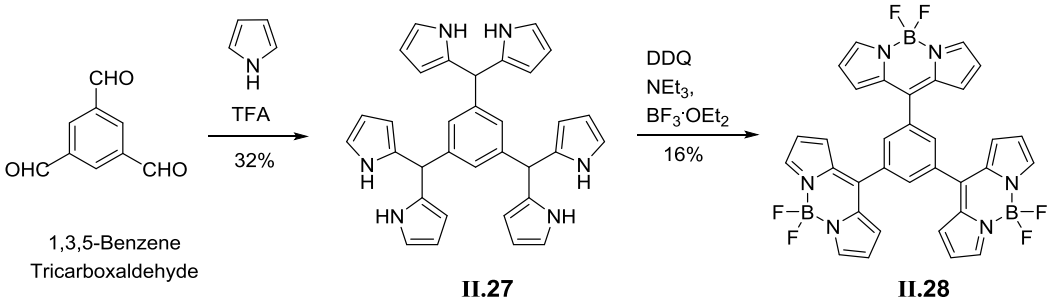

II.27 II.28

Scheme II.11: Synthesis of 1,3,5-Tis BODIPY Benzene (**II.28**).

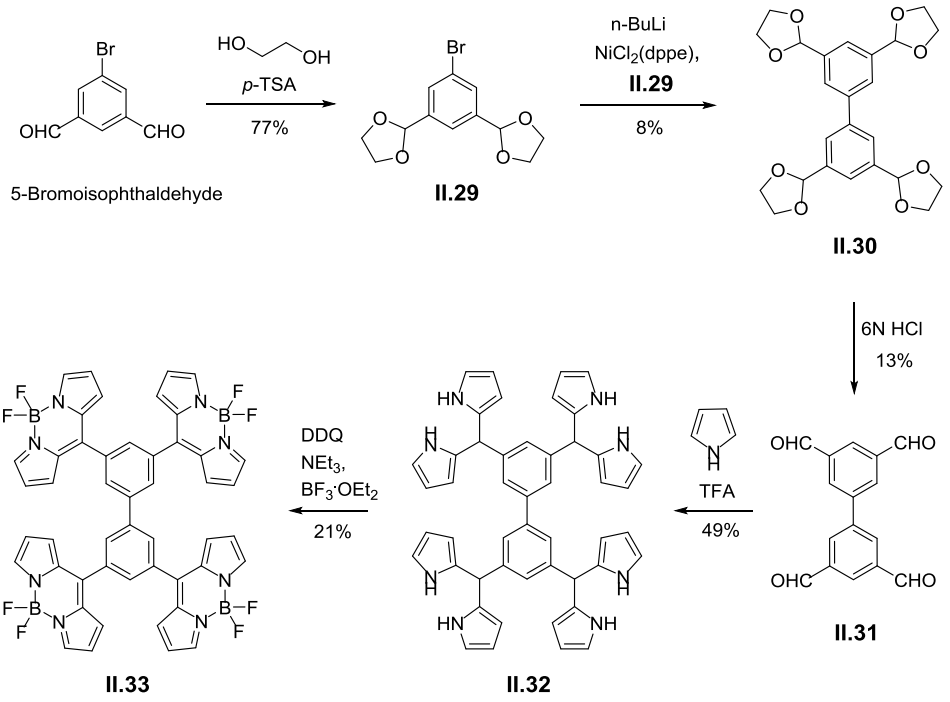

Scheme II.12: Synthesis of 1,1'-Biphenyl 3,3',5,5'-Tetra BODIPY (**II.33**)

II.4: Characterization BODIPY Derivatives:

All these molecules were characterized by HRMS and NMR techniques (Experimental Section). ^{1}H-NMR spectrum for 1,3-bis BODIPY benzene **II.24** displayed three sets of signal at δ = 6.59, 6.95 and 7.98 ppm for BOIDPY moiety and multiplet between 7.71-7.82 ppm corresponding to unsymmetrical benzene unit (Figure II.3). In the DEPT-90 spectrum, the six set of CH signals at 119, 129, 131, 132, 133, 145 ppm were observed suggesting the unsymmetrical structure of **II.24** (Figure II.4).

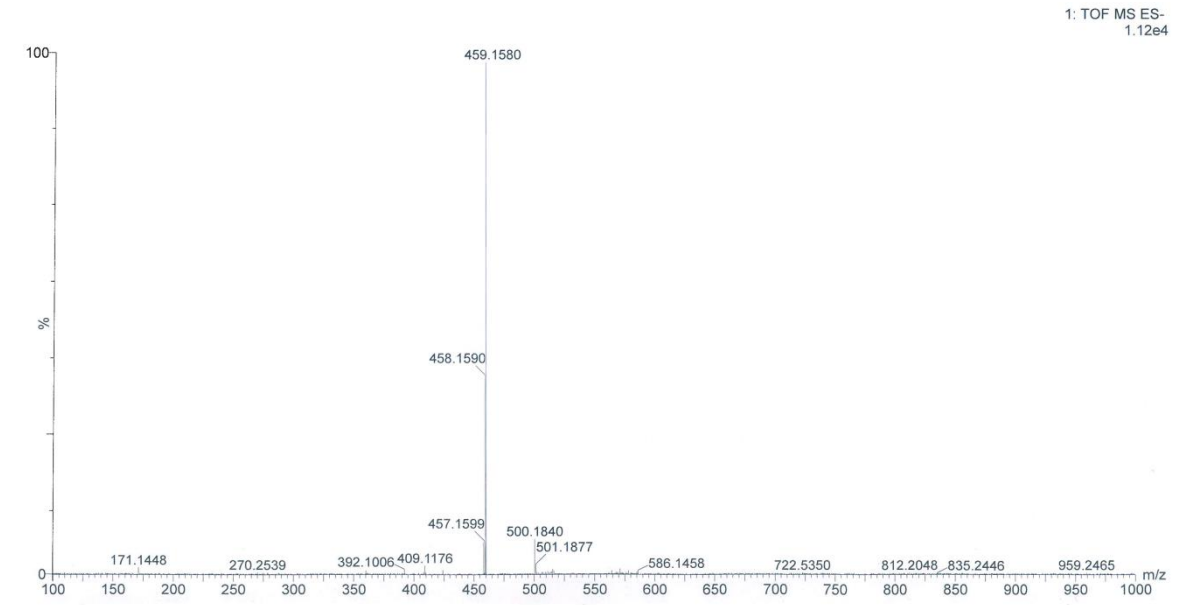

Figure II.2: HR-ESI-TOF mass spectrum of **II.24**

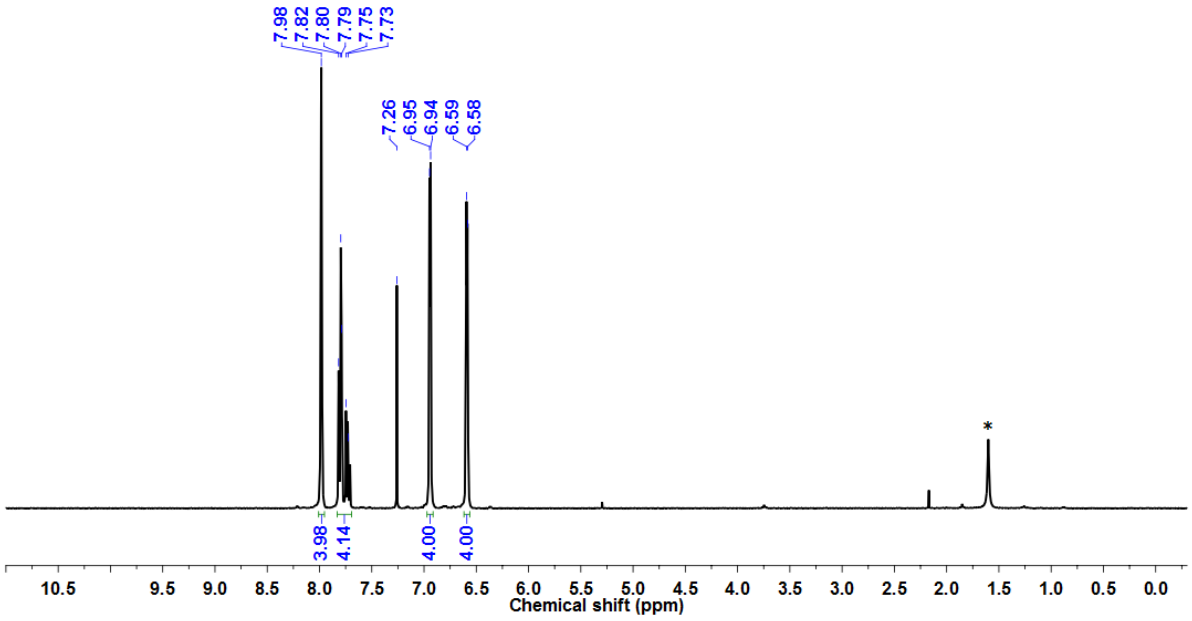

Figure II.3: ^{1}H-NMR spectrum of **II.24** in *Chloroform-d* at 295K

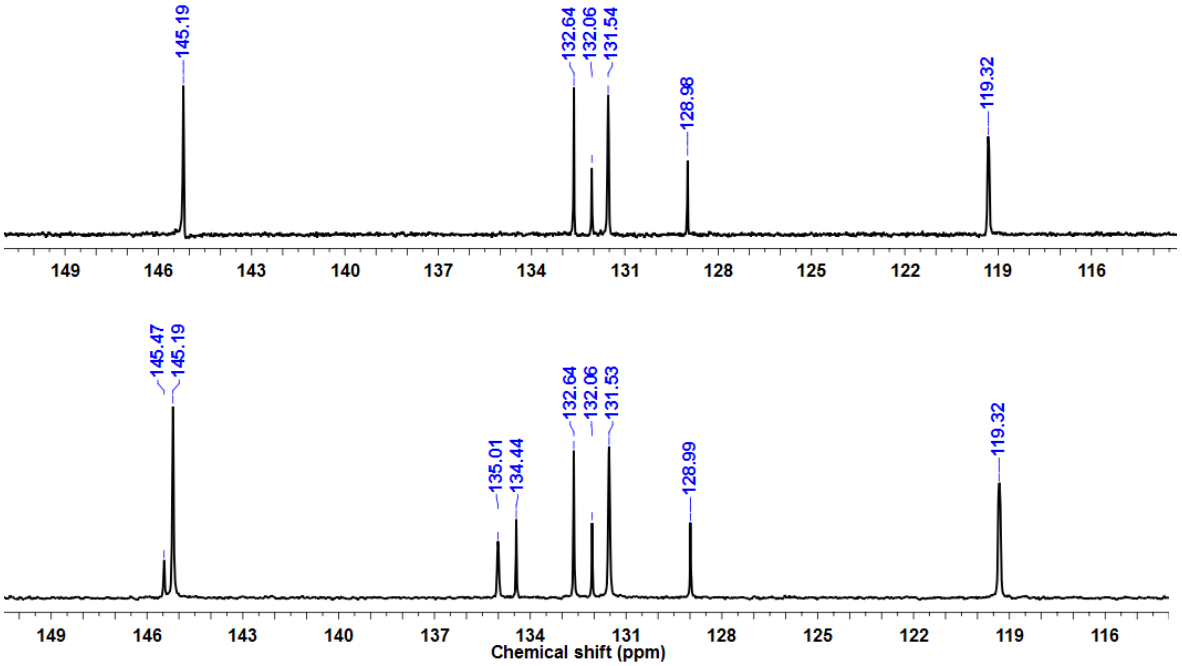

Figure II.4: (Top) DEPT-90 and (Bottom) ^{13}C-NMR spectrum of **II.24** in *Chloroform-d*

In ^{1}H-NMR spectrum of 1,4-bis BODIPY benzene **II.26**, the signal for BOIDPY moiety was observed at δ = 6.61, 7.00 and 8.01 ppm, while the symmetrical benzene unit displayed a singlet at 7.76 ppm (Figure II.6). DEPT-90 experiments indicated the four sets of CH signals at 119, 130, 131, 145 ppm, suggestive of symmetrical nature of this BODIPY isomer (Figure II.7).

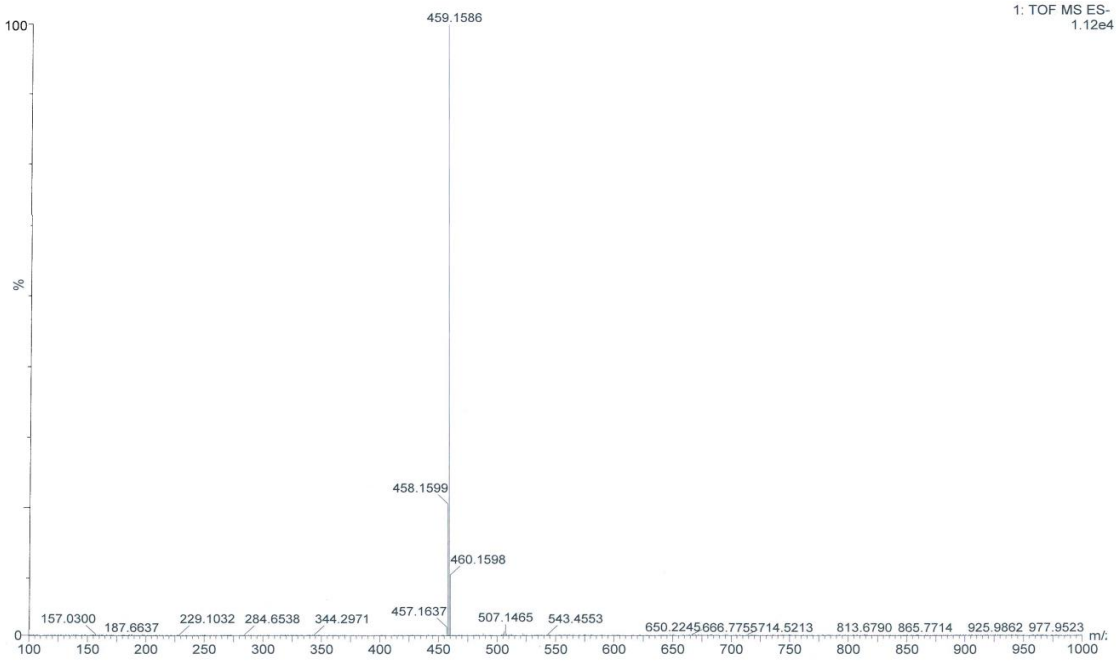

Figure II.5: HR-ESI-TOF mass spectrum of **II.26**

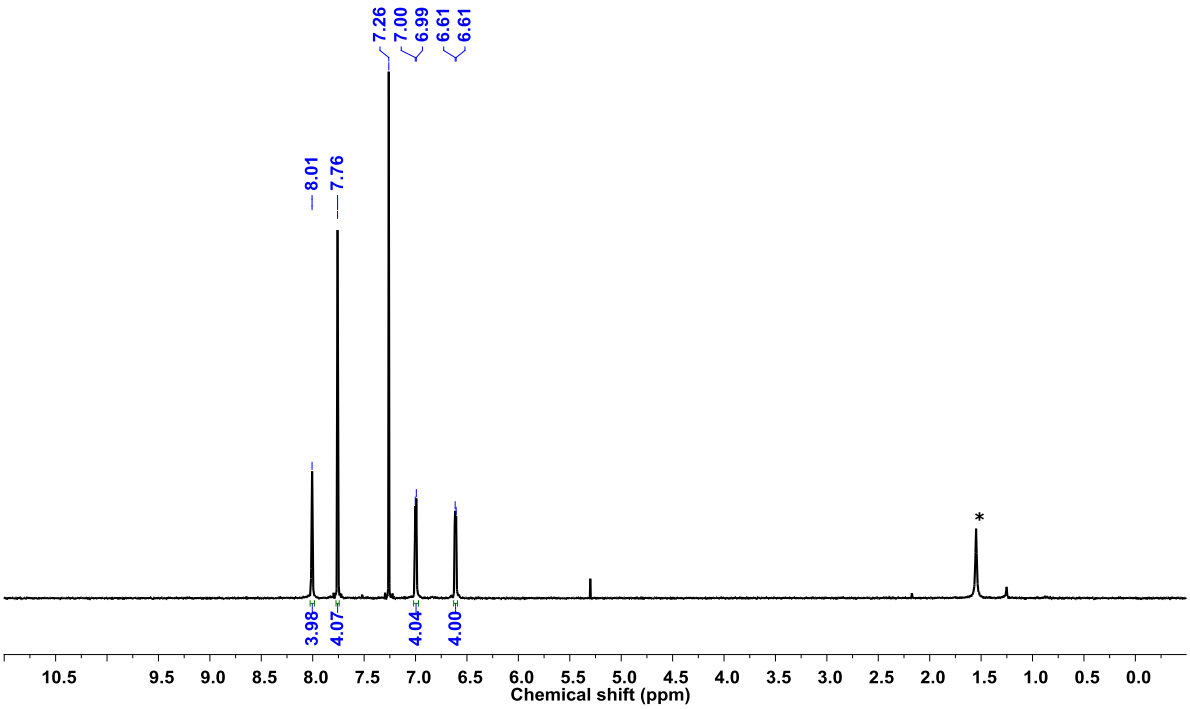

Figure II.6: [1]H-NMR spectrum of **II.26** in *Chloroform-d* at 295K

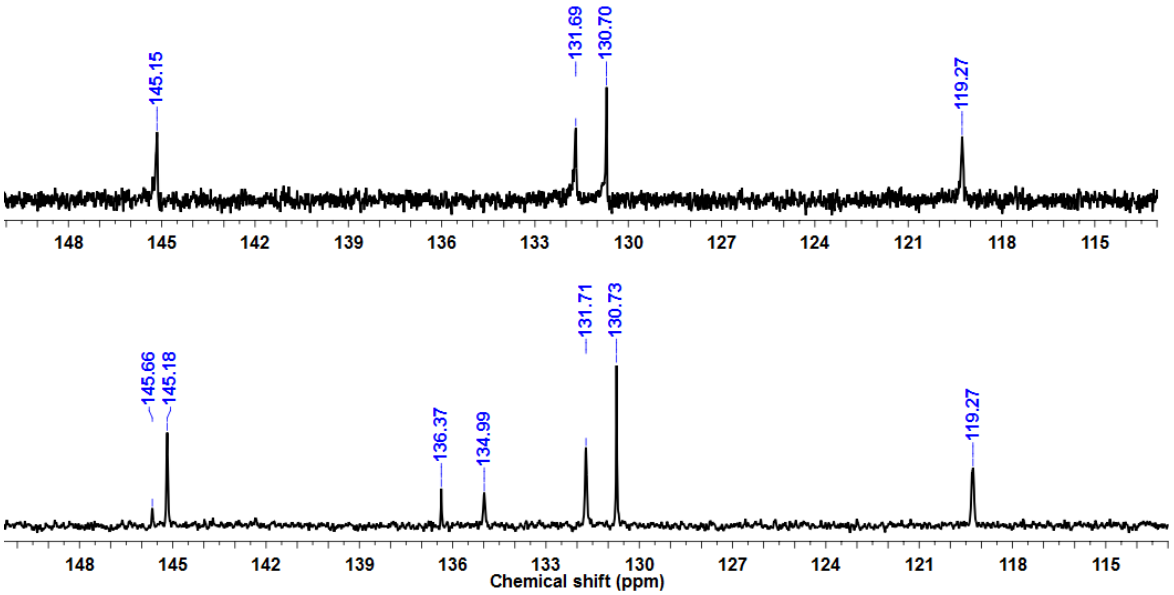

Figure II.7: (Top) DEPT-90 and (Bottom) [13]C-NMR spectrum of **II.26** in *Chloroform-d* at 295K

The [1]H NMR spectrum of 1,3,5-tris BODIPY benzene **II.28** displayed signals at 6.63, 6.96, 8.02 ppm for BOIDPY moiety and a signal for the benzene unit overlaps with BODIPY signal at 8.02 ppm (Figure II.9). The DEPT-90 spectrum matched as

per the expected structure of **II.28** with signals at 119, 131, 133, 145 ppm (Figure II.10).

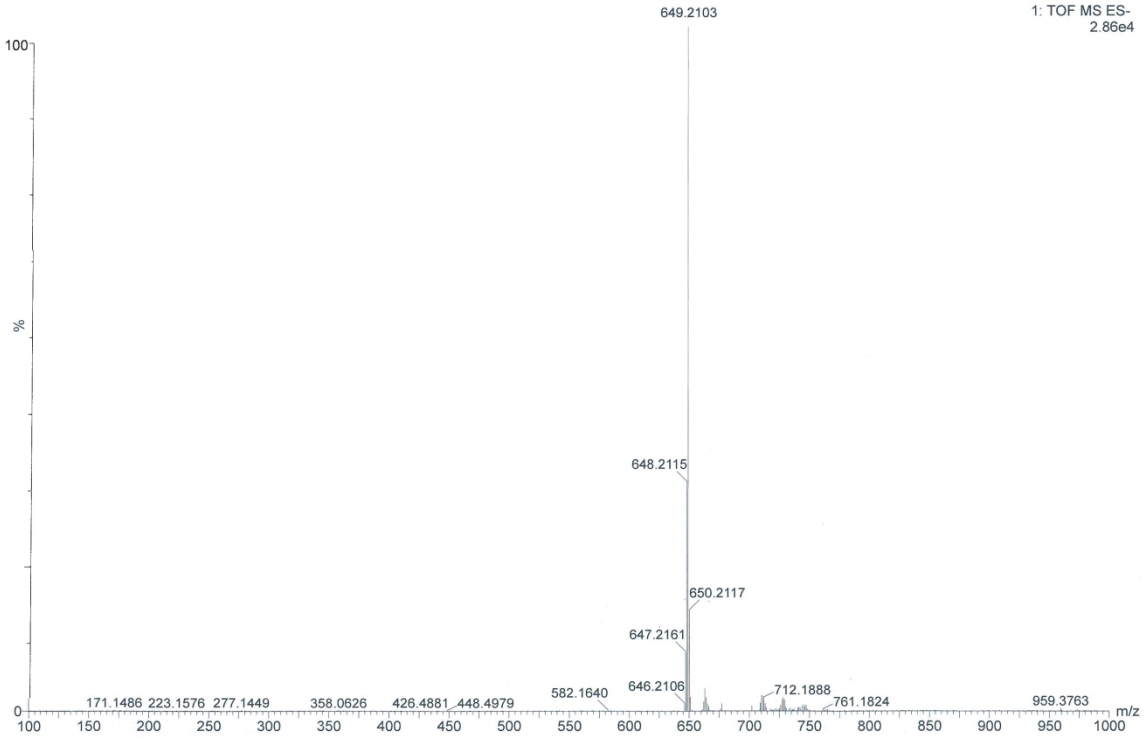

Figure II.8: HR-ESI-TOF mass spectrum of **II.28**

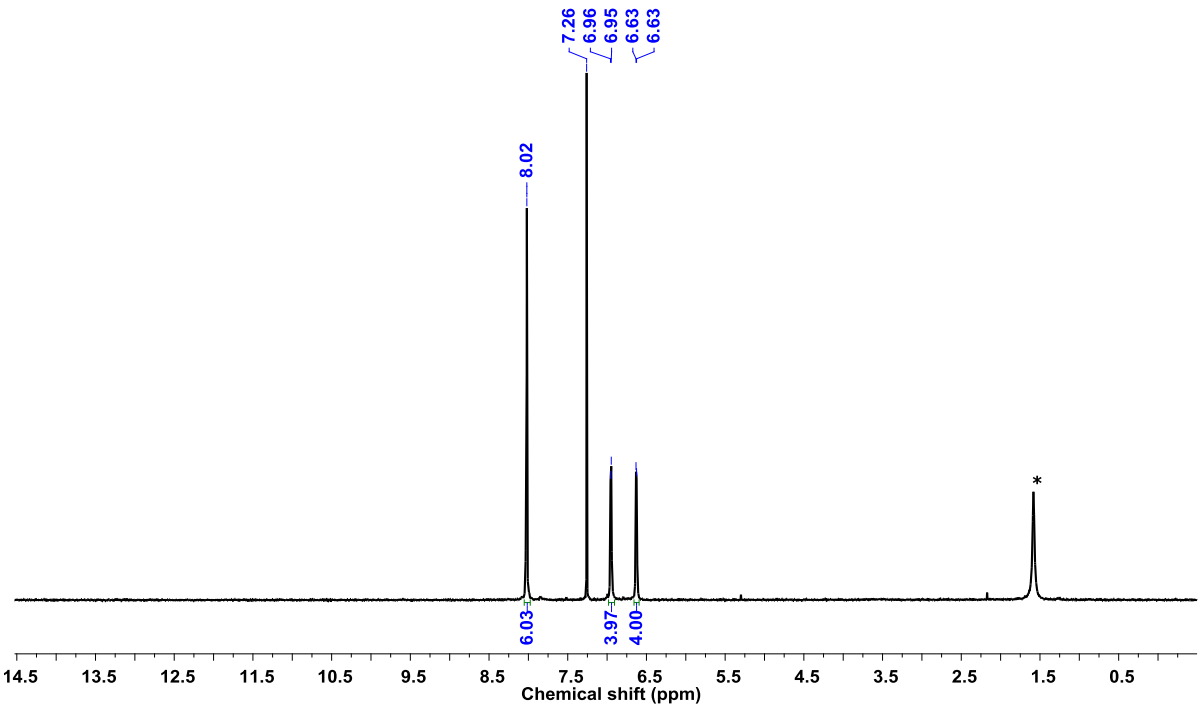

Figure II.9: ^{1}H-NMR spectrum of **II.28** in *Chloroform-d* at 295K

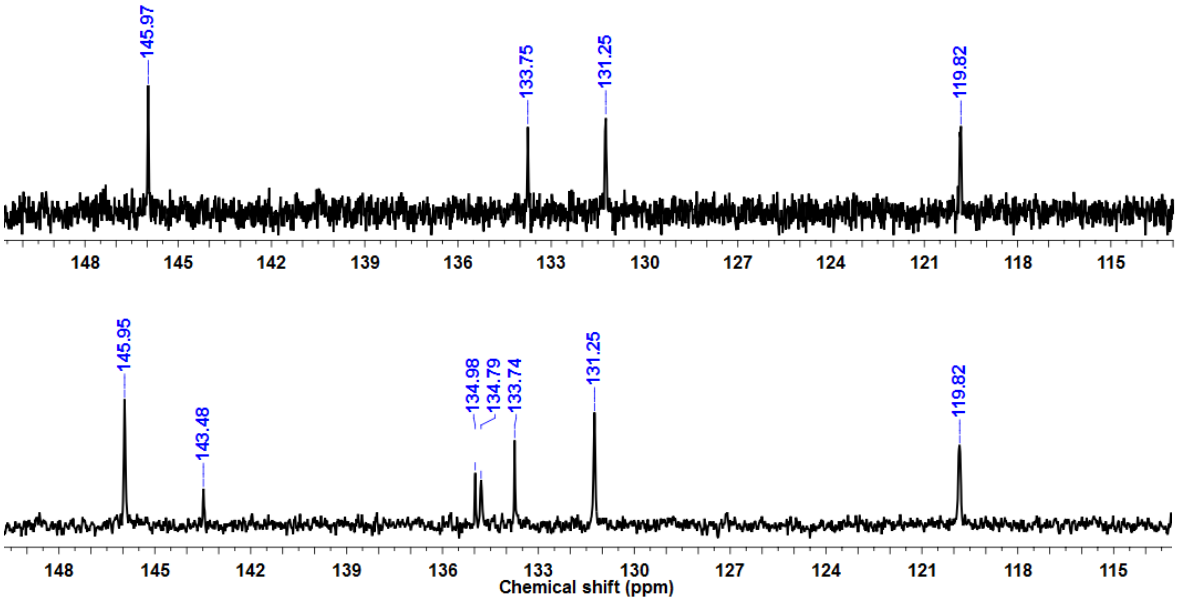

Figure II.10: (Top) DEPT-90 and (Bottom) ^{13}C-NMR spectrum of **II.28** in *Chloroform-d* at 295K

The 1,1'-biphenyl 3,3'5,5'-tetra BODIPY **II.33** exhibited BOIDPY moiety signals at 6.62, 6.98, 8.01 ppm, while the signals at 7.87, 8.03 ppm corresponded to biphenyl unit (Figure II.12). As expected five sets of CH signals at 119, 130, 131, 132, 145 were observed in DEPT-90 spectrum to further confirm its formation (Figure II.13).

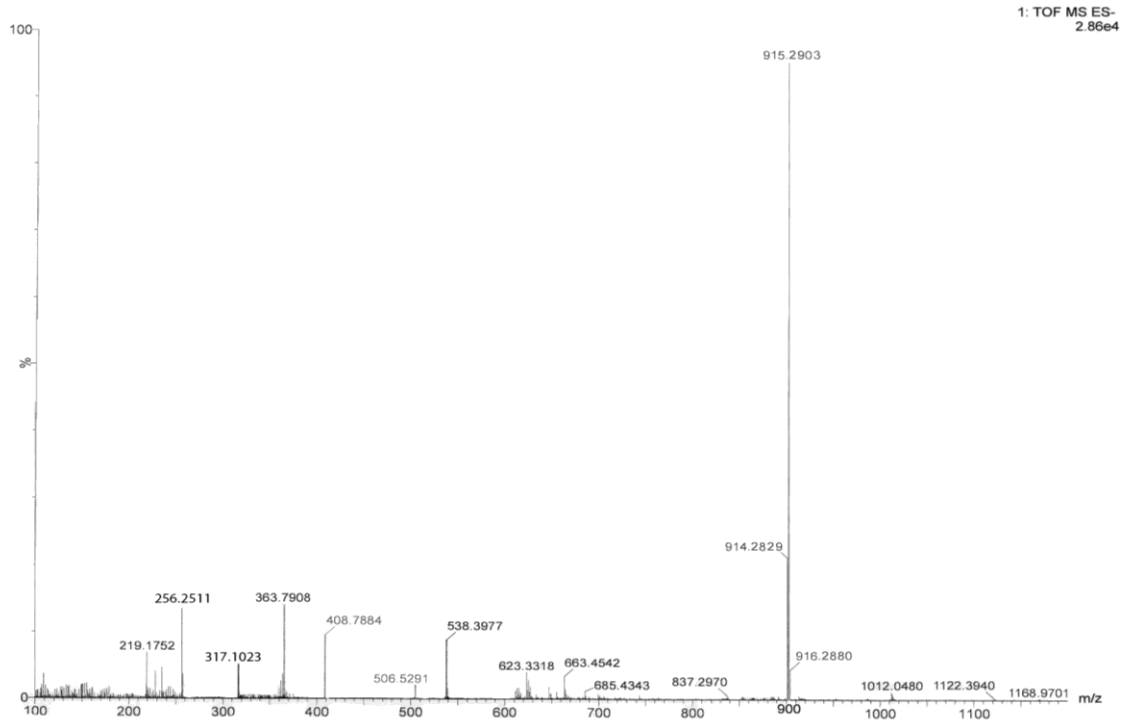

Figure II.11: HR-ESI-TOF mass spectrum of **II.33**

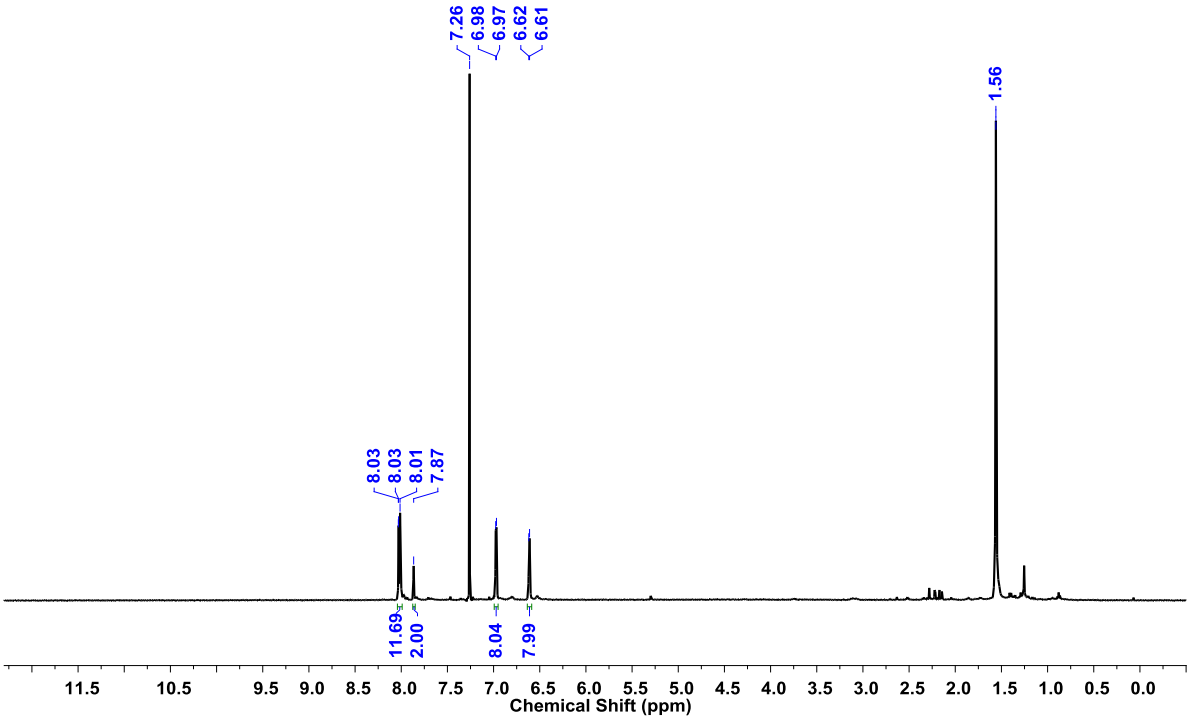

Figure II.12: ^{1}H-NMR spectrum of **II.33** in *Chloroform-d* at 295K

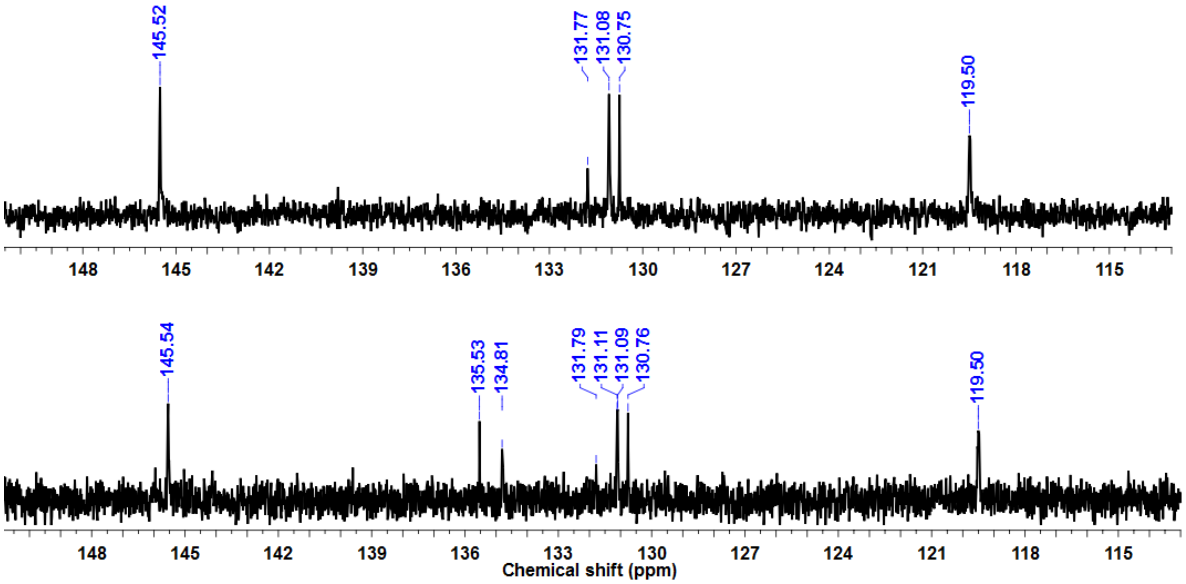

Figure II.13: (Top) DEPT-90 and (Bottom) ^{13}C-NMR spectrum of **II.33** in *Chloroform-d* at 295K

II.5: Single Crystal X-ray Diffraction Analysis:

Good quality of single crystals for X-ray diffraction analysis was grown by slow diffusion evaporation of dichloromethane solution of BODIPYs into n-hexane. The molecular structure of 1,3-bis BODIPY benzene **II.24** clearly indicated the connection between two BODIPY moieties at 1,3-position of benzene (Figure II.14a). The BODIPY moieties were found to make an angle of 88º (orthogonal) with each other and 52º to the benzene unit and hence molecule is in a locked conformation (Figure II.14b). Close observation confirmed the presence of strong intermolecular hydrogen bonding between the donor –CH of aromatic unit (pyrrole or benzene) and acceptor -BF of boron difluoride unit. The measured bond length and bond angle for β-pyrrolic C-H---F-B hydrogen bond is 2.3390(8)Å and 162º (Figure II.14c) and for benzene C-H---F-B hydrogen bond is 2.6926(12)Å and 142º (Figure II.14d) respectively.

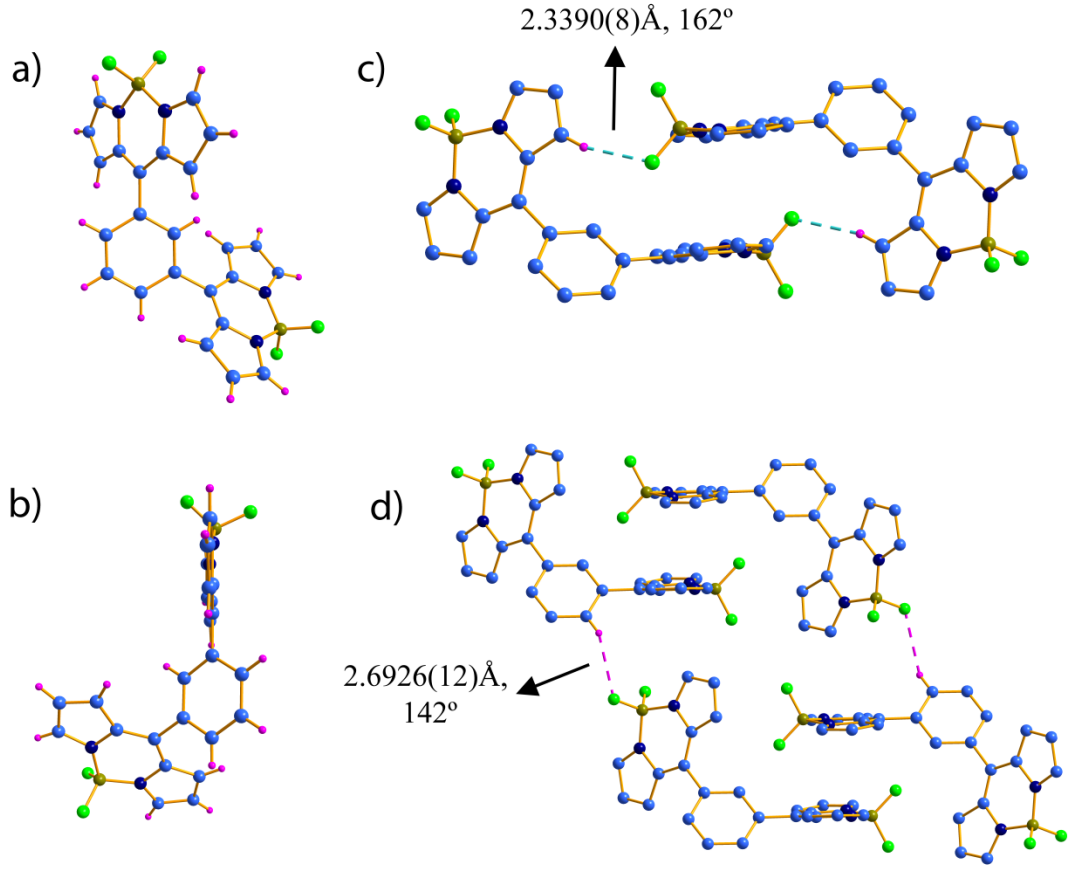

Figure II.14: Molecular Structures of 1,3-Bis BODIPY Benzene **II.24** a) View 1, b) View 2, c) hydrogen bonded dimer, d) another hydrogen bonded dimer.

In the molecular structure of 1,4-bis BODIPY benzene **II.26**, the two BODIPY moieties are co-planar at 1,4-postion of benzene (Figure II.15a) and make an angle of 53º with the benzene unit (Figure II.15b). Similar to 1,3-bis BODIPY **II.24**, 1,4-bis BODIPY **II.26** also exhibited two different types of strong intermolecular hydrogen bonds. The first has bond length and bond angle 2.4515(10)Å and 175º between one β-pyrrolic doner –CH and acceptor –BF of boron difuoride unit and second shows bond length and bond angle 2.4275(8)Å and 161º between another β-pyrrolic doner –CH and acceptor –BF of boron difluoride unit respectively (Figure II.15c). These two intermolecular hydrogen bonds help to form supramolecular architecture shown in following figure II.5d.

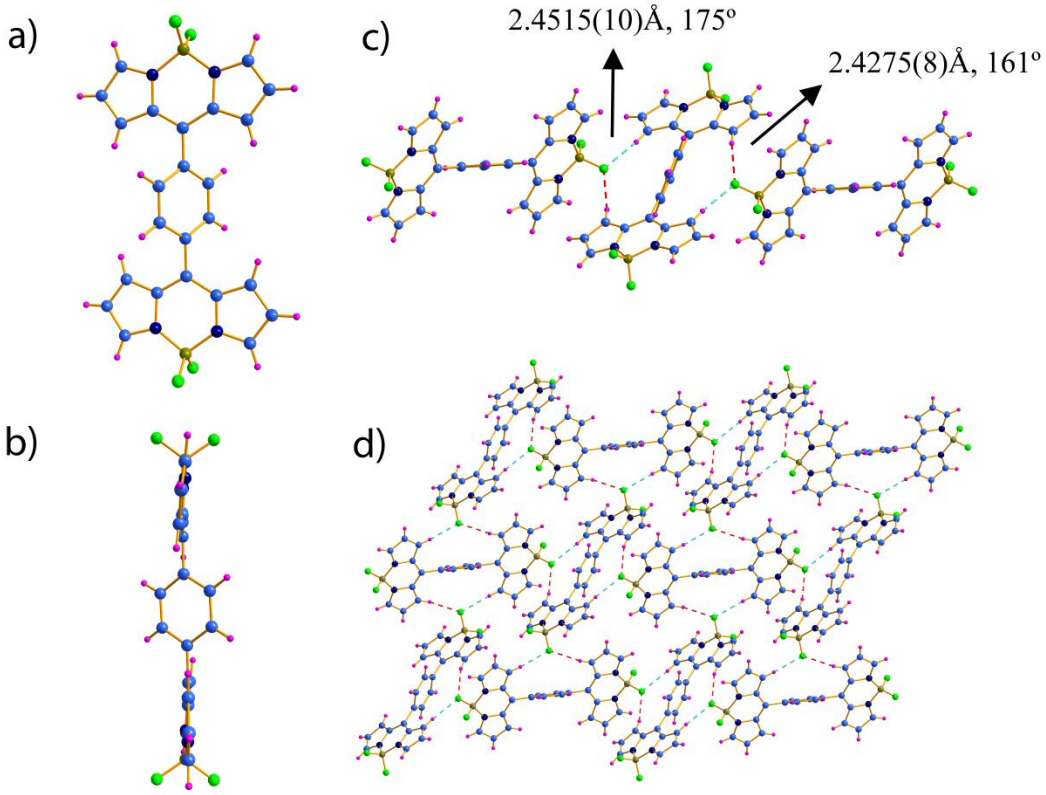

Figure II.15: Molecular Structures of 1,4-Bis BODIPY Benzene **II.26** a) View 1, b) View 2, c) hydrogen bonded network, d) packing diagram.

Furthermore, molecular structure of 1,3,5-tris BODIPY benzene **II.28** also confirmed the location of three BODIPY moieties at 1,3,5-positions of benzene. The angle made by the three BODIPY moieties with the benzene plane is found to be 46º (Figure II.16a). This BODIPY also exhibited strong intermolecular hydrogen bonding between two BODIPY molecules. The two hydrogen bond parameters were found to have (a) 2.3127(27)Å, 163º and (b) 2.7917(21)Å, 120º bond length and bond angle

respectively leading to the formation of a hexameric structure (Figure II.16b). The third strong hydrogen bond (c) 2.4320(19)Å, 158.271(237)º was found to connect the six BODIPY molecules to each other and forms another hexameric structure (Figure II.16c). Interestingly it has been observed that these two hexameric structures are then interconnected to each other by two more different types of hydrogen bonds (d) 2.761(2)Å, 115º (Figure II.16d) (e) 2.7676(18)Å, 119º (Figure II.16e) and forms hydrogen bonded organic framework (HOF) which has the 9.52Å pore diameter (Figure II.16f).

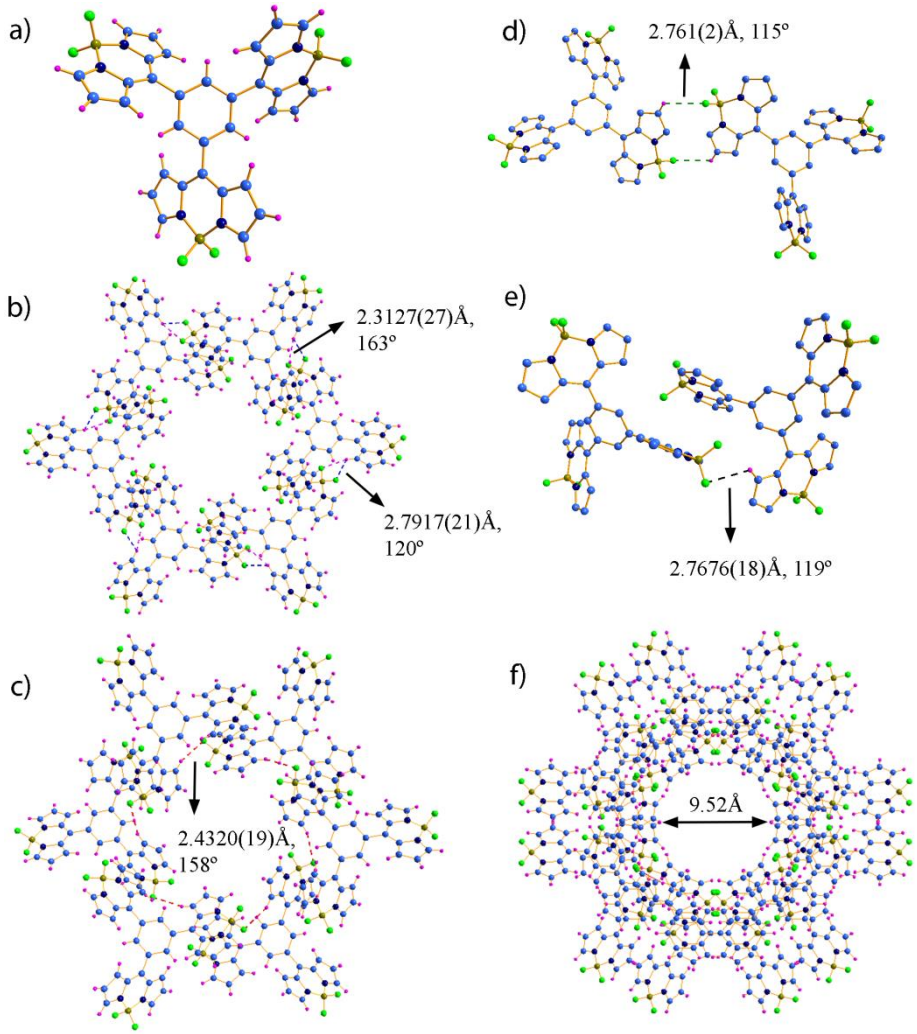

Figure II.16: Molecular Structures of 1,3,5-Tris BODIPY Benzene **II.28** a) single molecule structure, b) hexameric hydrogen bonded network, c) another hexameric hydrogen bonded hetwork , d) hydrogen bonded dimer, e) another hydrogen bonded dimer f) packing diagram indicate the formation of hydrogen bonded organic framework (HOF).

The molecular structure obtained for 1,1'-biphenyl 3,3'5,5'-tetra BODIPY **II.33** again confirms the presence of four BODIPY moiety at the 3,3',5,5'-position on the biphenyl unit (Figure II.17a). Surprisingly, the molecular structure displayed planar geometry of biphenyl unit indicating the effective delocalization of π-electron between two benzene rings. The BODIPY moiety makes an angle of 49º with the plane of biphenyl unit. The strong intermolecular hydrogen bond (a) 2.3540(39)Å, 163º connect the two molecules leading to the dimeric structure (Figure II.17b). The other two intermolecular hydrogen bonds (b) 2.3038(38)Å, 143º and (c) 2.7898(51)Å, 136º also facilitate the formation of another dimer (Figure II.17c). The two strong intermolecular hydrogen bonds (d) 2.5987(47)Å, 172º and (e) 2.6784(48)Å, 178º link the four molecules of BODIPY with each other to provide tetrameric structure (Figure II.17d).

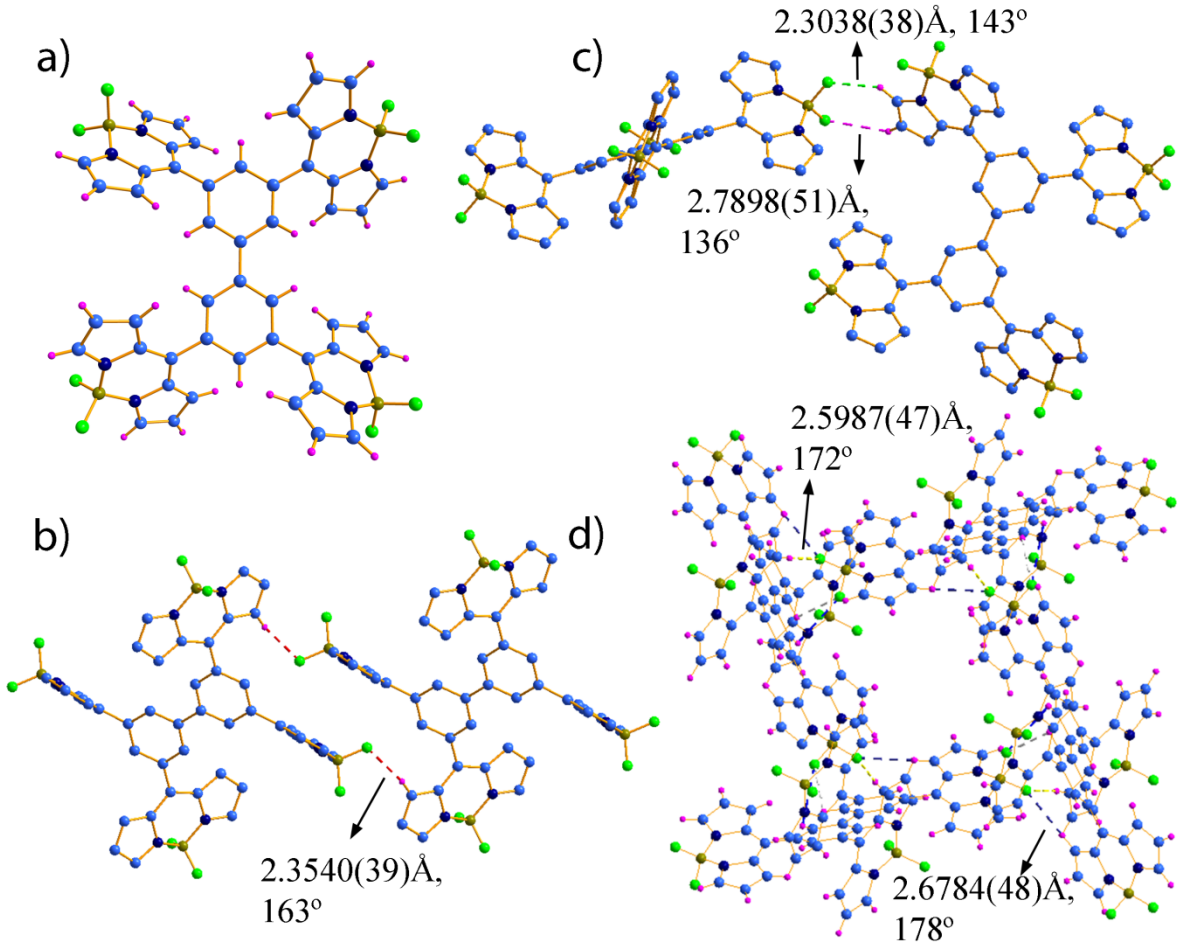

Figure II.17: Molecular Structures of 1,1'-biphenyl 3,3'5,5'-tetra BODIPY **II.33** a) single molecule structure, b) hydrogen bonded dimer, c) another hydrogen bonded dimer, d) tetrameric hydrogen bonded network.

All the above solid state studies highlight importance of these BODIPYs demonstrating different types of strong intermolecular hydrogen bonds for supramolecular chemistry.

II.6: Photophysical Properties:

The UV/Vis absorption spectra for mono, bis, tris and tetra BODIPY are shown in Figure II.18 and their optical properties are summarized in Table 1. The intense absorption maxima observed at 502, 505, 505 and 502 nm in dichloromethane corresponds to mono BODIPY dyes, **II.24**, **II.26**, **II.28** and **II.33** respectively. The fluorescence measurements performed in same solvent exhibited the emission at 523, 532, 532 and 528 nm and the calculated quantum yields are 2.6, 0.8, 1.7 and 2.7% with respect to Rhodamine 6G for **II.24**, **II.26**, **II.28** and **II.33** respectively. BODIPY **II.24** displayed greater quantum yield than BODIPY **II.26** due to locked conformation as observed in solid state (Figure II.14b) which can decrease the free rotation of around BODIPY moiety and *meso*-phenyl group leading to decreased non-radiative decay. Our study indicates that absorption and emission wavelength were red shifted with respect to the mono BODIPY dye. Molar extinction coefficient also increased for our synthesized molecules as compared to the mono BODIPY dye.

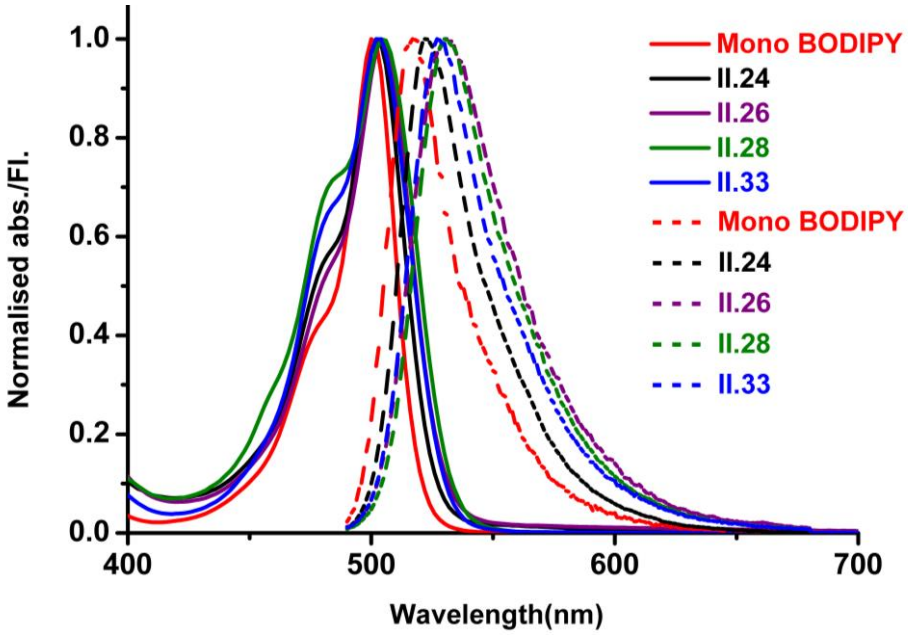

Figure II.18: UV-Visible absorption spectra (straight line) and fluorescence spectra (dashed line) of Mono BODIPY, **II.24**, **II.26**, **II.28** and **II.33** in dichloromethane.

Time dependent fluorescence decay measurements were carried out by the Time Correlated Single Photon Counting (TCSPC) technique using a 459 nm diode laser as excitation source (Table 1). The luminescence decay profiles were collected for these at their emission maxima, and their profiles are shown in Figure II.19. The τ_1 values decreased in the following trend for BODIPYs: **II 24** < **II 33** < **II 28** << **II 26**. The contribution from τ_2 for **II 33** is minor as compared to the τ_1 values. The first lifetime ($\tau_{1)}$ observed for the **II 24** and **II 33** are very much similar hence indicate nearly same quantum yield and molar extinction coefficient value. It is very clear from the decay plots that the **II 26** showed much faster decay compared to that of **II 24**, **II 28** and **II 33**.

Table 1. Optical properties of Mono BODIPY **II.24**, **II.26**, **II.28** and **II.33** in CH_2Cl_2.

BODIPY	λ_{abs} [nm]	λ_{em} [nm]	log ε [L mol^{-1} cm^{-1}])	Φ_F	τ_1 (ns)	τ_2 (ns)	χ^2
II.24	502	523	37620	0.026[a]	0.29	-	1.187[b]
II.26	505	532	50580	0.008[a]	0.03	-	1.182[b]
II.28	505	532	110160	0.017[a]	0.22	-	1.119[b]
II.33	502	528	39250	0.027[a]	0.26	2.27	0.902[b]

[a]Rhodamine 6G in ethanol was used as the reference (Φ_F = 0.95), [b]Luminescence decay lifetime was measured by using 459 nm LED as the excitation source.

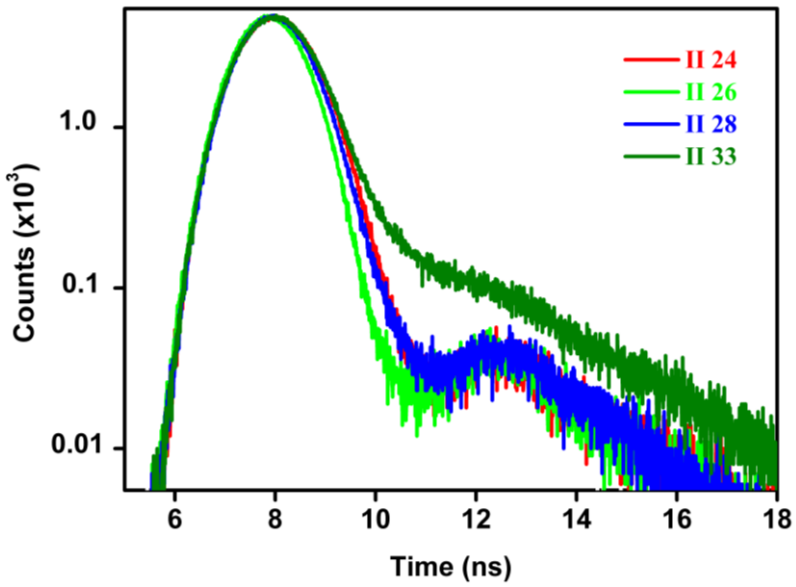

Figure II.19: TCSPC decay profile of BODIPYs **II.24**, **II.26**, **II.28** and **II.33** in the solid state

These observations indicate that with respect to mono BODIPY dye, there is an effect of increase in the number of BODIPY moiety from two to three and four on the biphenyl unit.

II.7: Conclusion:

This chapter describes the successful synthesis of 1,3-Bis **II.24**, 1,4-Bis **II.26**, 1,3,5-Tris **II.28** BODIPY benzene and 1,1'-biphenyl 3,3'5,5'-tetra **II.33** BODIPY and their structural characterization through SCXRD and other spectroscopic techniques. Emission measurements indicated the fluorescence quenching in 1,4-Bis BODIPY **II.26** due to free rotation between BODIPYs moiety and *meso*-phenyl ring. All these fluorescent compounds exhibited strong intermolecular hydrogen bonding between donors -CH of the aromatic part (pyrrole and benzene) and acceptor -BF of the boron difluoride part hence act as a sythons for supramolecular architecture. 1,3,5-Tris BODIPY **II.28** especially forms the hydrogen bonded organic framework (HOF) with the use of five different types strong intermolecular hydrogen bonding. The presence of BODIPY substitution on benzene and biphenyl unit at various positions affected their photophysical properties.

II.8: Experimental Section:

All reagents and solvents were of commercial reagent grade and used without further purification except where noted. Dry THF was obtained by refluxing and distillation over pressed Sodium metal whereas dry CH_2Cl_2 was obtained by refluxing and distillation over CaH2. Column chromatography was performed on silica gel (100-200) in glass columns. ^{1}H, ^{13}C, $^{19}F$and ^{11}B NMR spectra were recorded either on a JEOL 400 MHz or Bruker 500 MHz spectrometer and chemical shifts were reported as the delta scale in ppm relative to $CHCl_3$(δ = 7.26 ppm), $(CH_3)_2CO$ (δ = 2.05 ppm) or $(CH_3)_2SO$ (δ = 2.50 ppm) as internal reference for ^{1}H. High Resolution Mass spectra were obtained using WATERS G2 Synapt Mass Spectrometer. Electronic spectra were recorded on a Perkin-Elmer λ-900 ultraviolet−visible (UV−vis) spectrophotometer. Single crystals were grown in suitable organic solvent and single crystal X-ray diffraction were performed at 100K on BRUKER KAPPA APEX II CCD Duo diffractometer (operated at 1500 W power: 50 kV, 30 mA) using graphite-monochromated Mo Kα radiation (λ = 0.71073 Å).

Procedure for Synthesis of II.24

1,3-Bis-dipyrromethane **II.23** (500 mg, 1.3661 mmol, 1 equiv.) was dissolved in 25 ml dry tetrahydrofuran in 100 ml round bottom flask under N_2 inert atmosphere. DDQ (680 mg, 3 mmol, 2.2 equiv.) was dissolved separately in 25 ml dry tetrahydrofuran under N_2 inert atmosphere and added drop wise into reaction vessel containing dissolved **II.23** and stirred reaction mixture for one hour. Then reaction mixture was quenched with water, washed with water and extracted in dichlormethane. The organic phase was separated, dried over anhydrous sodium sulphate (Na_2SO_4) and the solvent was evaporated under vacuum. The residue obtained was dissolved in 20 ml dry dichlormethane under N_2 inert atmosphere in 25 ml round bottom flask. Triethyl amine (9.53 ml, 68.3060 mmol, 50 equiv.) added, after half an hour borontrifluoride etherate (8.43 ml, 68.3060 mmol, 50 equiv.) was added and reaction mixture was stirred overnight. The reaction mixture was diluted with dichloromethane and washed three times with water. The organic phase was separated and dried over anhydrous Na_2SO_4. The solvent was removed on rota-evaporator, the residue obtained was purified by silica gel (100-200 mesh) column chromatography gives **II.24**. Yield: 200 mg (32%); brown color solid; Melting Point = 250ºC. **^{1}H-NMR** (*Chloroform-d*,

400MHz, 295K): δ = 6.59(d, J = 4.0 Hz, 4H), 6.95(d, J = 4.0 Hz, 4H), 7.71-7.82(m, 4H), 7.98(s, 4H); **^{13}C-NMR**: δ = 119.32, 128.99, 131.53, 132.06, 132.64, 134.44, 135.01, 145.19, 145.74 ppm; **^{19}F-NMR**: δ = -144.86 (q, 4F); **^{11}B-NMR**: δ = 0.29 (t, 2B); **UV-Vis** (CH_2Cl_2): $\lambda_{max}(\varepsilon)Lmol^{-1}cm^{-1}$ = 502 nm (37620); **HRMS**: *m/z* calcd. for $(C_{24}H_{16}B_2F_4N_4+H)^+$= 459.1575, Observed = 459.1580; **Crystal data**: $C_{24}H_{16}B_2F_4N_4$(Mr = 458.03), monoclinic, space group C2/c (No.15), a = 19.943(3), b = 10.3684(12), c = 13.142(2)Å, α = 90.00, β = 130.765(5), γ = 90.00°, V = 2058.1(5)Å^3, Z = 4, ρcalcd = 1.478 mg/m^3, T = 150K, Rint (all data) = 0.0348, R1(all data) = 0.0380, RW (all data) = 0.1493, GOF = 1.361.

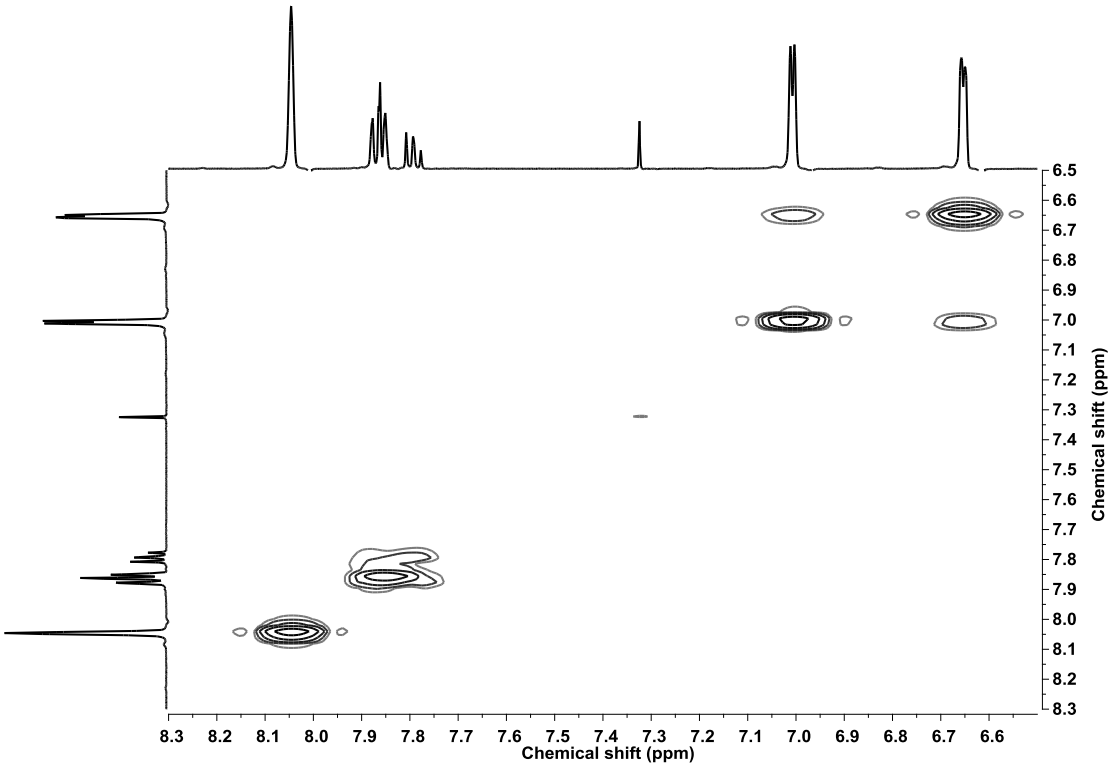

Figure II.19: ^{1}H-^{1}H COSY spectrum of **II.24** in *Chloroform-d*

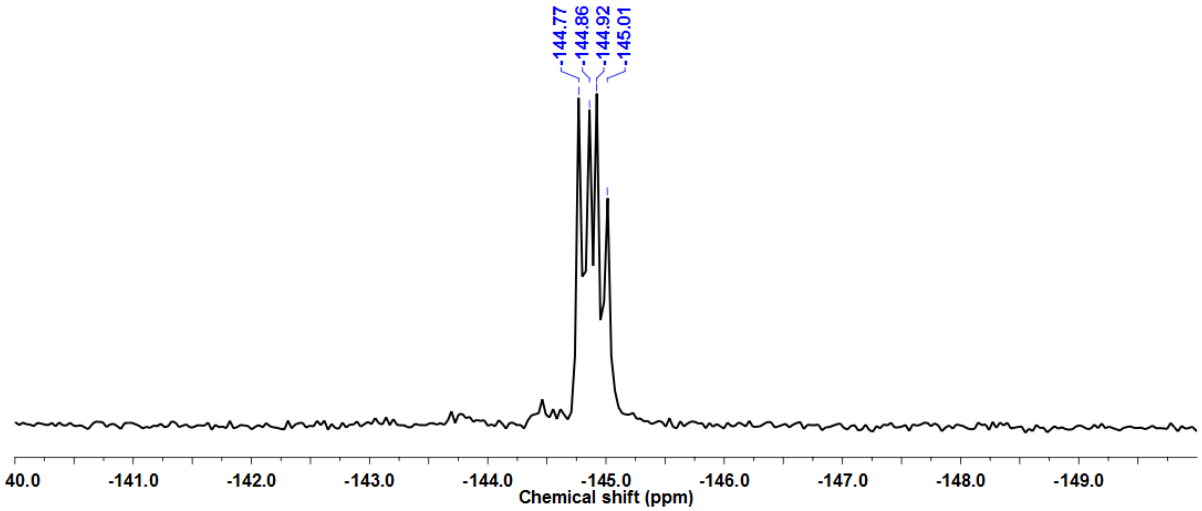

Figure II.20: ^{19}F-NMR spectrum of **II.24** in *Chloroform-d* at 295K

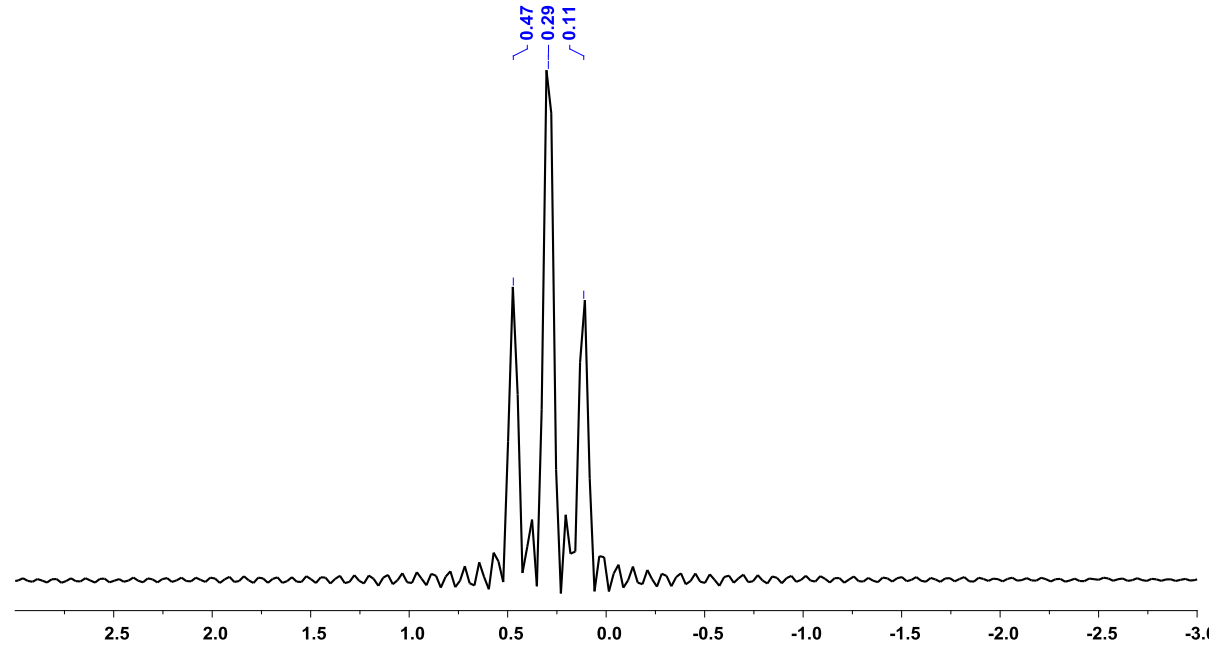

Figure II.21: ^{11}B-NMR spectrum of **II.24** in *Chloroform-d* at 295K

Procedure for Synthesis of II.26

1,4-Bis-dipyrromethane **II.25** (500 mg, 1.3661 mmol, 1 equiv.), DDQ (680 mg, 3 mmol, 2.2 equiv.), Triethyl amine (9.53 ml, 68.3060 mmol, 50 equiv.) and borontrifluoride etherate (8.43 ml, 68.3060 mmol, 50 equiv.) were reacted as per

procedure mentioned for synthesis of **II.24**. Yield: 150 mg (24%); brown color solid; Melting Point = >300ºC. **^{1}H-NMR** (*Chloroform-d*, 400MHz, 295K): δ = 6.61(d, J = 4.0 Hz, 4H), 7.00(d, J = 4.0 Hz, 4H), 7.76(s, 4H), 8.01(s, 4H); **^{13}C-NMR**: δ = 119.27, 130.73, 131.71, 134.99, 136.37, 145.18, 145.66 ppm; **^{19}F-NMR**: δ = -144.83 (q, 4F); **^{11}B-NMR**: δ = 0.32 (t, 2B); **UV-Vis** (CH_2Cl_2): $\lambda_{max}(\varepsilon)Lmol^{-1}cm^{-1}$ = 505 nm (50580); **HRMS**: *m/z* calcd. for $(C_{24}H_{16}B_2F_4N_4+H)^+$= 459.1575, Observed = 459.1586; **Crystal data**: $C_{24}H_{16}B_2F_4N_4$(Mr = 458.03), monoclinic, space group P 21/n (No.14), a = 6.0762(17), b = 11.767(3), c = 14.512(4)Å, α = 90.00, β = 95.829(4), γ = 90.00°, V = 1032.2(5)Å^3, Z = 2, ρcalcd = 1.474 mg/m^3, T = 150K, Rint (all data) = 0.0400, R1(all data) = 0.0515, RW (all data) = 0.1437, GOF = 1.075.

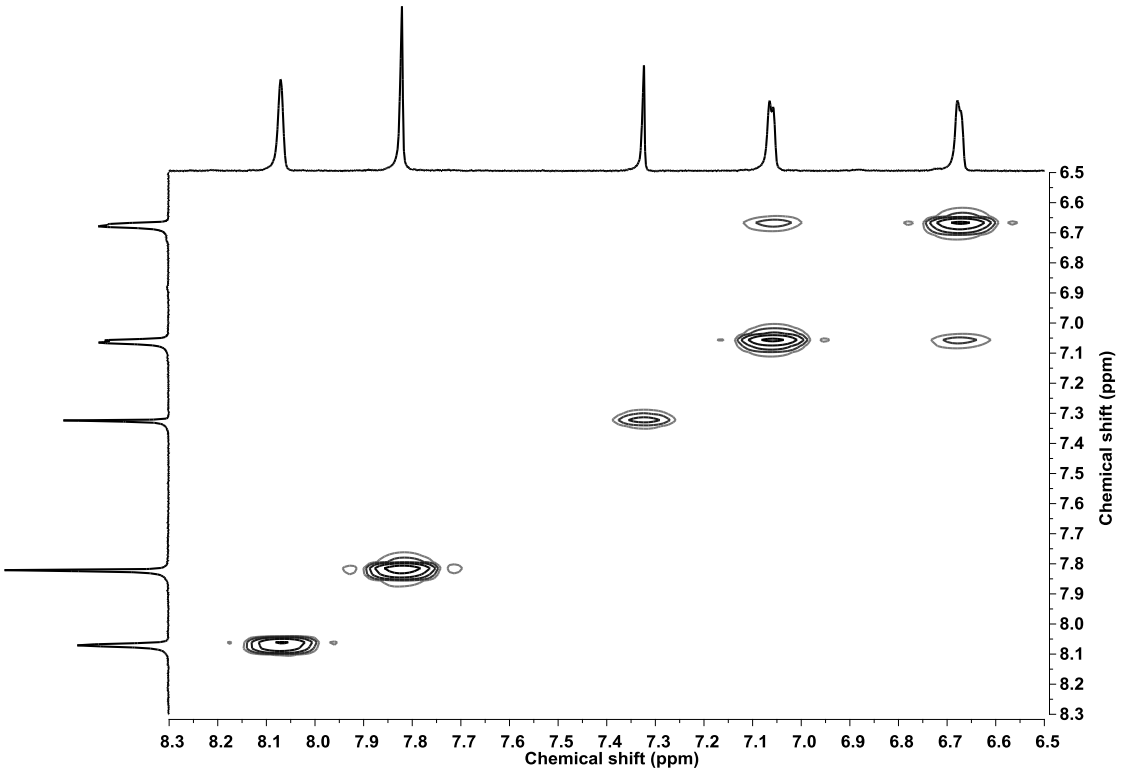

Figure II.22: ^{1}H-^{1}H COSY spectrum of **II.26** in *Chloroform-d* at 295K

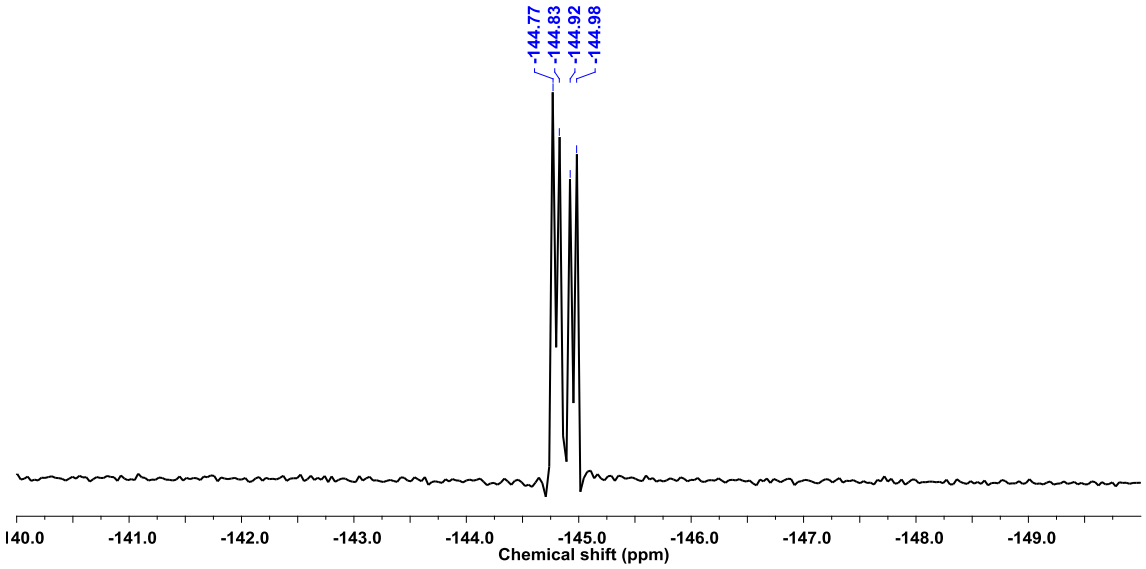

Figure II.23: ^{19}F-NMR spectrum of **II.26** in *Chloroform-d* at 295K

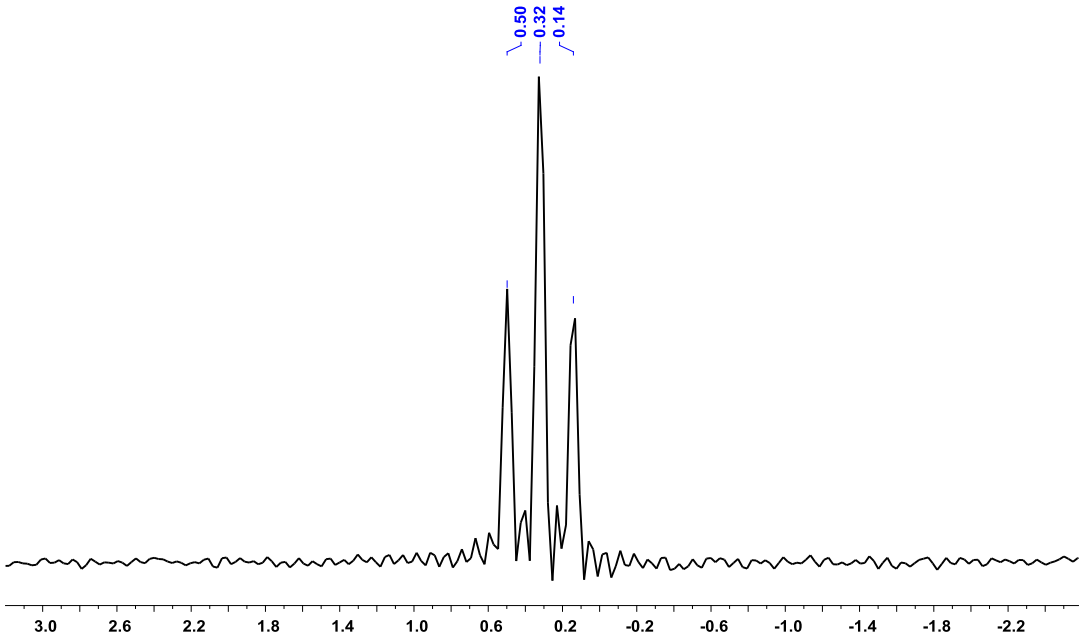

Figure II.24: ^{11}B-NMR spectrum of **II.26** in *Chloroform-d* at 295K

Procedure for Synthesis of II.27

1,3,5-Benzene tricarboxaldehyde was synthesised as per literate procedure. 1,3,5-Benzene tricarboxaldehyde (0.500 gm, 3.0864 mmol, 1 equiv.) was dissolved with pyrrole (32 ml, 462.9630 mmol, 150 equiv.) in 100 ml round bottom flask under inert N_2 atmosphere and trifluoroacetic acid (0.071 ml, 0.9260 mmol, 0.3 equiv.) added. After 30 minute, reaction was quanched by adding 50 ml dichloromethane and 50 ml 0.1 N NaOH. The organic layer was extracted from aqueous layer with dichloromethane, dried over anhydrous Na_2SO_4 and solvent were evaporated in vacuo. The residue was chromatographed to get pure compound **II.27**. Yield: 0.51 gm (32%); faint greenish-yellow color powder; Melting Point = Decomposes above 156ºC. **^{1}H-NMR** (*Dimethyl Sulphoxide-d_6*, 400MHz, 295K): δ = 5.19(s, 3H), 5.57(m, 6H), 5.85(m, 6H), 6.55(m, 6H), 7.00(s, 3H), 10.43(bs, 6H, exchangeable with D_2O); **^{13}C-NMR**: δ = 44.25, 106.45, 107.31, 117.01, 126.73, 133.81, 143.27 ppm; **HRMS**: *m/z* calcd for $(C_{33}H_{30}N_6+H)^+$=511.2610; observed= 511.2606.

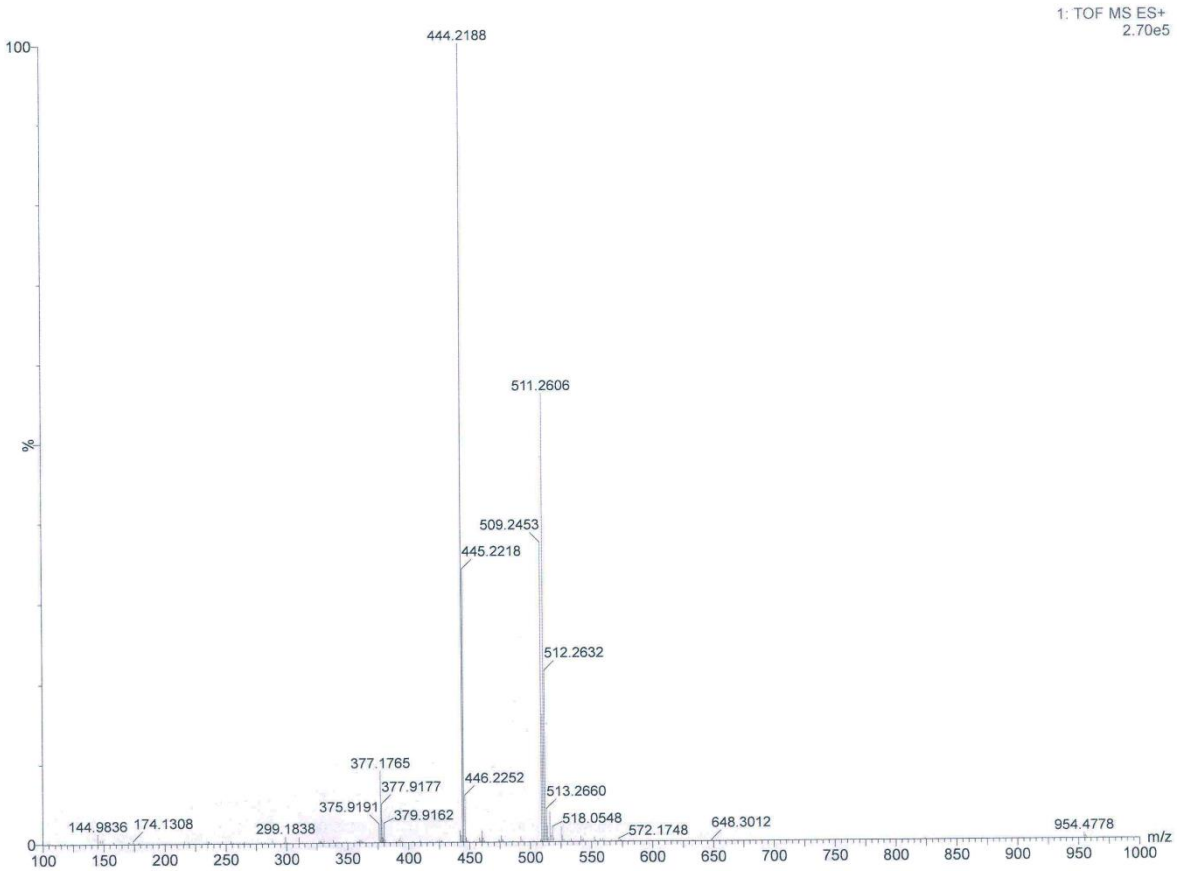

Figure II.25: HR-ESI-TOF mass spectrum of **II.27**

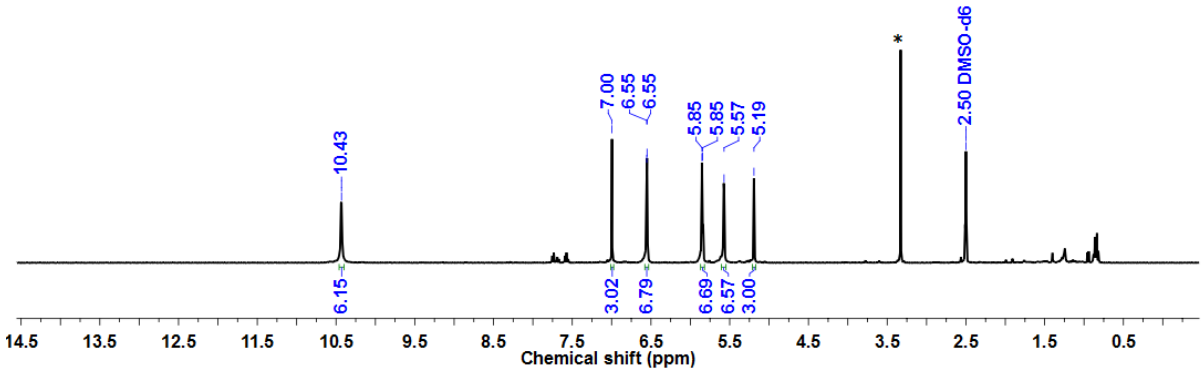

Figure II.26: ^{1}H-NMR spectrum of **II.27** in *Dimethyl Sulphoxide-d_6* at 295K

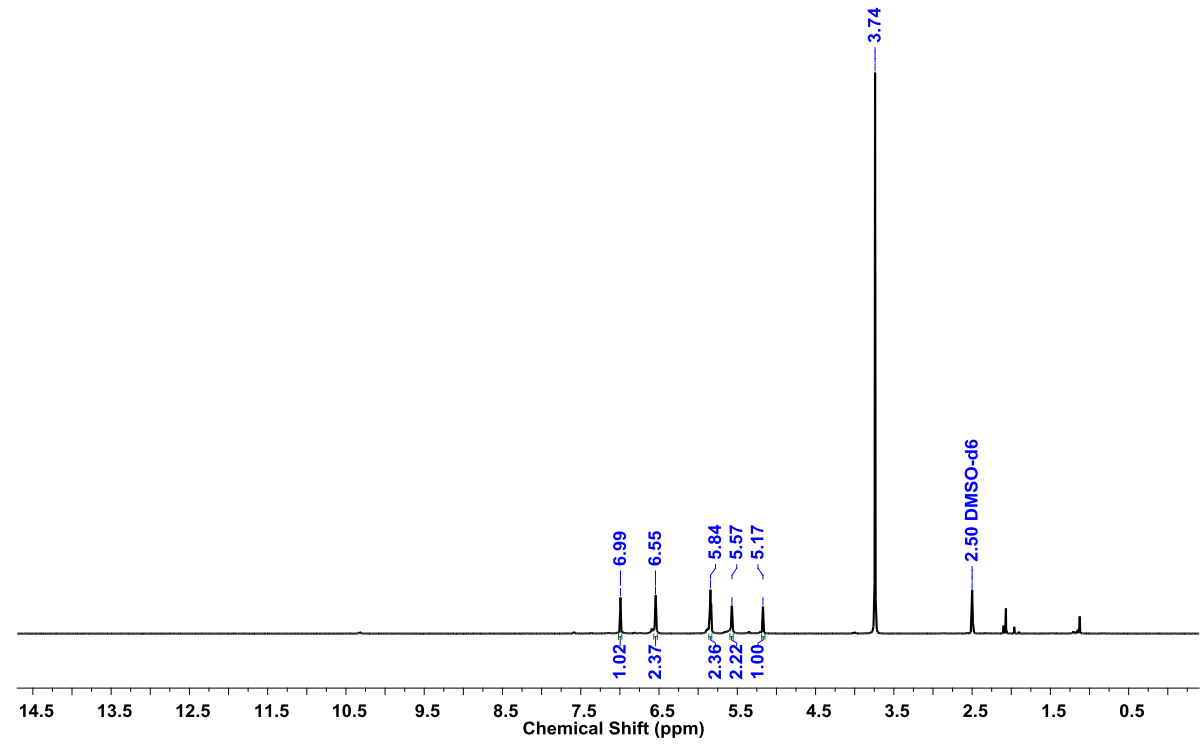

Figure II.27: ^{1}H-NMR spectrum of **II.27** after D_2O exchange in *Dimethyl Sulphoxide-d_6*.

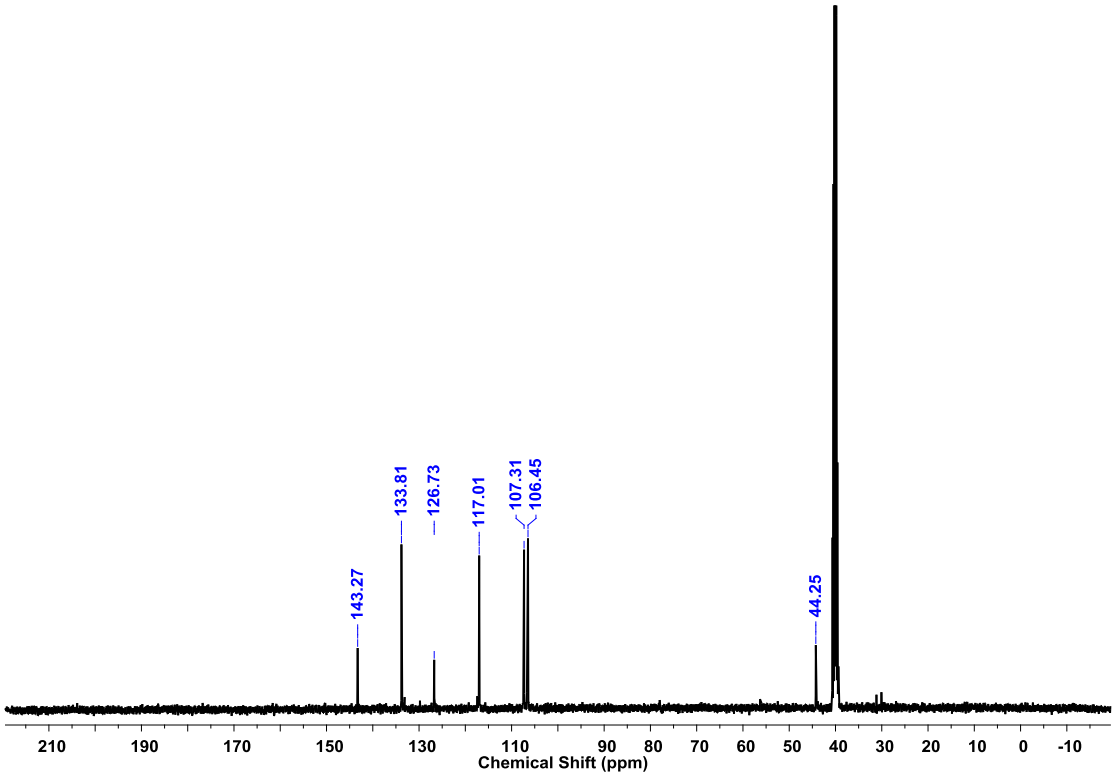

Figure II.28: ^{13}C-NMR spectrum of **II.27** in *Dimethyl Sulphoxide-d_6* at 295K

Procedure for Synthesis of II.28

1,3,5-Tris-dipyrromethane **II.27** (510 mg, 1 mmol, 1 equiv.), DDQ (749 mg, 1.10 mmol, 3.3 equiv.), Triethyl amine (10.47 ml, 75 mmol, 75 equiv.) and borontrifluoride etherate (9.25 ml, 75 mmol, 75 equiv.) were reacted as per our regular procedure for synthesis of BODIPY **II.24**. Yield: 102 mg (16%); brown color solid; Melting Point = >300ºC. **^{1}H-NMR** (*Chloroform-d*, 400MHz, 295K): δ = 6.63(d, J = 4.0 Hz, 6H), 6.96(d, J = 4.0 Hz, 6H), 8.02(s, 9H); **^{13}C-NMR**: δ = 119.82, 131.25, 133.74, 134.79, 134.98, 143.48, 145.95 ppm; **^{19}F-NMR**: δ = -144.77 (q, 6F); **^{11}B-NMR**: δ = 0.27 (t, 3B); **UV-Vis** (CH_2Cl_2): $\lambda_{max}(\varepsilon)Lmol^{-1}cm^{-1}$ = 505 nm (110160); **HRMS**: *m/z* calcd. for $(C_{33}H_{21}B_3F_6N_6+H)^+$= 649.2089, Observed = 649.2103; **Crystal data**: $C_{33}H_{21}B_3F_6N_6$(Mr = 647.99), trigonal, space group R -3c (No.167), a = 31.202(3), b = 31.202(3), c = 20.028(2)Å, α = 90.00, β = 90.00, γ = 120.00°, V = 16886(3)Å^3, Z = 18, ρcalcd = 1.147 mg/m^3, T = 150K, Rint(all data) = 0.0652, R1(all data) = 0.1442, RW (all data) = 0.1550, GOF = 1.040.

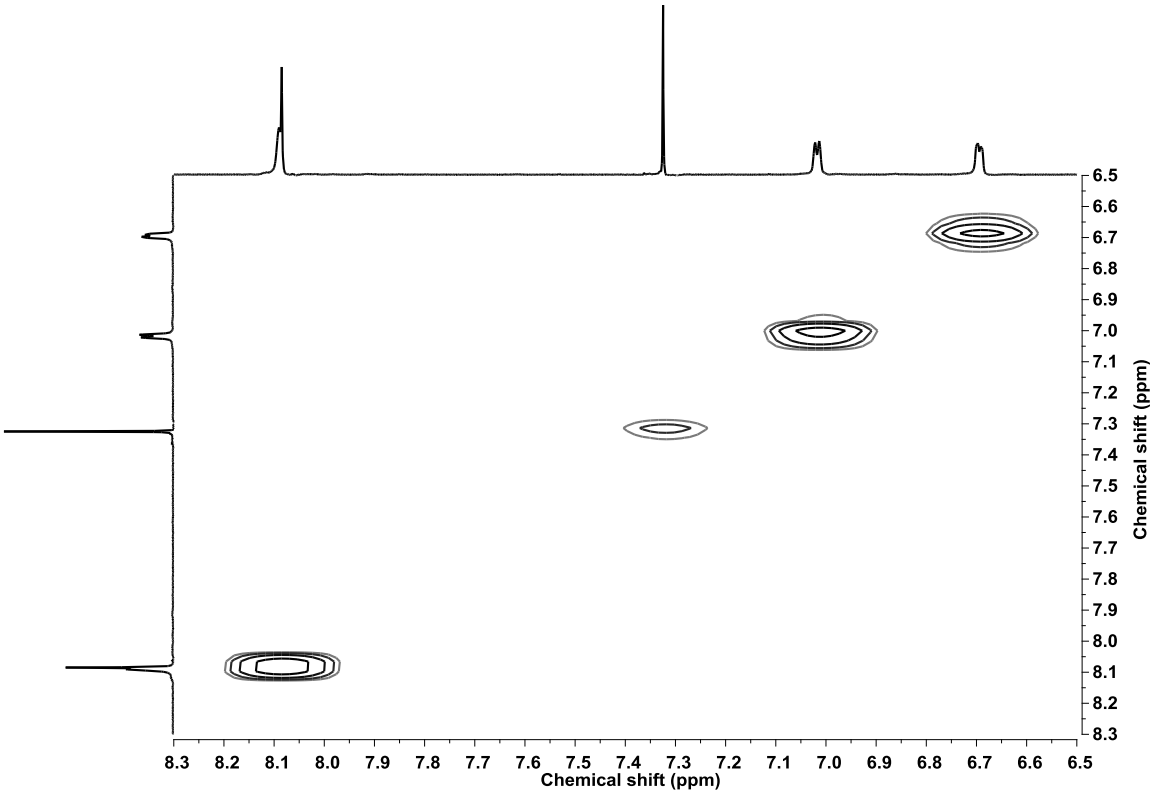

Figure II.29: ^{1}H-^{1}H COSY spectrum of **II.28** in *Chloroform-d* at 295K

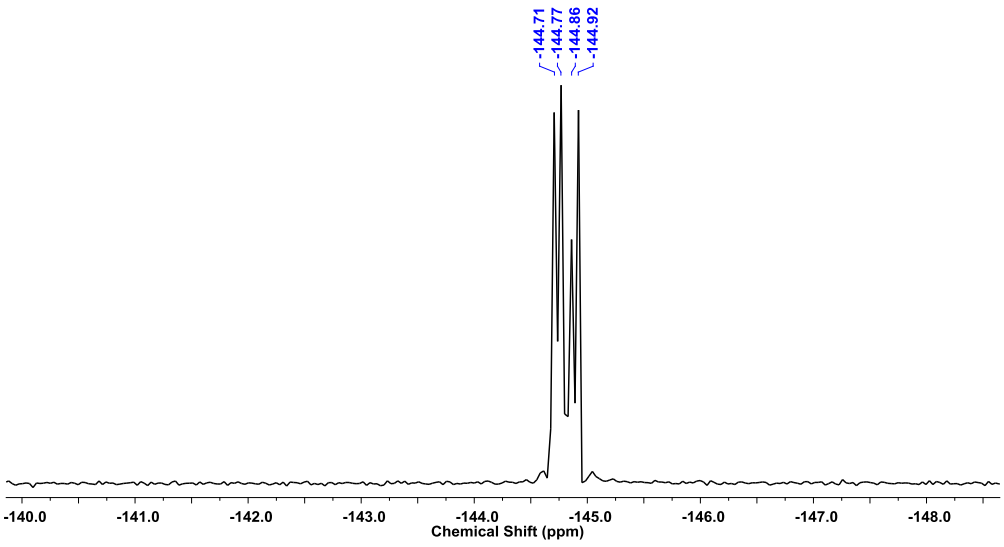

Figure II.30: ^{19}F-NMR spectrum of **II.28** in *Chloroform-d* at 295K

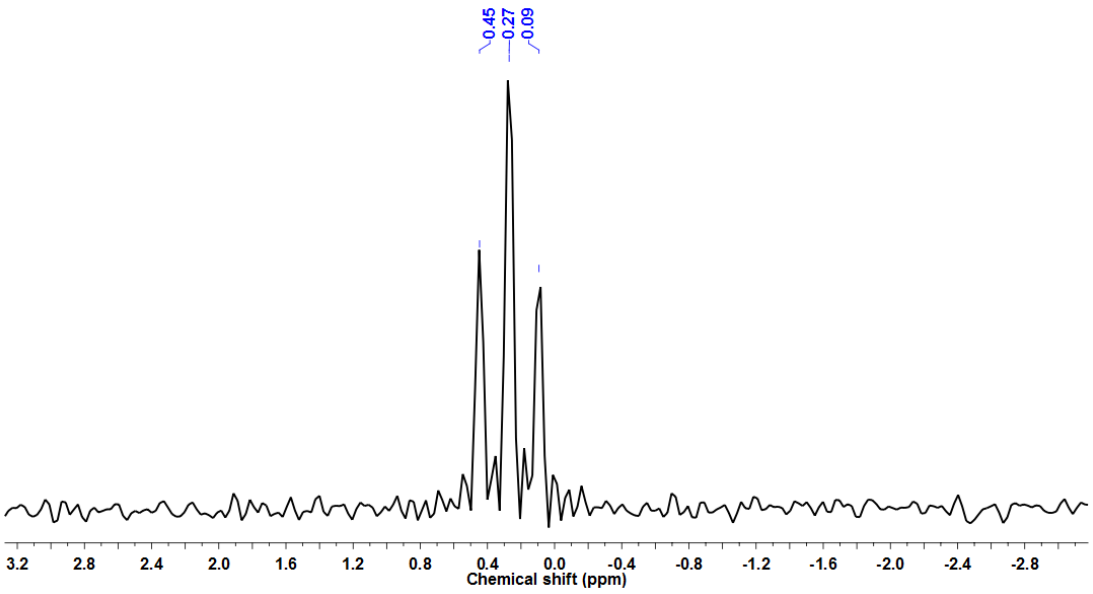

Figure II.31: ^{11}B-NMR spectrum of **II.28** in *Chloroform-d* at 295K

Procedure for Synthesis of II.29

5-Bromoisophthaldehyde was prepared as per literature procedure. 5-Bromoisophthaldehyde (5 gm, 24 mmol, 1 equiv.), ethylene glycol (4 ml, 71 mmol, 3 equiv.) and p-Toluene Sulfonic Acid (40 mg) were refluxed with 50 ml dry toluene in Dean Stark apparatus to get protected 5-bromoisophthaldehyde, **II.29**. Yield: 5.60 gm (77%); colorless oil. **^{1}H-NMR** (*Chloroform-d*, 400MHz, 295K): δ = 4.10(m, 8H), 5.80(s, 2H), 7.50(s, 1H), 7.62(d, 2H); **^{13}C-NMR**: δ = 65, 102, 122, 123, 130, 140 ppm; **HRMS**: *m/z* calcd. for $(C_{12}H_{13}BrO_4+H)^+$= 301.0075, Observed = 301.0076.

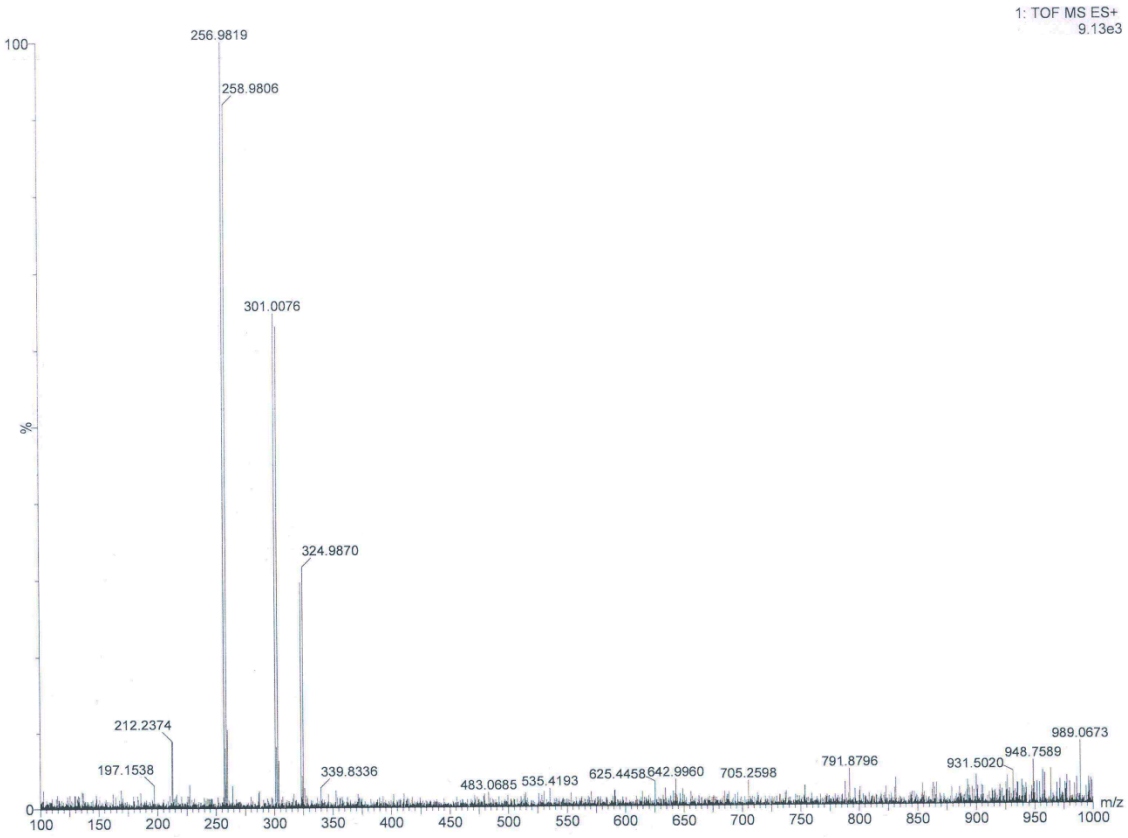

Figure II.32: HR-ESI-TOF mass spectrum of **II.29**

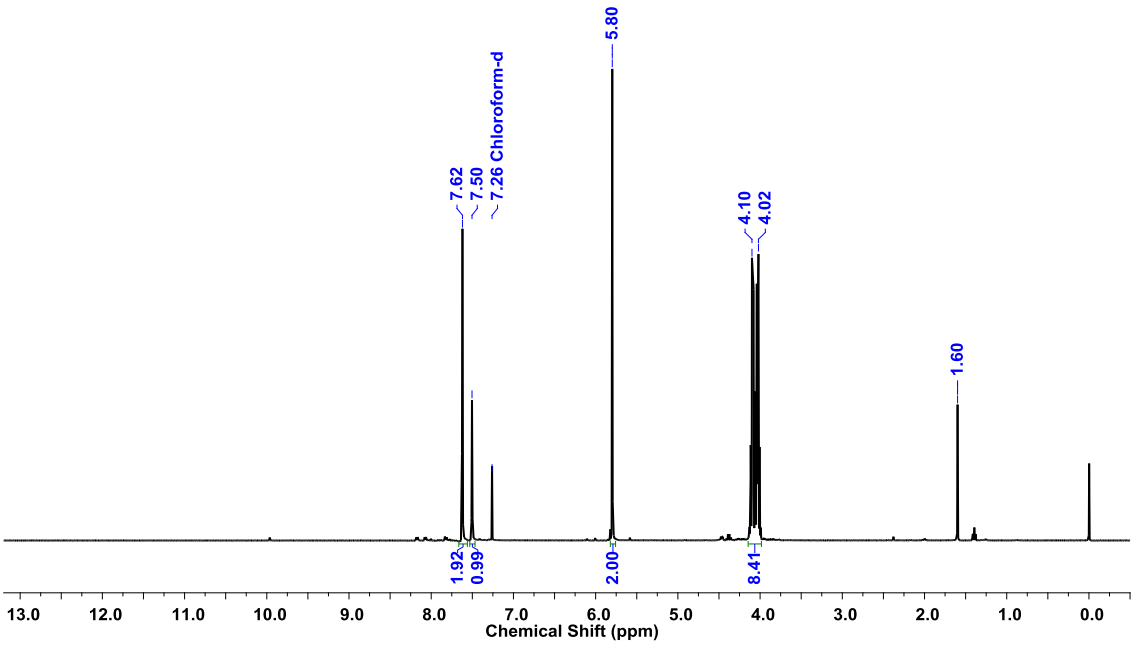

Figure II.33: ^{1}H-NMR spectrum of **II.29** in *Chloroform-d* at 295K

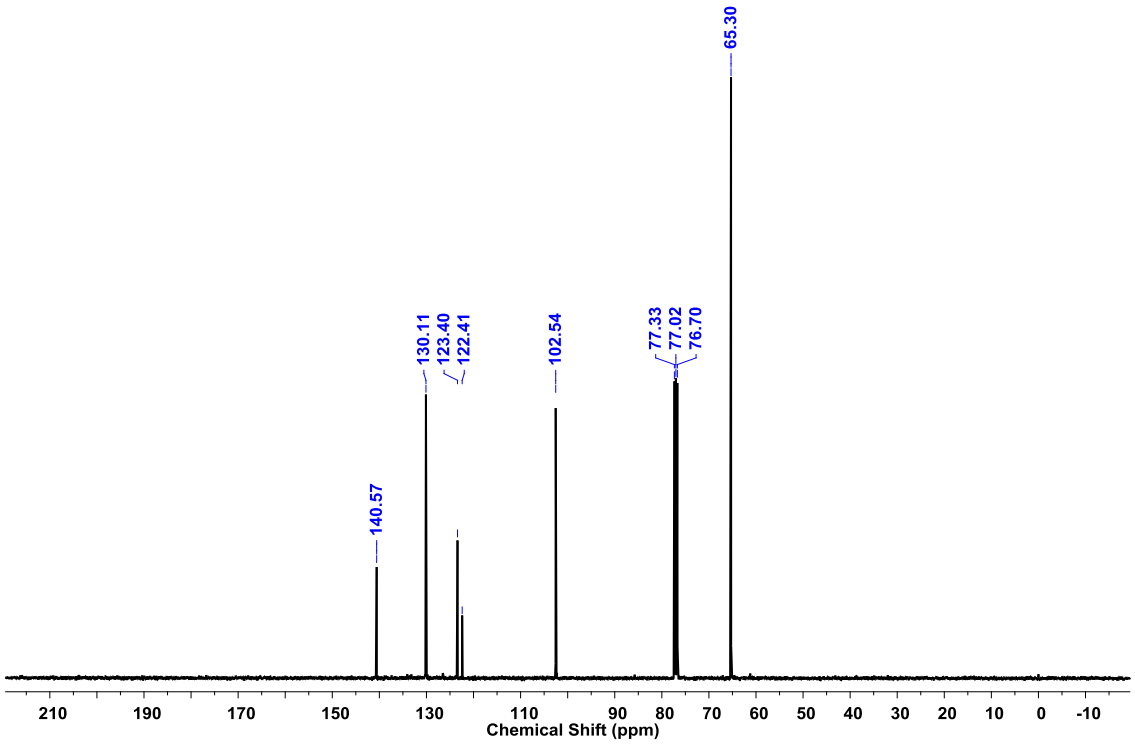

Figure II.34: ^{13}C-NMR spectrum of **II.29** in *Chloroform-d* at 295K

Procedure for Synthesis of II.30

Protected 5-bromoisophthaldehyde **II.29** (500 mg, 1.6667 mmol, 1 equiv.) was dissolved in 10 ml dry THF in 100 ml round bottom flask under N_2 inert atmosphere and reaction mixture temperature brought to -78ºC. After stirring reaction mixture for 5 minute, 1.2 ml 1.6 M n-BuLi in n-hexane was added. Thereafter 30 minute, 90 mg $NiCl_2$(dppe) dissolved separatly in 5 ml dry THF was added to the reaction mixture and finally protected 5-bromoisophthaldehyde **II.29** (500 mg, 1.6667 mmol, 1 equiv.) dissolved separatly in 5 ml dry THF was added and reaction mixture were refluxed for two hours. Reaction progress was monitored with TLC and quenched with distilled water. Organic compound was extracted with ethyl acetate, dried over anhydrous Na_2SO_4 and solvent evaporated on rota-evaporator to get crude reaction mixture. Pure product was obtained after performing silica gel column chromatography. Yield: 61 mg (8%); colorless solid; Melting Point = 195ºC. **^{1}H-NMR** (*Chloroform-d*, 400MHz, 295K): δ = 4.10(m, 16H), 5.90 (s, 4H), 7.60(s, 2H), 7.72(s, 4H); **^{13}C-NMR**: δ = 65.29,

103.43, 123.74, 126.14, 138.91, 141.03 ppm; **HRMS**: *m/z* calcd. for $(C_{24}H_{26}O_8+H)^+$= 443.1706, Observed = 443.1707.

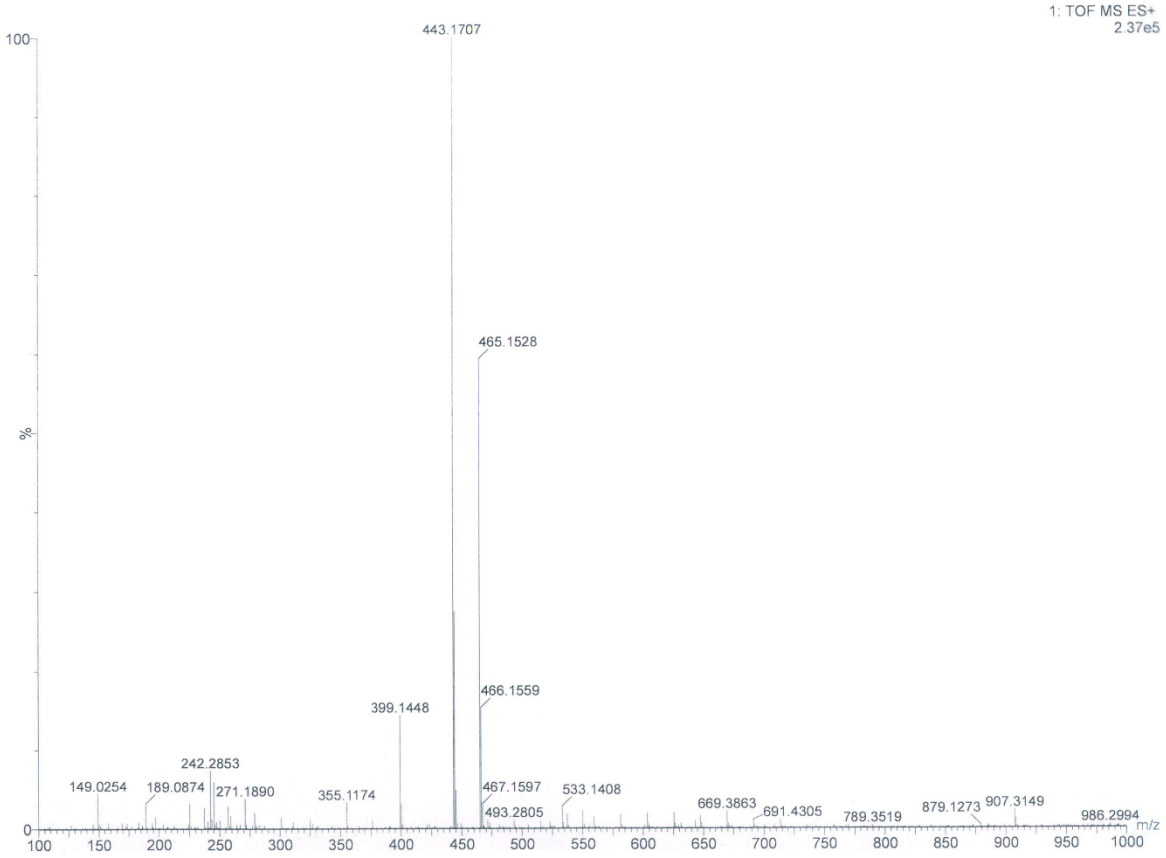

Figure II.35: HR-ESI-TOF mass spectrum of **II.30**

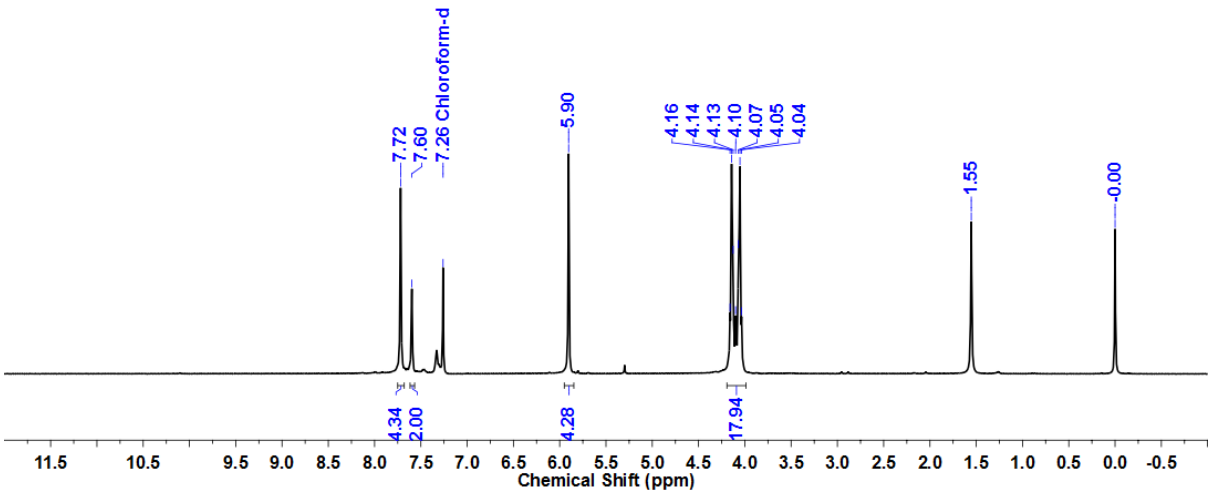

Figure II.36: ^{1}H-NMR spectrum of **II.30** in *Chloroform-d* at 295K

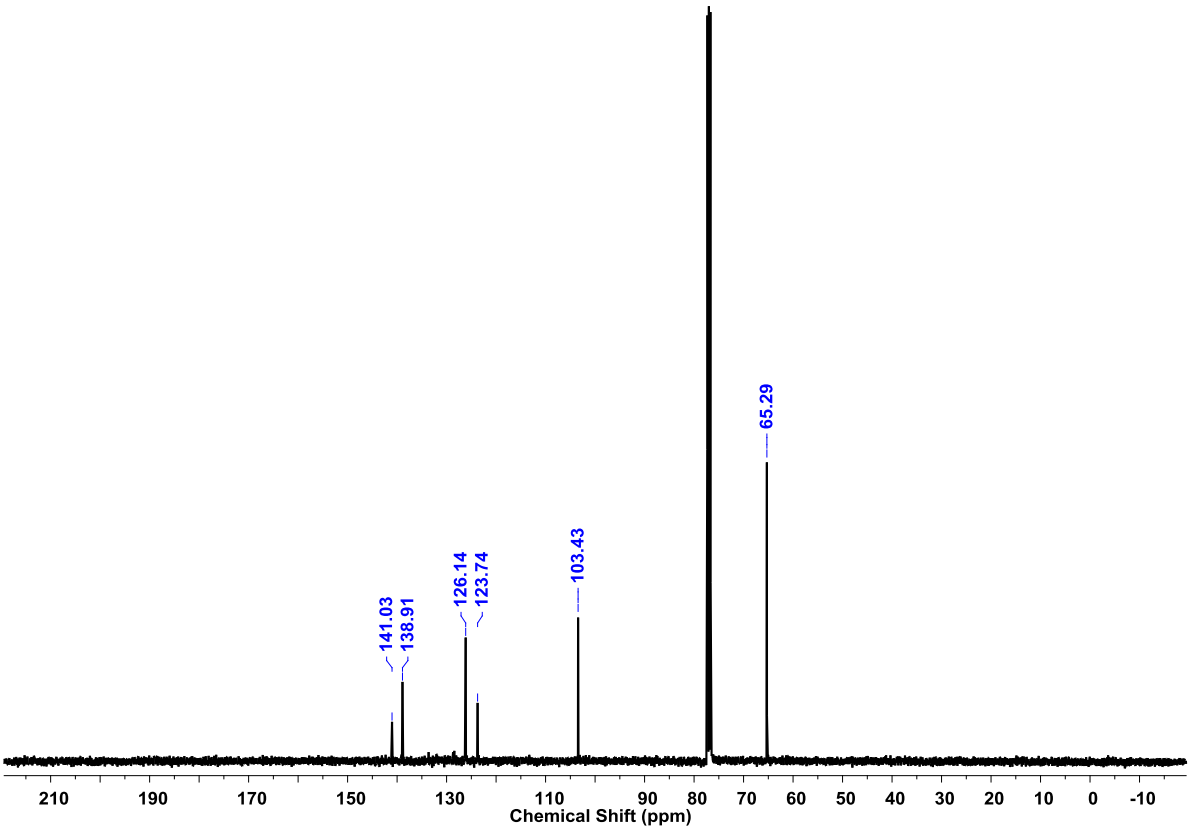

Figure II.37: ^{13}C-NMR spectrum of **II.30** in *Chloroform-d* at 295K

Procedure for Synthesis of II.31

Compound **II.30** (1 gm) is dissolved in a minimum amount of dichloromethane, then 50 ml tetrahydrofuran and 10 mL 6N HCl was added and this solution is stirred for one hour at room temperature. The solvent was removed under vacuo and to the residue dichloromethane was added. This organic solution was washed with 15 % aqeous K_2CO_3 (2X150 mL), distilled water (100 ml) and dried over Na_2SO_4. The solvent was removed under vacuo and obtained residue was purified by column chromatography. Yield: 80 mg (13%); colorless solid; Melting Point = 132ºC. **^{1}H-NMR** (*Chloroform-d*, 400MHz, 295K): δ = 8.26(d, J = 1.6 Hz, 4H), 8.30(t, J = 1.6 Hz, 2H), 10.05(s, 4H); **^{13}C-NMR**: δ = 124.39, 129.21, 137.17, 138.46, 189.44 ppm; **HRMS**: *m/z* calcd. for $(C_{16}H_{10}O_4+H)^+$= 267.0657, Observed = 267.0676.

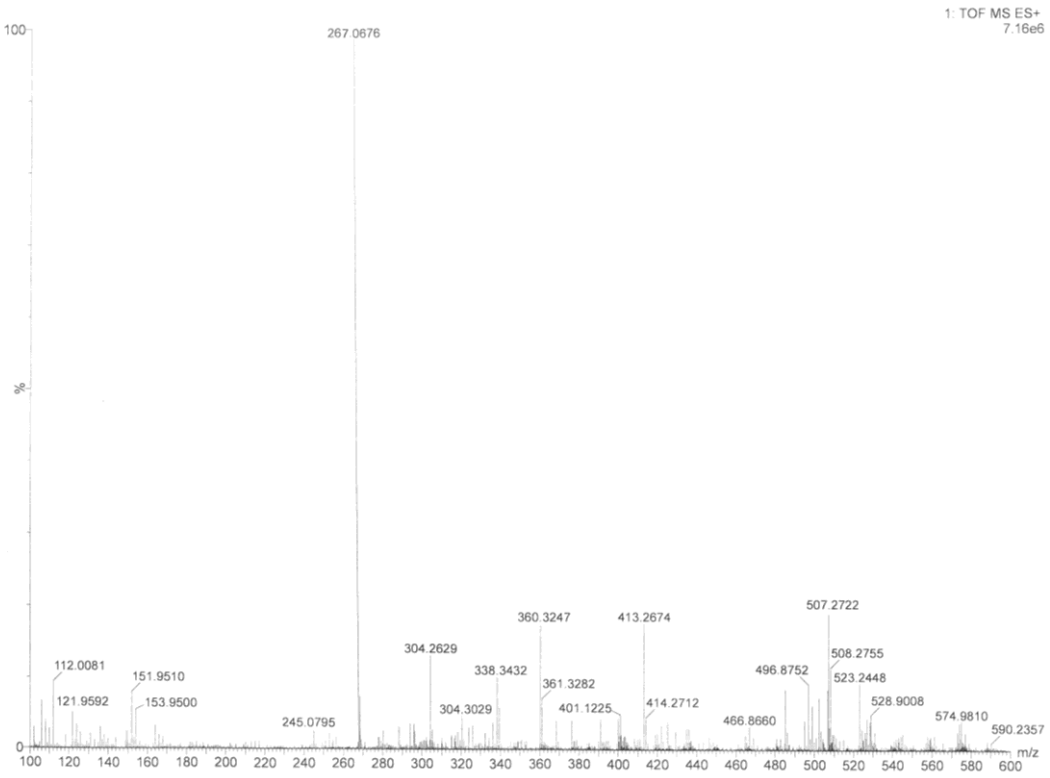

Figure II.38: HR-ESI-TOF mass spectrum of **II.31**

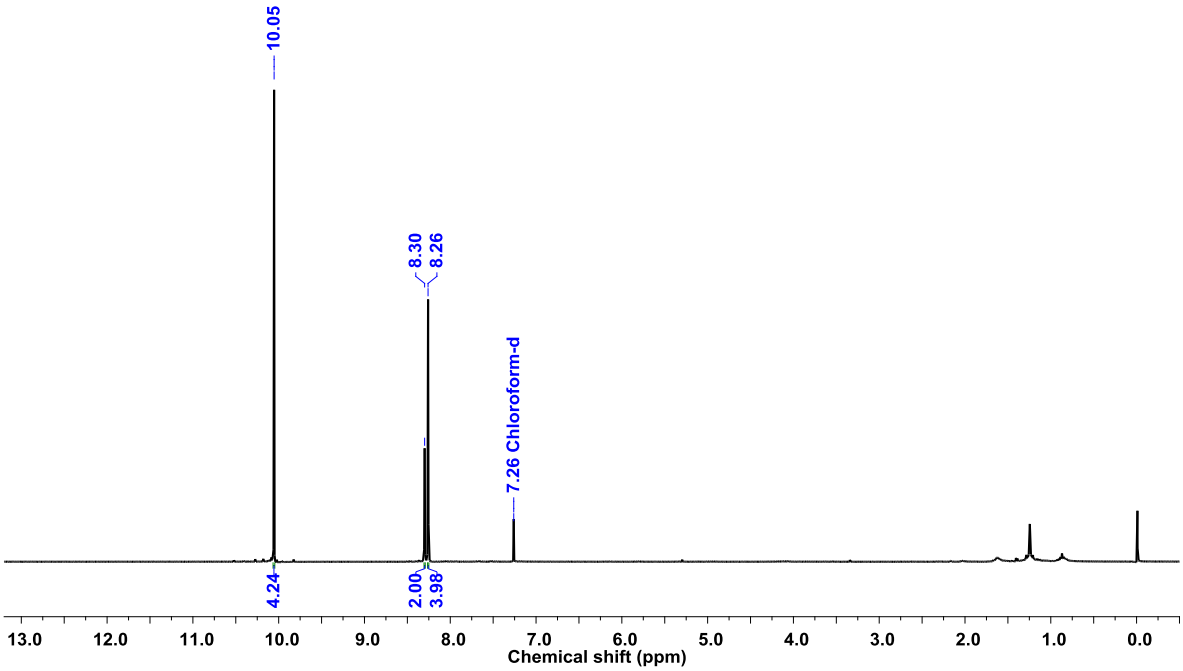

Figure II.39: ^{1}H-NMR spectrum of **II.31** in *Chloroform-d* at 295K

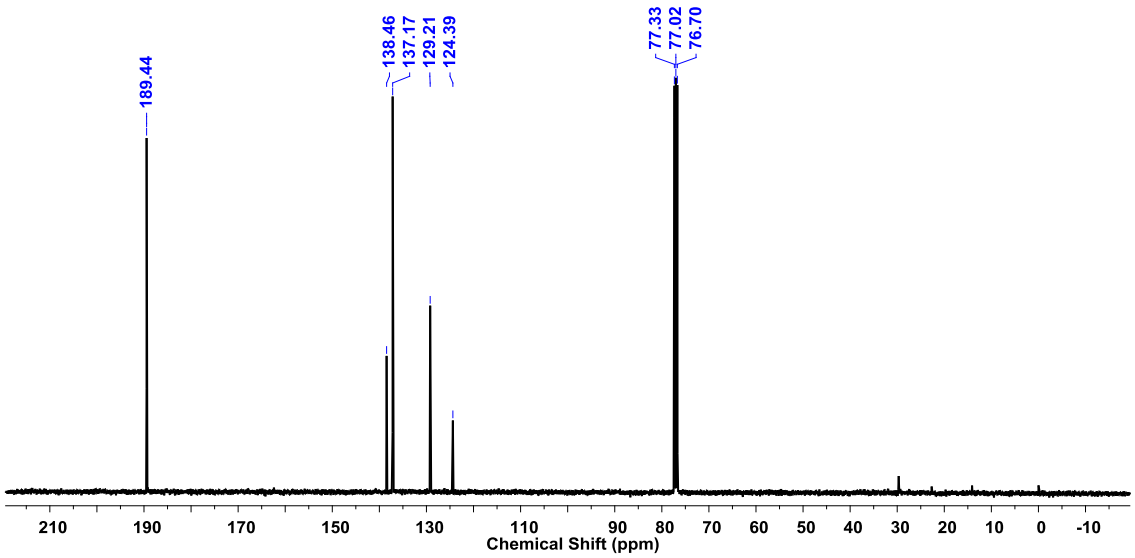

Figure II.40: ^{13}C-NMR spectrum of **II.31** in *Chloroform-d* at 295K

Procedure for Synthesis of II.32

Similar protocol to synthesis of **II.27** was employed for synthesis of **II.32**. 1,1'-Biphynyl-3,3',5,5'-Tetra-aldehyde **II.31** (60 mg, 0.2256 mmol, 1 equiv.) and pyrrole (3.12 ml, 45.1128 mmol, 200 equivalent) reacted using TFA (6.90 µlit, 0.09023 mmol, 0.4 equiv.). Yield: 100 mg (49%); colorless sticky compound. **^{1}H-NMR** (*Acetone-d_6*, 400MHz, 295K): δ = 5.41(s, 4H), 5.72(m, 8H), 5.97(m, 8H), 6.67(m, 8H), 7.19(s, 4H), 7.21(s, 2H), 9.72(bs, 8H, exchangeable with D_2O); **^{13}C-NMR**: δ = 43.76, 106.76, 107.39, 117.17, 121.55, 127.86, 129.16, 132.42, 146.03 ppm; **HRMS**: *m/z* calcd for $(C_{48}H_{42}N_8+H)^+$: 731.3611; observed: 731.3628.

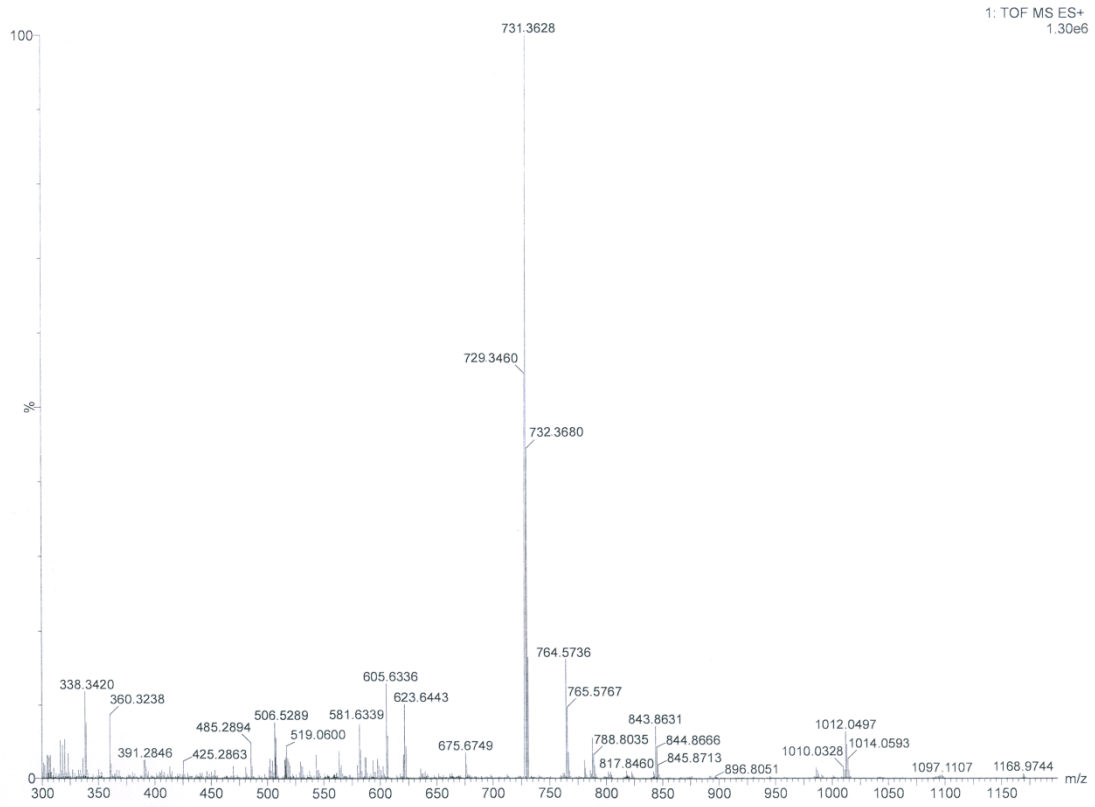

Figure II.41: HR-ESI-TOF mass spectrum of **II.32**

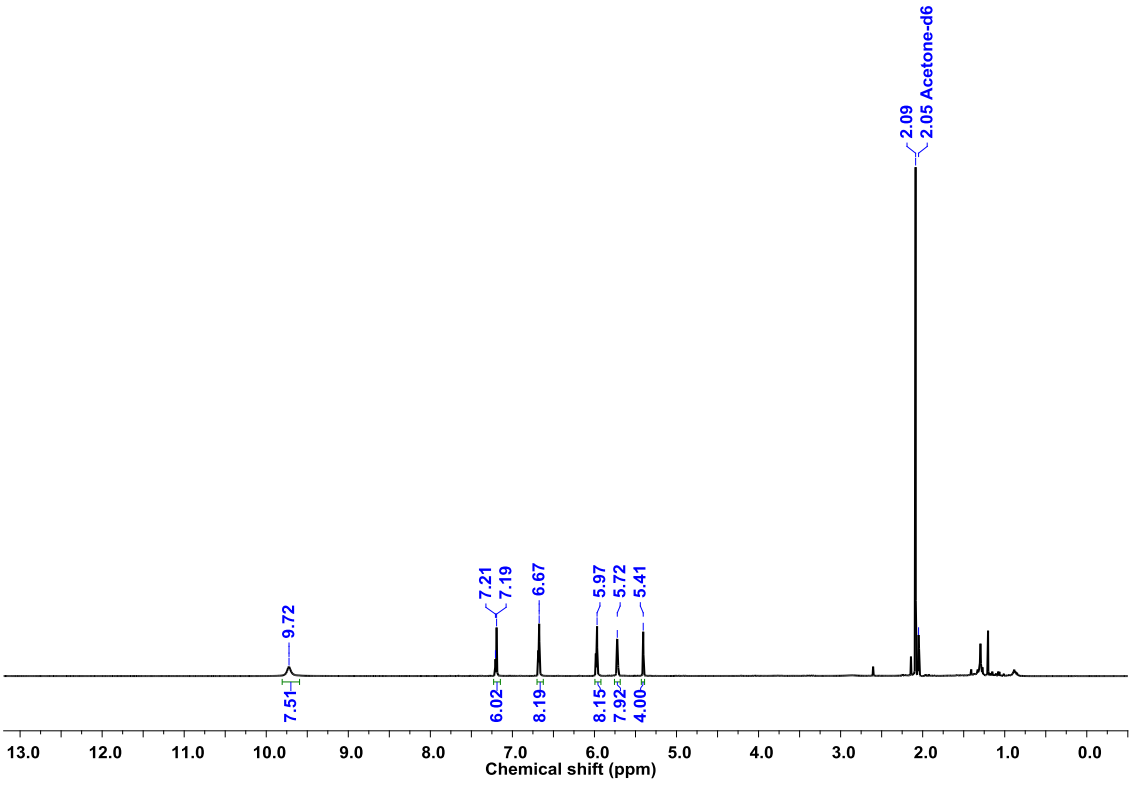

Figure II.42: ^{1}H-NMR spectrum of **II.32** in *Acetone-d_6* at 295K

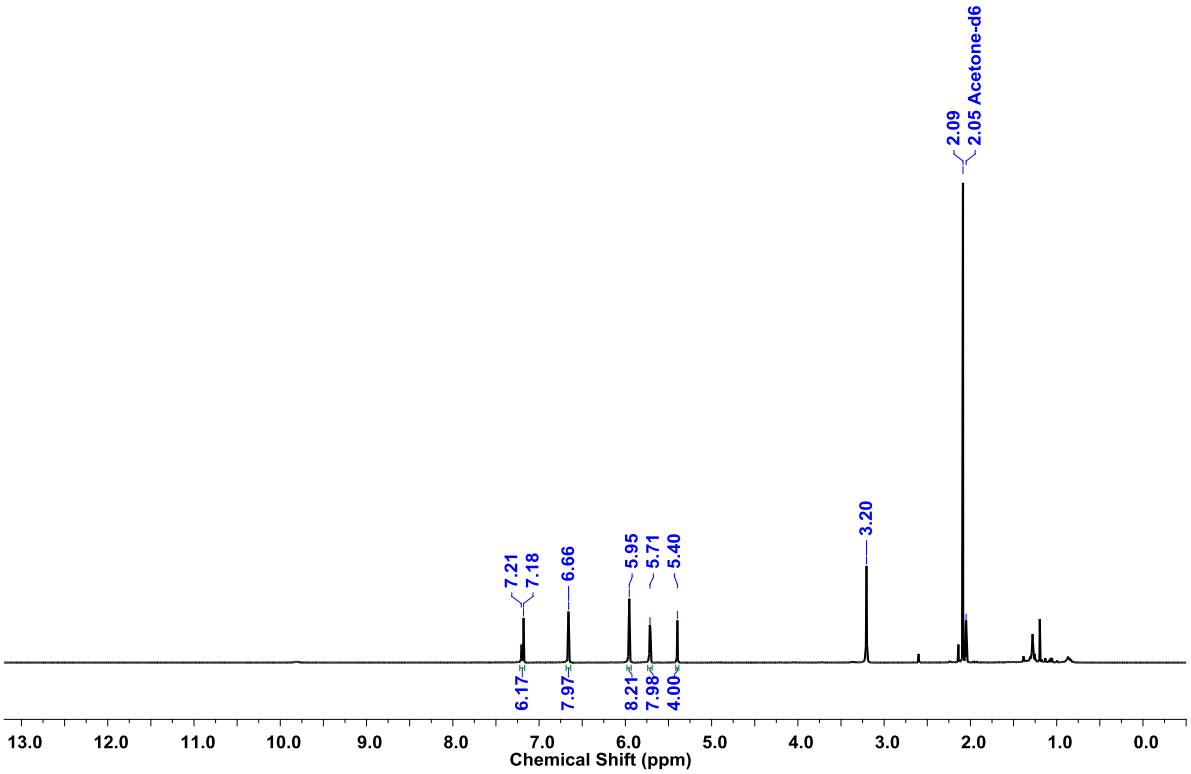

Figure II.43: ^{1}H-NMR spectrum of **II.32** after D_2O exchange in *Acetone-d_6* at 295K

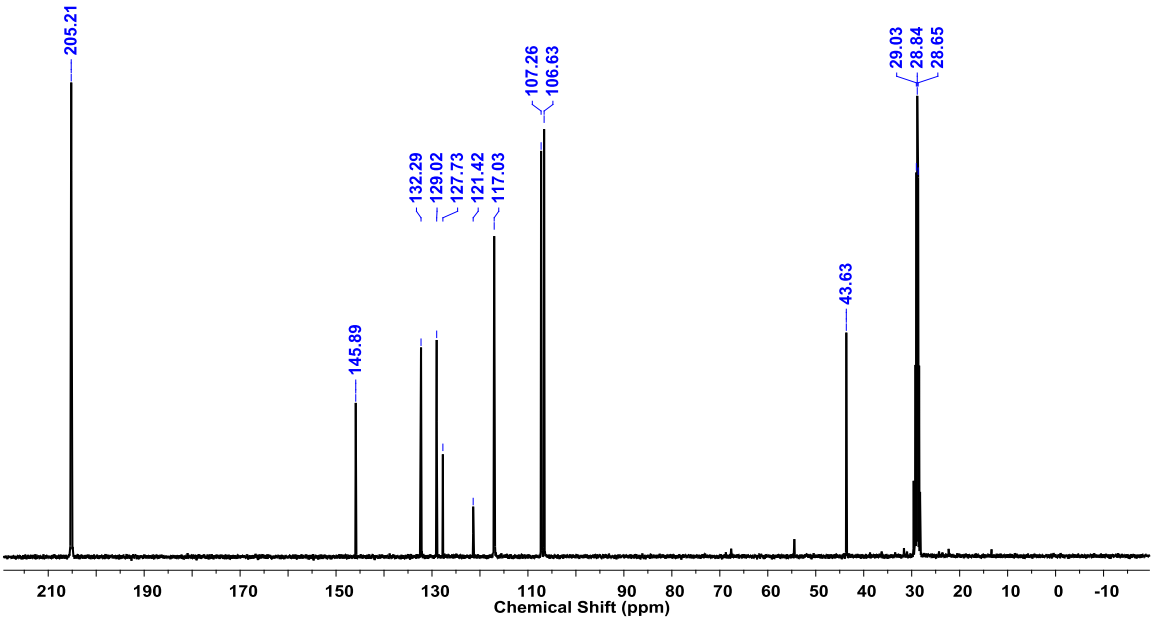

Figure II.44: ^{13}C-NMR spectrum of **II.32** in *Acetone-d_6* at 295K

Procedure for Synthesis of II.33

1,1'-Biphynyl-3,3',5,5'-Tetra-dipyrromethane **II.32** (90 mg, 0.1232 mmol, 1 equiv.), DDQ (123 mg, 0.5424 mmol, 4.4 equiv.), Triethyl amine (1.72 ml, 12.32 mmol, 100 equiv.) and borontrifluoride etherate (1.52 ml, 12.32 mmol, 100 equiv.) were reacted as per procedure used for synthesis of **II.24**. Yield 24 mg (21%); brown color solid; Melting Point = Decomposes above 250ºC. **^{1}H-NMR** (*Chloroform-d*, 400MHz, 295K): δ = 6.62(d, J = 4.0 Hz, 8H), 6.98(d, J = 4.0 Hz, 8H), 7.87(s, 2H), 8.01-8.03(m, 12H); **^{13}C-NMR**: δ = 119.50, 130.76, 131.09, 131.11, 131.79, 134.81, 135.53, 145.54 ppm; **^{19}F-NMR**: δ = -144.59 (q, 8F); **^{11}B-NMR**: δ = 0.03 (t, 4B); **UV-Vis** (CH_2Cl_2): $\lambda_{max}(\varepsilon)Lmol^{-1}cm^{-1}$ = 502 nm (39250); **HRMS**: *m/z* calcd. for $(C_{48}H_{30}B_4F_8N_8+H)^+$= 915.2916, observed = 915.2903; **Crystal data**: $C_{48}H_{30}B_4F_8N_8$(Mr = 914.04), monoclinic, space group P 21/c (No.14), a = 13.045(2), b = 14.548(3), c = 15.682(3)Å, α = 90.00, β = 107.016(4), γ = 90.00°, V = 2845.8(9)Å^3, Z = 2, ρcalcd = 1.067 mg/m^3, T = 100K, Rint (all data) = 0.0662, R1(all data) = 0.1544, RW (all data) = 0.2455, GOF = 0.690.

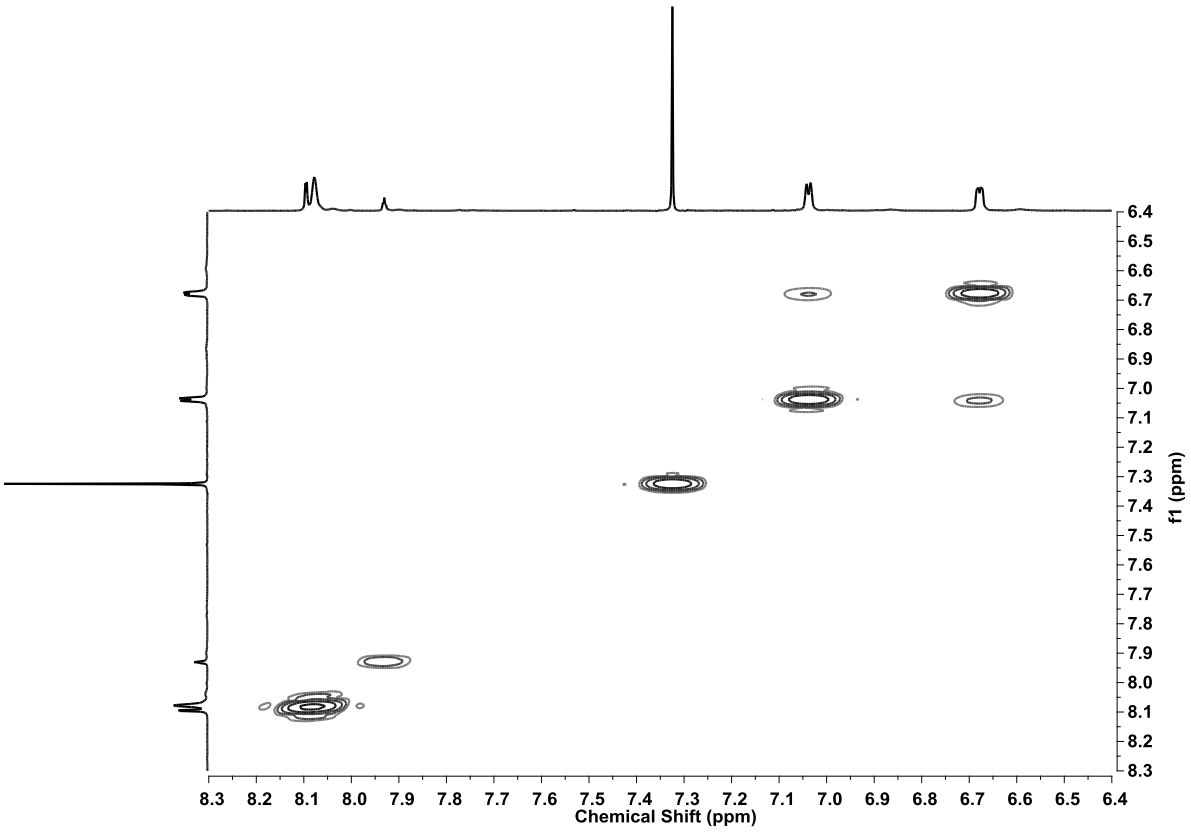

Figure II.45: ^{1}H-^{1}H COSY spectrum of **II.33** in *Chloroform-d* at 295K

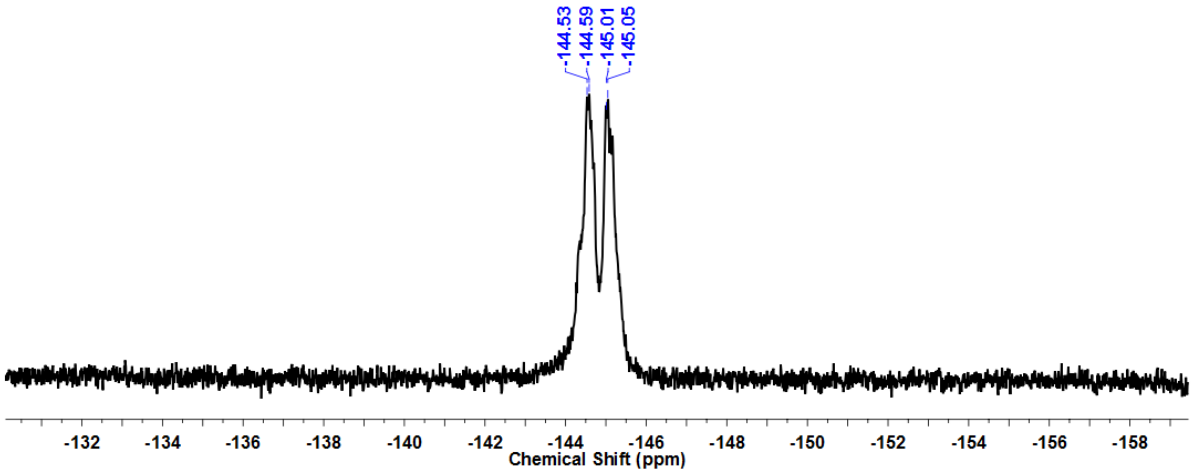

Figure II.46: ^{19}F-NMR spectrum of **II.33** in *Chloroform-d* at 295K

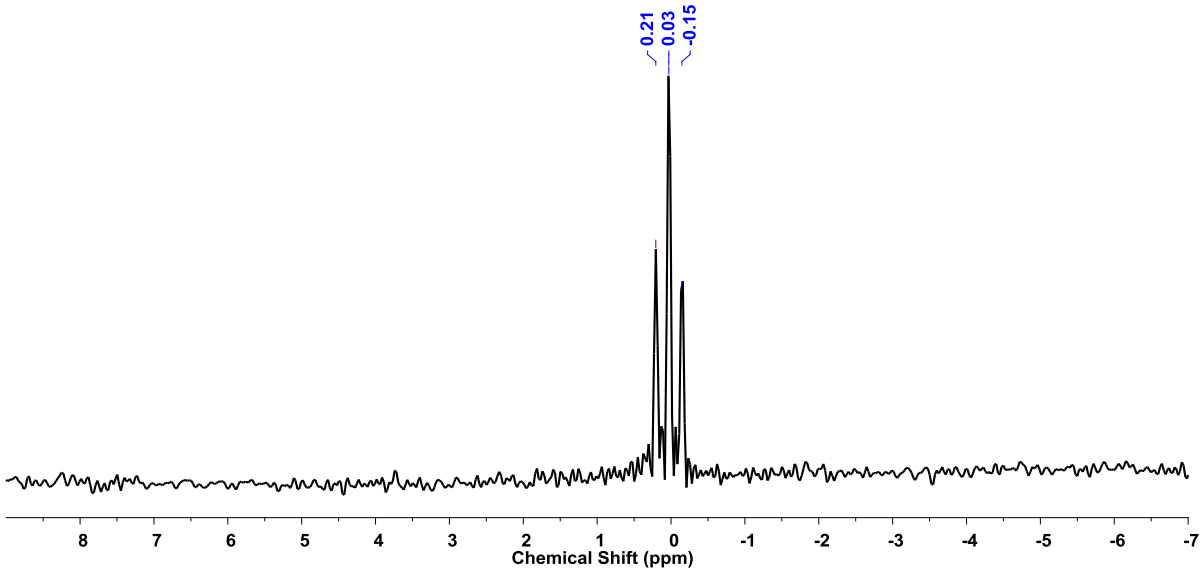

Figure II.47: ^{11}B-NMR spectrum of **II.33** in *Chloroform-d* at 295K

Chapter III

Reactivity of N-Confused Dipyrrins and Doubly N-Confused Dipyrrins with Metal Salts

Section A: Reactivity of N-Confused Dipyrrins with Metal Salts

III.A.1: Introduction:

Porphyrin and corrole are the tetrapyrrolic aromatic molecules containing NNNN core. These macrocycles are excellent ligand for various metal ions and also have potential for applications in material science, biology and medicines. Recently, porphyrinoids with a N-confused pyrrole ring has gained significant interest owning to their unusual structural and chemical properties. N-confused porphyrin **III.A.1**[46] and N-confused corrole **III.A.2**[47] represent the simplest examples of N-confused porphyrinoids (Figure III.A.1).

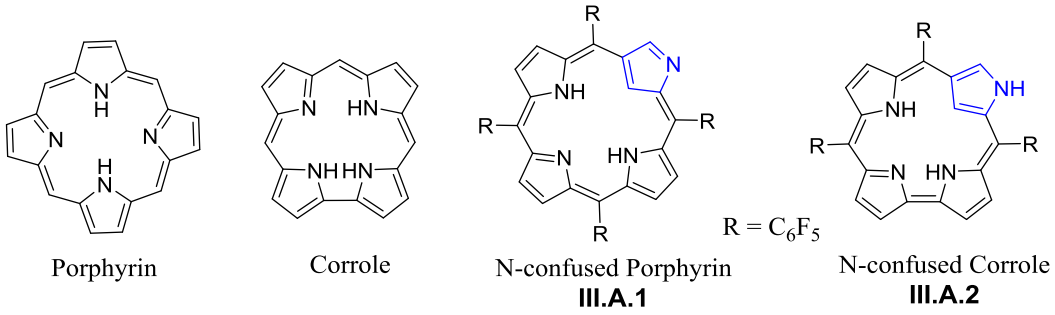

Figure III.A.1: Structures of Porphyrin, Corrole, N-confused Porphyrin and N-confused corrole

N-confused porphyrin (NCP) was reported independently by Furuta and Latos-Grazynski in 1994[46]. Like porphyrin, NCP is also composed of four pyrrole rings and four *meso*-carbon atoms, but possesses a confused pyrrole ring which is connected to the neighbouring *meso*-carbon atoms through α and β-carbon atoms. Therefore, the pyrrolic β-CH is facing the center of the macrocycle and the imine nitrogen pointed outside the core of the macrocycle and hence NCP contains NNNC core. In contrast to porphyrin, NCP exhibits an unsymmetrical structure and non-planar geometry. The loss of planarity as observed from the molecular structure of NCP, displayed the tilting of the confused pyrrole ring from the mean NCP plane by an angle of 30º.

The induced change due to the unorthodox connectivity of a pyrrole ring paves the way for tautomeric structures of NCP as realized by the observed color change in different organic solvents[48]. NCP forms red colored solution in dichloromethane

(non-polar solvent) and green in dimethyl formamide (polar solvent). The ^{1}H-NMR, X-ray diffraction analysis and UV-Visible spectroscopy confirmed the presence of tautomer **NCP III.A.1** in dichloromethane and the less aromatic tautomer **NCP III.A.2** in dimethyl formamide (Figure III.A.2).

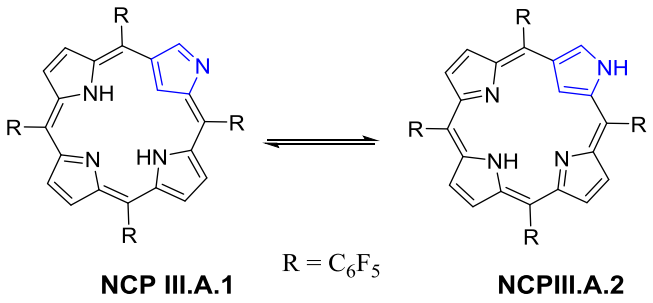

Figure III.A.2: Tautomerism in N-confused Porphyrin (NCP)

There were similar attempts to accommodate a confused pyrrole unit in a corrole framework. Furuta and co-workers targeted the synthesis of N-confused corrole **III.A.4** using N-confused bilane **III.A.3**. Apart from the expected N-confused corrole **III.A.4**, an unusual type of N-C linked corrole isomer called norrole **III.A.5** was also obtained as a minor byproduct (Scheme III.A.1)[47] in this reaction. The neo-confused pyrrole ring in Norrole is connected to the *meso*-carbon by a β-carbon atom, while the nitrogen of the neo-confused pyrrole ring forms a bond with the α-position of the neighboring pyrrole. Due to this arrangement of the pyrrole, the neo-confused pyrrole ring is tilted by 36.4º from mean macrocyclic plane of the norrole.

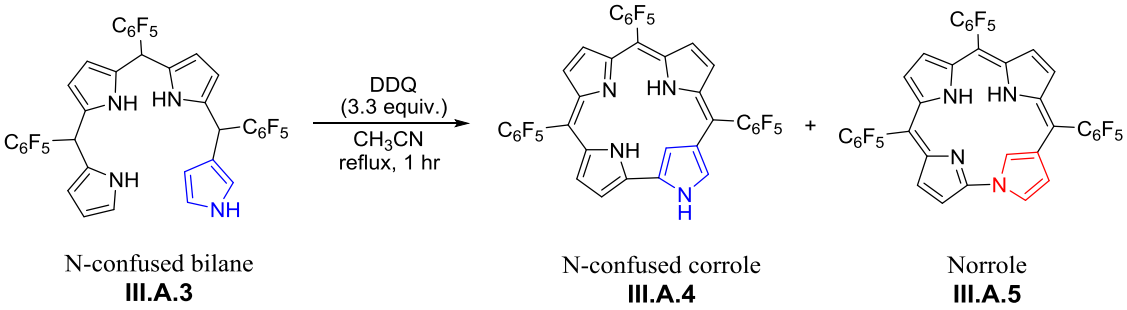

Scheme III.A.1: Synthesis of N-confused Corrole and Norrole

During the synthesis of N-confused norrole **III.A.7** from doubly N-confused bilane **III.A.6**, under harsh reaction conditions, C-fused norroles **III.A.8** was also identified in the reaction mixture (Scheme III.A.2)[49]. The driving force for

intramolecular C-C coupling could be the availability of a narrow space inside macrocycle and flexibility of N-linked and N-confused pyrrole ring in N-confused norrole.

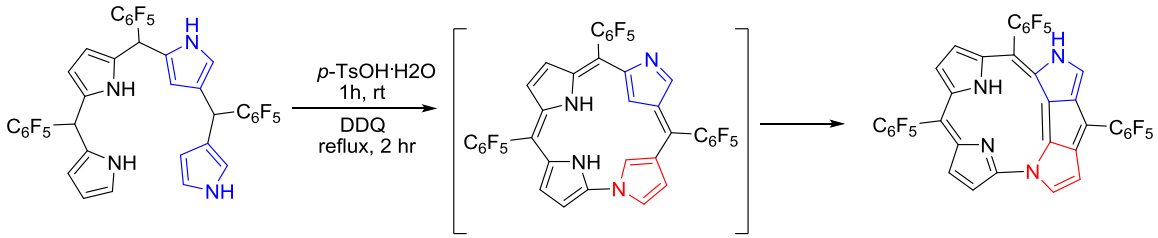

Doubly N-confused bilane
III.A.6

N-confused norrole
III.A.7

C-fused norrole
III.A.8

Scheme III.A.2: Synthesis of C-fused Norrole

Lash and co-workers considered this novel method of norrole synthesis as neo-confused approach, and coined the term "neo-confusion". They employed a different synthetic approach to synthesize the unknown porphyrin isomer with N-linked *meso*-carbon and called such systems as neo-confused porphyrin[50]. Neo-confused porphyrin possesses neo-confused pyrrole ring connected to the *meso*-carbon atom by nitrogen atom on one side and the other end is connected through a β-carbon atom of the same pyrrole unit. The MacDonald 2+2 condensation of dialdehyde **III.A.9** with dipyrromethane **III.A.10** using *p*-toluenesulphonic acid in methanol/dichloromethane produced the neo-confused phlorin **III.A.11**, as confirmed by proton NMR spectrum. The phlorin was further oxidized with DDQ to the corresponding benzoporphyrin isomer or neo-confused porphyrin **III.A.12** (Scheme III.A.3). Neo-confused porphyrin **III.A.12** forms a square planar nickel (II) complex with metal-carbon bond and hence act as an organometallic ligand.

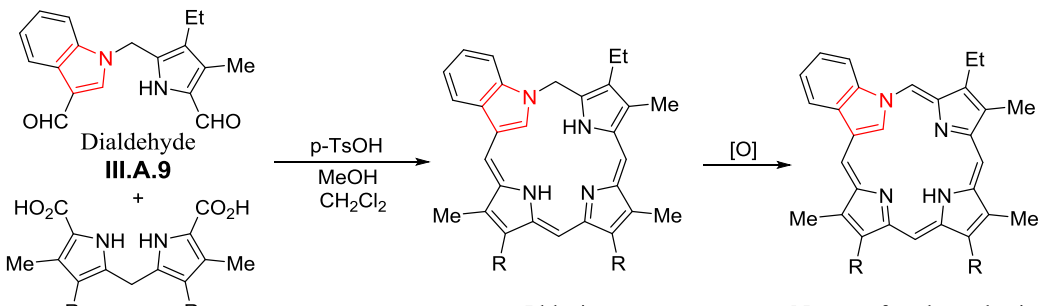

Dialdehyde
III.A.9

+

Dipyrromethane
III.A.10

Phlorin
III.A.11

Neo-confused porphyrin
III.A.12

Scheme III.A.3: Synthesis of Neo-confused Porphyrin

Formation of C-fused norrole **III.A.8**[49] and organometallic complex of neo-confused porphyrin **III.A.12**[50] indicate the high reactivity of inner carbon (α-carbon) atom of norrole and neo-confused porphyrin respectively. Substituted pyrrole play a significant role in the synthesis of norrole compared to N-confused corrole. When indole was employed as a substituted pyrrole, the target molecule benzonorrole was obtained in high yields. N-confused benzobilane **III.A.13** was also synthesized by same strategy as used for N-confused bilane **3**. Oxidative cyclization of N-confused benzobilane **III.A.13** with *p*-chloranil and copper(II) acetate leads to Cu(III) benzonorrole **III.A.14** and further demetalated to free base benzonorrole **III.A.15**[51]. This benzonorrole undergoes dimmerization to *cis*-benzonorrole dimer (*cis*-BNdimer) **III.A.16** and *trans*-benzonorrole dimer (*trans*-BNdimer) **III.A.17** when treated with DDQ under reflux in CH_3CN (Scheme III.A.4). Both the structures were confirmed by single crystal X-ray diffraction analysis.

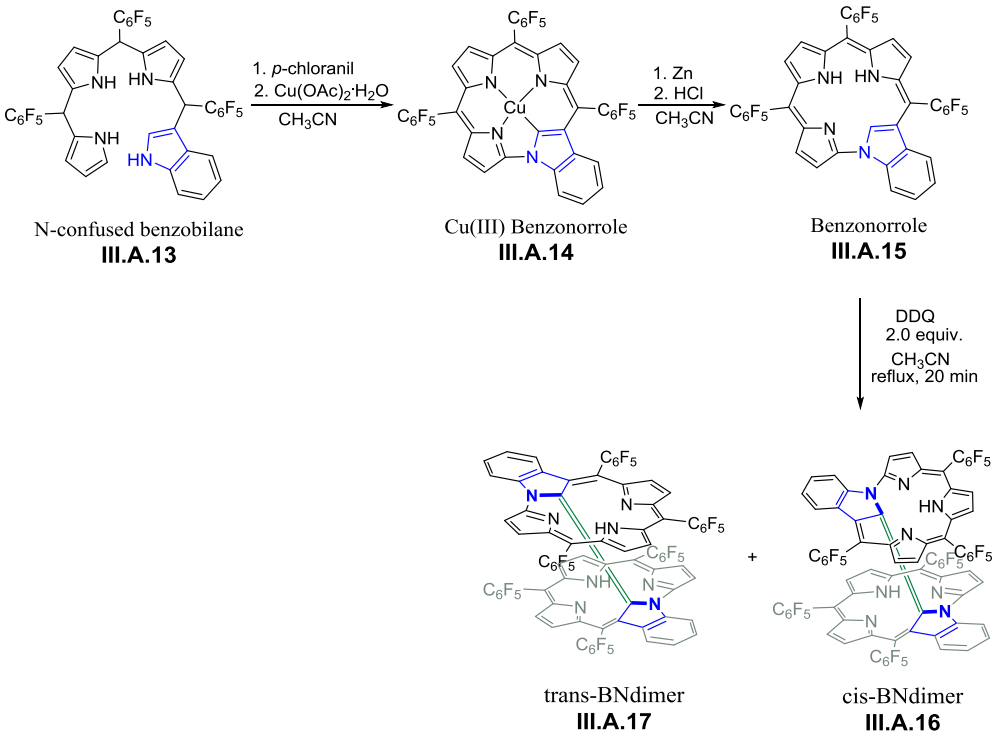

Scheme III.A.4: Synthesis of Benzonorrole and its dimerization

Cis-BNdimer can be further reduced with $TsNHNH_2$ to $BNdimerH_2$ and $BNdimerH_2$ was oxidized back to *cis*-BNdimer with DDQ. However a similar reduction of *trans*-BNdimer with $TsNHNH_2$ did not yield expected product.

III.A.2: Objectives:

The synthesis of Norrole and Neo-confused porphyrins add a new dimension to the versatile structural diversity of the porphyrin ring. However, these molecules are known to be synthesized through multi-step procedure which requires an oligopyrrole with a confused pyrrole unit. However similar reactivity of N-confused dipyrromethane as a potential metal chelating agent remins unexplored till date. It was observed that the oxidized diprromethane displayed reactivity uncharacteristic of a metal complexing agent and it underwent oxidative coupling to yield large macrocycles, in presence of metal ions, with structure features similar to norrole. Hence it was decided to employ this reaction as a simple and effective strategy to synthesize contracted and expanded norroles.

III.A.3: Synthesis and Characterization of N-confused Dipyrrin boron trifluoride Complex III.A.20:

The oxidation of N-confused dipyrromethane **III.A.18**[52] with DDQ (2,3-Dichloro-5,6-dicyano-1,4-benzoquinone) can lead to two tautomers, **III.A.19a** and **III.A.19b**, of N-confused dipyrrin depending on presence of imine nitrogen on one of the pyrrole ring (Scheme III.A.5). Further, upon reacting the confused dipyrrin **III.A.19** with boron trifluoride etherate, it was expected to yield a boron difluoride N-confused dipyrrin complex. However only a boron trifluoride complex **III.A.20** was obtained, similar to Lewis acid-base adducts. The formation of boron trifluride complex **III.A.20** was confirmed by mass spectroscopy (Figure III.A.3) and single crystal X-ray diffraction analysis (Figure III.A.4). This complex confirmed the oxidation of N-confused pyrrole ring rather than the normal pyrrole ring of N-confused dipyrromethane, **III.A.18**, with DDQ.

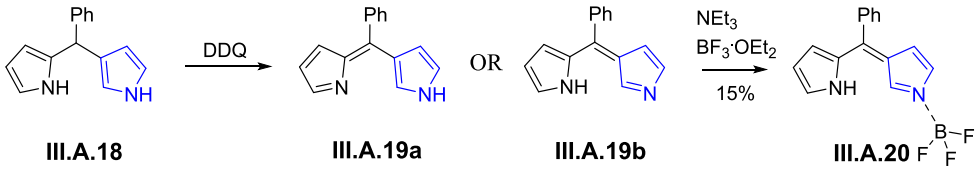

III.A.18 III.A.19a III.A.19b III.A.20

Scheme III.A.5: Oxidation of N-confused Dipyrromethane and its boron trifluoride complex

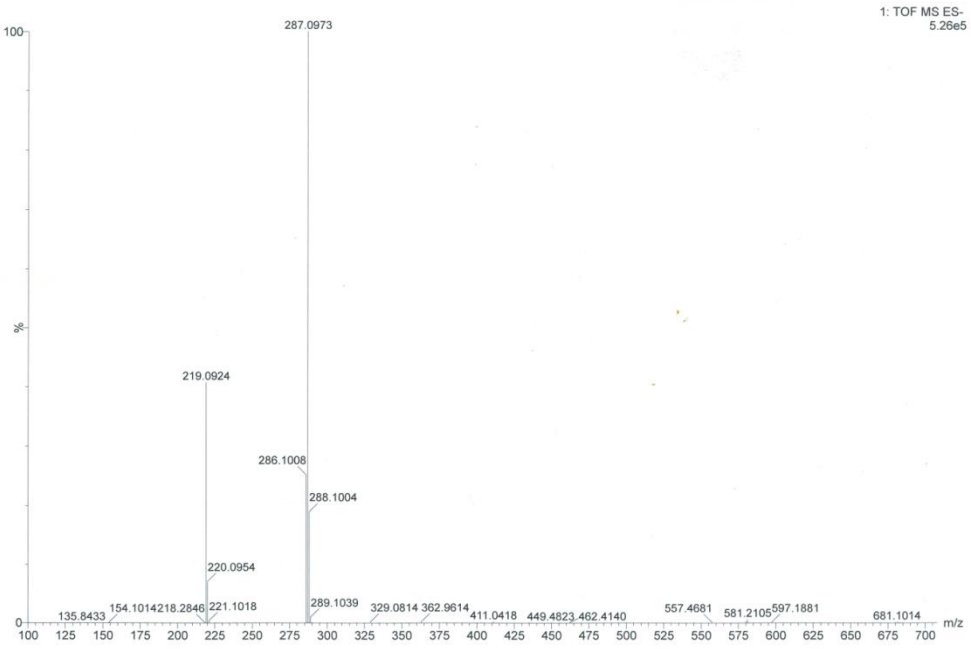

Figure III.A.3: HR-ESI-TOF mass spectrum of **III.A.20**

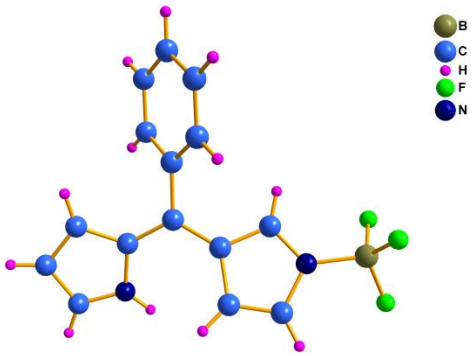

Figure III.A.4: Molecular Structure of **III.A.20**

III.A.4: Synthesis of Expanded Norroles:

Since the imine nitrogen of the N-confused dipyrrin **III.A.19b** was coordinated to the boron atom of the boron trifluoride, a similar reactivity was expected with metal salts too. The dipyrrin derived from pentafluorophenyl N-confused dipyrromethane was stirred overnight with anhydrous copper(II) acetate in dry tetrahydrofuran (Scheme III.A.6). Surprisingly, the High Resolution Mass Spectrum (HRMS) displayed a *m/z* ratio 925.1188 (Figure III.A.5) and 1233.1587 (Figure III.A.6) corresponding to the cyclotrimer **III.A.21a** and cyclotetramer **III.A.22** of the dipyrrin respectively[53]. Same products were obtained with other metal salts such as Co^{2+}, Zn^{2+}, Mn^{2+}, Fe^{2+}, Fe^{3+}, Ti^{4+} and Sn^{2+} under similar reaction

conditions. Along with cyclotrimer and cyclotetramer, cyclodimer (norcorrole isomer)[34b, 54], cyclopentamer and cyclohexamer were also observed in MALDI-TOF mass spectrum, but their yield was too low for further separation and characterization. Similarly, the reaction of phenyl derivative of the N-confused dipyrrin with metal salt also afforded cyclotrimer **III.A.21b** as the major product.

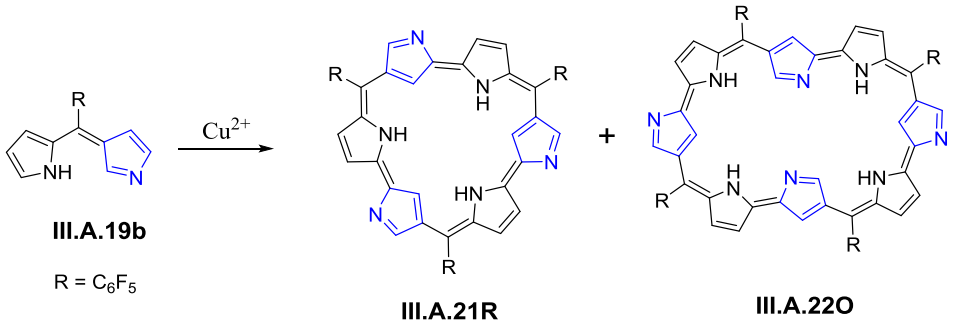

Scheme III.A.6: Expected Molecules

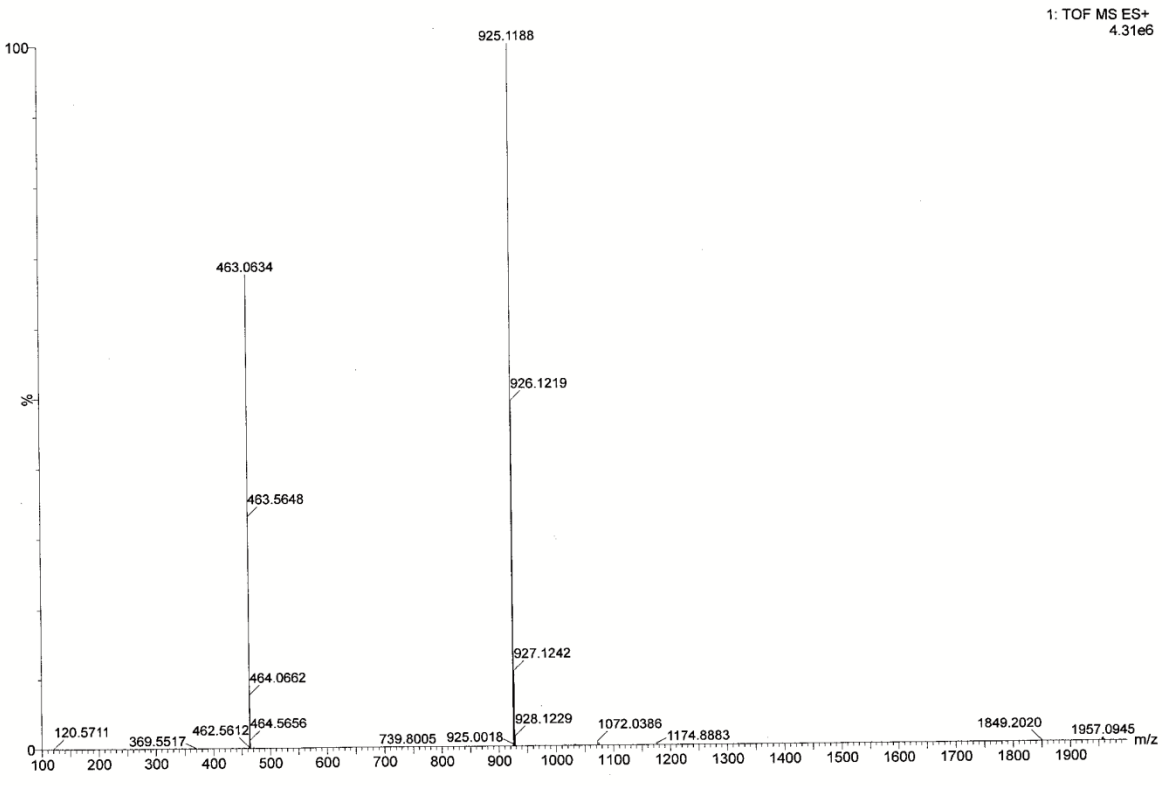

Figure III.A.5: HR-ESI-TOF mass spectrum of **III.A.21a**.

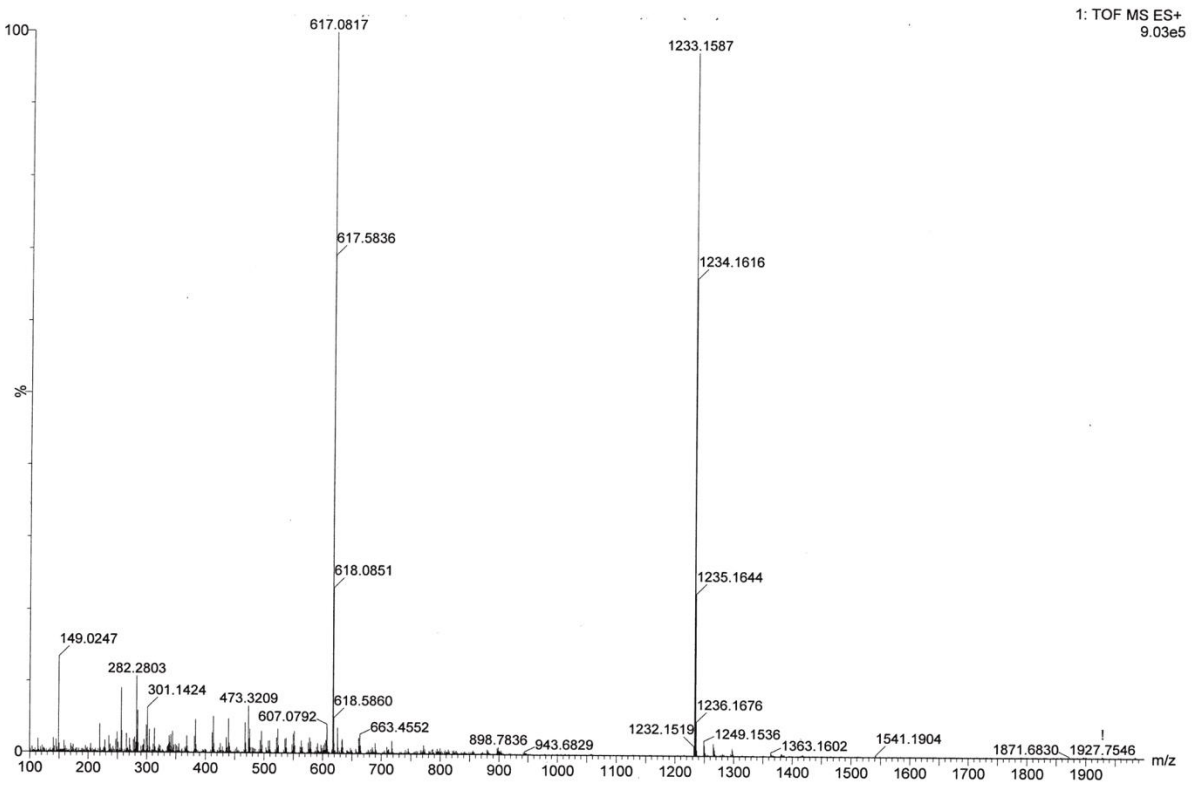

Figure III.A.6: HR-ESI-TOF mass spectrum of **III.A.22**.

Since α-α coupling is a well known synthetic methodology for synthesis of expanded porphyrinoids, the observed cyclotrimer and cyclotetramer of N-confused dipyrrin indicated possibility of formation of N-confused rosarin **III.A.21R** and N-confused octaphyrin **III.A.22O** respectively

In this regard, the formation of N-confused rosarin **III.A.21R** represents a structural isomer of rosarin **III.A.23**, while N-confused ocatphyrin **III.A.22O** can represent a structural isomer of octaphyrin **III.A.24**. (Figure III.A.7).

Rosarin is a hexapyrrolic expanded porphyrin or hexaphyrin(1,0,1,0,1,0) macrocycle **III.A.25**[55] reported by Sessler and co-workers. It was synthesized through an acid catalyzed condensation of bipyrrole with aromatic aldehyde. Formally, the macrocycle accounts for 24 π-electrons and expected to be anti-aromatic in nature. Structural elucidation confirmed a distorted conformation and hence its spectroscopic features displayed structure induced loss of paratropicity. Further it could not be oxidized to a 22 π-electron aromatic system. Very recently, they also synthesized a planar rosarian **III.A.26**[56] which exhibited anti-aromatic characteristics due to its planar structure. This was also synthesized through acid

catalyzed condensation of 1,10-dihydrobenzo[e]pyrrolo[3,2-g]indole and pentaflurobenzaldehyde (Figure III.A.8).

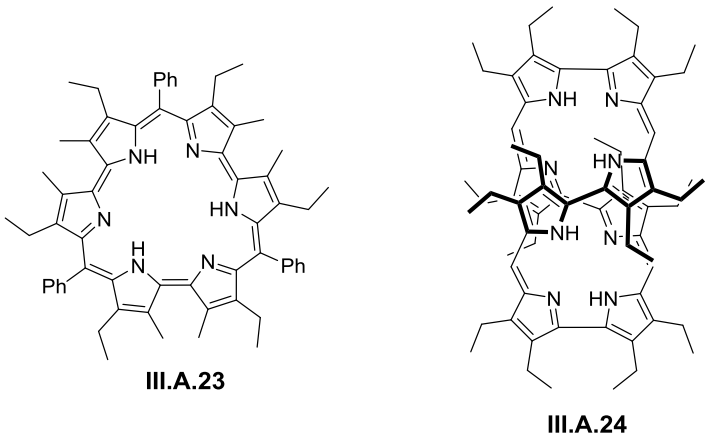

Figure III.A.7: Rosarin **III.A.23** and the octaphyrin **III.A.24** are the other reported **s**tructural isomers till date of **III.A.21R** and **III.A.22O**

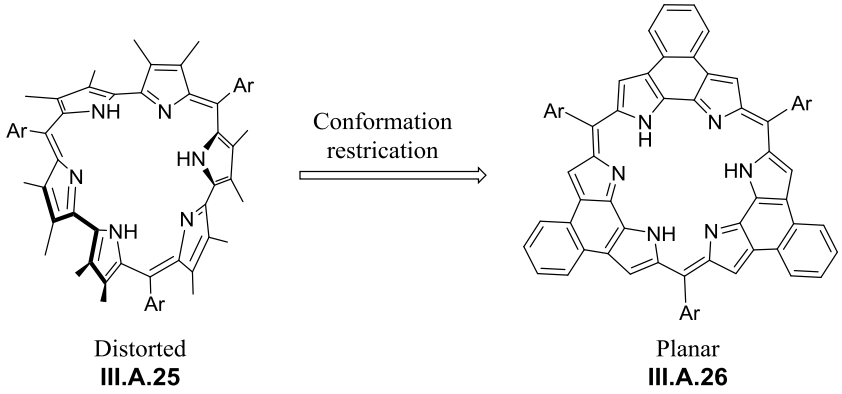

Figure III.A.8: Distorted and planar conformations for 24π Rosarin

III.A.5: Single Crystal X-Ray Diffraction Analysis of Expanded Norroles:

The expected structures of III.A.21R and III.A.22O were elucidated by single crystal X-ray diffraction analysis. Good quality crystals were grown by slow evaporation of *n*-hexane into chloroform solution of the macrocycles. Unexpectedly, the obtained crystal structures confirmed the presence of C-N bond between the pyrroles in bipyrrole subunit similar to that observed for Norrole. Hence it can be considered as Expanded Norroles. The hexapyrrolic expanded norrole **III.A.21a** confirmed three C-N bonds in the three bipyrrole subunits (Figure III.A.9). So the

molecule contains alternate arrangement of three normal and three N-linked pyrroles through a head-to-tail connection between three N-confused dipyrrins. Therefore, N-linked pyrrole shows one of the α-carbon inside and other α and β-carbon pointing outside the macrocycle. All the pyrrole rings are found to be coplanar hence prove that lone pair of electron on nitrogen atom of the N-linked pyrroles delocalized over the macrocycle. The dihedral angle between two pyrrole connected by C-N bond in bipyrrole subunit is 16^0, so deviated from perfect planarity.

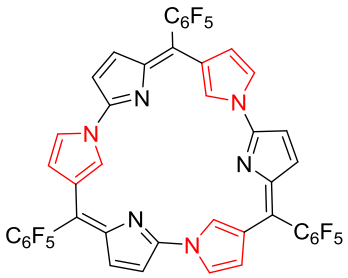

III.A.21a

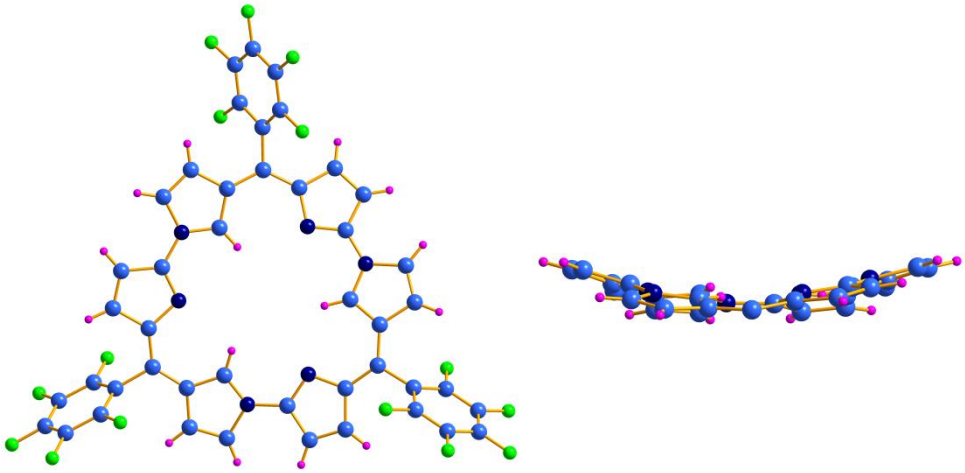

Figure III.A.9: Molecular Structure of **III.A.21a** top view (left) and side view (right)

Macrocycle **III.A.22** displayed a near planar structure with a rectangular shape in solid state (Figure III.A.10). In a fashion similar to **III.A.21a**, four N-confused dipyrrins are interconnected through C-N bond by head-to-tail arrangement leading to four C-N linked four bipyrrole units. This type of bonding is very similar to that observed in Norrole and hence this macrocycle can also be considered as "Expanded Norroles". Vogel and co-workers have reported octaphyrins with eight pyrroles and four or more *meso*-carbon atoms. Such systems were found to adopt a twisted conformation and hence considered as anti-aromatic in nature[57]. The expanded

norrole **III.A.22** is the first octaphyrin with a near planar conformation. The molecular structure of **III.A.22** indicates two different N-linked pyrroles (i) A, E pyrroles with α and β-carbon pointing inside and other α-carbon pointing outside the central cavity of macrocycle and (ii) C, G pyrrole exhibited similar orientation as observed in **III.A.21a** N-linked pyrrole. The distance between the two nitrogen of the pyrrole ring (B, H and D, F) is 7.0Å. It is sufficient enough to accommodate two carbon atoms inside the cavity and hence favor an inverted configuration for N-linked pyrrole. The distance between the nitrogen of the two pyrrole rings (B, D and F, H) is 5.0Å is insufficient for pyrrole rings to be inverted. This inversion of N-linked pyrrole reduces the symmetry of molecule **III.A.22** which gives two different signals for N-linked pyrrole in its ^{1}H-NMR spectrum. The C-N linked pyrroles (A, H and D, E) are coplanar while other two pair of N-linked pyrrole (B, C and G, F) makes a dihedral angel of 18^{0} with each other. The pair of pyrrole rings C, G and B, F make an angle of 17º and 4º, respectively, with the plane formed by the four *meso*-carbon atoms. These observed deviations prevent the macrocycle to adopt a perfect planar structure. The near planar structure of macrocycle **III.A.22** indicates the lone pair of electron on nitrogen atom of N-linked pyrroles is delocalized over molecular plane. Also C-C bond length in **III.A.21a** and **III.A.22** is in between single and double bond distance suggesting the π electron delocalization all over molecule (CCDC 933257 for **III.A.21a** and CCDC 933258 for **III.A.22**)[58].

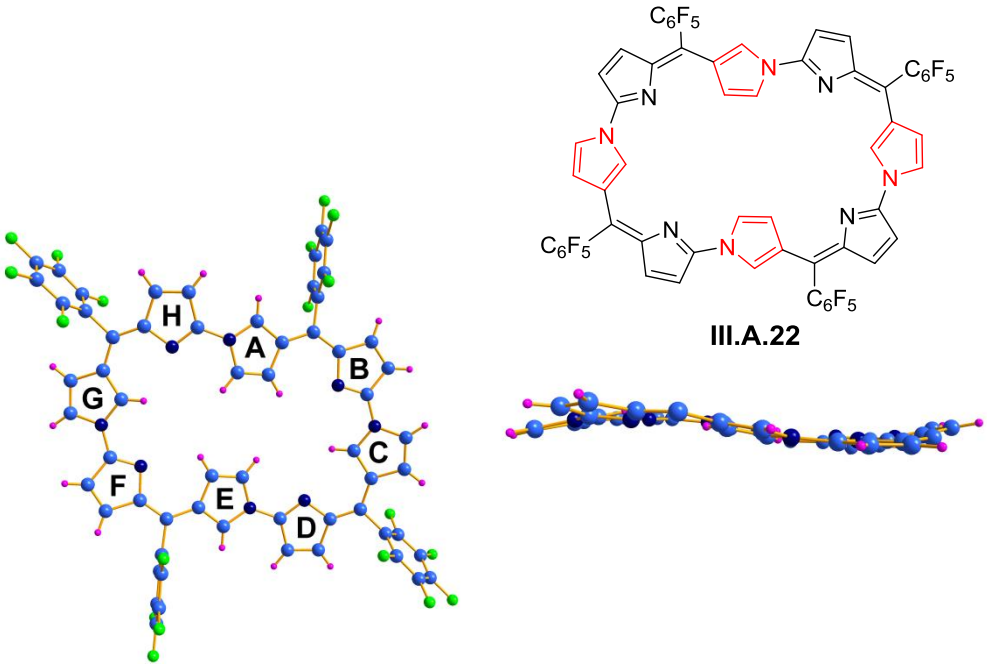

Figure III.A.10: Molecular Structure of **III.A.22** top view (left) and side view (right).

III.A.6: Characterization of Expanded Norroles

The ^{1}H-NMR spectrum of expanded norrole **III.A.21a** displayed multiplets at δ = 11.16, 6.78, and 5.62 ppm and two doublets at δ = 6.50 and 6.48 ppm (Figure III.A.11). ^{1}H-^{1}H COSY demonstrated the correlation between two doublets at δ =6.50 and 6.48 ppm, while the other three signals were found to be coupled with each other (Figure III.A.13). These observations suggested the possibility of normal pyrrole and confused pyrrole rings with two and three different protons respectively. D_2O experiment did not change the spectral pattern indicating absence of NH in the macrocycle. Also DEPT-90 spectrum confirmed five different ^{13}C signals corresponding to CH group (Figure III.A.12). Overall four signals appeared between δ =126 to 112 ppm and the fifth downfield signal appeared at 136 ppm. All these analysis prove the formation of **III.A.21a** as a macrocyclic product with three bipyrrole units having an unusual connection amongst themselve. The upfield and downfield chemical shift values observed in the ^{1}H spectrum signified paratropic ring current effect and delocalization of π electron occurs such that the loan pair of electron present on N also contributed to the anti-aromatic nature.

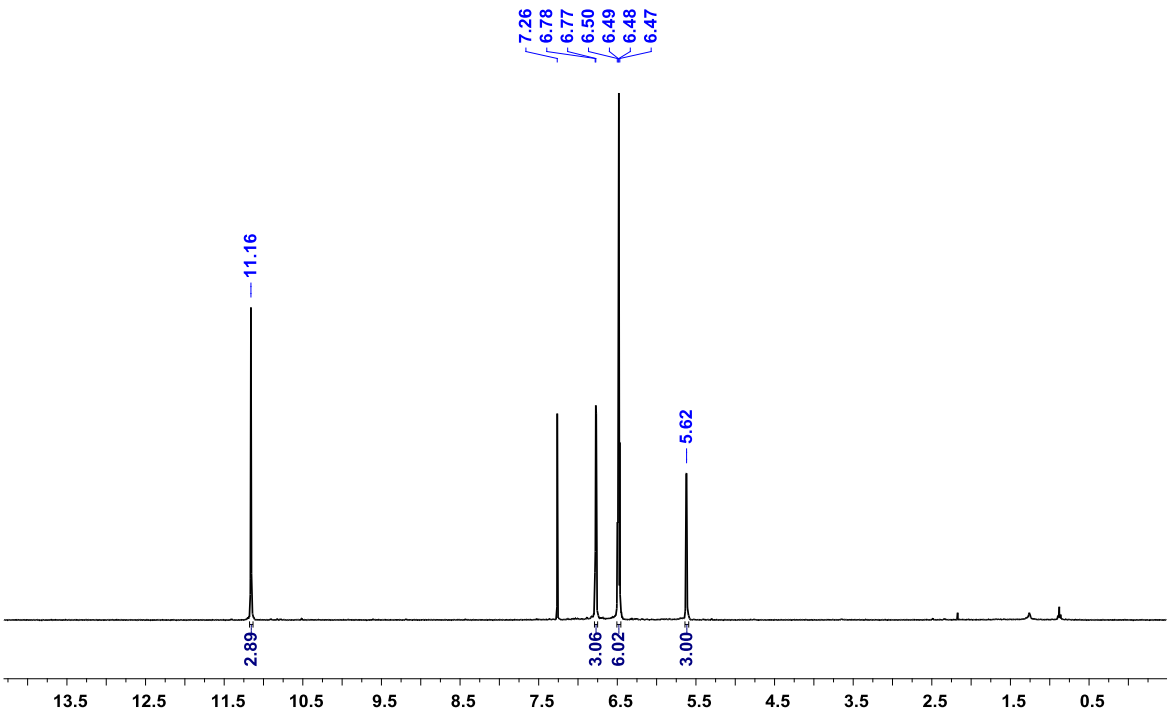

Figure III.A.11: ^{1}H NMR Spectrum of **III.A.21a** in $CDCl_3$ at room temperature.

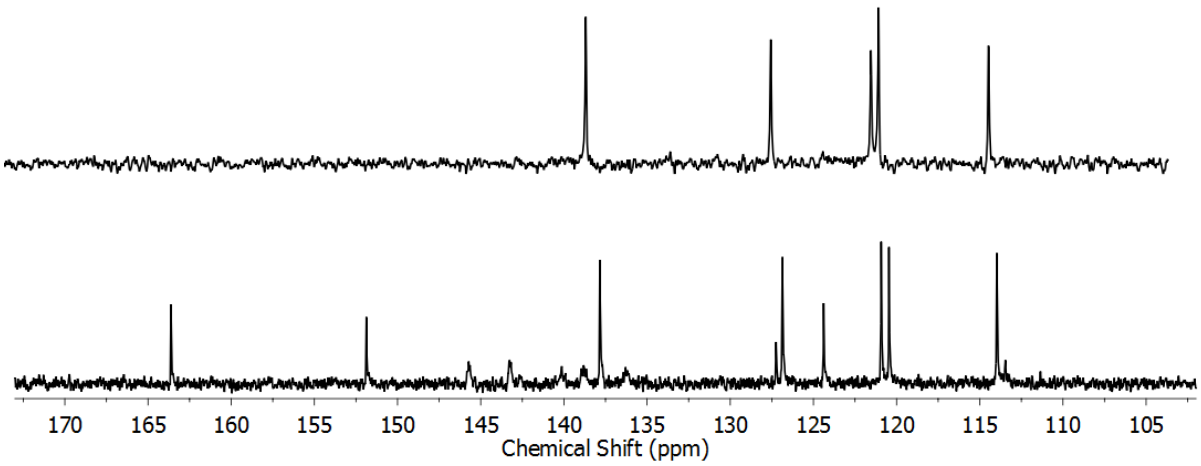

Figure III.A.12: (Top) DEPT-90 NMR Spectrum, (Bottom) ^{13}C NMR Spectrum of **III.A.21a** in $CDCl_3$ at toor temperature.

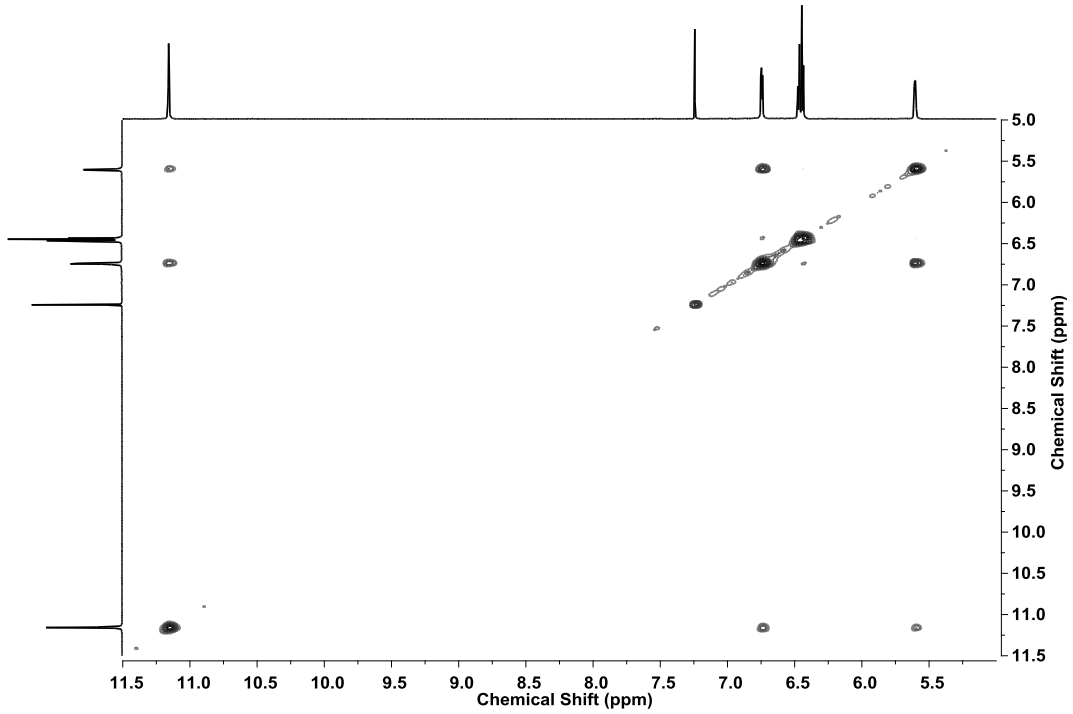

Figure III.A.13: ^{1}H-^{1}H COSY Spectrum of **III.A.21a** in $CDCl_3$ at room temperature.

The ^{1}H-NMR spectrum of expanded norrole **III.A.22** displayed double the number of signals as observed for **III.A.21a** in the region between δ = 10.00 and 6.00 ppm (Figure III.A.14). The ^{1}H-^{1}H COSY corroborated two different types of correlation (i) two sets of correlation was observed for the four doublets between δ =

7.25-6.97 ppm corresponds to normal pyrrole rings, (ii) Other six signals δ = 9.97, 8.69, 8.54, 7.64, 7.53 and 6.22 ppm showed two sets of symmetrical correlation which are assigned for confused pyrrole rings (Figure III.A.16). Addition of D_2O did not change the spectral pattern showing absence of NH in the macrocycle. DEPT-90 experiment gave eight different ^{13}C signals between δ = 127 to 114 ppm and a downfield signal at 138 ppm were observed for other two carbons (Figure III.A.15). The downfield signal at 10 ppm in ^1H NMR and at 138 ppm in DEPT 90 spectrum indicated the paratropic ring current effect for anti-aromatic macrocycle **III.A.22**. All these observations clearly suggest the presence of two pair of confused ring with dissimilar orientation in macrocycle **III.A.22**. The 32π octaphyrin **III.A.24**, with eight pyrrole unit was found to take twisted conformation, hence characterized as non-aromatic in nature[59]. But observed shielding and deshielding in ^1H-NMR spectrum of **III.A.22** indicate the planar conformation for 32π system and anti-aromaticity.

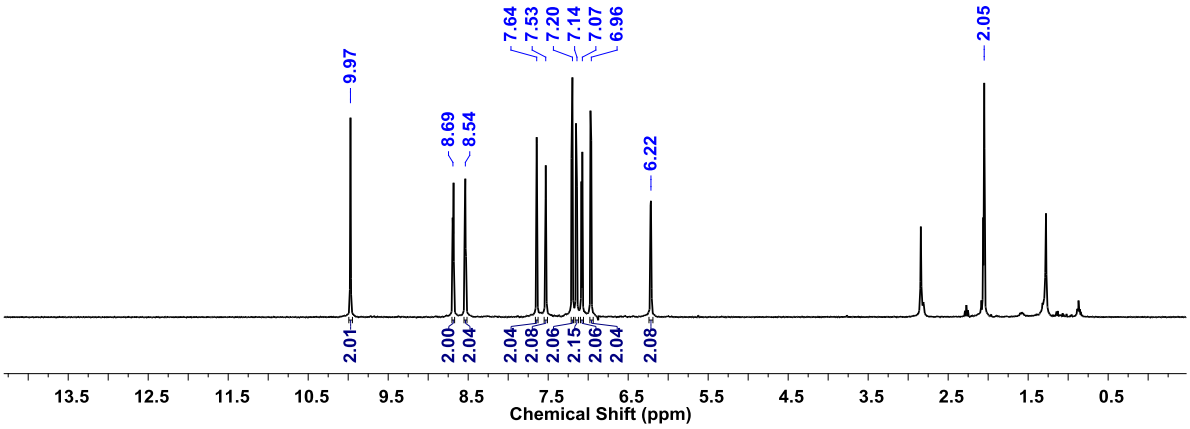

Figure III.A.14: ^1H NMR Spectrum of **III.A.22** in *Acetone-d_6*.

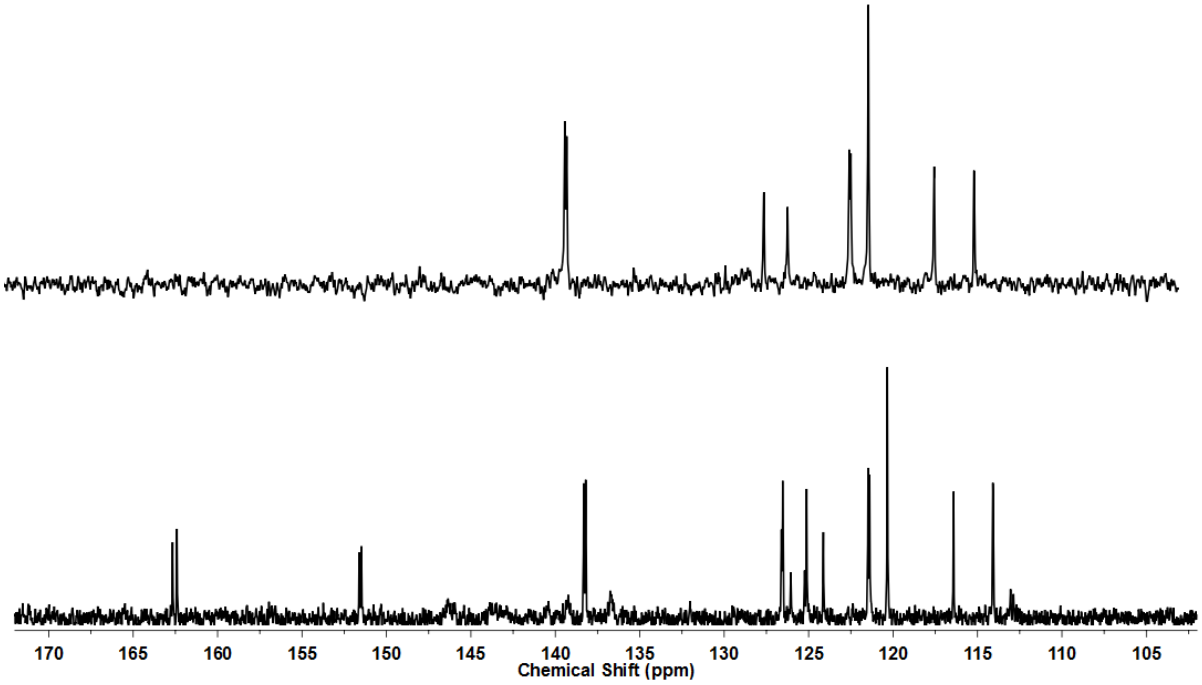

Figure III.A.15: (TOP) DEPT-90 NMR Spectrum (Bottom) ^{13}C NMR Spectrum of **III.A.22** in *Acetone-d_6*

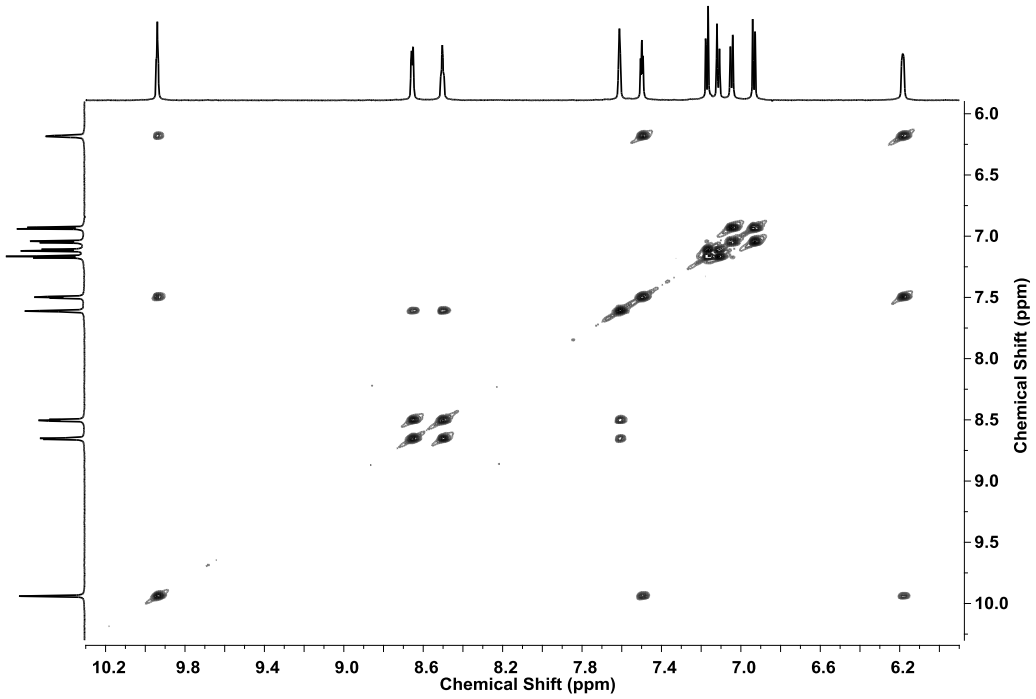

Figure III.A.16: ^{1}H-^{1}H COSY Spectrum of **III.A.22** in *Acetone-d_6*.

Similarly the obtained expanded norrole **III.A.21b** was also confirmed by HRMS (Figure III.A.17), ^{1}H-NMR (Figure III.A.18) and single- crystal X-ray diffraction analysis (Figure III.A.19).

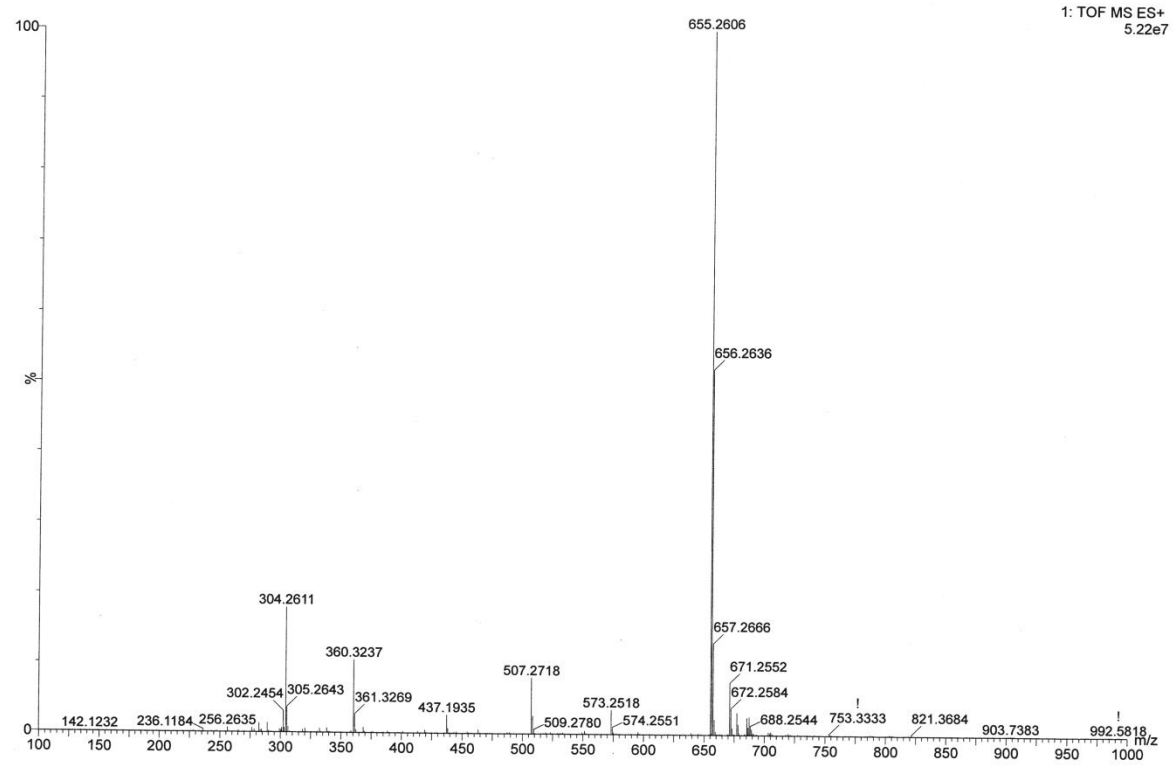

Figure III.A.17: HR-ESI-TOF mass spectrum of **III.A.21b**.

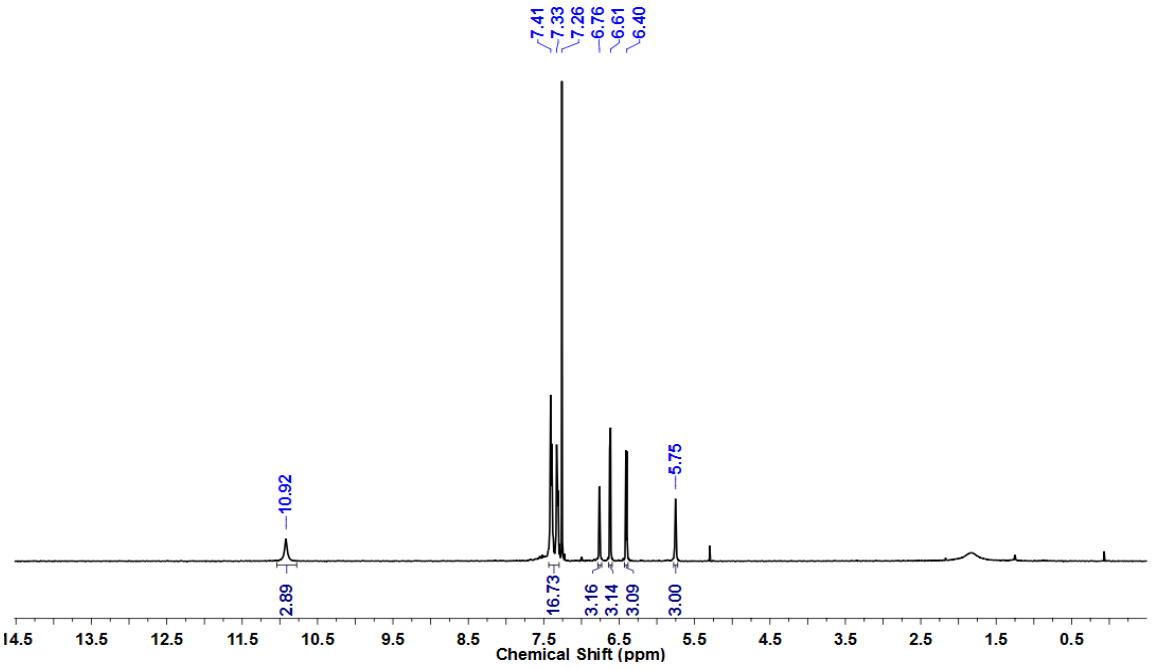

Figure III.A.18: ^{1}H NMR Spectrum of **III.A.21b** in $CDCl_3$.

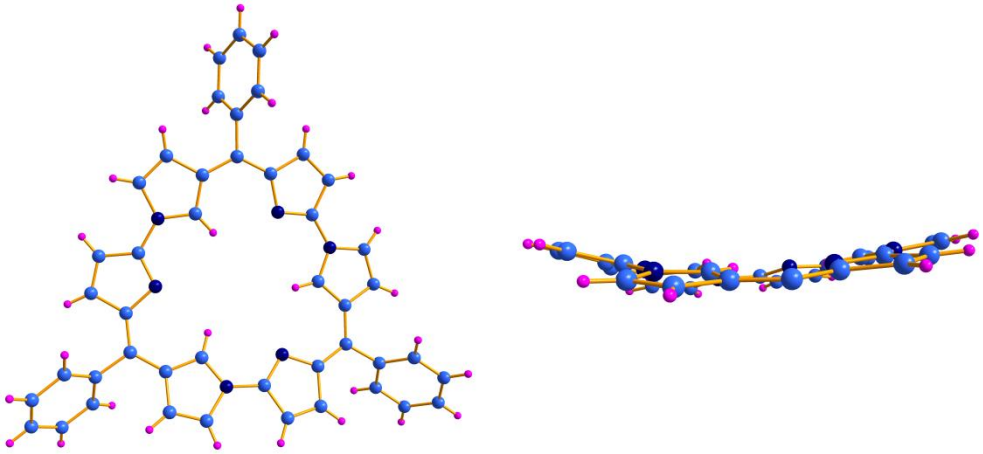

Figure III.A.19: Molecular Structure of **III.A.21b** top view (left) and side view (right).

III.A.7: Optical Properties

The **III.A.21a** and **III.A.22** form yellowish-green and red colored solution in common organic solvents respectively due to their extensive conjugation. The compound **III.A.21a** shows a maximum absorption at λ = 402 nm (ε = 45000) and a weak absorption at λ = 526 nm. The compound **III.A.22** exhibited maximum absorption at λ = 423 nm (ε = 152000) and two weak absorption at λ = 518 and 550 nm (Figure III.A.20). The observed weak and broad absorption suggested the anti-aromatic nature of these macrocycles. The computed nucleus independent chemical shift (NICS)[60] for these molecules using Gaussian 09[61] for qualitative and quantitative determination of π electron delocalization in macrocycle. The computed NICS(0) values for **III.A.21a**, **III.A.21b** and **III.A.22** are found to be δ = 4.5, 3.5 and 1.5 ppm respectively. These obtained positive NICS(0) values are indicative of weak anti-aromatic character of macrocycles.

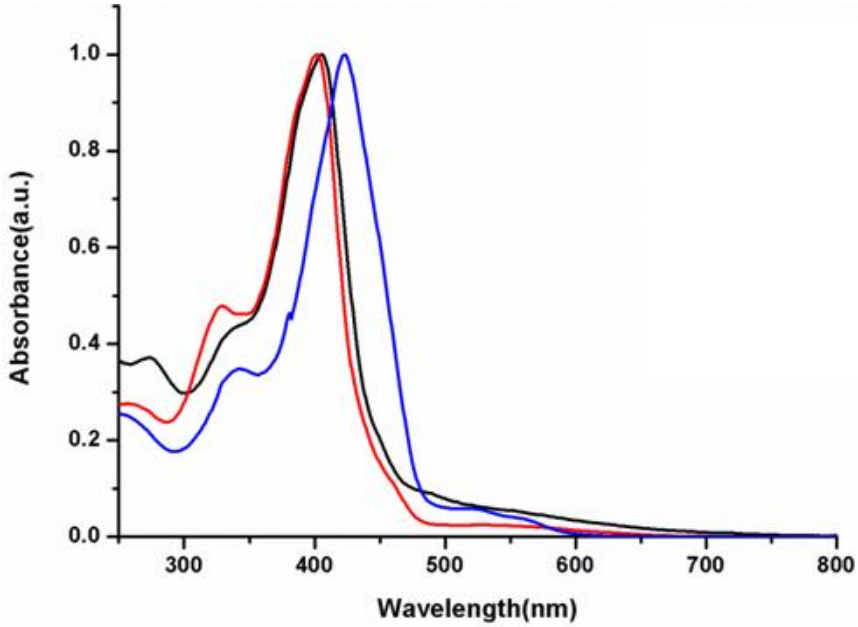

Figure III.A.20: Electronic spectra of ~10^{-6} M solutions of **III.A.21a**, **III.A.21b and III.A.22** in dichloromethane.

III.A.8: Conclusion

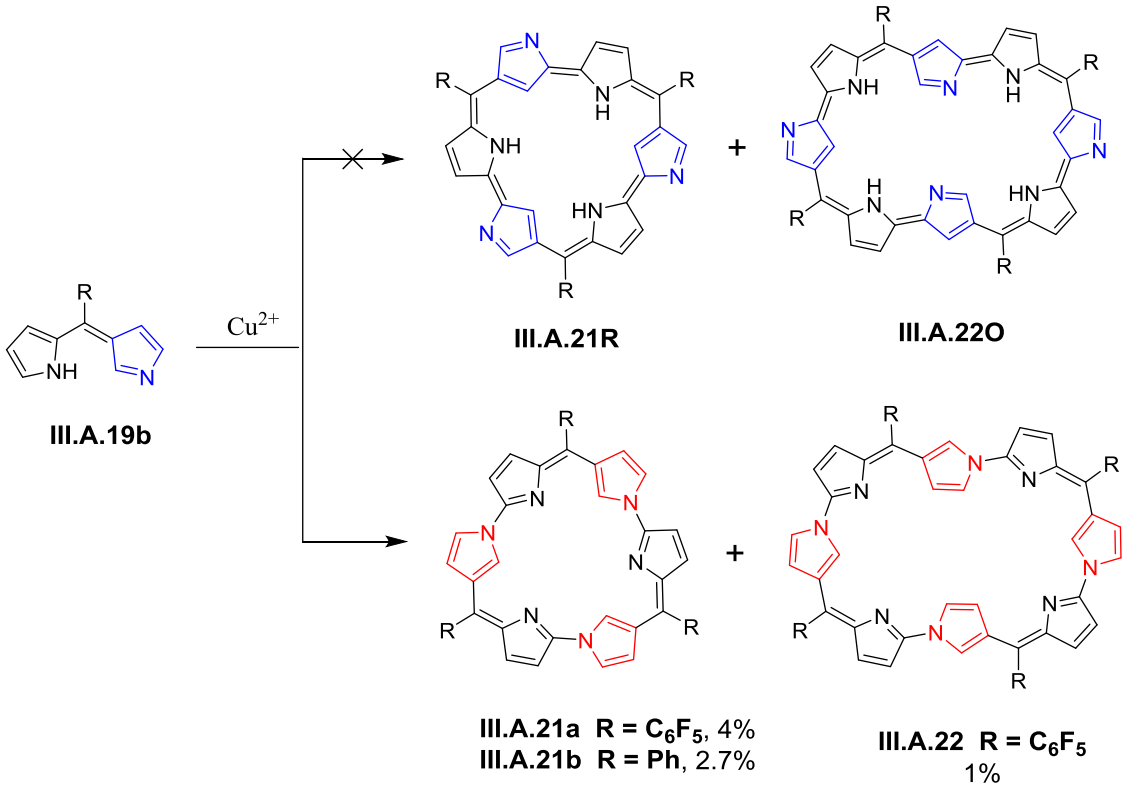

N-confused dipyrrin exhibits different reactivity with metal salts as compared to regular dipyrrin. Interestingly it undergoes intermolecular cyclomerization to form novel expanded norroles. These expanded norroles contain multiple C-N linkage along the conjugated pathway of the macrocyclic framework. The upfield and downfield chemical shift values in their ^{1}H NMR spectra suggest paratropic ring current effects in the solution state and anti-aromatic in nature. The synthetic protocol is very simple and can be catalyzed with a variety of metal salts. Compound **III.A.22** is the first example planar 32π octaphyrin and shows anti-aromatic in nature. These molecules are formed by accommodating more than two neo-confused pyrrole rings hence represent the novel class of stable, anti-aromatic expanded porphyrinoids with unusual π electron conjugation.

III.A.9: Experimental Section:

All reagents and solvents were of commercial reagent grade and used without further purification except where noted. Dry THF was obtained by refluxing and distillation over pressed Sodium metal. Column chromatography was performed on silica gel (230-400) in glass columns. ^{1}H NMR spectra were recorded either on a JEOL 400 MHz spectrometer, and chemical shifts were reported as the delta scale in ppm relative to $CHCl_3$ (δ = 7.26 ppm) or $(CH_3)_2CO$ (δ = 2.1 ppm) as internal reference for ^{1}H. Electronic spectra were recorded on a Perkin-Elmer λ-900 ultraviolet−visible (UV−vis) spectrophotometer. High Resolution Mass spectra were obtained using WATERS G2 Synapt Mass Spectrometer. Single crystals were grown by using chloroform and hexanes. Single crystal X-ray diffraction were performed on BRUKER KAPPA APEX II CCD Duo diffractometer (operated at 1500 W power: 50 kV, 30 mA) using graphite-monochromated Mo Kα radiation (λ = 0.71073 Å). Quantum mechanical calculations were carried out on Gaussian 09 program suite to estimate the NICS(0) values at the centre of the molecular plane of all the three macrocycles. Density functional theory (DFT) with Becke's three-parameter hybrid exchange functional and the Lee-Yang-Parr correlation functional (B3LYP) and 6-31G (d,p) basis set for all the atoms were employed in the calculations. The molecular structures obtained from single crystal analysis were used to obtain the geometry optimized structures. All the three macrocycles were found to have large

and positive NICS(0) values confirming their anti-aromatic nature. Computational calculations were carried out on the Supercomputer facility at IISER, Pune

Synthesis of III.A.20:

DDQ (0.56 g, 2.477 mmol, 1.1 equiv.) was added to *meso* phenyl N-confused dipyrromethane **III.A.18** (0.5 g, 2.25 mmol, 1 equiv.) dissolved in 25 ml dry tetrahydrofuran. The reaction was stirred for one hour reaction and then quenched with water. The organic phase extracted with dichloromethane, dried over sodium sulphate (Na_2SO_4) and evaporated in vacuo. Then, the crude product was dissolved in 25ml dry dichloromethane and triethyl amine (4.71 ml, 33.78 mmol, 15 equiv.). After 30 minutes, boron triflouride (4.17 ml, 33.78 mmol, 15 equiv.) was added and stirring continued overnight. The reaction was quenched with water and the organic phase extracted with dichloromethane and evaporated in vacuo. The residue obtained was purified by silica gel chromatography to yield 100 mg (15%) of **III.A.20** as a yellowish orange colored solid. ^{1}H NMR: Spectrum shows very broad signals that cannot be assigned properly. **UV-Vis** (CH_2Cl_2): λ_{max} = 445 nm; **HRMS** m/z calcd. for $[C_{15}H_{12}BF_3N_2\text{-}H]^+$ = 287.0968, Observed = 287.0973. **Crystal data:** $C_{15}H_{12}BF_3N_2$ (*Mr* = 288.08), Orthorhombic, space group P 21 21 21, *a* = 5.5466(16), *b* = 15.127(5), *c* = 15.528(5)Å, $\alpha = \beta = \gamma = 90.00°$, V = 302.8(7)Å^3, Z = 4, ρcalcd = 1.469 mg/m^3, T = 150K, Rint (all data) = 0.0599, *R*1(all data) = 0.1282 , *R*W (all data) = 0.2337, GOF = 0.676.

Synthetic Procedure for Expanded Norroles:

DDQ (0.8 g, 3.5 mmol, 2.2 equiv) was added to a stirred solution of *meso* pentafluorophenyl N-confused dipyrromethane (0.5 gm, 1.6 mmol, 1 equiv.) in tetrahydrofuran under nitrogen atmosphere. After stirring for 1hour, copper acetate (0.15 gm, 0.8 mmol, 0.5 equiv.) was added and stirring continued overnight. The reaction was quenched with water and the organic phase was extracted thrice with CH_2Cl_2. The combined organic phase was washed repeatedly with water, dried over Na_2SO_4 and the solvent evaporated in vacuo. The residue was purified by SiO_2 column chromatography using a mixture of hexane and ethyl acetate as the eluent. The first yellowish green fraction afforded **III.A.21a** (60 mg, 4%) followed by a reddish coloured fraction yielded **III.A.22** (20mg, 1%).

III.A.21a: **^{1}H NMR** ($CDCl_3$, 400 MHz, 298 K) δ = 11.16 (m, 3H), 6.78 (m, 3H), 6.50 (d, J = 4Hz, 3H), 6.48 (d, J = 4Hz, 3H), 5.62 (m, 3H); **^{13}C NMR** ($CDCl_3$, 100 MHz, 298K) δ = 113.97, 120.45, 120.95, 124.38, 126.86, 127.24, 137.84, 151.87, 163.62; **UV-Vis** (CH_2Cl_2): $\lambda_{max}(\varepsilon)Lmol^{-1}cm^{-1}$: 402 nm (45,000), 526 nm (1092); **HRMS** *m/z calcd.* for $[C_{45}H_{15}F_{15}N_6+H]^+$ = 925.1197, Observed = 925.1188; **Crystal data**: $C_{45}H_{15}F_{15}N_6$(*Mr* = 927.65), monoclinic, space group *P21/n*, *a* = 10.493(2), *b* = 20.963(4), *c* = 34.490(7)Å, *α* = 90.00, *β* = 81.887(7), *γ* = 90.00°, V = 7510(3)Å^3, Z = 8, *ρ*calcd = 1.641 mg/m^3, T = 150 K, Rint (all data) = 0.0687, R1 (all data) = 0.2224, RW (all data) = 0.2330, GOF = 0.960.

III.A.22: **^{1}H NMR** (Acetone-d_6, 400 MHz, 298K) δ = 9.97 (m, 2H), 8.69 (d, J = 4.0 Hz, 2H), 8.54 (m, 2H), 7.64 (m, 2H), 7.53 (m, 2H), 7.21 (d, J = 4.0 Hz, 2H), 7.15 (d, J = 4.0 Hz, 2H), 7.08 (d, J = 4.0 Hz, 2H), 6.97 (d, J = 4.0 Hz, 2H), 6.22 (m, 2H); **^{13}C NMR** (Acetone-d_6, 100 MHz, 298K) δ 114.08, 116.42, 120.34, 120.39, 120.48, 124.13, 125.12, 125.24, 126.06, 126.53, 138.20, 138.31, 151.48, 151.62, 162.41, 162.66; **UV-Vis** (CH_2Cl_2): $\lambda_{max}(\varepsilon)Lmol^{-1}cm^{-1}$ = 423 nm (1,52,400), 518 nm (9150), 550 nm (6550); **HRMS** *m/z calcd*. for $[C_{60}H_{20}F_{20}N_8+H]^+$ = 1233.1570, Observed = 1233.1587; **Crystal data**: $C_{60}H_{20}F_{20}N_8$ (Mr = 1232.84), Triclinic, space group P-1(No. 2), *a* =16.937(6), *b* =17.127(6), *c* = 19.802(7)Å, *α* = 69.219(5), *β* = 73.707(5), *γ* = 60.742(6)°, V = 4645(3)Å^3, Z = 3, ρcalcd = 1.322 mg/m^3, T = 150K, Rint (all data) = 0.0718, R1(all data) = 0.1983, RW (all data) = 0.2505, GOF = 0.592.

Synthesis of III.A.21b:

The procedure mentioned above was employed with *meso*-phenyl N-confused dipyrromethane (0.5 g, 2.25 mmol, 1 equiv.), DDQ (1.125 g, 4.955 mmol, 2.2 equiv.) and copper acetate (0.2027 g, 1.125 mmol, 0.5 equiv.). Yield 40 mg (2.7%). **^{1}H NMR** ($CDCl_3$, 400MHz, 298K) δ = 5.75 (s, 3H), 6.41 (d, J = 4.0 Hz, 3H), 6.63 (d, J = 4.0 Hz, 3H), 6.77(m, 3H), 7.31-7.41(m, 15H) 10.92(s, 3H); **UV-Vis** (CH_2Cl_2): $\lambda_{max}(\varepsilon)Lmol^{-1}cm^{-1}$ = 405 nm (141,200); **HRMS** *m/z* calcd. for $[C_{45}H_{30}N_6+H]^+$ = 655.2611, Observed = 655.2606; **Crystal data:** $C_{45}H_{30}N_6$(*Mr* = 654.75), monoclinic, space group *P21/c (No.14)*, *a* = 8.7927(17), *b* = 17.4956(16), *c* = 21.281(2)Å, *α* = 90.00, *β* = 106.110(2), *γ* = 90.00°, V = 6722.0(11)Å^3, Z = 8, *ρ*calcd = 1.294 mg/m^3, *T* = 150K, Rint (all data) = 0.0628, *R*1(all data) = 0.1643, *R*W (all data) = 0.1857, GOF = 0.977.

Section B: Reactivity of Doubly N-Confused Dipyrrins with Metal Salts

III.B.1: Introduction:

Dipyrrin consists of two pyrrole units attached to the *meso*-carbon atom through an alpha carbon atom whereas N-confused dipyrrin contains of a pyrrole unit connected through a beta carbon to the nitrogen. However, the role of N-confused dipyrrin as a metal complexing agent has eluded chemists probably due to its unconventional orientation of the pyrrole rings. The earlier part of this chapter described the altered reactivity of dipyrrin with various metal salts upon changing the connectivity between the two pyrroles in a dipyrrin framework. Interestingly, as compared to the regular dipyrrins, N-confused dipyrrins undergoes intermolecular oxidative cyclomerization in the presence of metal ions into new macrocyclic products known as expanded norroles[53].

The tetrapyrene **III.B.1** with two terminal N-confused pyrrole rings undergoes intramolecular oxidative cyclization reaction with DDQ in acetonitrile into corrorin **III.B.2** (Scheme III.B.1)[62]. The corrorin **III.B.2** was previously obtained by [2+2] acid catalyzed condensation reaction of N-confused dipyrromethane[63].

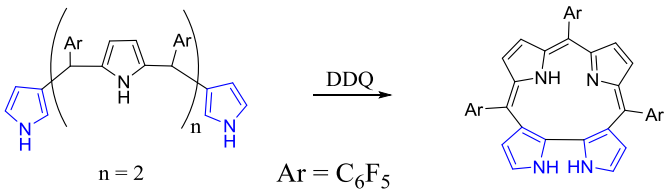

III.B.1 **III.B.2**

Scheme III.B.1: Synthesis of Corrorin

The two terminal N-confused pyrrole rings in pentapyrrane **III.B.3** undergoes unique ring closure reaction to doubly N-confused sapphyrin involving the two confused pyrrole in the bipyrrolic unit. However cyclization reaction proceeds by β,α-α,β coupling instead of expected β',α-α,β' coupling as like cyclization of the doubly N-confused bilane to corrorin[62] to provide the dihydrosapphyrinarin **III.B.4** with sp^3 *meso*-carbon[64]. As understood from the conversion of corrorin to oxyindolophyrin[63], the bipyrrolic unit in **III.B.4** is also reactive and experiences ring

contraction with triethyl amine to form the tetrapyrrolic macrocycle pyrrolyl norrole **III.B.5** (Scheme III.B.2). The **III.B.5** also underwent ring expansion reaction with DDQ to a new pentacyclic macrocycle **III.B.6** described as isosmaragdyrin[65] analogue in which two confused pyrrole rings are connected by N,α-α,β linkage.

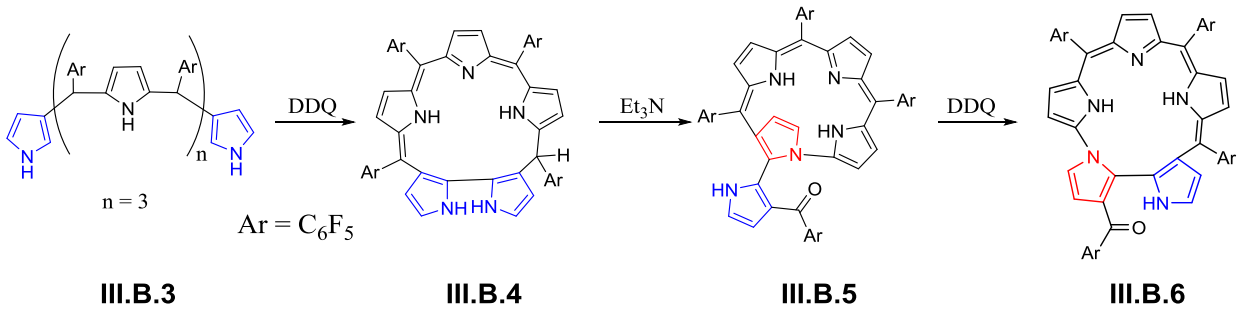

III.B.3 **III.B.4** **III.B.5** **III.B.6**

Scheme III.B.2: Synthesis of dihydrosapphyrinarin and its reactivity

In contrast to the ring closure at both the α-positions of the confused pyrroles observed with **III.B.3**, the hexapyrrane **III.B.7** with two terminal N-confused pyrroles undergoes oxidative ring closure reaction with β,N-α,β linkage mode to a new example of neo-confused hexaphyrin **III.B.8** which contain two confused pyrrole rings[66]. Further, **III.B.8** provided neo-fused hexaphyrin **III.B.9** containing 5,5,5,7-tetracyclic ring in the framework by oxidative intramolecular ring closure reaction with DDQ (Scheme III.B.3).

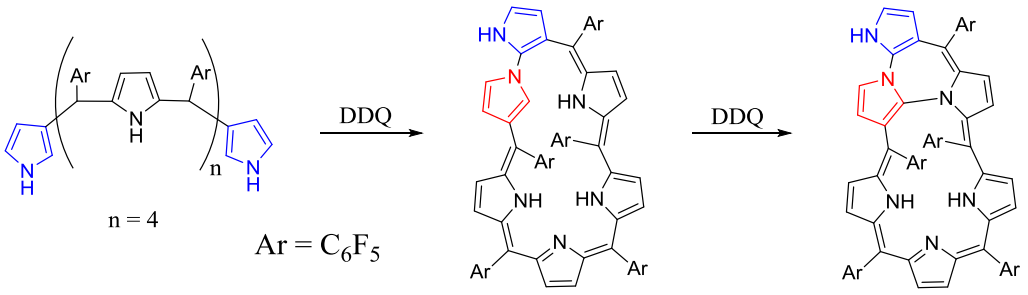

III.B.7 **III.B.8** **III.B.9**

Scheme III.B.3: Synthesis of Neo-fused hexaphyrin and its reactivity

III.B.2: Objective:

The unsuccessful attempt at the synthesis of N-confused dipyrrin metal complex inspired to explore reactivity of doubly N-confused dipyrrin with different metal salts by following the similar protocol as used for dipyrrins.

III.B.3: Synthesis of Aza-Heptalenes:

Dipyrrin **III.B.11** (doubly N-confused dipyrrin) was obtained by the facile oxidation of 3,3'-dipyrromethane[49] **III.B.10** and it was further reacted with metal salts in dry THF without additional purification (Scheme III.B.4). A pink colored solution was obtained upon Overnight stirring of **III.B.12** with copper(II) acetate yielded a pink colored solution which displayed a *m/z* value 615.0664 (Figure III.B.5) in its HR –MS spectrum (insert the mass spectrum here). It was two units less than the expected nornorrole **III.B.15** (Figure III.B.17). The nature of the products formed from **III.B.11** was dependent on the metal salt used in the reaction. When **III.B.11** was reacted with iron(III) acetylacetonoate under similar reaction conditions, two

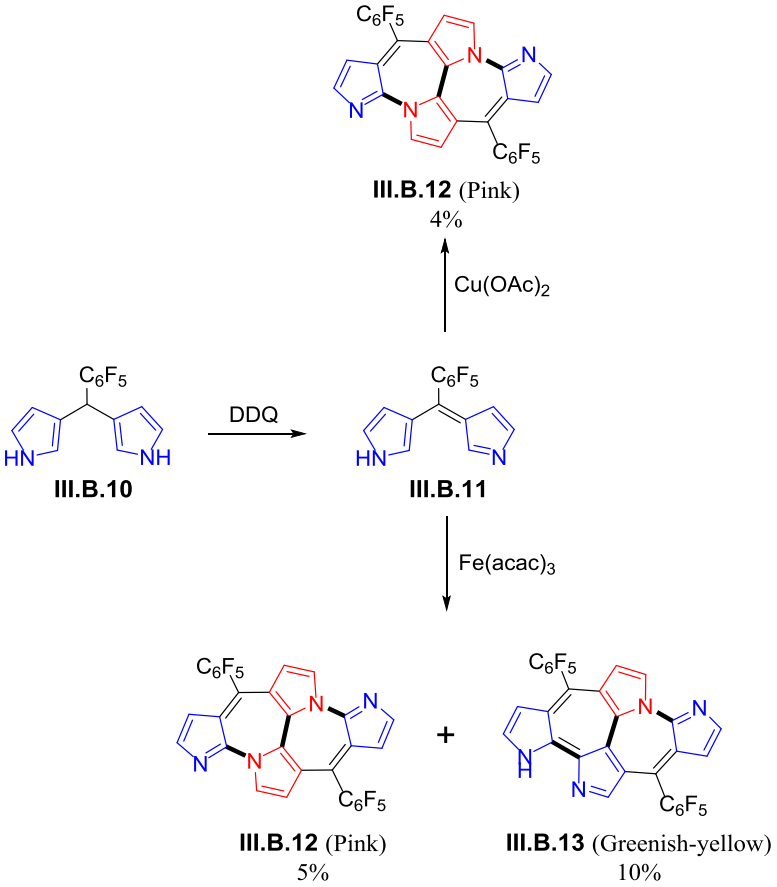

Scheme III.B.4: Synthesis of Aza-heptalenes

different products were obtained in 5% and 10% yields respectively. Apart from the pink colored solution mentioned above, a greenish-yellow colored solution was isolated by column chromatographic separation. Surprisingly, the high resolution mass spectrum obtained for pink and greenish-yellow color solution displayed the same *m/z* value suggestive of structural isomers for the unexpected cyclodimer (Figure III.B.5 and III.B.8).

III.B.4: Single Crystal X-Ray Diffraction Analysis of Aza-Heptalenes:

Both the pink and greenish-yellow color solutions were allowed to crystallize in dichloromethane by slow vapor diffusion of n-hexane. Unambiguous determination of molecular structures by single crystal X-ray diffraction studies confirmed the cyclodimers **III.B.12** and **III.B.13**[67]. Molecular structure of **III.B.12** confirmed the formation of an unusual bicyclic C-fused ring embedded in a macrocyclic framework similar to that of ‘‘nornorrole’’ **III.B.15**. This can be envisaged by the oxidative coupling induced ring closure reaction between the inwardly pointed α-carbons of the neo-confused pyrrole in the contracted macrocycle **III.B.15**. Both the doubly N-confused dipyrrin units are connected to each other in a head-to-tail fashion leading to the formation of two C_α-N linked bipyrrole units (Figure III.B.1). Both the neo-confused pyrrole rings with their α-carbon atoms pointed towards the macrocyclic core were found to be at a distance of 1.413(3) Å. This closeness is good enough for oxidative ring closure reaction to afford another C_α-C_α linked bipyrrolic unit. The highly flat conformation of this molecule suggested effective delocalization of lone pair of electron on N-linked pyrrole. The planar nature of this molecule also aids weak π stacking as seen in its crystal packing.

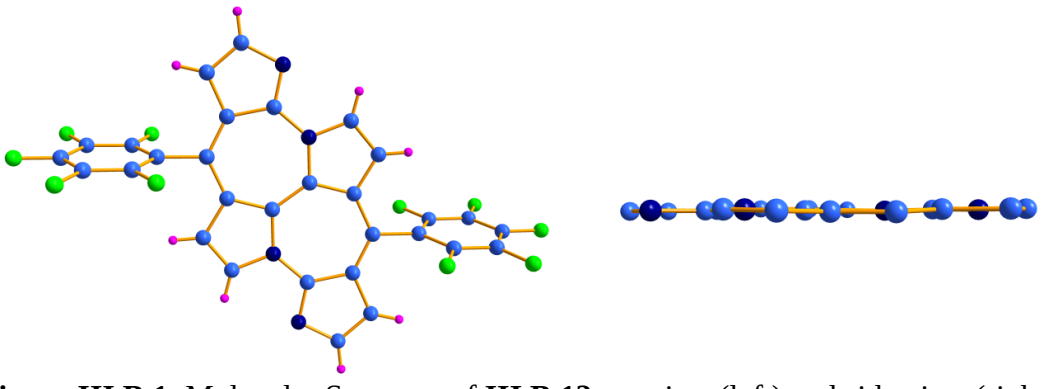

Figure III.B.1: Molecular Structure of **III.B.12** top view (left) and side view (right).

The molecular structure of **III.B.13** disclosed the flat geometry with unsymmetrical connectivity between the two doubly N-confused dipyrrin units due to the three different bipyrrole units. As compared to the **III.B.12**, the unconventional connectivity leading to C_α-N and C_α-C_α linkage was observed between the two doubly N-confused dipyrrin units (Figure III.B.2). The α-carbon of the N-linked pyrrole in one dipyrrin unit and β-carbon of the other pyrrole B present in the other dipyrrin are separated by a distance of 1.401(7) Å. The induced ring closure due to oxidative coupling between these carbon atoms leads to the unconventional C_α-C_β bipyrrole unit at the centre of macrocycle. This bond distance is shorter than the 1.49 Å reported for similar bond in C-fused norrole[49]. The flat conformation indicates the lone pair of electron present on N-linked pyrrole is delocalized over the macrocycle framework.

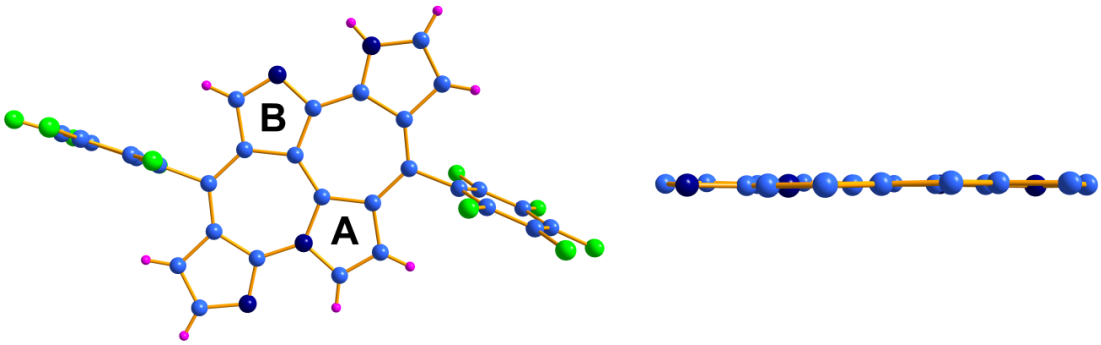

Figure III.B.2: Molecular Structure of **III.B.13** top view (left) and side view (right).

However, the single crystal X-ray diffraction studies were not precise enough to identify the location of the proton with respect three pyrrole nitrogen atoms in **III.B.13**. The molecule suggested the tautomeric structures with possible location of hydrogen on any of these pyrrole nitrogens. Therefore, the N-methylated derivative of this molecule was synthesized to locate the exact position of the NH in this macrocycle. The X-ray diffraction analysis of **III.B.Me-13** derivative confirmed the location of methyl group on the nitrogen of the C_α-C_α linked bipyrrolic unit (Figure III.B.3). The structure of the methyl derivative **III.B.Me-13** is similar to that of parent molecule **III.B.13** with fused seven membered bicyclic rings at the centre. All the pyrrole rings and the heptalene[68] moiety are planar enough to suggest the delocalization of the lone pair of electrons of N-linked pyrrole nitrogen with the π-electron cloud of molecule (CCDC 1024460 for **III.B.12**, 1024461 for **III.B.13** and 1024462 for **III.B.Me-13**)[58].

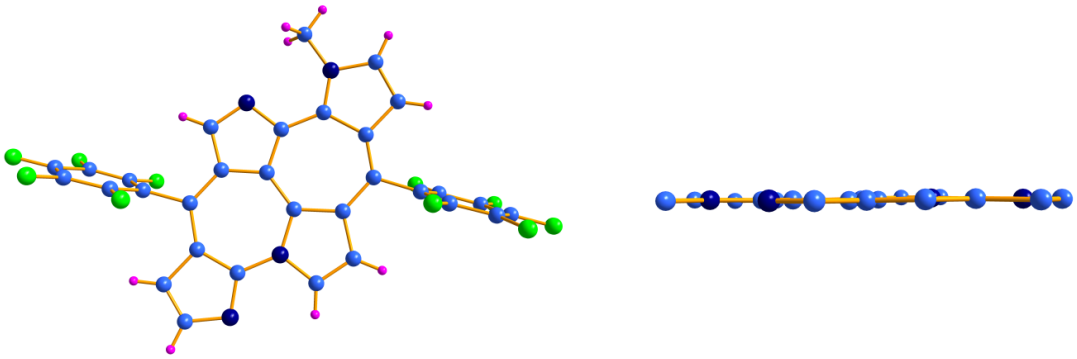

Figure III.B.3: Molecular Structure of **III.B.Me-13** top view (left) and side view (right).

III.B.5: Discussion on Heptalenes:

The cyclodimers **III.B.12**, **III.B.13** and **III.B.Me-13** represent the examples of substituted heptalenes whose planarity is favored by the fusion of two pyrrole rings to the central bicyclic core. Planar bicyclic non-benzenoid aromatic compounds such as pentalene and heptalene are of fundamental interest. Pentalene composed of two fused cyclopentadiene rings and heptalene contains two fused cycloheptatriene rings. Pentalene is anti-aromatic because it has 4nπ electron hence too unstable. But its substituted derivatives such as 1,3,5-tri-*tert*-butylpentalene[69] and dibenzopentalene[70] are thermally stable. Heptalene was first synthesized by by Dauben and Bertelli in 1961[71] and described as unstable, non-planar and non-aromatic compound while its dianion is thermally stable, planar and aromatic[72]. The substituted heptalene such as dicyclopenta[ef,kl]heptalene[68] is a thermodynamically stable non-benzenoid isomer of pyrene that constitutes the Huckel 14π aromatic peripheral systems perturbed by a central double bond. The valence bond formulae of **A** and **B** contain 14 π electron system peripheral to the ethylene bridge (Figure III.B.4). These kinds of polycyclic conjugated aromatic hydrocarbons are of fundamental interest for their relationship between structure and aromaticity.

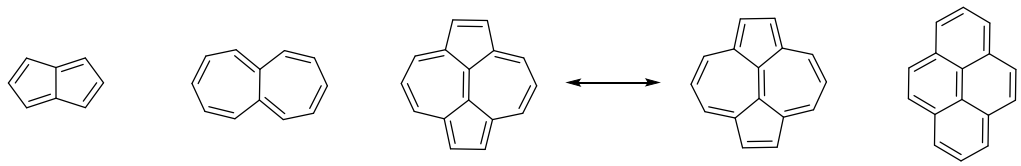

Figure III.B.4: Bicyclic non-benzenoid molecules

III.B.6: Characterization of Aza-Heptalenes:

This macrocycle **III.B.12** has poor solubility in common organic solvents. The ^{1}H NMR spectrum of **III.B.12** indicated the symmetrical structure with four doublets at δ = 6.84, 7.79, 7.96 and 9.53 ppm corresponding to equal number of protons (Figure III.B.6). The ^{1}H–^{1}H COSY spectrum displayed two types of correlations for doublets at (i) 6.84 and 7.79, (ii) 7.96 and 9.53 ppm corresponding to the two different sets of proton on α-carbon and β-carbon atoms of the four pyrrole rings (Figure III.B.7).

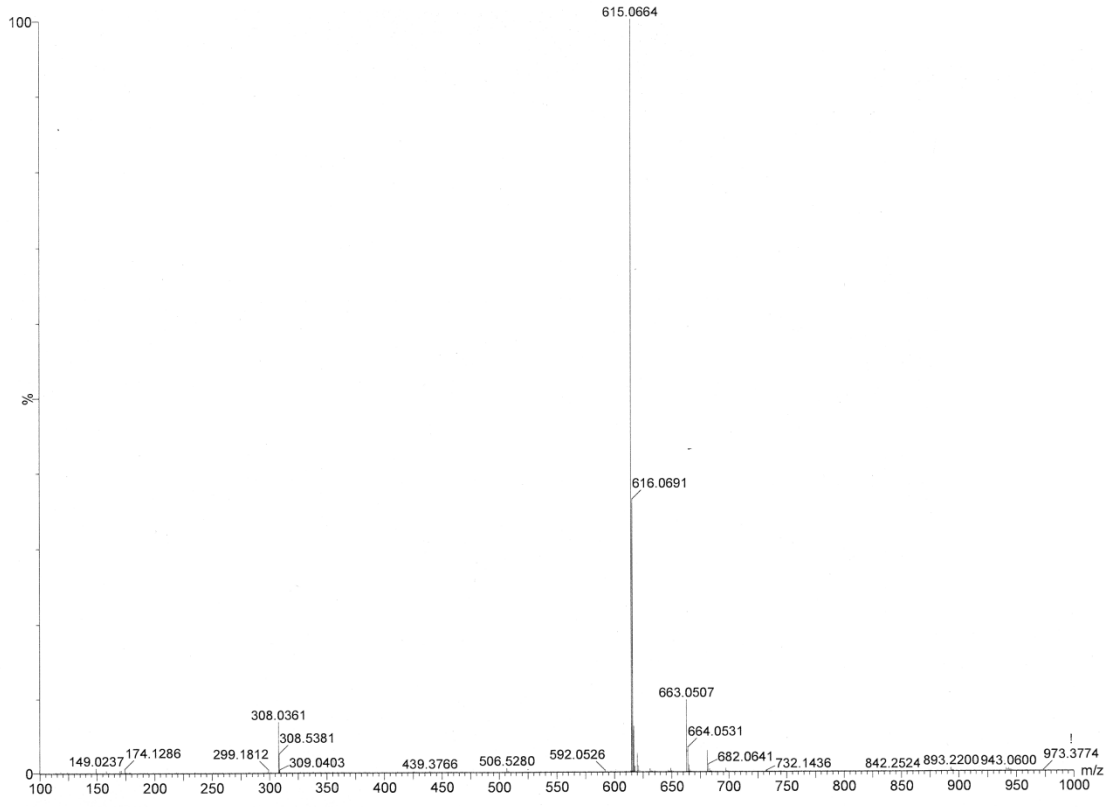

Figure III.B.5: HR-ESI-TOF mass spectrum of **III.B.12**

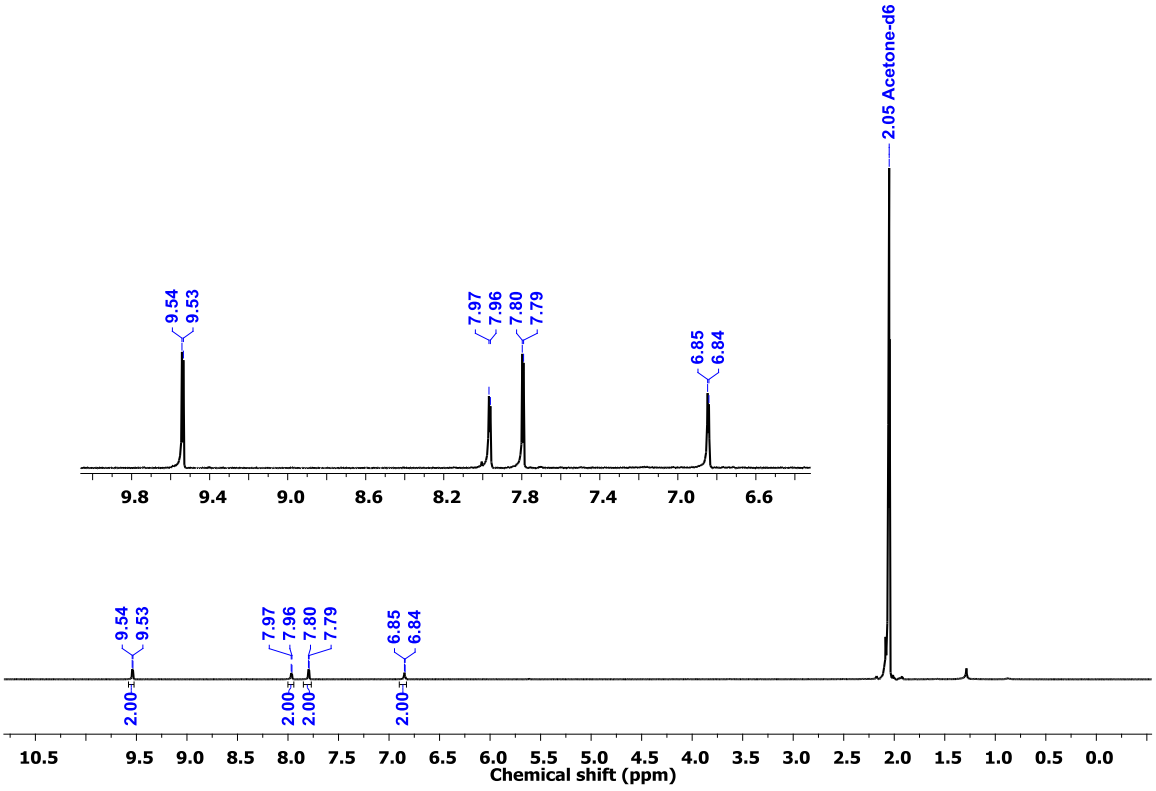

Figure III.B.6: ^{1}H-NMR spectrum of **III.B.12** in *Acetone-d_6* at 295K.

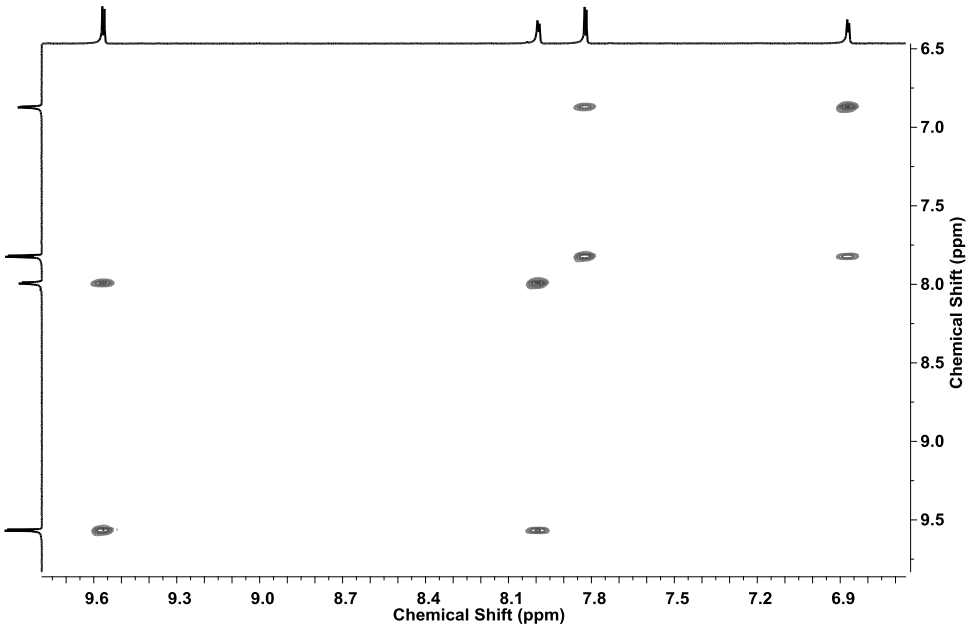

Figure III.B.7: ^{1}H-^{1}H COSY Spectrum of **III.B.12** in *Acetone-d_6* at 295K.

In contrast to the **III.B.12**, the ^{1}H NMR spectrum for **III.B.13** recorded in *Dimethyl Sulphoxide-d_6* indicated the unsymmetrical nature of compound. Eight signals were observed in the region δ = 6.00 to 13.50 ppm at ambient temperature. The six doublets at δ = 6.28, 6.73, 7.19, 7.50, 7.82 and 9.28 ppm along with a sharp singlet at 8.71 ppm and a broad singlet at 13.46 ppm were observed corresponding to equal number of protons (Figure III.B.9). The broad singlet at 13.46 ppm disappeared upon addition of D_2O suggesting the presence of one NH in the molecule (Figure III.B.10). In the ^{1}H-^{1}H COSY spectrum, the singlet at 8.71 ppm is corresponds to the proton on the α-carbon of the pyrrole ring **B** and three correlations were observed between six doublets which justified for the other protons on the α and β-carbon of the macrocycle (Figure III.B.11). DEPT-90 measurements indicated seven ^{13}C signals for the CH at 108.72, 112.25, 112.80, 126.97, 130.80, 140.26, and 149.92 ppm suggesting unsymmetrical structure of molecule (Figure III.B.12). The HMBS experiment also indicated seven different correlations as expected and support the above analysis (Figure III.B.13).

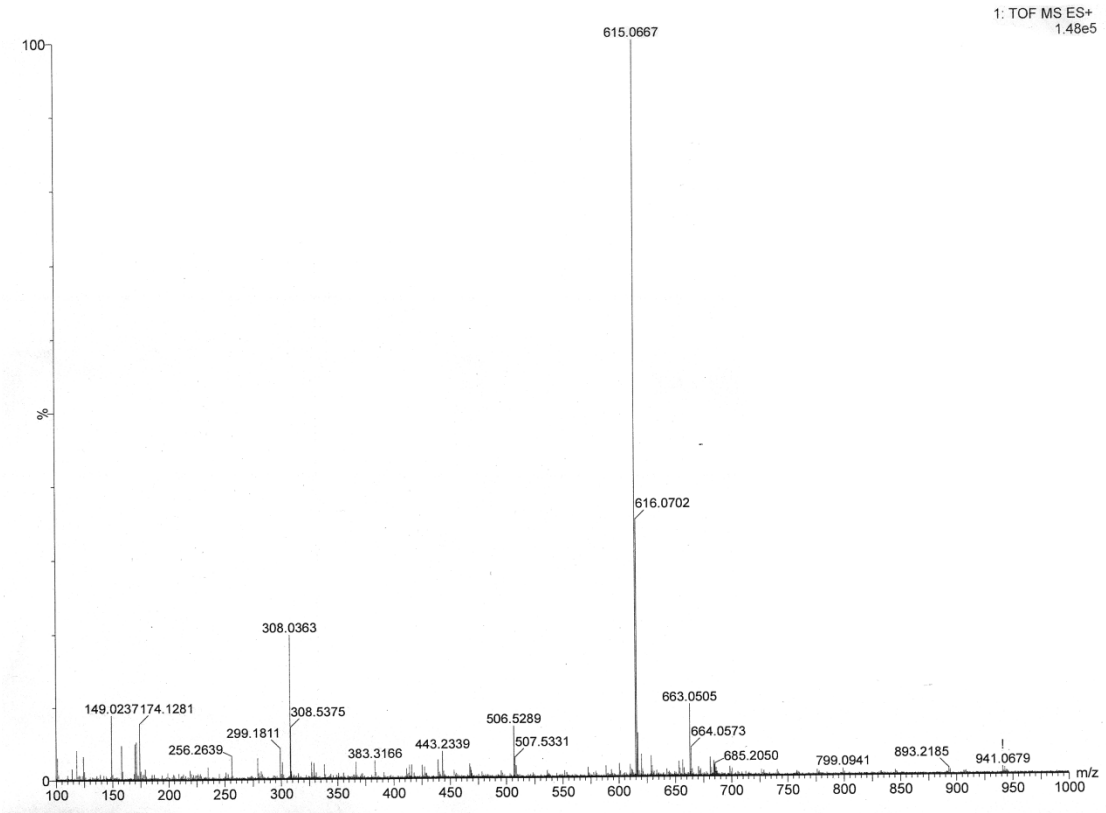

Figure III.B.8: HR-ESI-TOF mass spectrum of **III.B.13**

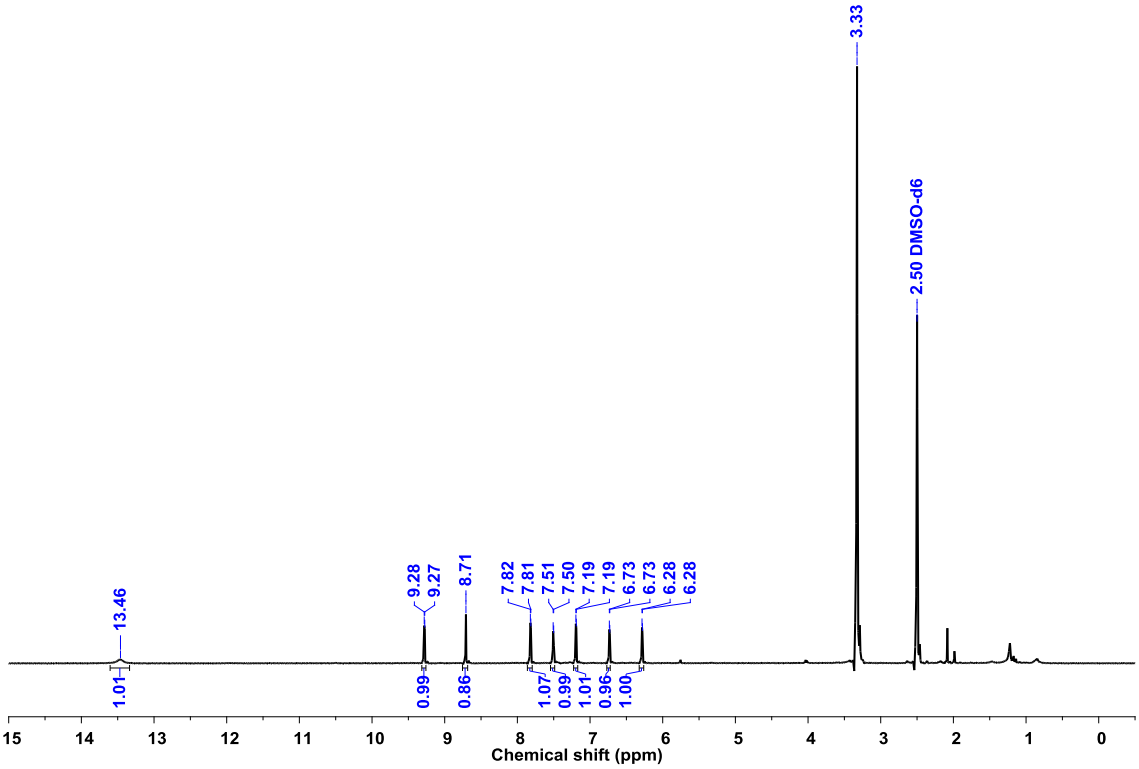

Figure III.B.9: ^{1}H-NMR spectrum of **III.B.13** in *Dimethyl Sulphoxide-d_6* at 295K.

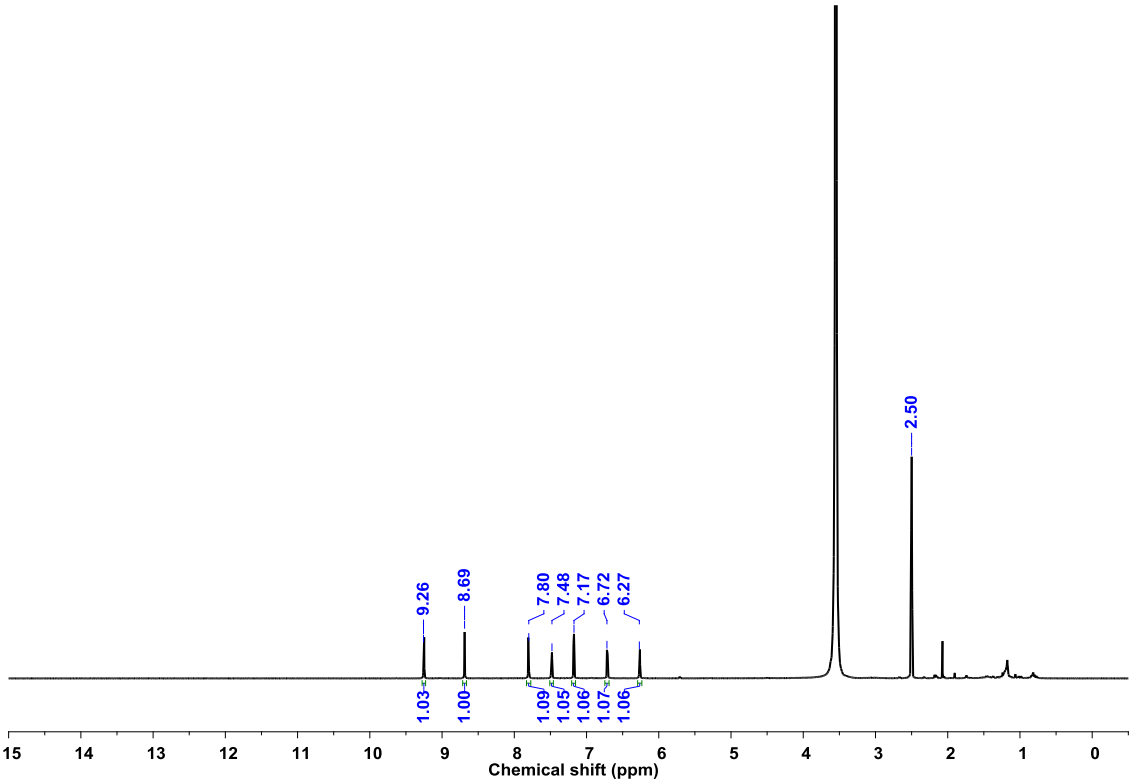

Figure III.B.10: ^{1}H-NMR spectrum of **III.B.13** after D_2O exchange in *Dimethyl Sulphoxide-d_6*

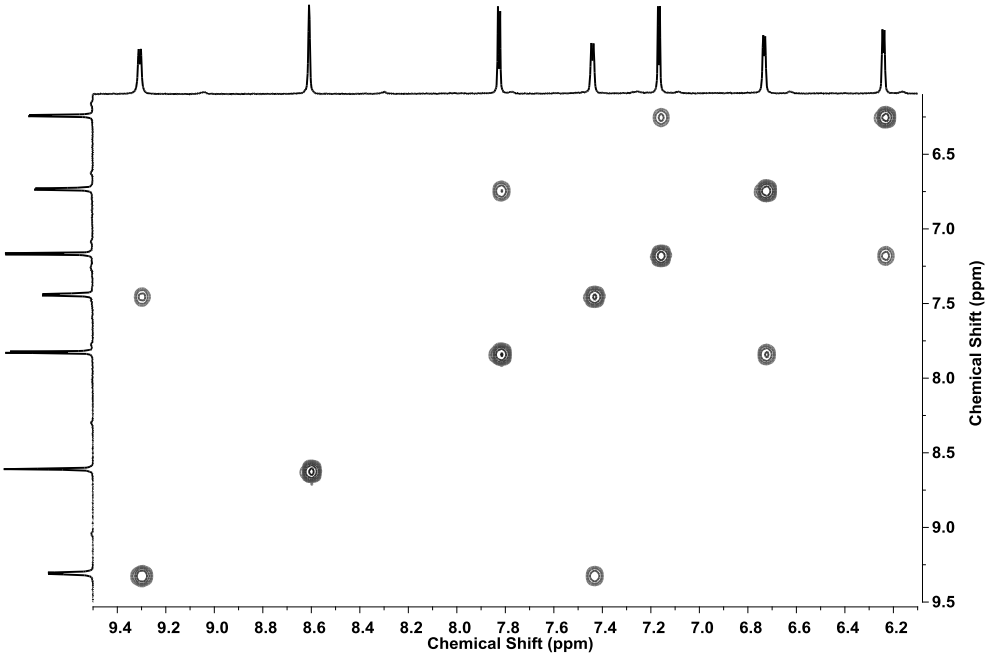

Figure III.B.11: ^{1}H-^{1}H COSY spectrum of **III.B.13** in *Dimethyl Sulphoxide-d_6* at 295K.

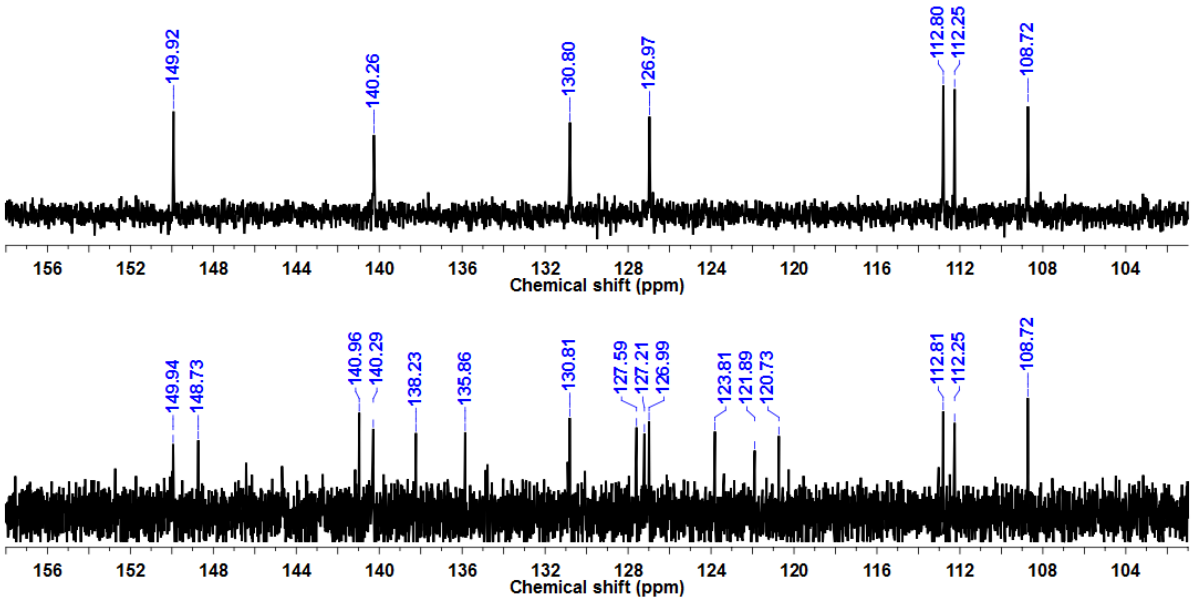

Figure III.B.12: (Top) DEPT-90 and (Bottom) ^{13}C-NMR spectrum of **III.B.13** in *Dimethyl Sulphoxide-d_6* at 295K.

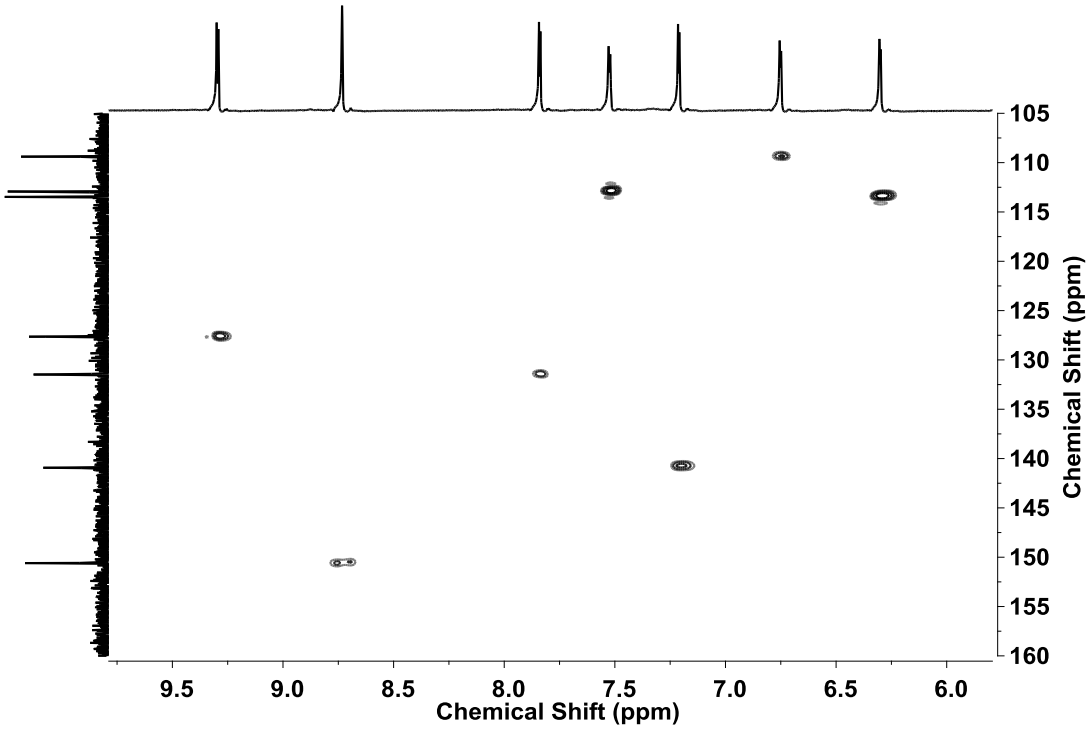

Figure III.B.13: HMBC spectrum of **III.B.13** in *Dimethyl Sulphoxide-d_6* at 295K.

The ^{1}H NMR spectrum for **III.B.Me-13** displayed a total of eight signals, with a singlet at 4.75 ppm corresponding to three protons which are assigned to the methyl group and remaining seven signals resonated at the same chemical shift as observed for the **III.B.13** (Figure III.B.15). The correlation observed in ^{1}H-^{1}H COSY spectrum was similar to **III.B.13** (Figure III.B.16).

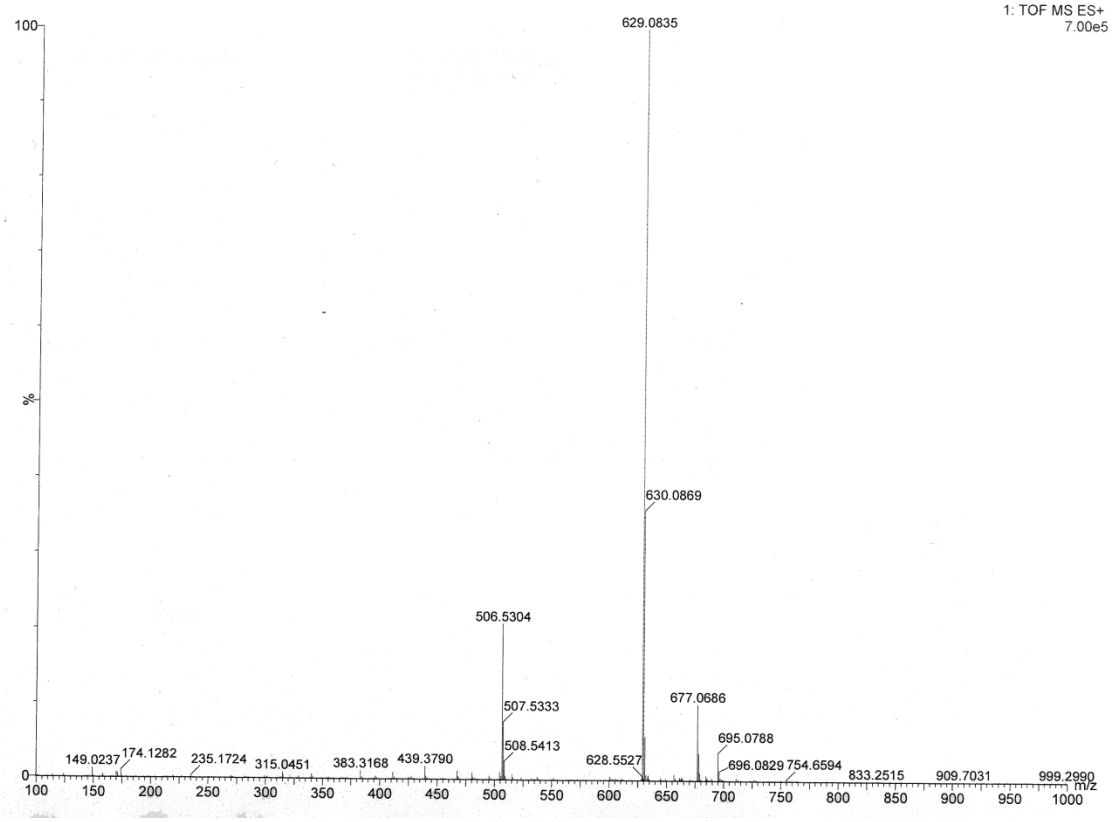

Figure III.B.14: HR-ESI-TOF mass spectrum of **III.B.Me-13**

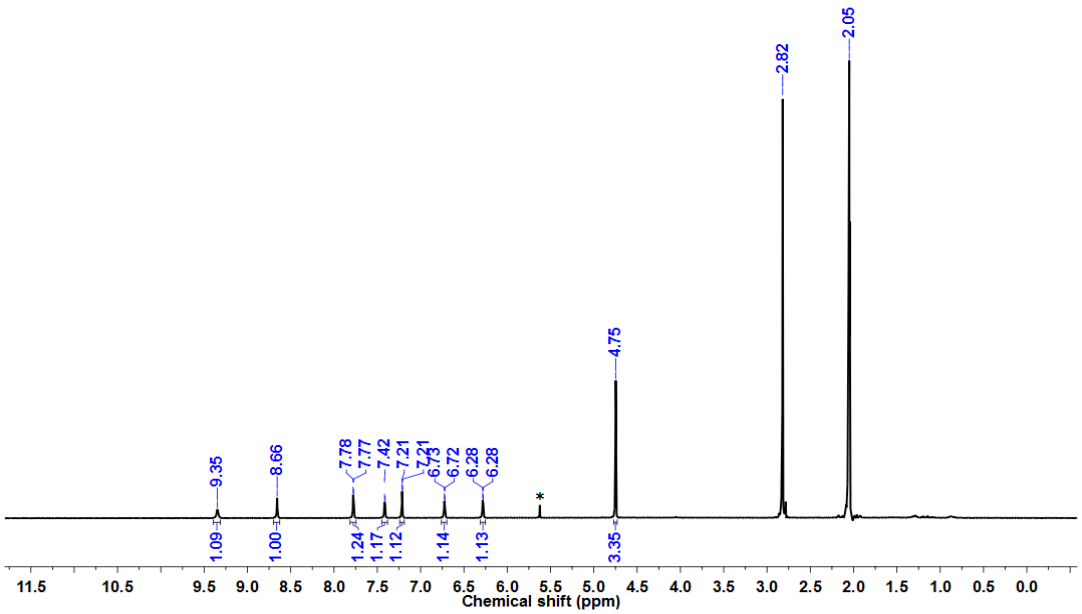

Figure III.B.15: ^{1}H-NMR spectrum of **III.B.Me-13** in *Acetone-d_6* at 295K.

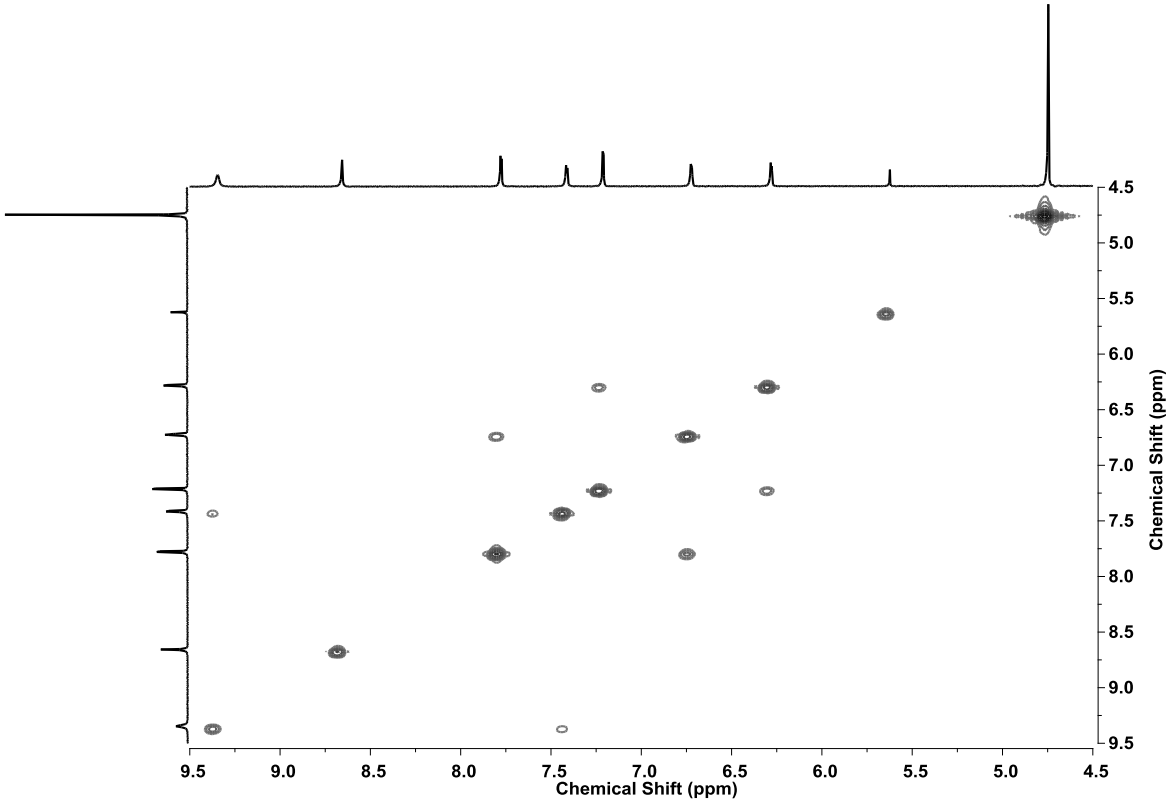

Figure III.B.16: ^{1}H-^{1}H COSY spectrum of **III.B.Me-13** in *Acetone-d_6* at 295K.

The observed downfield chemical shift values for **III.B.12** and **III.B.13** signified a diatropic ring current effect. However the expected nornorrole **III.B.15** is structural isomer of norcorrole **III.B.14**[34b, 54] and should be 20π anti-aromatic system with considerable upfield chemical shift values. The observed diatropic ring current effect for **III.B.12** and **III.B.13** suggested them as derivatives of substituted heptalenes, rather than typical porphyronoids, and hence can be aromatic in nature.

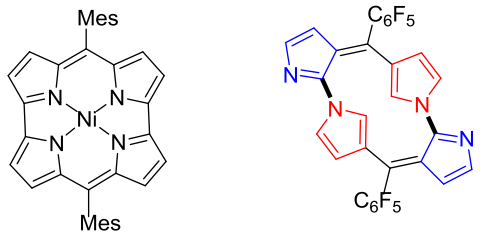

Norcorrole
III.B.14

Nornorrole
III.B.15

Figure III.B.17: Chemical structues of Norcorrole (**III.B.14**) and Nornorrole (**III.B.15**)

III.B.7: Optical Properties:

The electronic absorption spectrum was found to be similar for both the macrocycles, **III.B.12** and **III.B.13**, but different than norcorrole[34b, 54]. They exhibited multiple absorptions and relatively blue shifted as compared to the norcorrole. The aza-heptalene **III.B.12** exhibited absorptions at 262 nm (e = 17 800), 280 (17 800), 361 (10 000), 514 (6700) and **III.B.13** absorbed at 268 (32 600), 282 (32 500), 346 (33 600), 451 nm (8800) in dichloromethane (Figure III.B.18). Absorptions with similar energy were observed for the **III.B.Me-13** in dichloromethane. Porphyrinoids are known to absorb in the visible region of the electromagnetic spectrum followed by weak and low energy absorptions. These observed high energy absorptions are similar to heptalene like systems and therefore these molecules can be best described as aza-heptalenes.

III.B.8: TD-DFT Calculations and Redox Properties:

This understanding was further supported by TD-DFT calculations employed to simulate electronic absorption spectrum of **III.B.12** and **III.B.13**. At first it was calculated for the whole molecule and later by trimming molecules to the heptalene core. It was observed that the high energy absorptions were characteristic of heptalene, rather than that of the expected 20π nornorrole structure **III.B.15**. The molecule **III.B.12** trimmed to the heptalene core showed theoretical vertical excitation energies in the high energy region of the electromagnetic spectrum whereas those are red shifted for the molecule **III.B.12** due to extended π conjugation (Figure III.B.19). Similar results have been seen for molecule **III.B.13** (Figure III.B.20). This clearly supported the heptalene nature of these aromatic compounds.

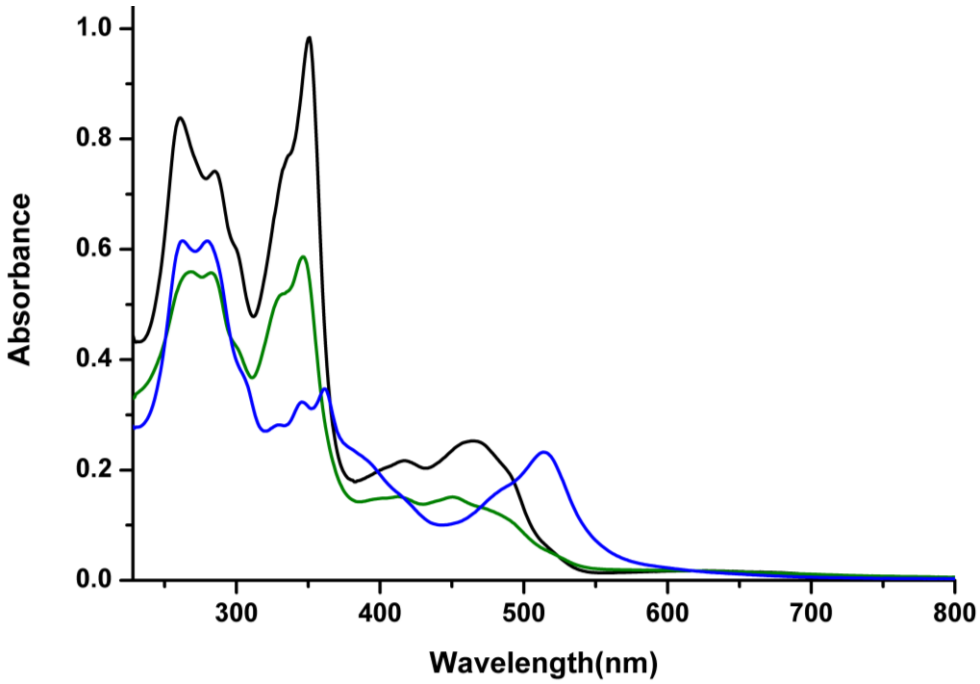

Figure III.B.18: UV-Visible absorption spectrum of aza-heptalenes **III.B.12**, **III.B.13** and **III.B.Me-13** in dichloromethane.

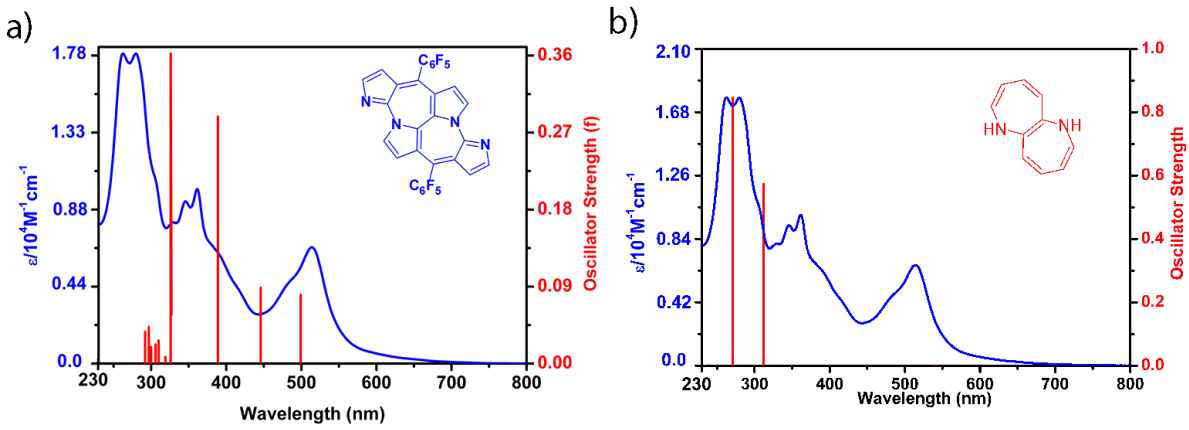

Figure III.B.19: The steady state absorption spectra (blue line) of **III.B.12** recorded in CH_2Cl_2 a) theoretical vertical excitation energies (red bar) for **III.B.12** and b) theoretical vertical excitation energies (red bar) after trimming molecule **III.B.12** to the heptalene core obtained from TD-DFT calculations carried out at the B3LYP/6-31G(d,p) level.

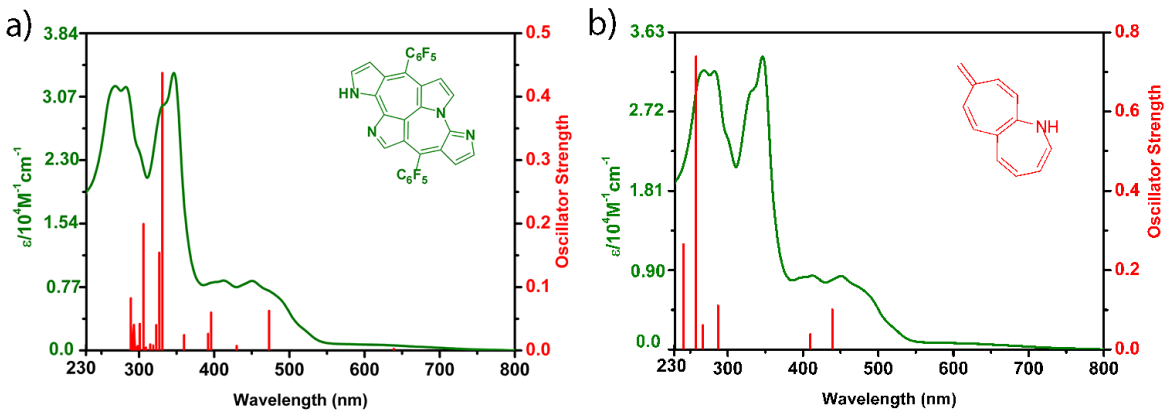

Figure III.B.20: The steady state absorption spectra (green line) of **III.B.13** recorded in CH_2Cl_2 a) theoretical vertical excitation energies (red bar) for **III.B.13** and b) theoretical vertical excitation energies (red bar) after trimming molecule **III.B.13** to the heptalene core obtained from TD-DFT calculations carried out at the B3LYP/6-31G(d,p) level.

The estimated NICS(0) value for **III.B.12** was found to be -0.5 ppm at the center of both the seven membered rings. A value of -5 ppm at the center of heterocyclic seven membered ring is and +2 ppm at carbon ring center was estimated for **III.B.13** (Figure III.B.21). These values are in agreement with the effective π electron delocalization expected for the bicyclic system of **III.B.13** than that of **III.B.12**. These values also support the aromatic nature of both the aza-heptlanes. In cyclic voltammetry studies, the reductions were observed at -0.78, -1.04 and -1.24 V and oxidation were not observed for **III.B.12**. Similarly for **III.B.13**, reduction at -0.88, -1.1 and -1.46 V along with a single irreversible oxidation at 1.25 V were observed (Figure III.B.22). These values suggest the redox feature dissimilar to porphyrin-like systems and also do not bind with metal ions contrary to porphyrinoids.

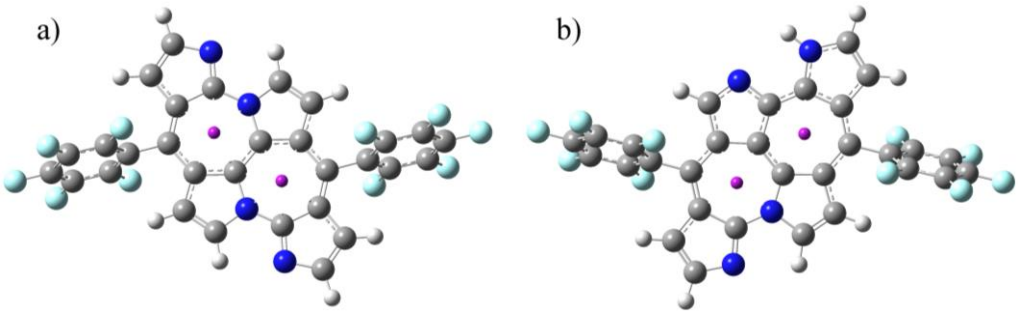

Figure III.B.21: Model structure **III.B.12** (a) and **III.B.13** (b) indicating NICS(0) point

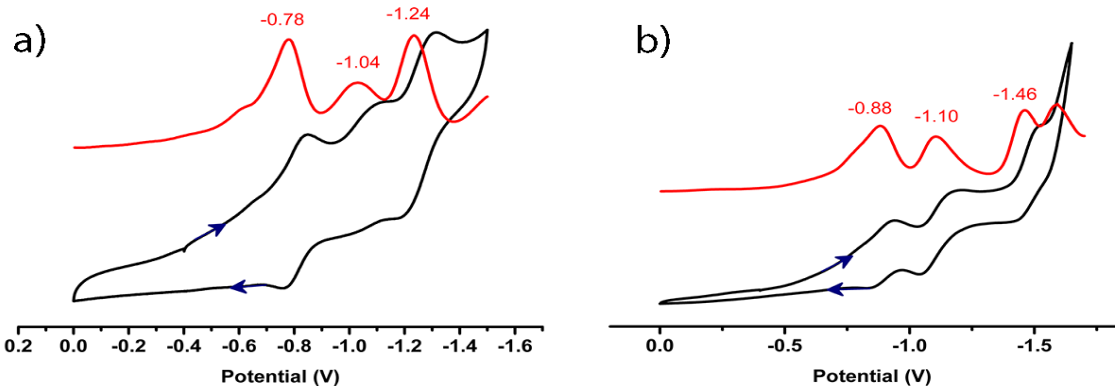

Figure III.B.22: Cyclic voltammogram (black line) and differential pulse voltammogram (red line) of a) **III.B.12** and b) **III.B.13** were recorded in CH_2Cl_2 using TBAP as a supporting electrolyte.

III.B.9: Conclusion:

Doubly N-confused dipyrrins undergo intermolecular cyclodimerization with metal salts into planar aza-heptalene isomers. The **III.B.12** and **III.B.13** molecular structures indicate the formation of probable macrocyclic intermediate such as **III.B.15** which forms the bipyrrolic unit at its center. The method of synthesis is very simple with respect to the obtained fused cyclic systems. Even though these molecules represent the features of N-confused corrole, norrole and nornorrole, but spectroscopic analysis and computational studies support **III.B.12** and **39** as examples of non-benzenoid aromatic molecules.

III.B.10: Experimental Section:

All reagents and solvents were of commercial reagent grade and were used without further purification except where noted. Dry THF was obtained by refluxing and distillation over pressed Sodium metal. Column chromatography was performed on silica gel (230-400) in glass columns. ^{1}H NMR and ^{19}F NMR spectra were recorded either on a JEOL 400 MHz or Bruker 500 MHz spectrometer, and chemical shifts were reported as the delta scale in ppm relative to $(CH_3)_2SO$ (δ = 2.50 ppm) or $(CH_3)_2CO$ (δ = 2.1 ppm) as internal reference for $_1H$. High Resolution Mass spectra were obtained using WATERS G2 Synapt Mass Spectrometer. Electronic spectra were recorded on a Perkin-Elmer »-900 ultraviolet−visible (UV−vis) spectrophotometer. Single crystals were grown in suitable organic solvent and Single crystal X-ray diffraction were performed at 100K on BRUKER KAPPA APEX II

CCD Duo diffractometer (operated at 1500 W power: 50 kV, 30 mA) using graphite-monochromated Mo K± radiation (» = 0.71073 Å). Quantum mechanical calculations were carried out on Gaussian 09 program suite using High Performance Computing Cluster facility of IISER PUNE. All calculations were carried out by Density Functional Theory (DFT) with Becke's three-parameter hybrid exchange functional and the Lee-Yang-Parr correlation functional (B3LYP) and 6-31G(d,p) basis set for all the atoms were employed in the calculations. To estimate the NICS(0) values at the center of the seven membered rings of molecular plane of all the macrocycles, the gauge independent atomic orbital (GIAO) method used based on the optimized geometries. The molecular structures obtained from single crystal analysis were used for geometry optimization. Cyclic voltammetry (CV) and Differential pulse voltammetry (DPV) measurements were carried out on a BAS electrochemical system using a conventional three-electrode cell in dry CH_2Cl_2 containing 0.1 M tetrabutylammonium perchlorate (TBAP) as the supporting electrolyte. Measurements were carried out under an Ar atmosphere. A glassy carbon (working electrode), a platinum wire (counter electrode), and saturated calomel (reference electrode) were used.

Procedure for Synthesis of III.B.12:

Meso-pentafluorophenyl doubly N-confused dipyrromethane (DNCDPM) was synthesized as per literature procedure. To a DNCDPM (300 mg, 0.9615 mmol, 1 equiv.), 10ml dry THF was added under N_2 inert atmosphere followed by addition of DDQ (480 mg, 2.1154 mmol, 2.2 equiv.). After stirring reaction mixture for one hour, copper(II) acetate (173 mg, 0.9615 mmol, 1 equiv.) was added and the reaction mixture was stirred for overnight. Reaction was quenched with 100ml distilled water and organic phase was extracted thrice with dichloromethane. The combined dichloromethane extracts was washed with water, dried over Na_2SO_4 and evaporated under vacuo. The crude product was purified by silica gel column chromatography using hexane/ethyl acetate as the eluent and pink color solution obtained as **III.B.12** (12 mg, 4%). It has been found that, this compound has poor solubility in common organic solvents hence hampered the ^{13}C-NMR studies. **^{1}H NMR** (Acetone-d_6, 400MHz, 295K) δ = 6.84 (d, J = 4.0 Hz, 2H), 7.79 (d, J = 4.0 Hz, 2H), 7.96 (d, J = 4.0 Hz, 2H), 9.53 (d, J = 4.0 Hz, 2H); **^{19}F NMR** (Acetone-d_6, 376MHz, 295K) δ = -141.62 (d, J = 11.28 Hz, 4F), -153.93 (t, J = 15.04 Hz, 2F), -162.07 (t, J = 15.04 Hz,

4F); **UV-Vis** (CH_2Cl_2): $\lambda_{max}(\varepsilon)Lmol^{-1}cm^{-1}$ = 262 nm (17,800), 280 nm (17,800), 361 nm (10,000) and 514 nm (6,700); **HRMS** *m/z* calcd. for $(C_{30}H_8N_4F_{10}+H)^+$ = 615.0668, Observed = 615.0664; **Crystal data:** $C_{30}H_8N_4F_{10}$ (*Mr* = 614.40), triclinic, space group *P-1 (No.2)*, *a* = 5.996(2), *b* = 7.348(3), *c* = 13.198(5)Å, α = 87.325(8), β = 86.010(8), γ = 71.490(8)°, V = 549.9(4)Å^3, Z = 1, ρcalcd = 1.855 mg/m^3, *T* = 100K, Rint (all data) = 0.0385, *R*1(all data) = 0.0576, *R*W (all data) = 0.1124, GOF = 1.043.

Procedure for Synthesis of III.B.13:

DNCDPM (100 mg, 0.3205 mmol, 1 equiv.) were dissolved in 100ml dry THF under inert atmosphere of N_2 and DDQ (160 mg, 0.7051 mmol, 2.2 equiv) was added. After one hour, Iron(III) acetylacetonoate (113 mg, 0.3205 mmol, 1 equiv.) was added and the reaction mixture stirred overnight. Furthermore, reaction mixture was passed through bed of basic alumina. The first fraction afforded pink color solution of **III.B.12** (5 mg, 5%) in dichlormethane and second fraction provided dark color solution in methanol/dichloromethane combination which was further purified by silica gel column chromatography using hexane/ethyl acetate as a eluent to give greenish yellow color solution as **III.B.13** (10 mg, 10%). **^{1}H NMR** (DMSO-*d_6*, 400MHz, 295K) δ = 6.28 (d, J = 4.0 Hz, 1H), 6.73 (d, J = 4.0 Hz, 1H), 7.19 (d, J = 4.0 Hz, 1H), 7.50 (d, J = 4.0 Hz, 1H), 7.82 (d, J = 4.0 Hz, 1H), 8.71 (s, 1H), 9.28 (d, J = 4.0 Hz, 1H), 13.46 (bs, 1H, exchangeable with D_2O); **^{19}F NMR** (DMSO-*d_6*, 376MHz, 295K) δ = -142.41 (d, J = 22.56 Hz, 4F), -155.63 (td, J = 15.04 Hz, 2F), -162.89 (td, J = 15.04 Hz, 4F); **UV-Vis** (CH_2Cl_2): $\lambda_{max}(\varepsilon)Lmol^{-1}cm^{-1}$ = 268 nm (32,600) 282 nm (32,500), 346 nm (33,600) and 451 nm (8,800); **HRMS** *m/z* calcd. for $(C_{30}H_8N_4F_{10}+H)^+$ = 615.0668, Observed = 615.0667; **Crystal data:** $C_{30}H_8N_4F_{10}O_1$ (*Mr* = 630.40), monoclinic, space group *P21/c (No.14)*, *a* = 28.021(12), *b* = 11.565(3), *c* = 7.319(3)Å, α = 90.00, β = 95.576(10), γ = 90.00°, V = 2360.6(17)Å^3, Z = 4, ρcalcd = 1.774 mg/m^3, *T* = 100K, Rint (all data) = 0.0793, *R*1(all data) = 0.1812, *R*W (all data) = 0.2303, GOF = 1.112.

Procedure for Synthesis of III.B.Me-13:

To a **III.B.13** (100 mg, 0.1628 mmol, 1 equiv.) in 5 ml dry dimethyl formamide under N_2 inert atmosphere, sodium hydride (1 equiv.) was added at 0ºC. After 30 minute, methyl iodide (1.5 equiv.) was added and reaction mixture brought to room temperature. Reaction mixture quenched with ice cold distilled water and organic

compound was extracted with ethyl acetate from ice cold reaction mixture. The organic layer was evaporated on rota evaporator to get crude solid which was further purified on silica gel in ethyl acetate/n-hexane combination to get yellowish colored compound **III.B.Me-13** (55 mg, 54%). **^{1}H NMR** (Acetone-d_6, 400MHz, 295K) δ = 4.75 (s, 3H), 6.28 (d, J = 4.0 Hz, 1H), 6.72 (d, J = 4.0 Hz, 1H), 7.21 (d, J = 4.0 Hz, 1H), 7.42 (d, J = 4.0 Hz, 1H), 7.77 (d, J = 4.0 Hz, 1H), 8.66 (s, 1H), 9.35 (s, 1H); **^{19}F NMR** (Acetone-d_6, 376MHz, 295K) δ = -140.01 (d, J = 76.96 Hz, 4F), -152.84 (d, J = 221.84 Hz, 2F), -160.65 (d, J = 206.80 Hz, 4F); **UV-Vis** (CH_2Cl_2): $\lambda_{max}(\varepsilon)Lmol^{-1}cm^{-1}$ = 261 nm (43,900), 285 nm (38,700) 351 nm (51,200) and 465 nm (13,000); **HRMS** m/z calcd. for $(C_{31}H_{10}N_4F_{10}+H)^+$= 629.0824, Observed = 629.0835; **Crystal data**: $C_{31}H_{10}N_4F_{10}$ (Mr = 628.43), triclinic, space group P 1 (No.1), a = 6.1461(11), b = 7.3648(13), c = 14.031(3)Å, α = 76.834(4), β = 82.082(4), γ = 72.763(4)°, V = 589.0(2)Å^3, Z = 1, ρcalcd = 1.772 mg/m^3, T = 100K, Rint (all data) = 0.0484, R1(all data) = 0.0927, RW (all data) = 0.1616, GOF = 0.963

Chapter IV

Reactivity of Benzo derivatives of N-Confused and Doubly N-Confused Dipyrrins with Metal Salts

IV.1: Introduction:

As described in the earlier chapter, attempts to prepare a metal complex of N-confused dipyrrin yielded the anti-aromatic expanded norroles, **III.A.21a** and **III.A.22** (Chart IV.1) wherein the dipyrrin units are connected to each other by multiple C-N bonds[53]. In a dipyrrin unit, the replacement of a pyrrole ring by N-confused pyrrole ring has significantly changed the reactivity of N-confused dipyrrins with metal salts. After the replacement of both the pyrrole rings with N-confused pyrrole rings in dipyrrin unit also displayed modified reactivity with metal salts a as observed by the formation of non-macrocyclic products such as aza-heptalenes, **III.B.12** and **III.B.13** rather than the expected expanded norroles.(Chart IV.1)[67].

Chart IV.1: Chemical structures of expanded norrole **(III.A.21a)** and **(III.A.22)**; aza-heptalene **(III.B.12)** and **(III.B.13)**.

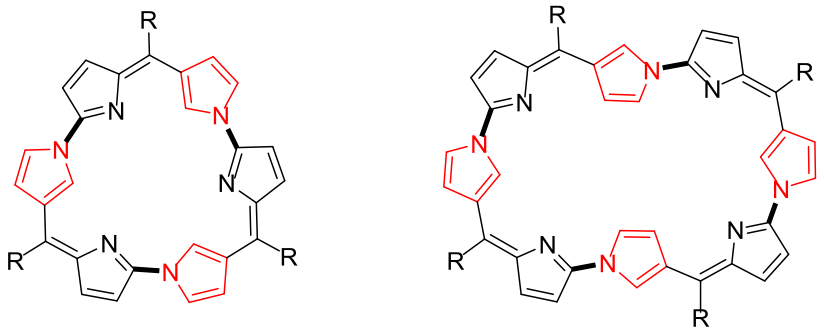

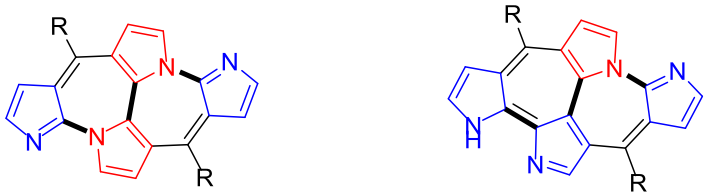

IV.2: Objectives:

This unexpected difference in the reactivity of modified dipyrrins was observed due to the introduction of one and two N-confused pyrrole rings into the normal dipyrrin units. Based on these altered reactivity for singly and doubly N-confused dipyrrins with respect to regular dipyrrins, it can be expected that the fusion approach on confused pyrrole rings will be interesting to explore reactivity of such

dipyrrins with metal salts. This chapter describes the attempts to explore the cyclomerization of mono benzofused N-confused dipyrromethane **IV.1** into macrocyclic product and dimer. The details of dimerization of mono and dibenzofused doubly N-confused dipyrrins (**IV.5** and **IV.7**) will also be explained in detail.

IV.3: Synthesis and Characterization of Trioxo Expanded Norroles:

IV.3.1: Trioxo Expnaded Norroles IV.2a:

The mono benzofused N-confused dipyrromethane **IV.1** was oxidized with DDQ to its dipyrrin, and further reacted with copper(II) acetate under concentrated reaction conditions (Scheme IV.1). The HRMS mass spectrum of this reaction mixture displayed a *m/z* value of 1122.1387 (Figure IV.1) which is forty eight units more than that of the expected cyclotrimer, suggesting the possibility of formation of trioxo-cyclotrimer **IV.2a**. This was identified as a red coloured band from column chromatographic purification and obtained as a red color solid in 3.9% yields. Another red coloured solid compound **IV.2b** was also obtained in 3.6% yield by similar protocol.

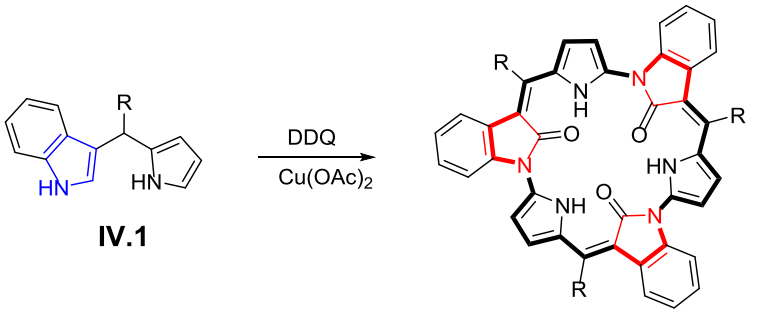

Scheme IV.1: Synthesis of Expanded Norrole **IV.2a** and **IV.2b**.

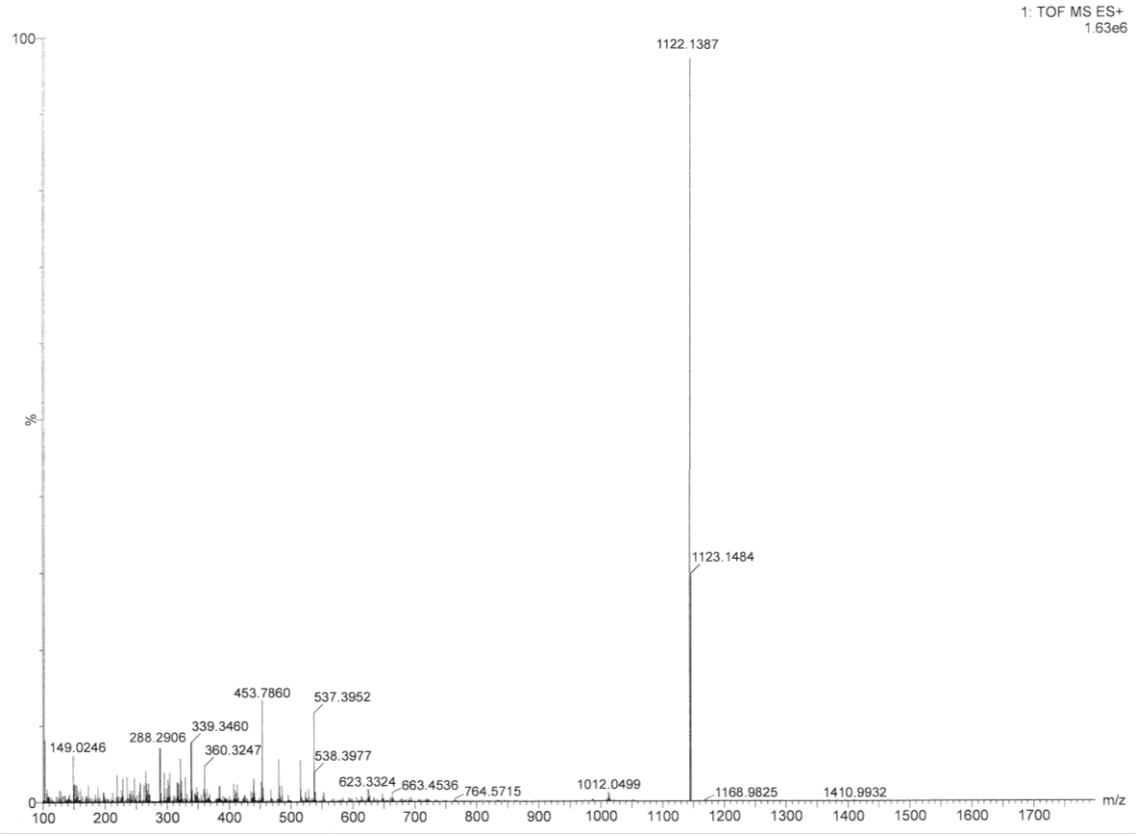

Figure IV.1: HR-ESI-TOF mass spectrum of **IV.2a**.

In order to confirm molecular structures of trioxo-expanded norrole **IV.2a**, good quality single crystals were grown by solvent diffusion of *n*-hexane vapours into the dichloromethane solution of the compound and subjected them for single crystal X-ray diffraction studies (Figure IV.2). The molecular structure of trioxo-expanded norrole, **IV.2a** proved the presence of three C-N linkage and the head-to-tail attachments of the three monobenzofused N-confused dipyrrin units. The α-carbons of the N-linked indole ring which are oriented towards the macrocyclic core, exhibited high reactivity and underwent oxidation to form the tri-oxygeneted expanded norrole **IV.2a** (Figure IV.2a). The benzene carbon atoms on the indole ring and α- and β-carbons of the normal pyrrole ring are pointed outside the macrocycle core. The **IV.2a** containing all the pyrrole and indole rings has near planar conformation indicating the delocalization of lone pair of electron present on the nitrogen, of the N-linked pyrrole of the indole, with π-electron cloud of the macrocyclic framework (Figure IV.2b). All these observations shows complete match for trioxo-expanded norroles **IV.2a**.

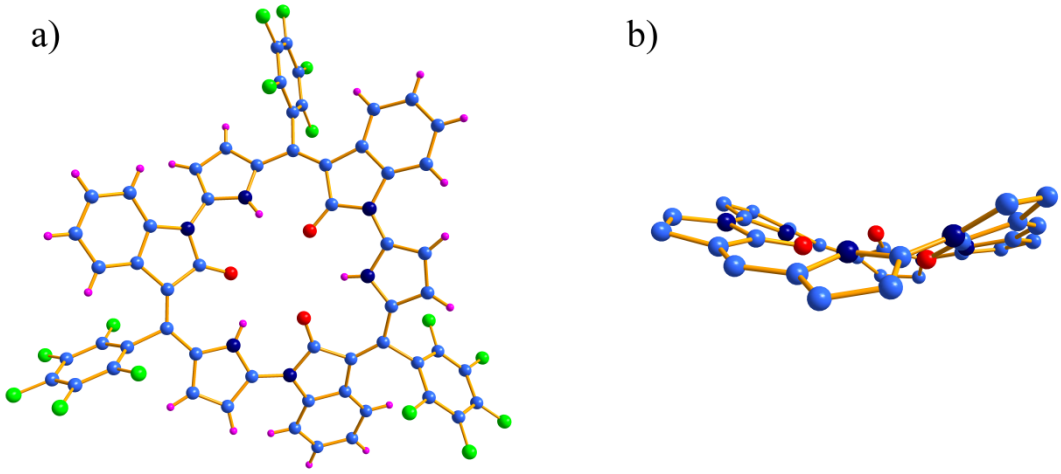

Figure IV.2: Molecular Structures of trioxydized expanded norrole **IV.2a**, a) top view and b) side view, the *meso* pentafluorophenyl groups and hydrogen atoms were omitted for clarity.

The ^{1}H NMR spectrum of **IV.2a** displayed multiplets at δ = 6.43 and 6.68, doublets at 6.01 and 7.55, triplet of doublet at 6.87 and 7.19 and broad singlet at 14.86 ppm (Figure IV.4). Upon addition of D_2O, the intensity of the signal at 14.86 ppm decreased significantly indicating the presence of NH in the macrocycle (Figure IV.5). ^{1}H-^{1}H NMR COSY indicated the strong correlation between the multiplets at δ = 6.43 and 6.68 corresponding to pyrrole ring protons and the other four signals at 6.01, 6.87, 7.19 and 7.55 were coupled amongst themselves corresponding to benzofused pyrrole ring protons (Figure IV.6). The ^{13}C NMR spectrum displayed inner carbonyl carbon signal at 166 ppm and DEPT-90 spectrum for CH groups has showed six different ^{13}C signals from 103 to 127 ppm (Figure IV.7). The presence of amine and imide functional groups in macrocycle **IV.2a** was also confirmed by IR studies (Figure IV.3). The observed downfield shift for the inner NH proton and inner carbonyl carbon clearly indicated the paratropic ring current effect expected of anti-aromatic macrocycles.

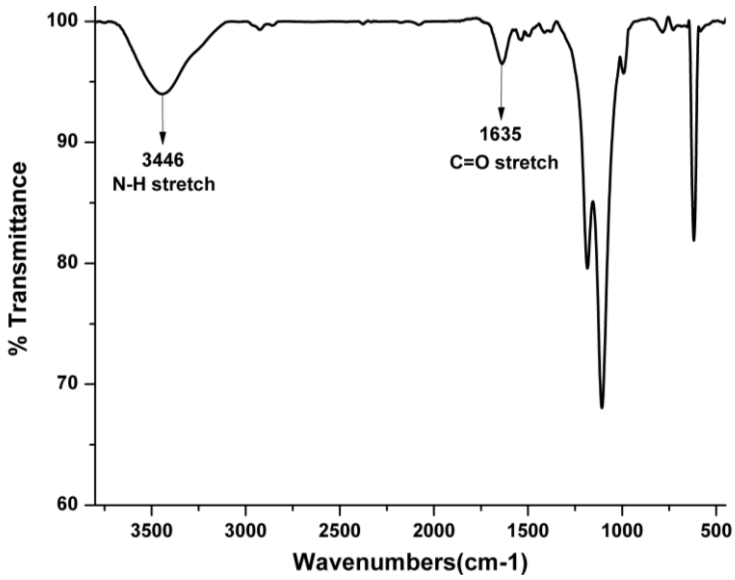

Figure IV.3: IR spectrum of **IV.2a**.

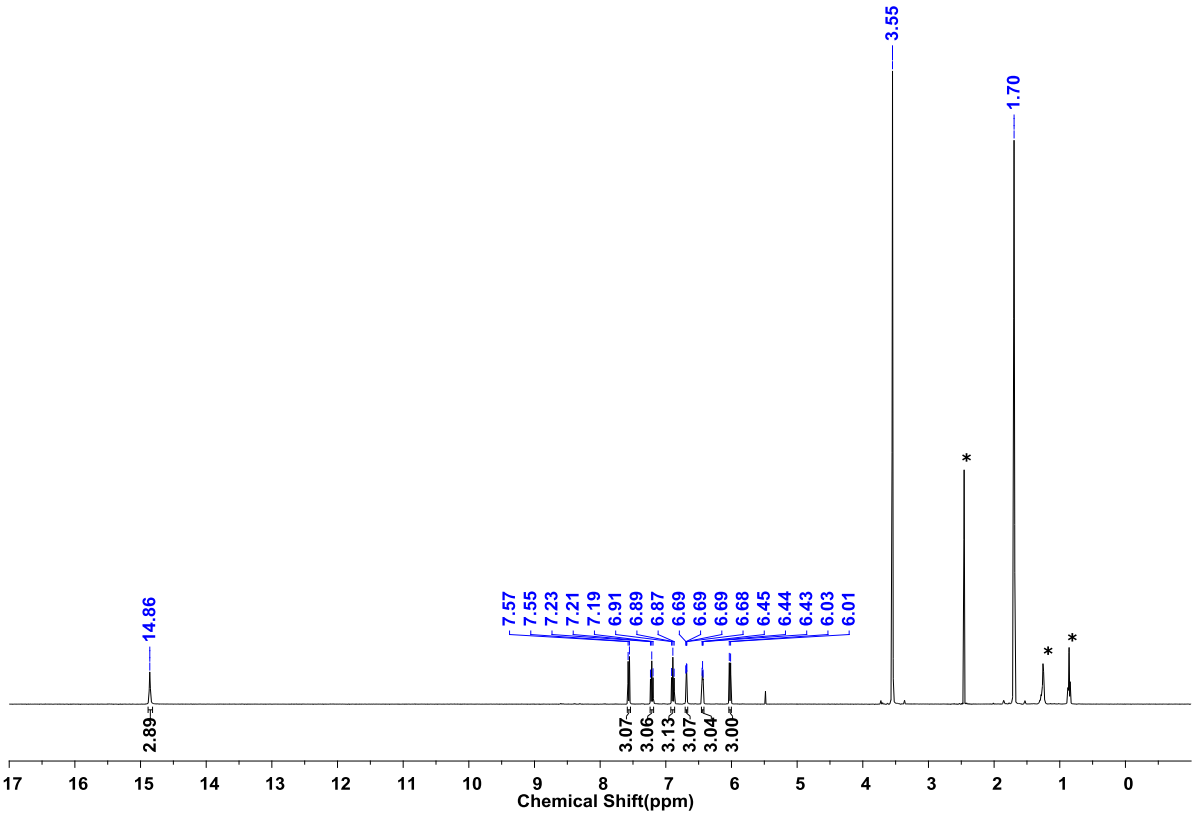

Figure IV.4: ^{1}H-NMR spectrum of **IV.2a** in *Tetrahydrofuran-d_8* at 295K.

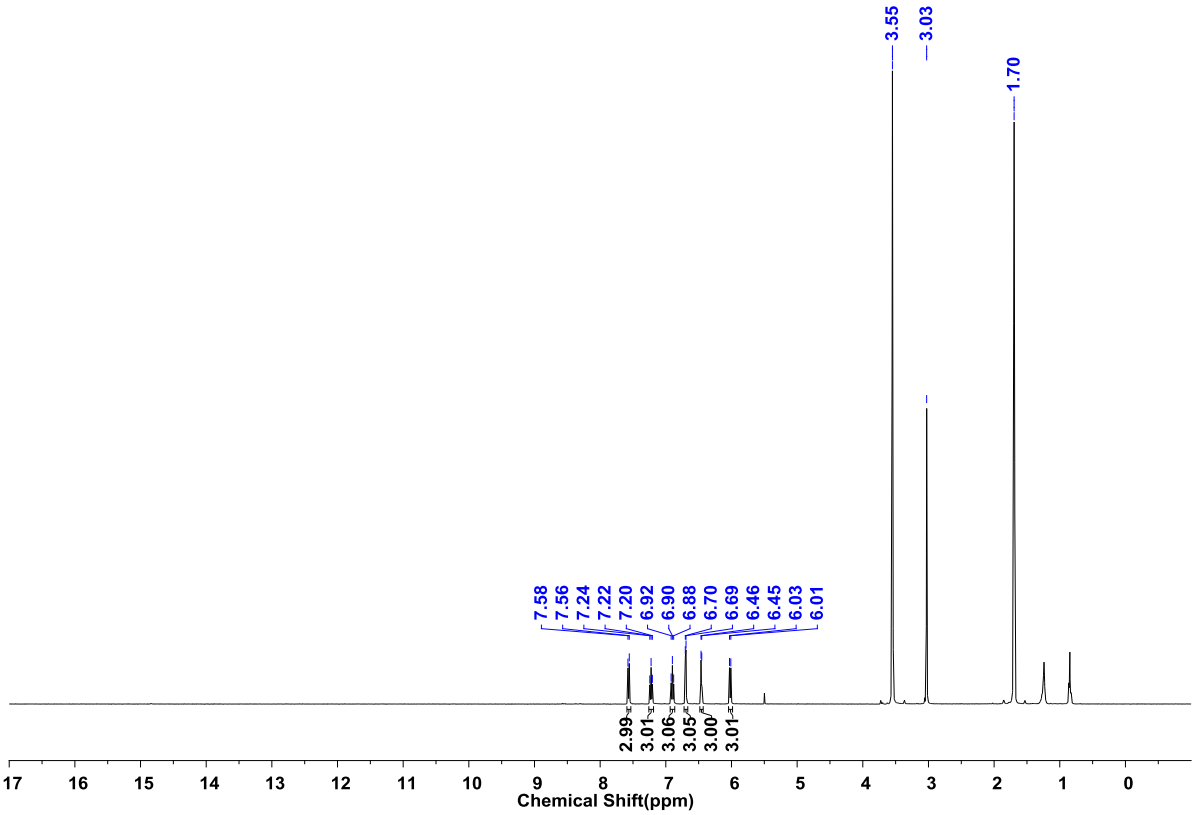

Figure IV.5: ^{1}H-NMR spectrum of **IV.2a** after D_2O exchange in *Tetrahydrofuran-d_8* at 295K

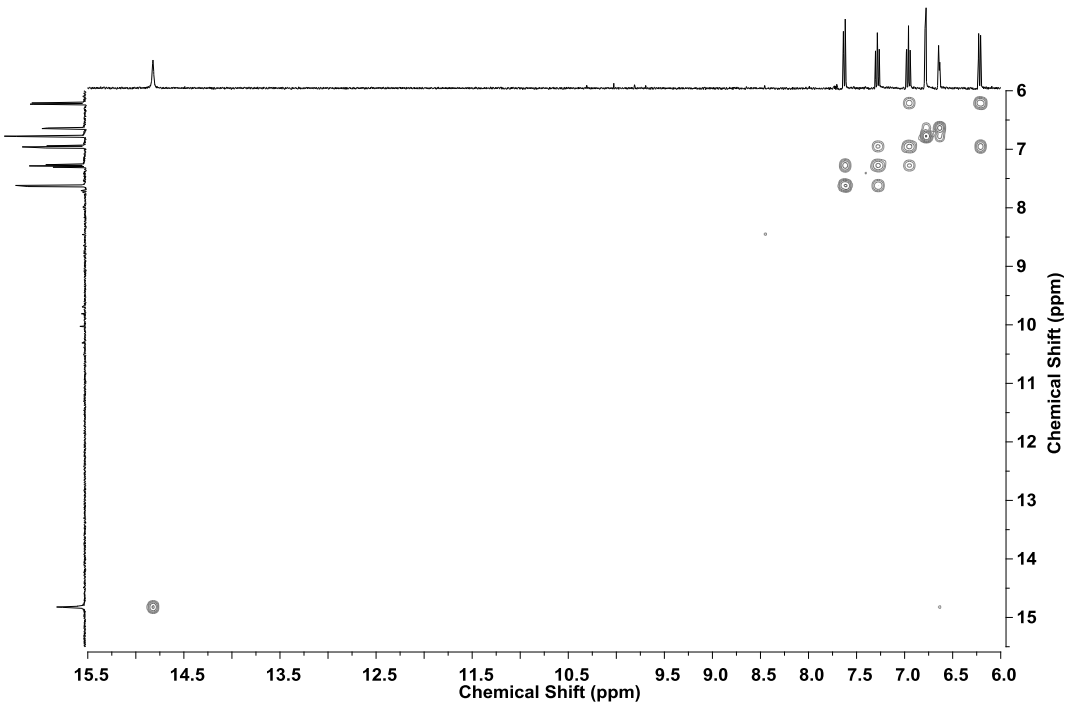

Figure IV.6: ^{1}H-^{1}H COSY spectrum of **IV.2a** in *Tetrahydrofuran-d_8* at 295K.

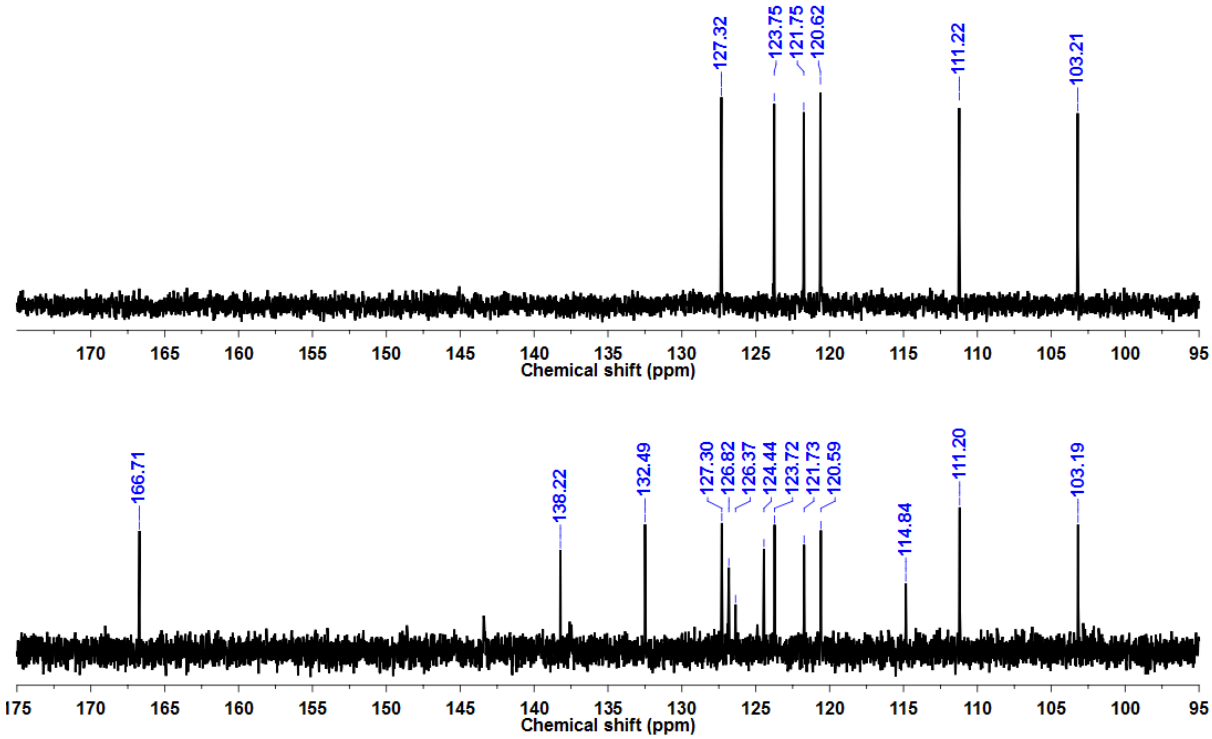

Figure IV.7: (Top) DEPT-90 and (Bottom**)** ^{13}C-NMR COSY spectrum of **IV.2a** in *Tetrahydrofuran-d_8* at 295K.

IV.3.2: Trioxo Expanded Norroles IV.2b:

Similarly the trioxidized expanded norrole **IV.2b** was also confirmed by IR (Figure IV.8), HRMS (Figure IV.9), NMR (Figure IV.10, 11) and single crystal X-ray diffraction analysis (Figure IV.12).

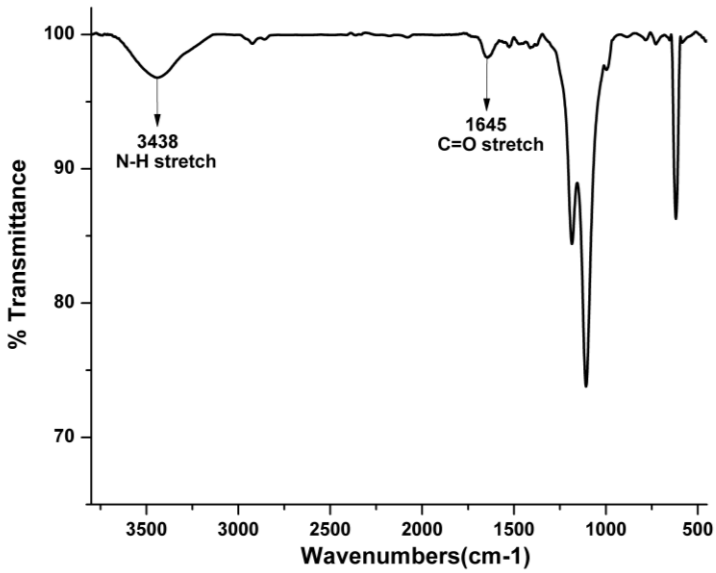

Figure IV.8: IR spectrum of **IV.2b**.

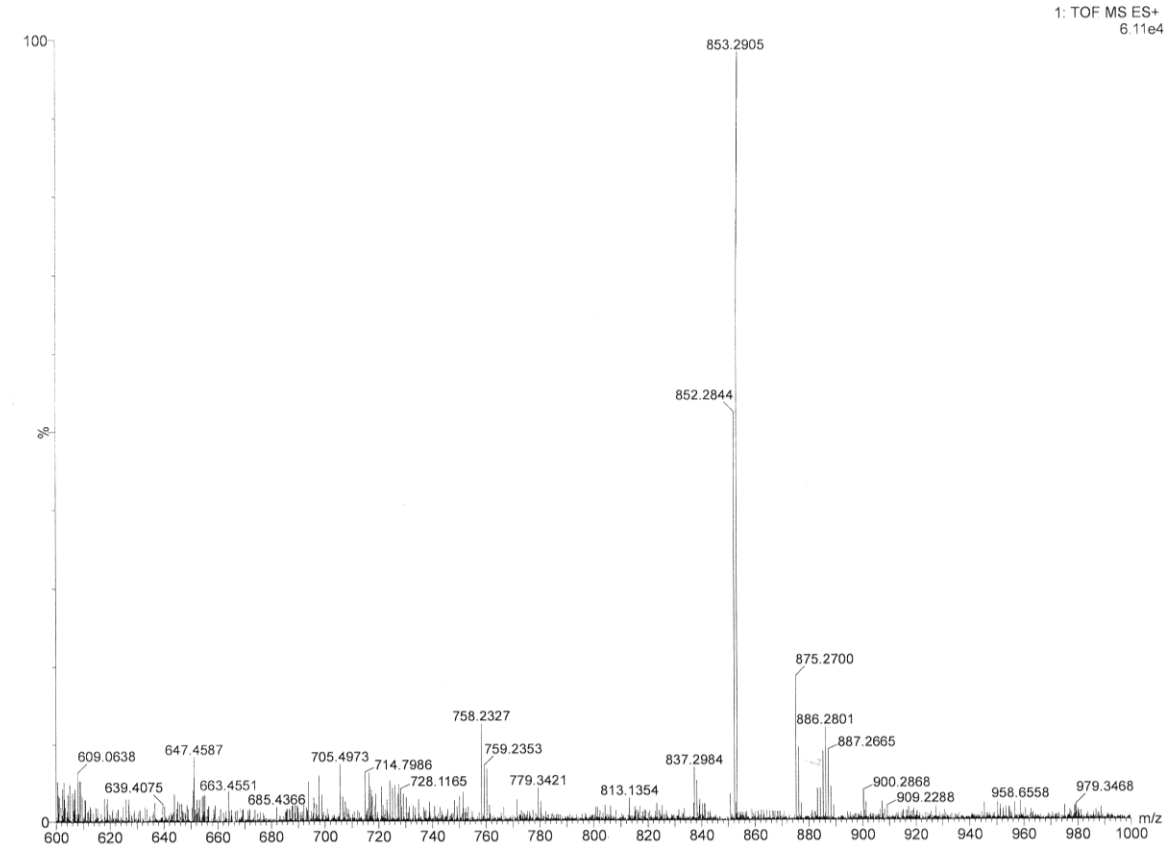

Figure IV.9: HR-ESI-TOF mass spectrum of **IV.2b**.

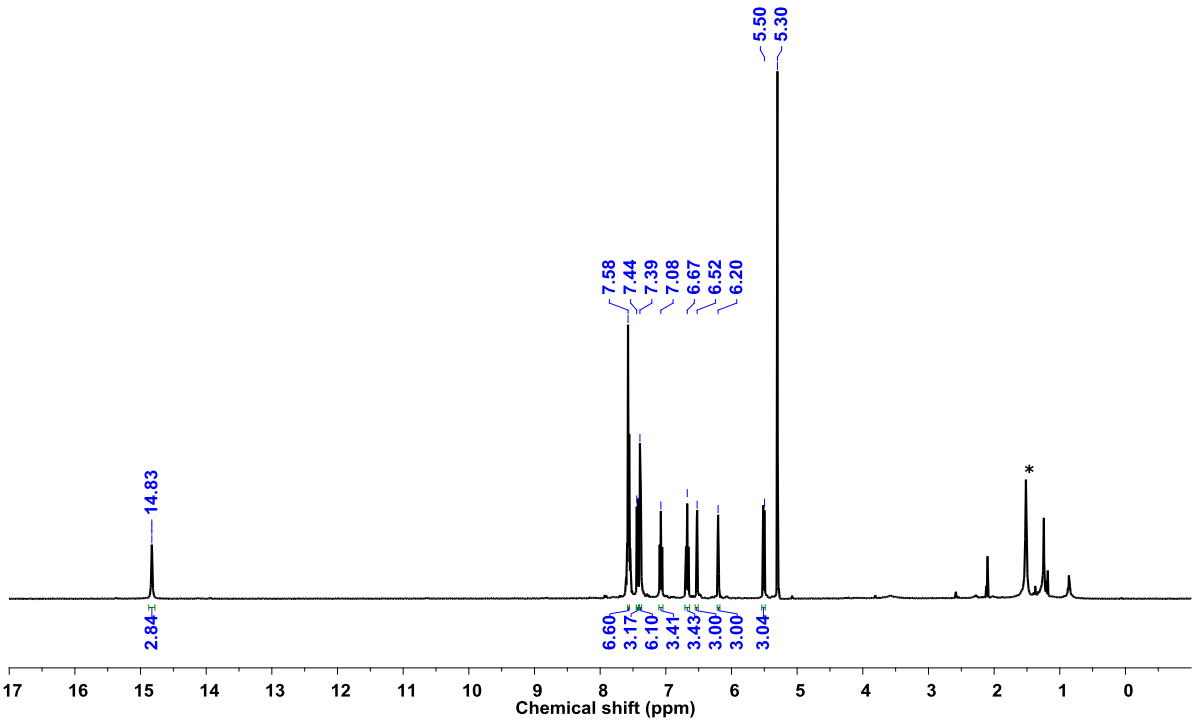

Figure IV.10: ^{1}H-NMR spectrum of **IV.2b** in *Dichloromethane-d_2* at 295K.

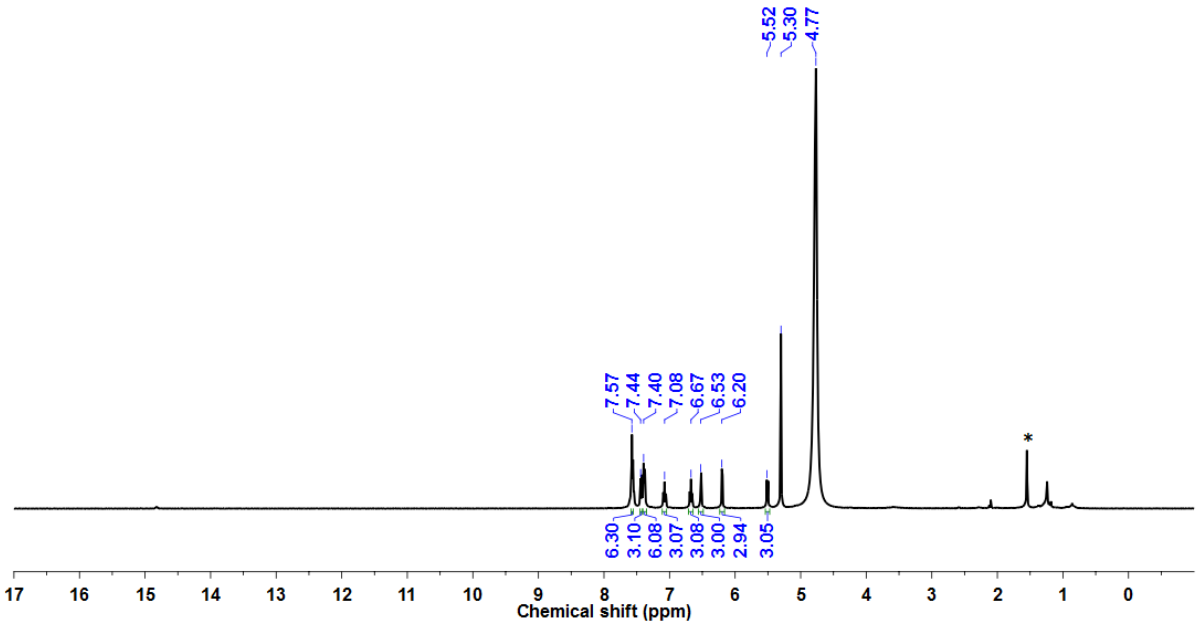

Figure IV.11: ^{1}H-NMR spectrum of **IV.2b** after D_2O exchange in *Dichloromethane-d_2* at 295K.

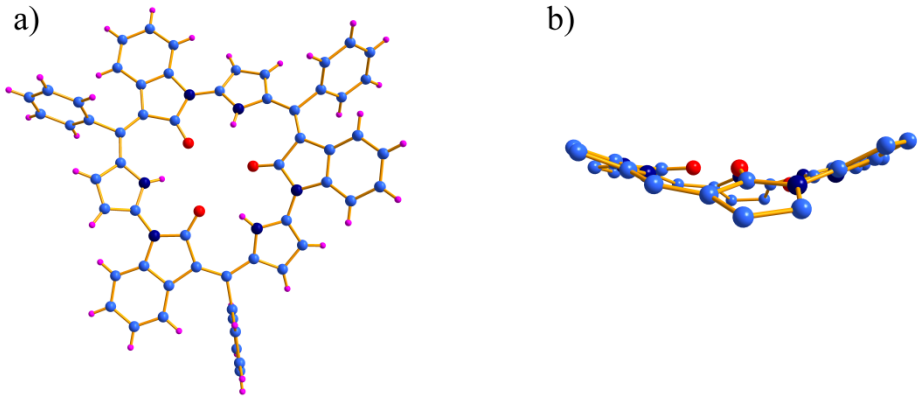

Figure IV.12: Molecular structures of trioxidized expanded norrole **IV.2b**, a) top view and b) side view, the *meso* phenyl groups and hydrogen atoms were omitted for clarity.

IV.4: Synthesis and Characterization of Dimer IV.3:

It was observed that either metal salt or the dilution factor of the reaction affects the mode of cyclization in dipyrrin. When **IV.1** was reacted under dilute reaction condition (see experimental section), HRMS analysis revealed *m/z* value

719.1288 (Figure IV.13) suggesting the formation of unusual dimer **IV.3** isolated in 4% yields apart from **IV.2a** in 3.4% yields (Scheme IV.2).

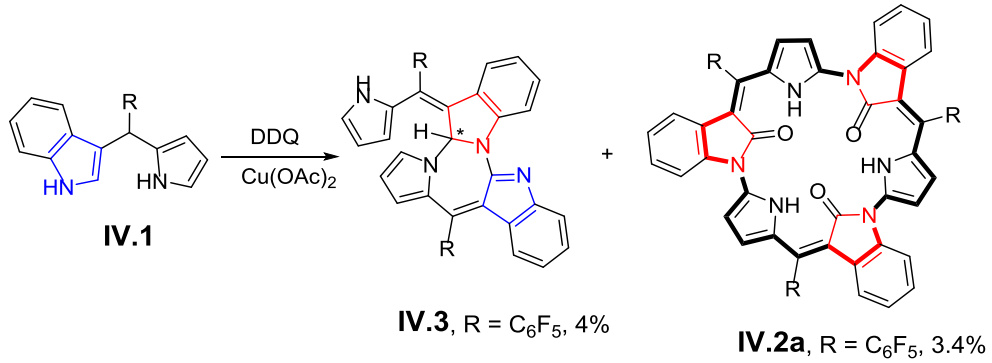

Scheme IV.2: Synthesis of Dimer **IV.3** and Expanded Norrole **IV.2a**.

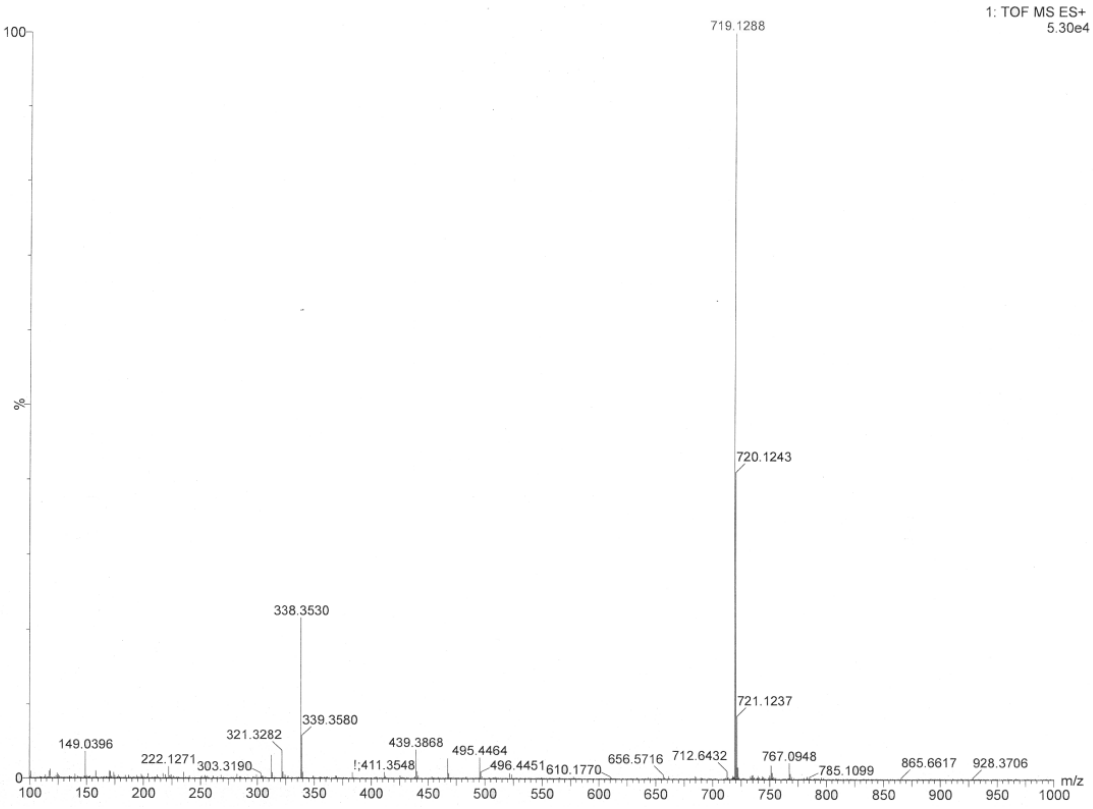

Figure IV.13: HR-ESI-TOF mass spectrum of **IV.3**.

The observed *m/z* value in HRMS spectrum of compounds **IV.3** also favors the formation of dihydro-nornorrole **IV.3NN** (Figure IV.14).

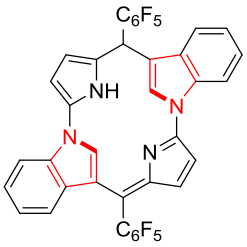

IV.3NN

Figure IV.14: Expected Structures of Contracted Norroles.

The molecular structure of **IV.3** displayed two mono benzofused N-confused dipyrrin unit connected to each other through two different types of C-N bonds in an unsymmetrical fashion leading to formation of one seven membered ring E. This molecule has two types C-N linkage: (a) indole A ring nitrogen of the one the mono benzofused N-confused dipyrrin is connected to other indole B ring at the α-carbon of the another monobenzofused N-confused dipyrrin forming N-Cα bond and (b) normal pyrrole C ring nitrogen of the one monobenzofused N-confused dipyrrin is connected to the other indole A ring at the α-carbon of the other monobenzofused N-confused dipyrrin creating the chiral center and forming another N-Cα bond (Figure IV.15a). The seven membered E ring having sp^3 chiral carbon atom is projected out of the plane whereas the other sp^2 carbon atoms form a planar structure (Figure IV.15b).

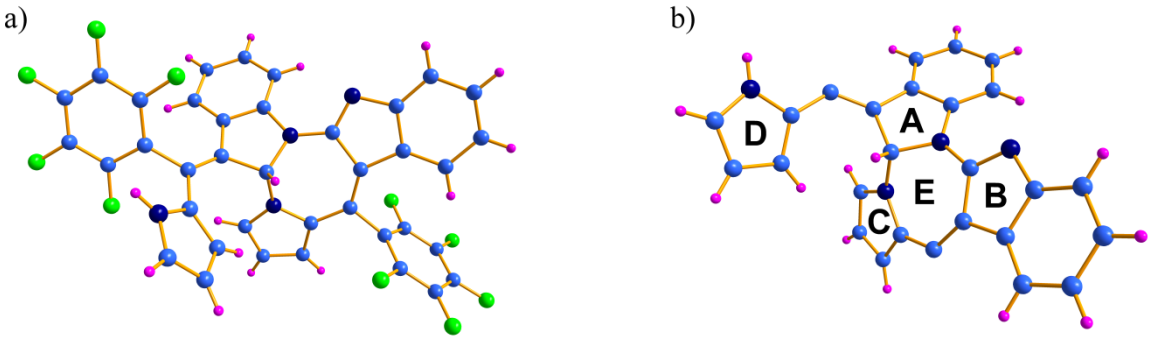

Figure IV.15: Molecular Structures of chiral dimer **IV.3**, a) top view and b) side view, the *meso* pentafluorophenyl groups were omitted for clarity.

The ^{1}H NMR spectrum of **IV.3** displays sixteen distinct signals from δ = 5.62 to 10.10 ppm (Figure IV.16). The intensity of the broad signal at 10.10 ppm decreased significantly after the addition of D_2O suggesting the presence of NH (Figure IV.17). The singlet at 5.62 ppm corresponds to the sp^3 chiral carbon proton. Also ^{1}H-^{1}H NMR COSY indicated no correlation for signal at 5.62 and 10.10 ppm, whereas signals

from 6.17 to 8.23 ppm showed multiple correlations (Figure IV.19). DEPT-90 spectrum for CH groups showed total fifteen numbers of ^{13}C signals and chiral carbon signal observed at 73 ppm (Figure IV.18). All these observations indicate the formation of dimer **IV.3** and not the **IV.3NN**.

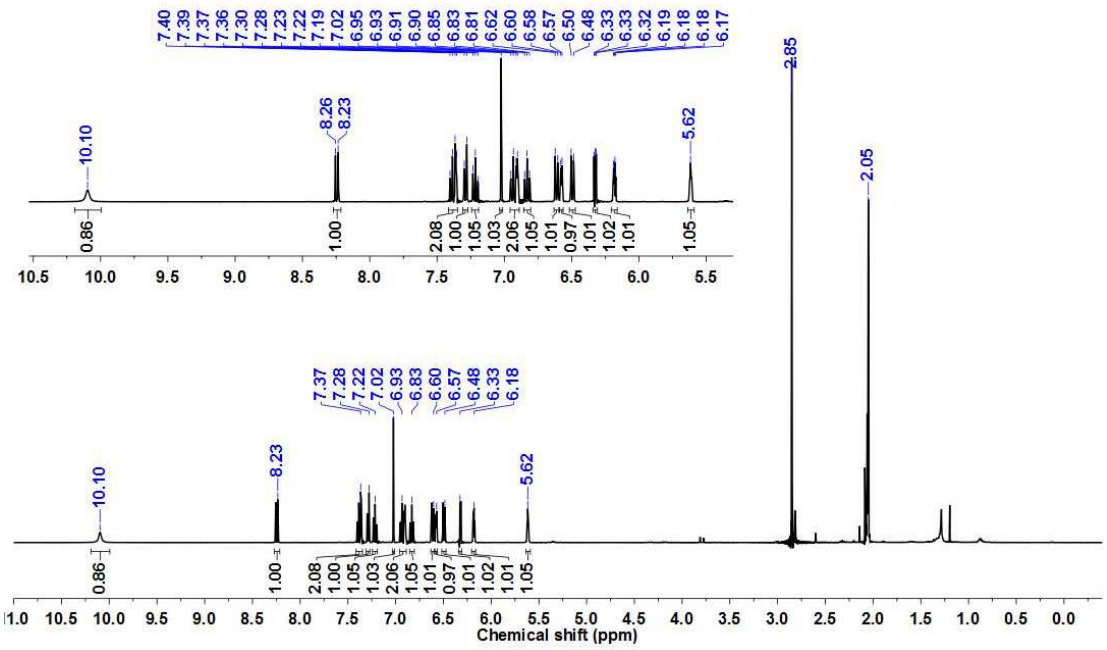

Figure IV.16: ^{1}H-NMR spectrum of **IV.3** in *Acetone-d_6* at 295K.

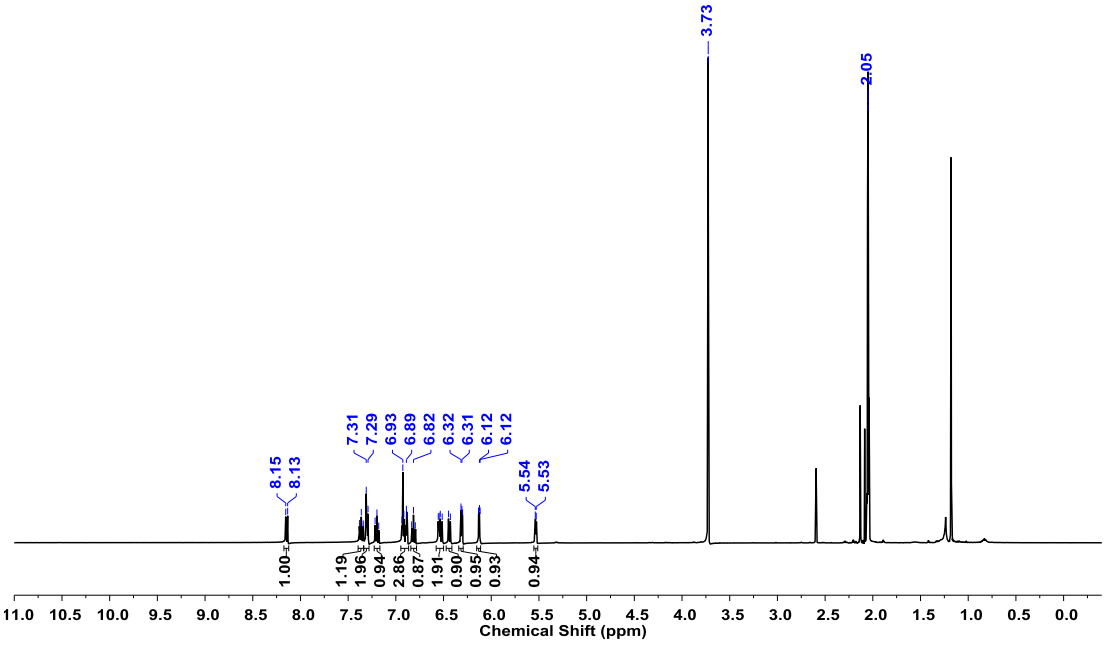

Figure IV.17: ^{1}H-NMR spectrum of **IV.3** after D_2O exchange in *Acetone-d_6* at 295K.

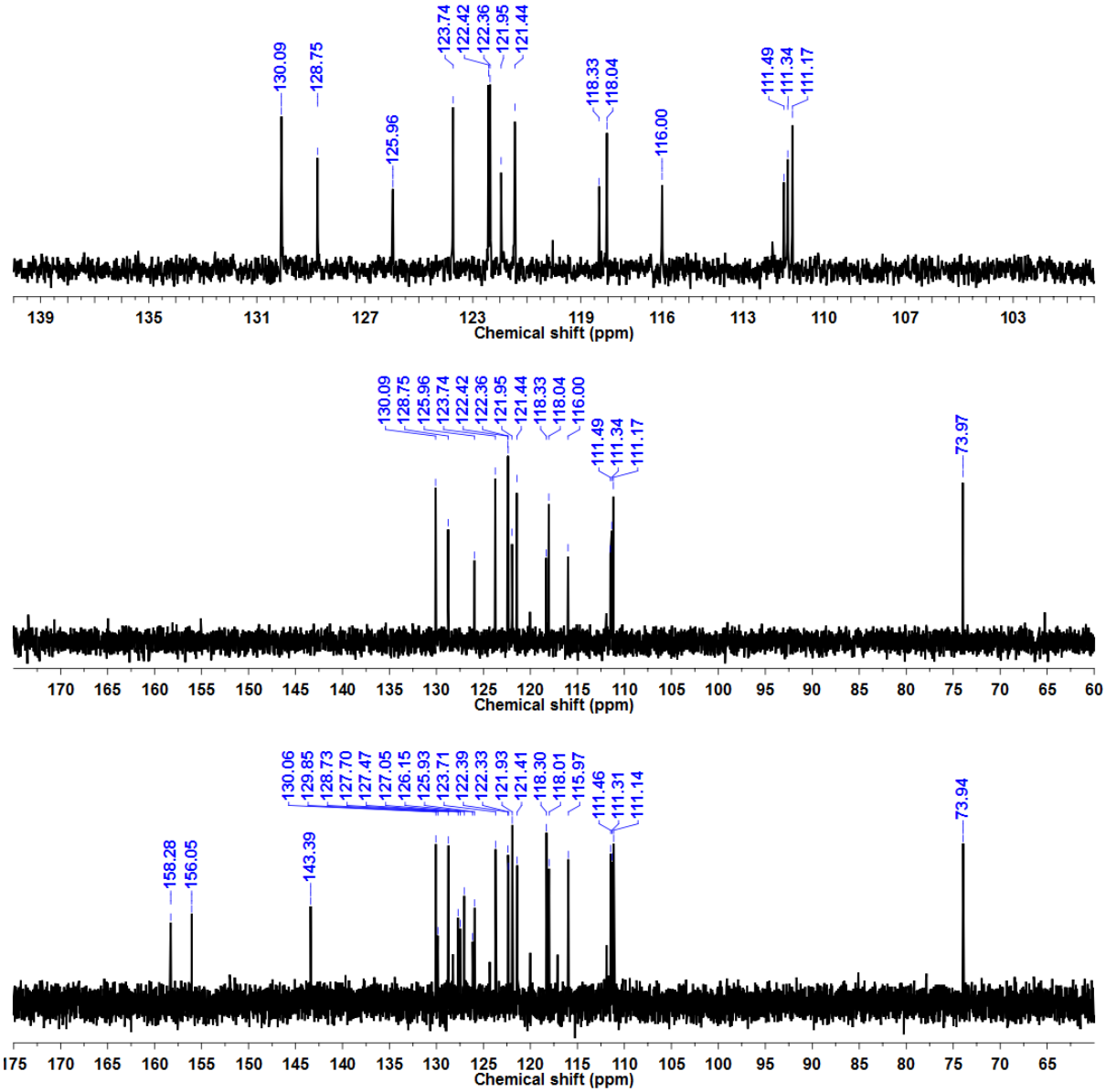

Figure IV.18: (Top) Zoomed-DEPT-90, (Middle) DEPT-90 and (Bottom**)** ^{13}C-NMR spectrum of **IV.3** in *Acetone-d_6* at 295K.

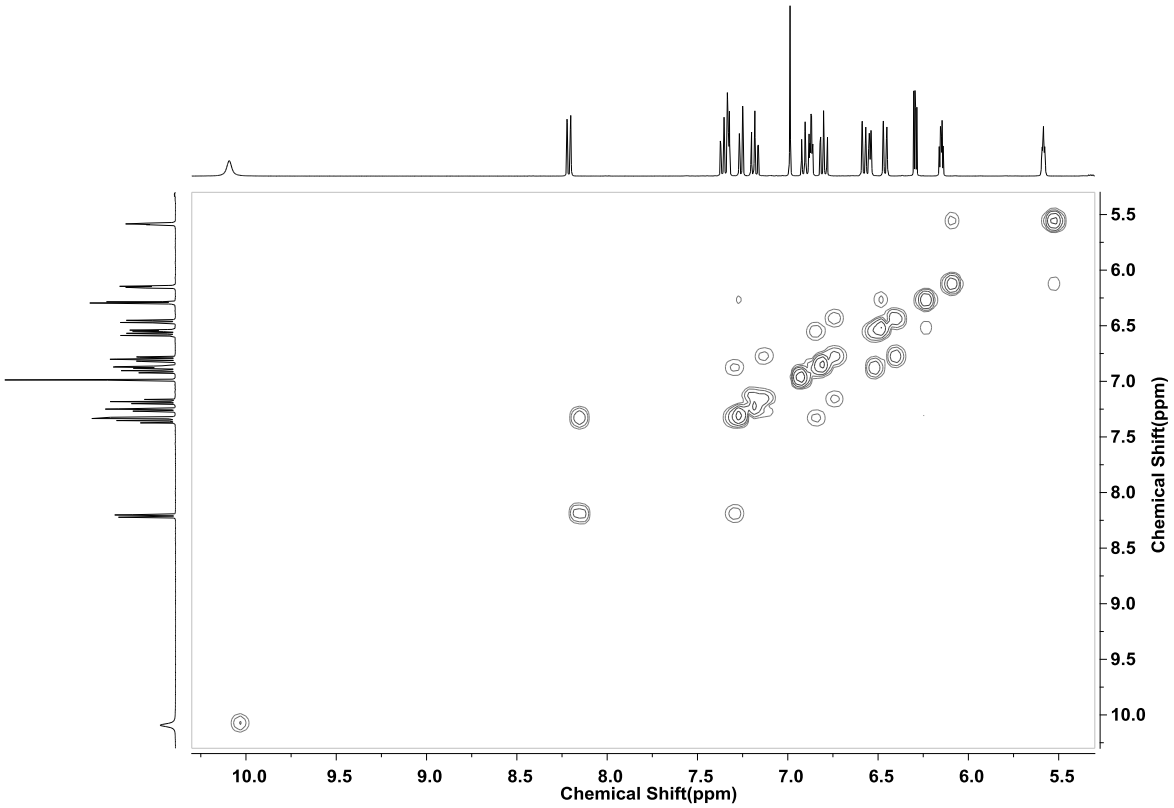

Figure IV.19: ^{1}H-^{1}H COSY spectrum of **IV.3** in *Acetone-d_6* at 295K.

IV.5: Synthesis and Characterization of Azaheptalene IV.6:

Monobenzo doubly N-confused dipyrromethane **IV.5** was obtained by deprotecting the Tri(isopropyl silyl) dipyrromethane derivative **IV.4**. The **IV.5** was oxidized with DDQ and treated with copper(II) acetate **(**Scheme IV.3). The HRMS displayed *m/z* value of 715.0965 (Figure IV.20) corresponding to the expected dimer **IV.6** with 1% reaction yield.

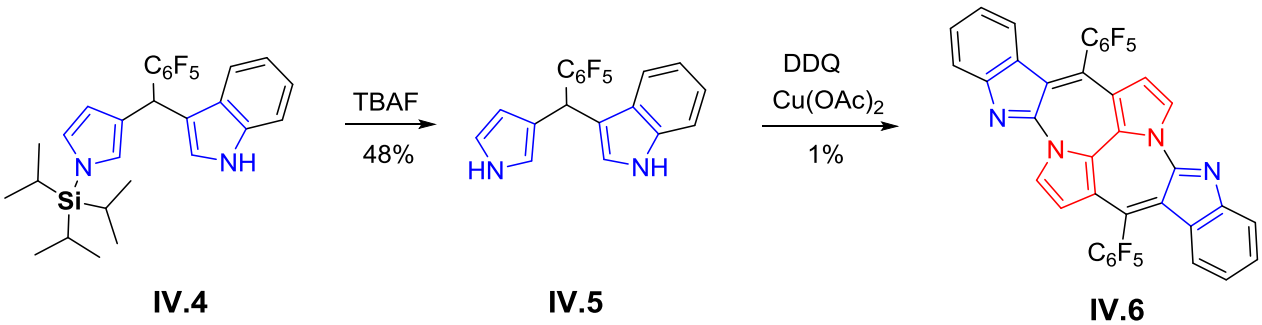

IV.4 **IV.5** **IV.6**

Scheme IV.3: Synthesis of Dimer **IV.6.**

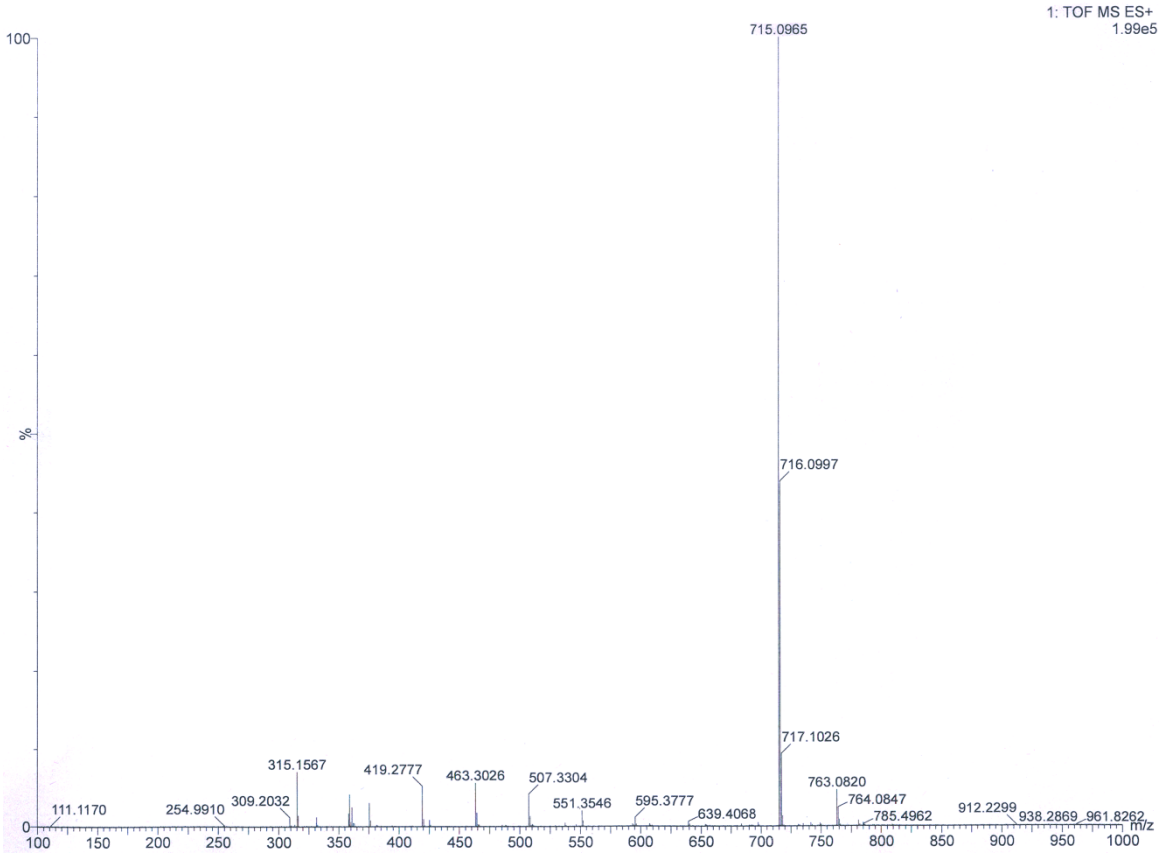

Figure IV.20: HR-ESI-TOF mass spectrum of **IV.6**.

The molecular structure of **IV.6** confirmed symmetrical coupling which connect pyrrole ring nitrogen of one dipyrrin at the α-position to the indole ring of another dipyrrin forming C-N bond. The α-carbons of both the neo-confused pyrrole rings were found to be coupled with each other, through a C_α-C_α bond length of 1.408(10) Å and this provides heterocyclic seven membered bicyclic systems to be structurally similar to aza-heptalene. This molecule also represents the linear fusion of three different aromatic rings (6, 5 and 7 membered) similar to hexacene (Figure IV.21a). The planar molecule also exhibited strong π-π stacking with inter-planar distance found to be 3.307 Å (Figure IV.21b) in the crystal packing.

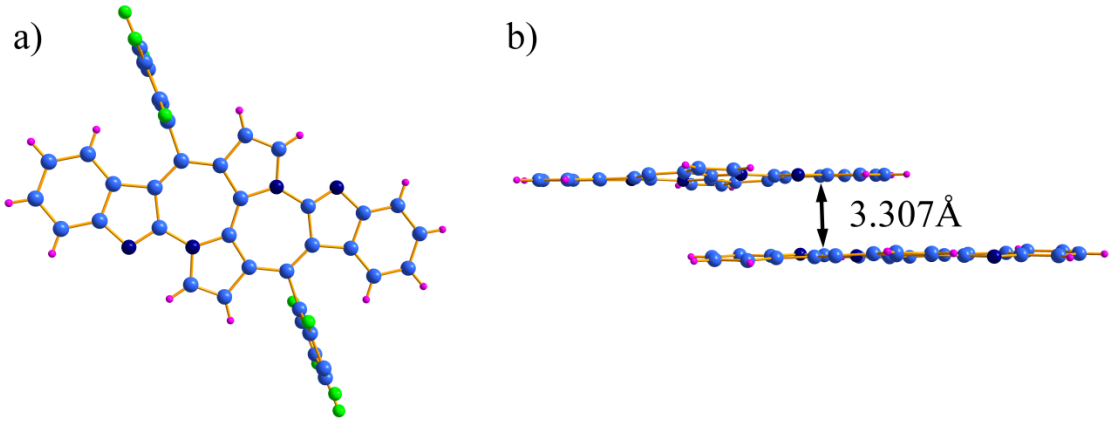

Figure IV.21: Molecular Structures of aza-heptalene **IV.6**, a) top view and b) side view shows intermolecular π-π stacking interactions, the *meso* pentafluorophenyl groups were omitted for clarity.

The ^{1}H NMR spectrum of molecule **IV.6** indicated signals at δ = 6.35, 6.94, 7.13, 7.48 7.71 and 9.35 ppm (Figure IV.22). ^{1}H-^{1}H COSY spectrum displayed coupling between the doublets at δ = 6.35 and 9.35 ppm (coupling constant, J = 4 Hz) corresponding to the pyrrole ring protons. A second set of correlations suggested signals at δ = 6.94, 7.13, 7.48 and 7.71 ppm represented the benzofused ring protons (Figure IV.23). DEPT-90 spectrum exhibited six different ^{13}C signals at δ = 114, 119, 121, 124, 125 and 129 ppm (Figure IV.24). All these NMR studies confirmed the formation of molecule **IV.6**.

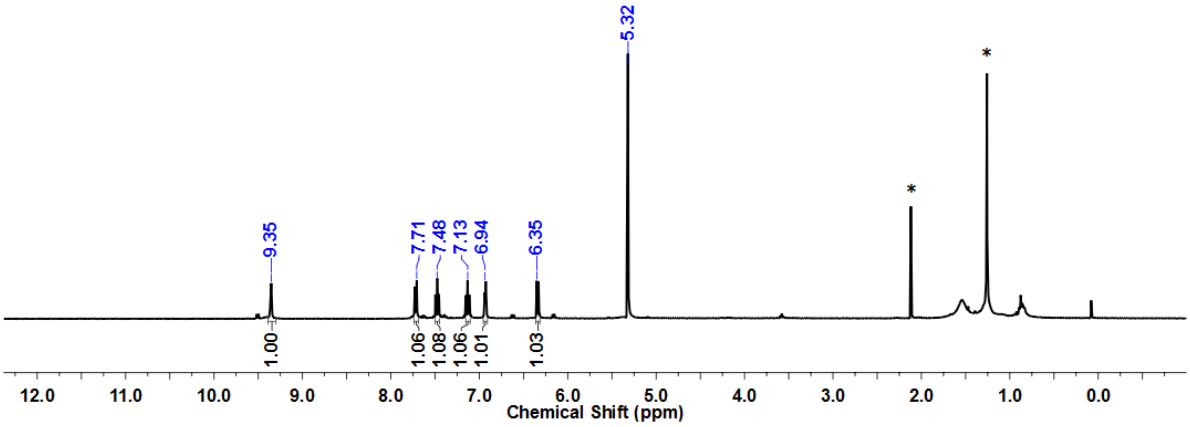

Figure IV.22: ^{1}H-NMR spectrum of **IV.6** in *Dichloromethane-d_2* at 295K.

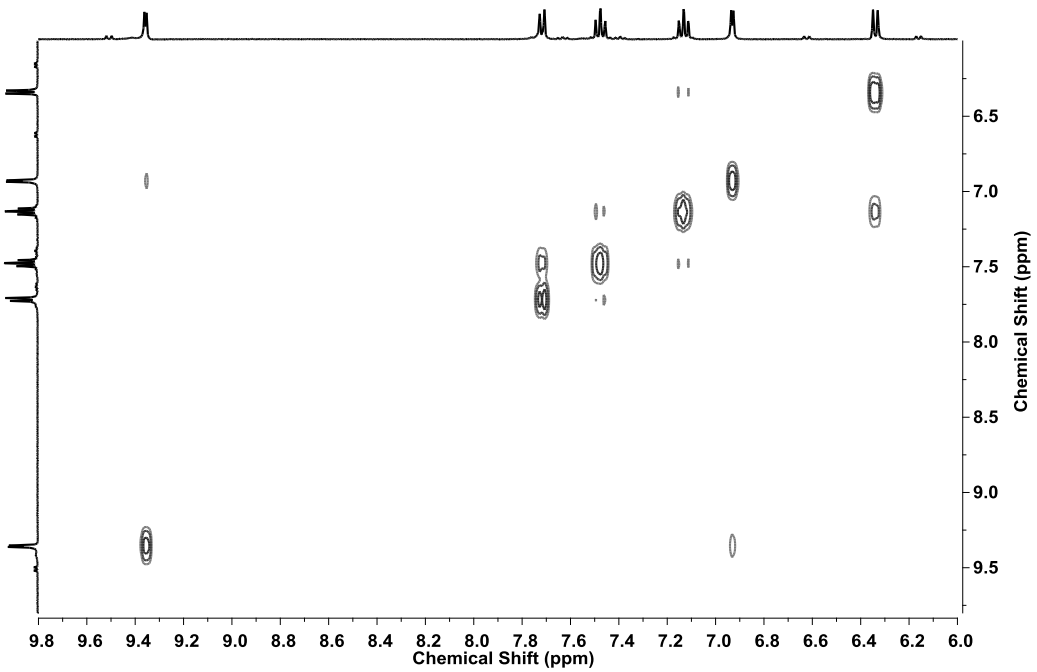

Figure IV.23: ^{1}H-^{1}H COSY spectrum of **IV.6** in *Dichloromethane-d_2* at 295K.

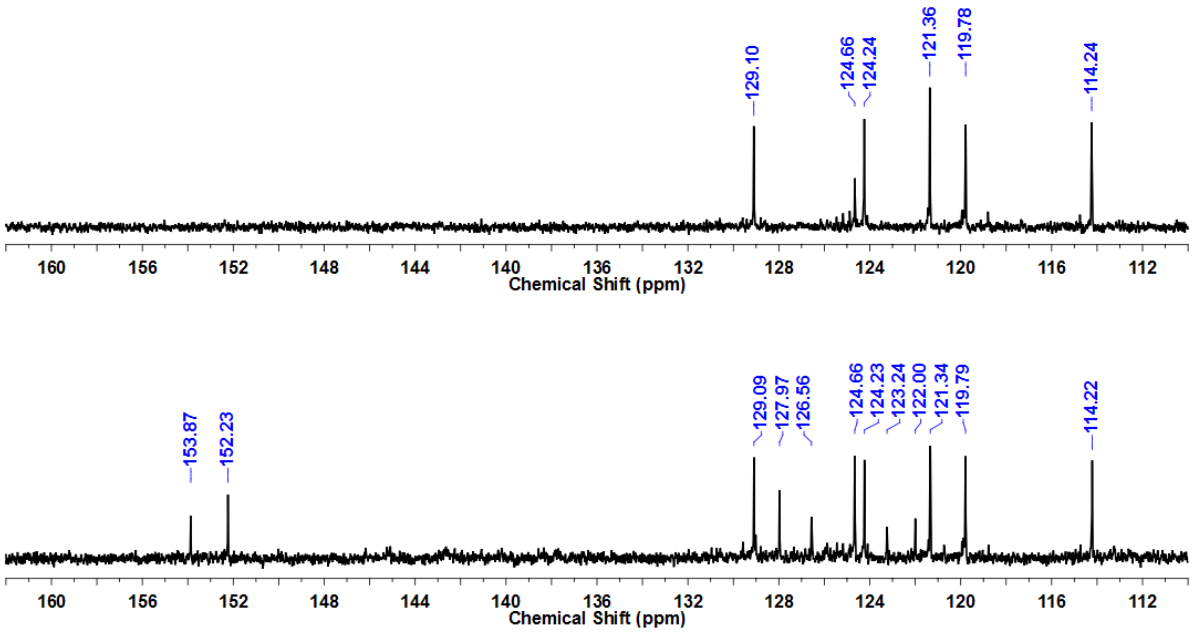

Figure IV.24:(Top) DEPT-90 and (Bottom**)** ^{13}C-NMR spectrum of **IV.6** in *Dichloromethane-d_2*.

IV.6: Synthesis and Characterization of Dimer IV.8:

Similarly the reaction of dibenzofused doubly N-confused dipyrromethane **IV.7** with copper(II) acetate yielded another unexpected dimer **IV.8** (Scheme IV.4) having *m/z* ratio 817.1436 in 3% yields (Figure IV.25).

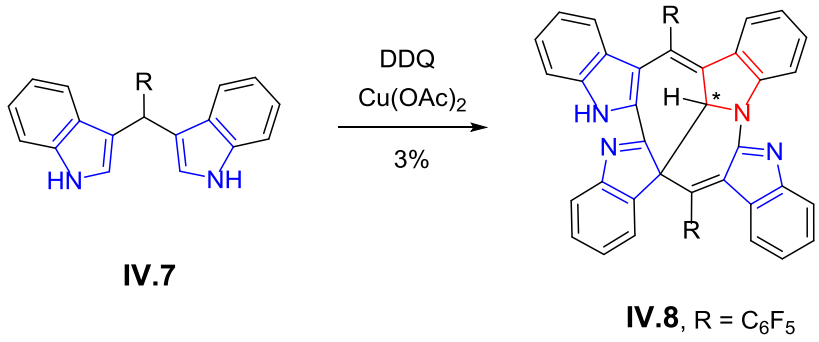

IV.7

IV.8, R = C_6F_5

Scheme IV.4: Synthesis of Dimer **IV.8.**

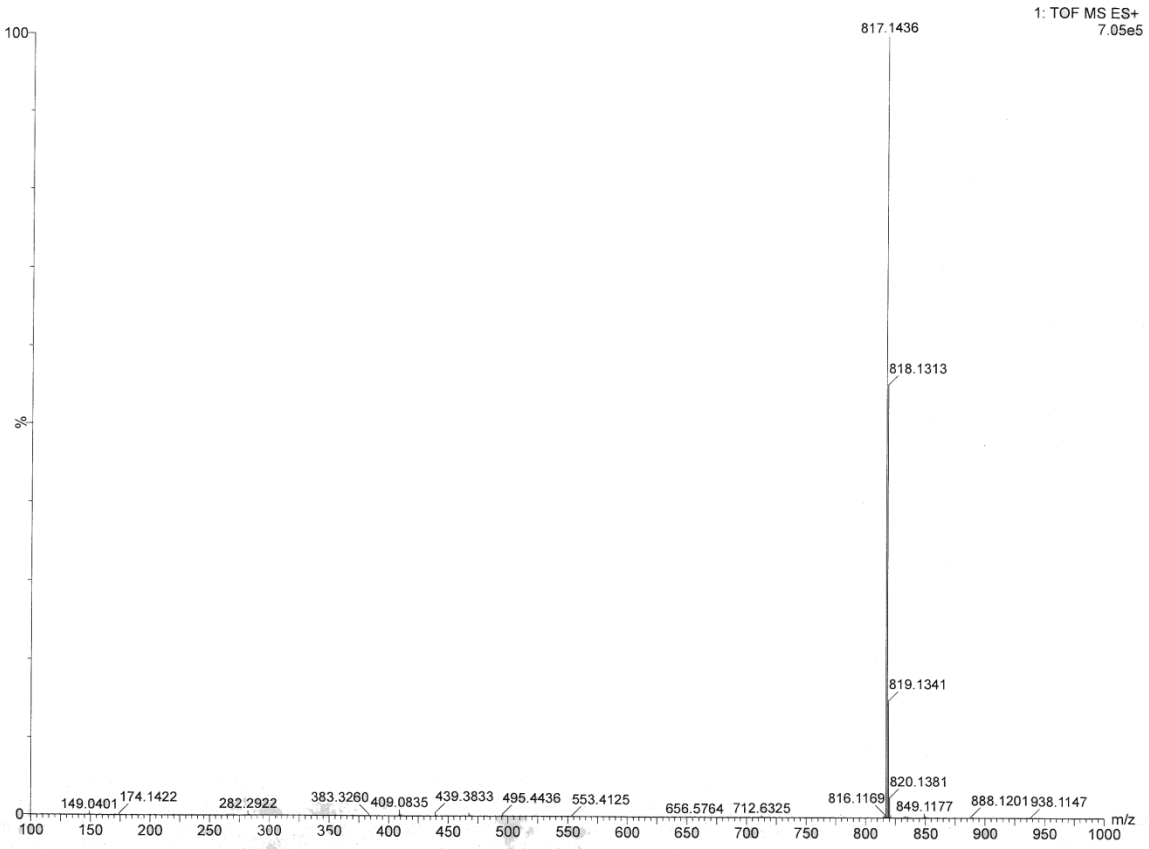

Figure IV.25: HR-ESI-TOF mass spectrum of **IV.8**.

The noticed *m/z* value of compounds **IV.8** in their HRMS spectrum also indicated the possibility of formation of N-confused nornorrole **IV.8NN** (Figure IV.26).

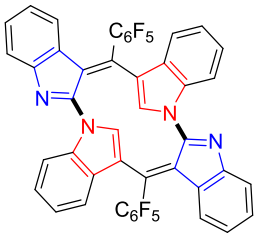

IV.8NN

Figure IV.26: Expected Structures of Contracted Norroles.

The molecular structure of **IV.8** indicated that the all the indole rings in F to I are involved in the unsymmetrical connectivity of two dibenzofused doubly N-confused dipyrrin units (Figure IV.27a). Also **IV.8** contains three types of connection between two dibenzofused doubly N-confused dipyrrin units (a) the nitrogen of indole (F ring) is connected to another indole (I ring) at the α-carbon of the another dibenzofused doubly N-confused dipyrrin leading to the formation of N-C_α bond, (b) the α-carbon of one dibenzofused indole (G ring) of the doubly N-confused dipyrrin forms a bond with anther indole (H ring) at the α-carbon of the another dibenzofused doubly N-confused dipyrrin forming C_α-C_α bond and (c) finally the α-carbon of the indole (F ring) and the indole H ring β-carbon which is connected to *meso* carbon of the dibenzofused doubly N-confused dipyrrin undergoes oxidative coupling reaction at the centre of macrocycle to form an unusual C_α-C_β bond (Figure IV.27b). This leads to formation of chiral carbon and bicyclic system having six and seven membered rings.

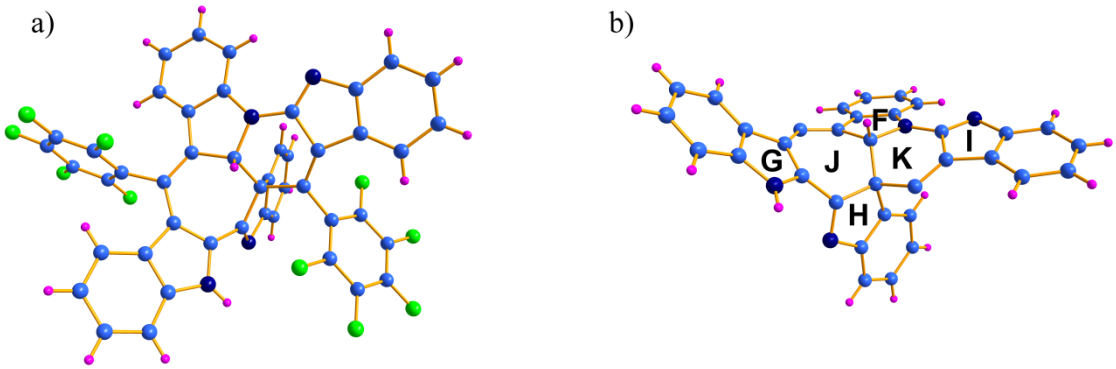

Figure IV.27: Molecular Structures of chiral dimer **IV.8**, a) top view and b) side view, the *meso* pentafluorophenyl groups were omitted for clarity.

The molecule **IV.8** displayed a total of eighteen signals from δ = 6.49 to 11.81 ppm in its ^{1}H NMR spectrum (Figure IV.28). The D_2O addition confirmed the presence of a lone NH in the molecule at 11.81 ppm and the chiral carbon proton resonated at 6.49 ppm (Figure IV.29). ^{1}H-^{1}H COSY exhibited absence of correlation for signal at 6.49 and 11.81 ppm, while the remaining sixteen signals from 6.62 to 8.26 ppm were involved in multiple correlations (Figure IV.30). Its DEPT-90 spectrum displayed seventeen number of ^{13}C signals with the sp^3 chiral carbon resonance at 69 ppm (Figure IV.31). All these observation confirmed the formation of **IV.8** instead of **IV.8NN**.

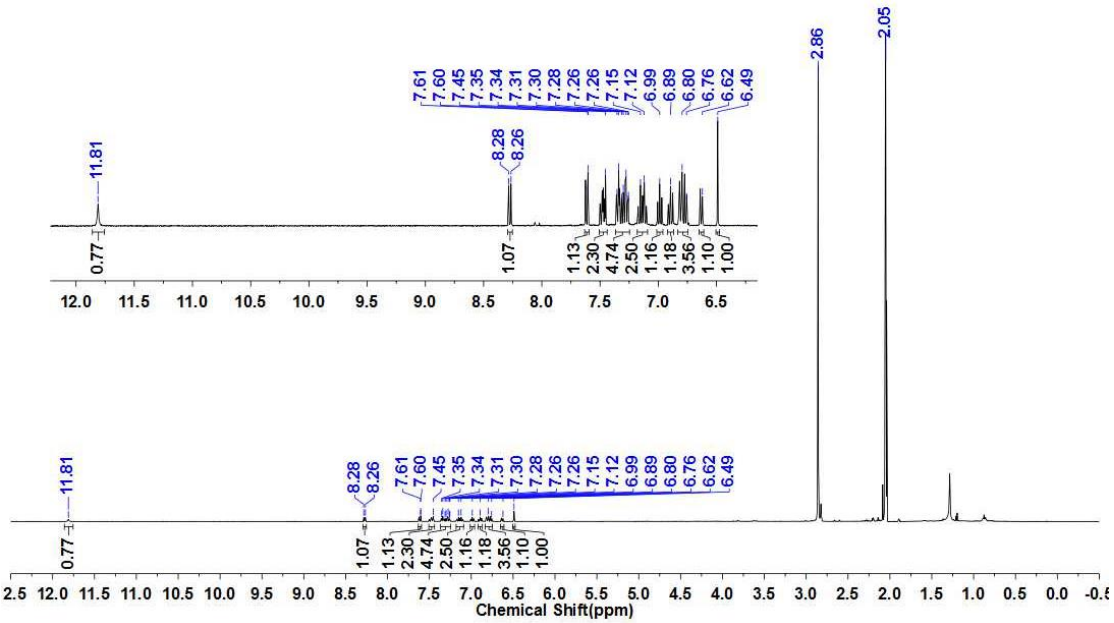

Figure IV.28: ^{1}H-NMR spectrum of **IV.8** in *Acetone-d_6* at 295K.

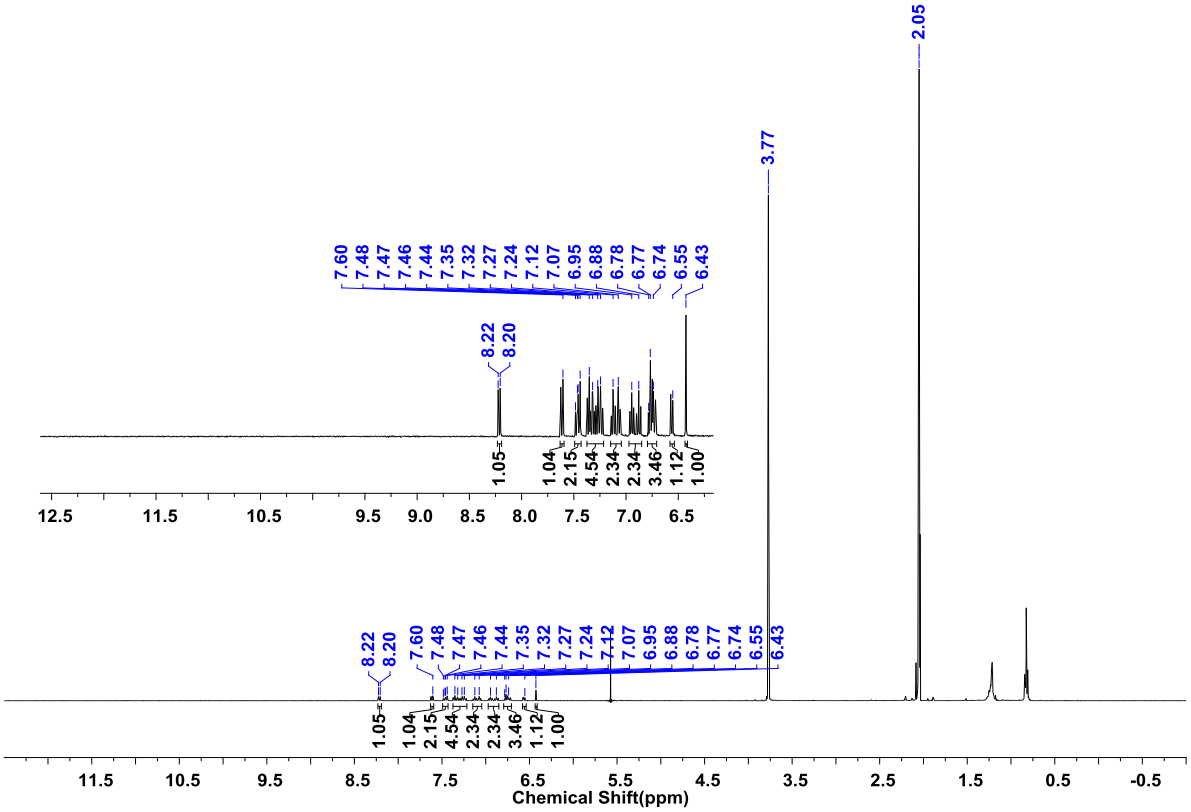

Figure IV.29: ^{1}H-NMR spectrum of **IV.8** after D_2O exchange in *Acetone-d_6* at 295K

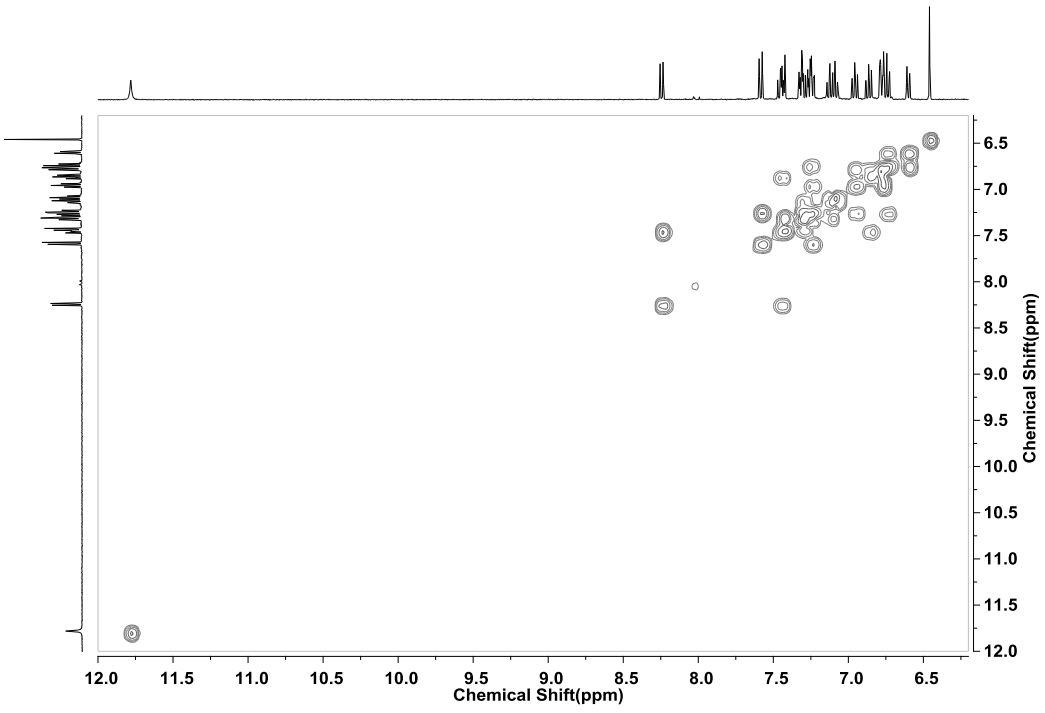

Figure IV.30: ^{1}H-^{1}H COSY spectrum of **IV.8** in *Acetone-d_6* at 295K.

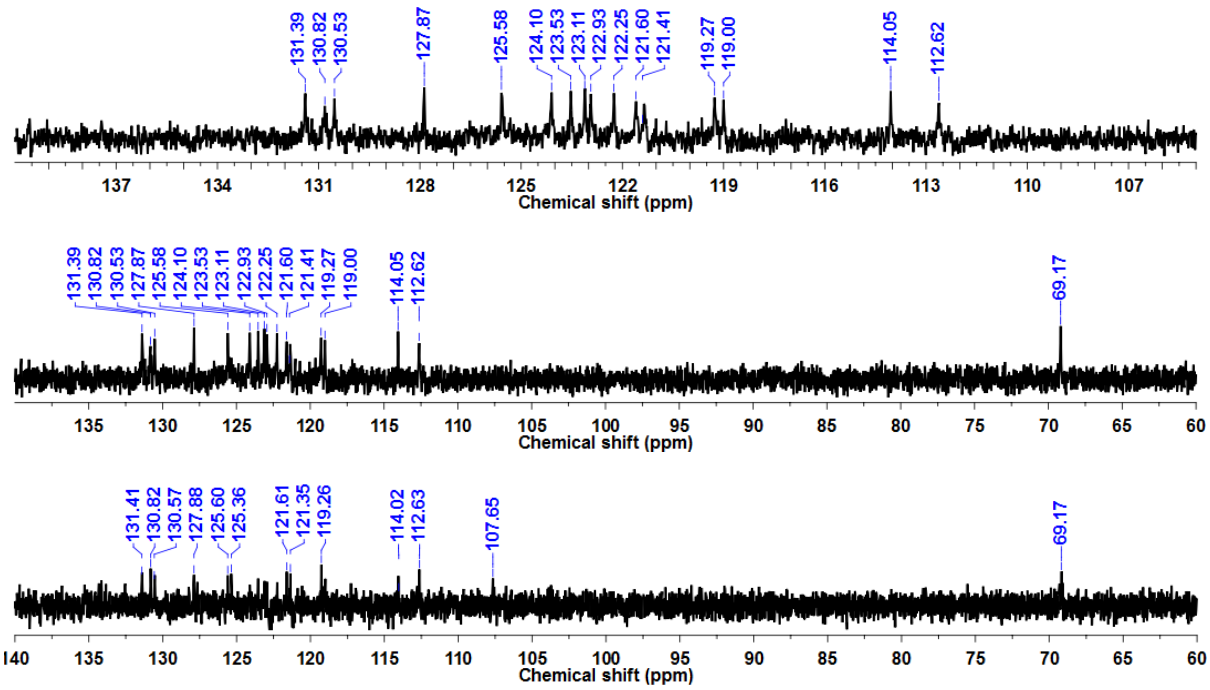

Figure IV.31: (Top) Zoomed-DEPT-90, (Middle) DEPT-90 and (Bottom) ^{13}C-NMR COSY spectrum of **IV.8** in *Acetone-d_6* at 295K.

IV.7: Optical Properties:

All these molecules displayed reddish colored solutions in dichloromethane with dissimilarities in their electronic spectrum. The compound **IV.2a** absorbs at λ = 271 nm (ε = 29580) and 440 nm (ε = 32210). Molecule **IV.6** absorbs at 322 nm (ε = 17900), 388 nm (ε = 14420) 503 nm (ε = 7460) and 540 nm (ε = 7960). The compound **IV.3** was found to absorb at λ = 281 nm (ε = 16830), 325 nm (ε = 16660), 342 nm (ε = 16760) and 391 nm (ε = 21350). The compound **IV.8** found to show absorbance at 283 nm (ε = 1430) and 338 nm (ε = 750) (Figure IV.31). Nucleus Independent Chemical Shift (NICS)[60] values were obtained by employing Gaussian 09[61] program for **IV.2a** and **IV.2b** to estimate the extent of π-electron delocalization in the macrocyclic framework. The computed NICS(0) values for both the macrocycles are δ = 2.1 ppm indicating the presence of weak paratropic ring current and hence can be classified as anti-aromatic in nature.

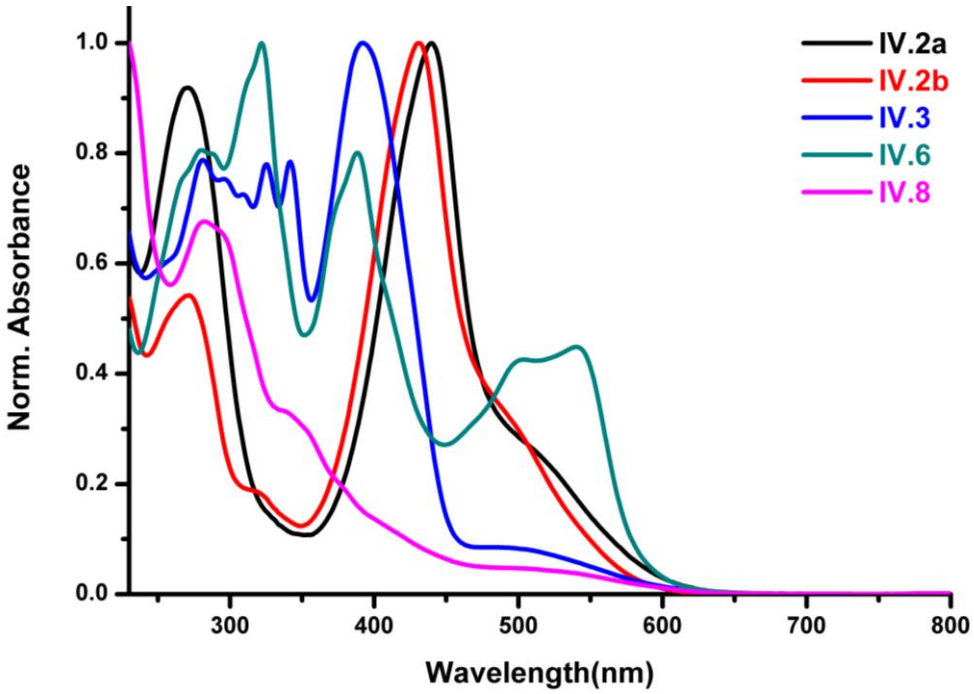

Figure IV.32: Electronic spectra of ~10^{-6} M solutions of **IV.2a, IV.2b, IV.3, IV.6** and **IV.8** in dichloromethane.

IV.8: Conclusions

In summary, with respect to dipyrrin as a chelating agent, the fusion approach on N-confused pyrrole ring of N-confused dipyrrin and doubly N-confused dipyrrin has modified its reactivity with the metal salts. A variety of novel dimers of confused dipyrrins **IV.3** and **IV.8** which contain unique N,α-N,α and α,α-N,α-β,α biyrrole linkages respectively have been synthesized. Their method of synthesis is very simple and can be catalysed with a variety of metal salts. They may not be the example of porphyrinoids but suggested the validity of confused dipyrrins derivatives to neo-confusion approach. The obtained macrocycles **IV.2a** and **IV.2b** are the first examples of oxygenated 24 π-electron expanded norroles which exhibited paratropic ring current effect thus anti-aromatic in nature. Also the dimer **IV.6** displayed the characteristics of aza-heptalene as well as aza-hexacene. Synthetic difficulties, stability and solubility of hexacene are the obstacle for further studies but aza-hexacene is free from all these issues.

IV.9: Experimental Section:

All reagents and solvents were of commercial reagent grade and were used without further purification except where noted. Dry THF was obtained by refluxing and distillation over pressed Sodium metal. Column chromatography was performed on silica gel (230-400) in glass columns. ^{1}H NMR and ^{19}F NMR spectra were recorded either on a JEOL 400 MHz or Bruker 500 MHz spectrometer, and chemical shifts were reported as the delta scale in ppm relative to $(CH_3)_2SO$ (δ = 2.50 ppm) or THF (δ = 1.73 ppm) or $(CH_3)_2CO$ (δ = 2.1 ppm) as internal reference for ^{1}H. High Resolution Mass spectra were obtained using WATERS G2 Synapt Mass Spectrometer. Electronic spectra were recorded on a Perkin-Elmer λ-900 ultraviolet−visible (UV−vis) spectrophotometer. Single crystals were grown in suitable organic solvent and Single crystal X-ray diffraction were performed at 100K on BRUKER KAPPA APEX II CCD Duo diffractometer (operated at 1500 W power: 50 kV, 30 mA) using graphite-monochromated Mo Kα radiation (λ = 0.71073 Å). Quantum mechanical calculations were carried out on Gaussian 09 program suite using High Performance Computing Cluster facility of IISER PUNE. All calculations were carried out by Density Functional Theory (DFT) with Becke's three-parameter hybrid exchange functional and the Lee-Yang-Parr correlation functional (B3LYP) and 6-31G(d,p) basis set for all the atoms were employed in the calculations. To estimate the NICS(0) values at the center of the seven membered rings of molecular plane of all the macrocycles, the gauge independent atomic orbital(GIAO) method used based on the optimized geometries. The molecular structures obtained from single crystal analysis were used for geometry optimization.

Procedure for Synthesis of IV.1

To a dissolved Indole-3-carboxaldehyde (1 gm, 6.8966 mmol, 1 equiv.) in 20 ml dry THF, pentafluorophenyl magnesium bromide (2.4 equiv.) was added and reaction mixture stirred overnight. The reaction was quenched with solution of saturated ammonium chloride and worked up with dichloromethane. Solvent were evaporated on rota evaporator. The carbinol (2 gm, 6.3898 mmol, 1 equiv.) obtained was condensed with pyrrole (22 ml, 319.4888 mmol, 50 equiv.) using trifluoroacetic acid (0.049 ml, 0.6390 mmol, 0.1 equiv.) in 100 ml round bottom flask under inert N_2 atmosphere. After 30 minute 50 ml dichloromethane was added and organic layer

extracted from 50 ml 0.1 N NaOH aqueous layer in dichloromethane, dried over sodium sulphate and solvent were evaporated in vacuo. The residue was chromatographed to get pure MonoBenzo N-Confused Dipyrromethane (MBNCDPM) **IV.1** (1.3 gm, Yield = 56%). **^{1}H NMR** (Acetone-d_6, 400MHz, 295K): δ = 6.00(m, 1H), 6.05(m, 1H), 6.15(s, 1H), 6.73(m, 1H), 6.97(m, 1H), 7.11(m, 2H), 7.26(d, J = 8.0 Hz, 1H), 7.41(d, J = 8.0 Hz, 1H), 9.95(bs, 1H, exchangeable with D_2O), 10.24(bs, 1H, exchangeable with D_2O); **^{13}C-NMR** (Acetone-d_6, 400MHz, 295K): δ = 31, 106, 107, 111, 113, 117, 118, 119, 121, 123, 126, 129 ppm; **HRMS** (EI): *m/z* calcd for $(C_{19}H_{11}F_5N_2\text{-}H)^+$ = 361.0764; observed = 361.0768

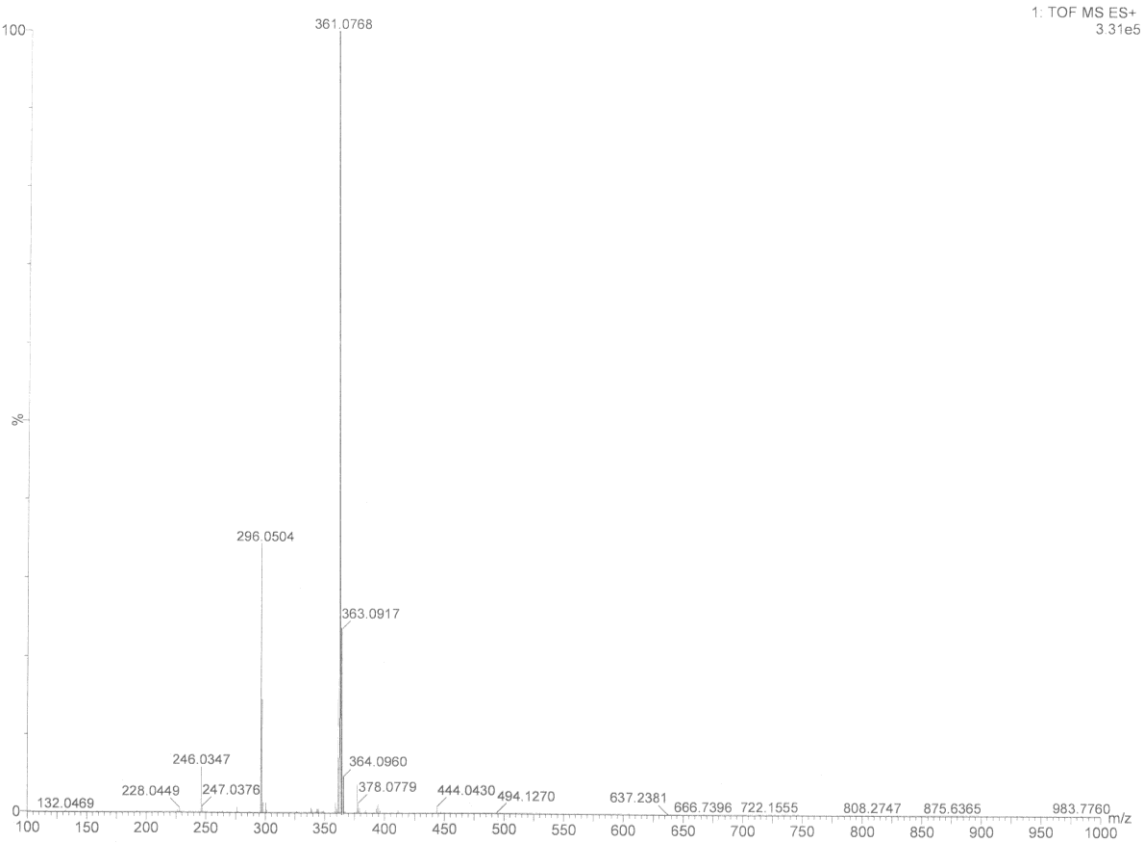

Figure IV.33: HR-ESI-TOF mass spectrum of **IV.1**.

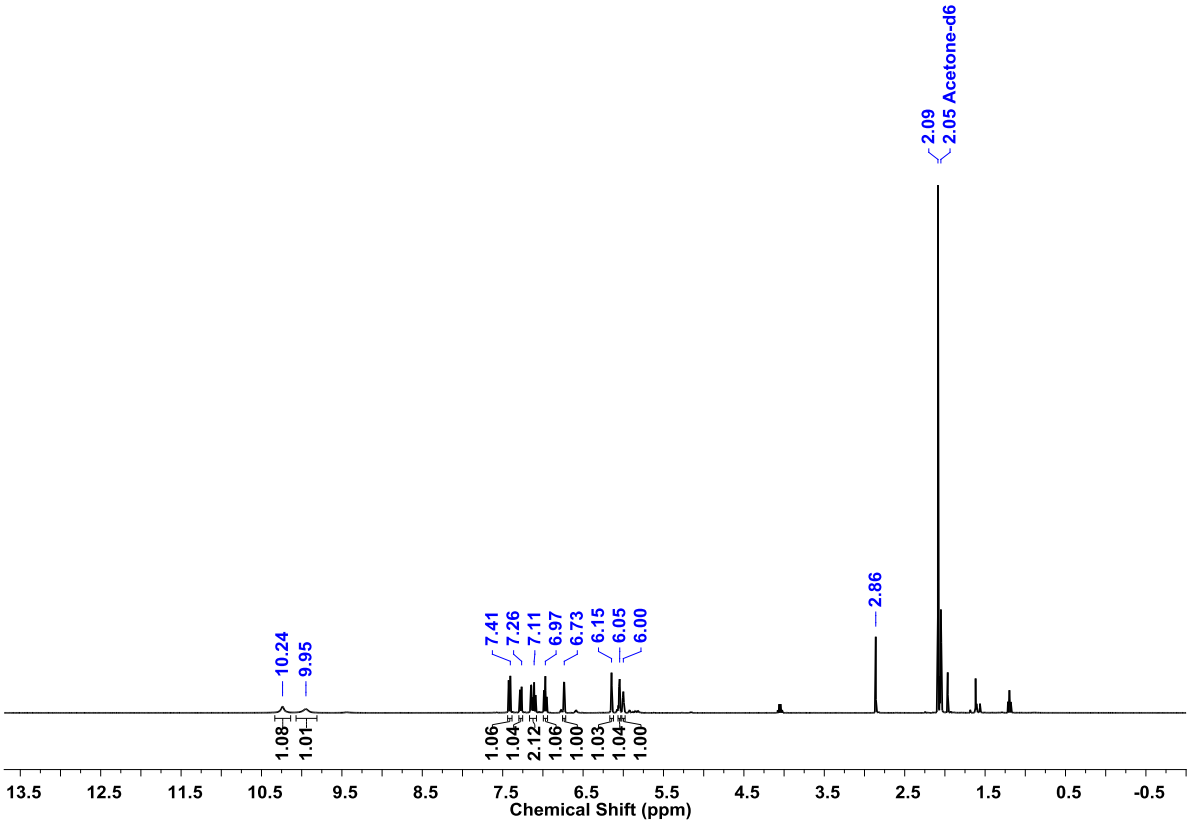

Figure IV.34: ^{1}H-NMR spectrum of **IV.1** in *Acetone-d_6* at 295K.

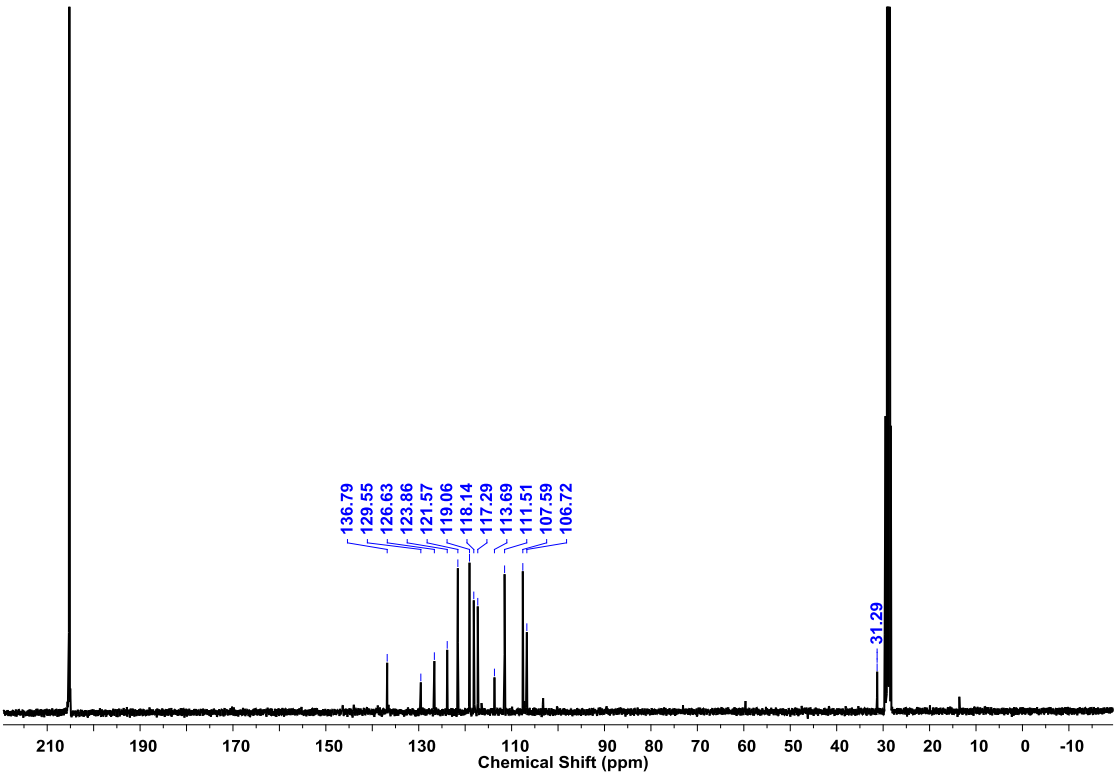

Figure IV.35: ^{13}C-NMR spectrum of **IV.1** in *Acetone-d_6* at 295K

Procedure for Synthesis of IV.2a:

In 25 ml two neck round bottom flask, MBNCDPM **IV.1a** (500 mg, 1.3812 mmol, 1 equiv.) dissolved in 10 ml dry THF and DDQ (690 mg, 3.0387 mmol, 2.2 equiv.) was added under N_2 atmosphere. Copper(II) acetate (248 mg, 1.3812 mmol, 1 equiv.) was added after 1 hour and reaction stirred overnight. Reaction mixture was directly chromatographed on silica gel (230-400 mesh) to get red colour **IV.2a** (21 mg, 3.9%) in 10% ethyl acetate/n-hexane as eluent. **^{1}H NMR** (THF-d_8, 400MHz, 295K): δ = 6.01(d, J = 8.0 Hz, 3H), 6.43(m, 3H), 6.68(m, 3H), 6.89(t, J = 8.0 Hz, 3H), 7.21(t, J = 8.0 Hz, 3H), 7.55(d, J = 8.0 Hz, 3H), 14.86(bs, 3H, exchangeable with D_2O); **^{13}C NMR** (THF-d_8, 400MHz, 295K)**:** δ = 103, 111, 115, 121, 122, 124, 125, 126, 127, 133, 138, 167 ppm; **^{19}F NMR** (THF-d_8, 376MHz, 295K): -162.27(t, J = 22.56 Hz, 6F), -154.56(t, J = 22.56 Hz, 3F), -142.51(d, J = 22.56 Hz, 6F); **HRMS** (EI): *m/z* calcd. for $(C_{57}H_{21}F_{15}N_6O_3)^+$ = 1122.1436, Observed = 1122.1387; **UV-Vis** (CH_2Cl_2): $\lambda_{max}(\varepsilon)$L $mol^{-1}cm^{-1}$ = 271 nm (29580) and 440 nm (32211); **Crystal data:**$C_{62}H_{21}N_6F_{15}O_3$(M_r = 1182.85), monoclinic, space group *P 21/c (No.14)*, *a* = 8.6387(19), *b* = 14.094(3), *c* = 42.764(10)Å, *α* = 90.00, *β* = 91.418(5), *γ* = 90.00°, V = 5205(2)Å^3, Z = 4, ρ_{calcd} = 1.510 mg/m^3, *T* = 100K, R_{int} (all data) = 0.1046, R_1(all data) = 0.1785, R_W (all data) = 0.2842, GOF = 1.554

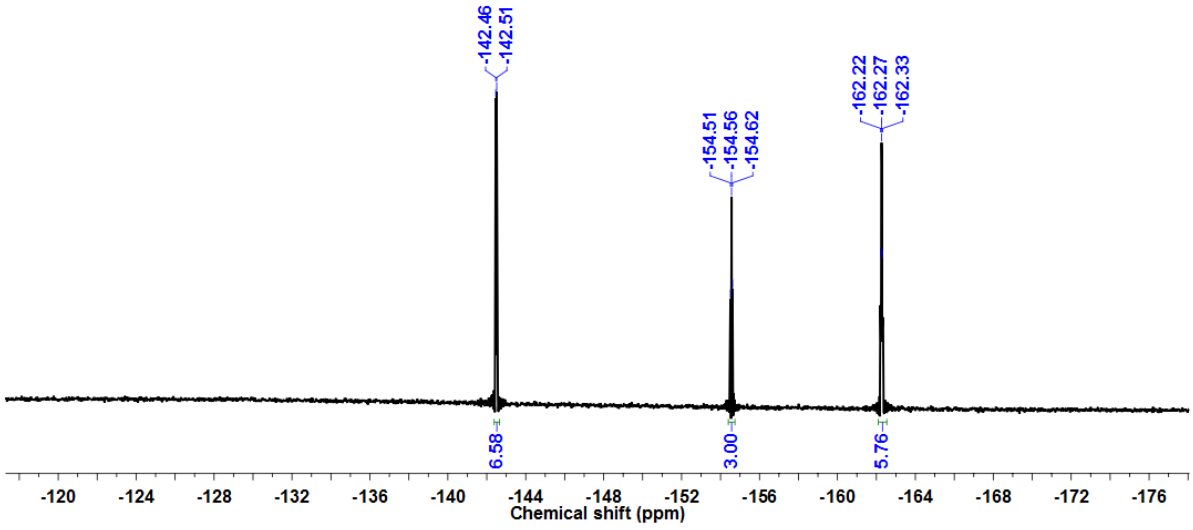

Figure IV.36: ^{19}F-NMR spectrum of **IV.2a** in *Tetrahydrofuran-d_8* at 295K.

Procedure for Synthesis of IV.2b:

MBNCDPM **IV.1b** (500 mg, 1.8382 mmol, 1 equiv.), DDQ (918 mg, 4.0412 mmol, 2.2 equiv.) and copper(II) acetate (330 mg, 1.8382 mmol, 1 equiv.) were reacted using similar protocol as mentioned above for **IV.2a**. **IV.2b** (19 mg, Yield 3.6%). **^{1}H NMR** (Dichloromethane-d_2, 400MHz, 295K): δ = 5.50 (d, J = 8.0 Hz, 3H), 6.20 (m, 3H), 6.52 (m, 3H), 6.67 (t, J = 8.0 Hz, 3H), 7.08 (t, J = 8.0 Hz, 3H), 7.39 (m, 6H), 7.44(d, J = 8.0 Hz, 3H), 7.58 (m, 6H), 14.83(bs, 3H, exchangeable with D_2O); **HRMS** (EI): *m/z* calcd. for $(C_{57}H_{36}N_6O_3+H)^+$= 853.2927, Observed = 853.2905; **UV-Vis** (CH_2Cl_2): $\lambda_{max}(\varepsilon)$L $mol^{-1}cm^{-1}$ = 271 nm (6177), 431 nm (11431); **Crystal data:**$C_{57}H_{36}N_6O_4$(M_r = 868.92), triclinic, space group *P -1 (No.2)*, a = 12.261(6), b = 13.380(6), c = 14.218(6)Å, α = 77.740(9), β = 81.518(10), γ = 89.721(12), V = 2253.5(18)Å^3, Z = 2, ρ_{calcd} = 1.281 mg/m^3, T = 100K, R_{int} (all data) = 0.1061, R_1(all data) = 0.2447, R_W (all data) = 0.3764, GOF = 1.000

Procedure for Synthesis of IV.3:

MBNCDPM **IV.1a** (200 mg, 0.5525 mmol, 1 equiv.) was dissolved in 200ml dry tetrahydrofuran in two neck 250ml round bottom flack under N_2 inert atmosphere and DDQ(276 mg, 1.2155 mmol, 2.2 equiv.) was added. After 1 hour copper(II) acetate (99 mg, 0.5525 mmol, 1 equiv.) added and reaction continued for overnight. Then reaction mixture was passed through a bed of basic alumina, a dark colour fraction obtained contains **IV.2a** and **IV.3**. The organic fraction was evaporated on rota evaporator to get crude reaction mixture which was further purified on silica gel (230-400 mesh) by column chromatography. First fraction gave red colour band **IV.2a** (7 mg, 3.4%) and second band corresponds to **IV.3** (8 mg, 4%). **^{1}H NMR** (Acetone-d_6, 400MHz, 295K): δ = 5.62(s, 1H), 6.18(m, 1H), 6.32(m, 1H), 6.48(d, J = 8.0 Hz, 1H), 6.57(d, J = 8.0 Hz, 1H), 6.60(d, J = 8.0 Hz, 1H), 6.83(t, J = 8.0 Hz, 1H), 6.90-6.95(m, 2H), 7.02(s, 1H), 7.22(t, J = 8.0 Hz, 1H), 7.28(d, J = 8.0 Hz, 1H), 7.36-7.40(m, 2H), 8.23(d, J = 8.0 Hz, 1H), 10.10(bs, 1H, exchangeable with D_2O); **^{13}C NMR** (Acetone-d_6, 400MHz, 295K)**:** δ = 74, 111, 112, 116, 118, 121, 122, 124, 126, 127, 128, 129, 130, 143, 156, 158 ppm; **^{19}F NMR** (Acetone-d_6, 376MHz, 295K): -162.60(t, J = 22.56 Hz, 1F), -162.11(q, J = 22.56 Hz, 2F), -161.84(t, J = 22.56 Hz, 1F), -154.89 (d, J = 22.56 Hz, 1F), -154.65 (d, J = 18.80 Hz, 1F), -143.37 (d, J = 22.56 Hz, 1F), -142.75 (d, J = 22.56 Hz, 1F), -142.03 (d, J = 22.56 Hz, 1F) -141.88 (d, J = 22.56 Hz, 1F);

HRMS (EI): *m/z* calcd. for $(C_{38}H_{16}N_4F_{10}+H)^+$= 719.1294, Observed = 719.1288; **UV-Vis** (CH_2Cl_2): $\lambda_{max}(\varepsilon)$L $mol^{-1}cm^{-1}$ = 281 nm (16830), 325 nm (16658), 342 nm (16759), 391 nm (21354); **Crystal data:**$C_{41}H_{22}N_4F_{10}O$(M_r = 776.63), triclinic, space group *P -1 (No.2)*, *a* = 9.9304(18), *b* = 12.231(2), *c* = 14.545(3)Å, α = 75.314(4), β = 82.512(4), γ = 80.770(4)°, V = 1679.3(5)$Å^3$, Z = 2, ρ_{calcd} = 1.536 mg/m^3, *T* = 100K, R_{int} (all data) = 0.0524, R_1(all data) = 0.1342, R_W (all data) = 0.1372, GOF = 0.941

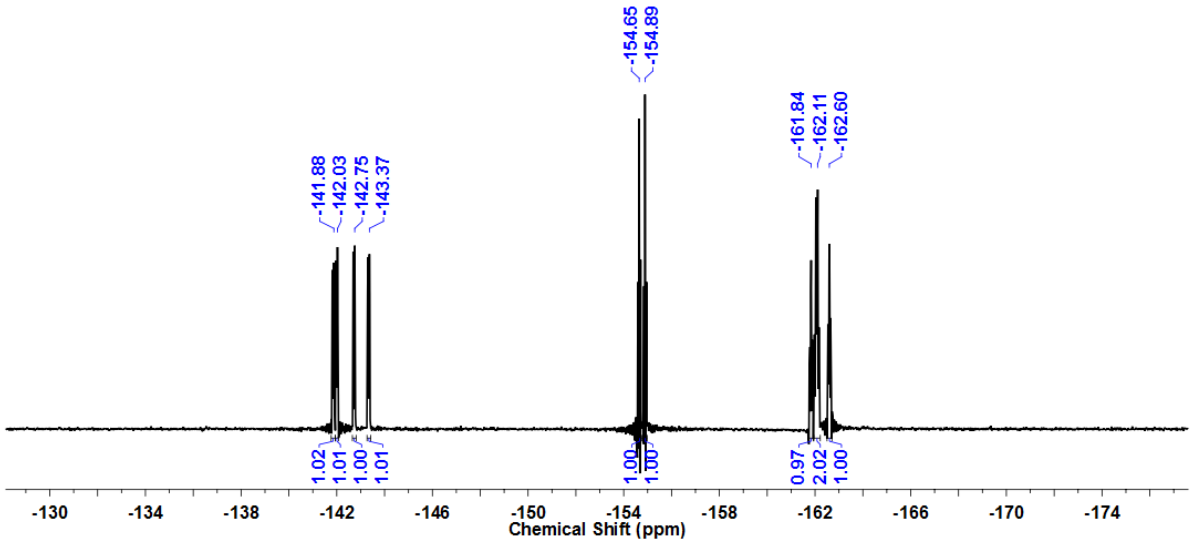

Figure IV.37: ^{19}F-NMR spectrum of **IV.3** in *Acetone-d_6* at 295K.

Procedure for Synthesis of IV.5:

The Indole-3-carboxaldehyde was reduced with pentafluorophenyl magnesium bromide to its carninol. Carbinol (2.5 gm, 7.9872 mmol, 1 equiv.) and 1-(triisopropylsilyl)pyrrole (4.45 gm, 19.9681 mmol, 2.5 equiv.) in 23 ml dry dichloromethane were stirred under N_2 at 0ºC for 10 min. Then $BF_3{\cdot}Et_2O$ (0.99 ml, 7.9872 mmol, 1 equiv.) was added and reaction mixture stirred at 0ºC for 5 min. The reaction mixture was passed through basic alumina using dichloromethane as eluent and solvent evaporated in vacuo. The concentrated reaction mixture was directly subjected to excess of tetrabutyl ammonium fluoride (1 M in THF) for 90 min., deprotected reaction mixture quenched with water and extracted with dichloromethane. The combined organic layer was dried over Na_2SO_4 and evaporated in vacuo. The residue obtained was purified by silica gel column chromatography using hexane/ethyl acetate eluent. The first fraction afforded MBNCDPM **IV.1a** (1 gm, Yield = 35%) and second fraction gave MonoBenzo Doubly N-Confused Dipyrromethane (MBDNCDPM) **IV.5** (1.4 gm, Yield = 48%). **^{1}H NMR** (Acetone-d_6,

400MHz, 295K): δ = 6.01(s, 1H), 6.17(s, 1H), 6.75(s, 1H), 6.79(m, 1H), 6.95(t, J = 8.0 Hz, 1H), 7.09(t, J = 8.0 Hz, 1H), 7.17(s, 1H), 7.29(d, J = 8.0 Hz, 1H), 7.39(d, J = 8.0 Hz, 1H), 9.97(bs, 1H, exchangeable with D_2O), 10.14(bs, 1H, exchangeable with D_2O); **^{13}C-NMR** (Acetone-d_6, 400MHz, 295K): δ = 31, 108, 111, 115, 116, 118, 119, 121, 122, 123, 127 ppm; **HRMS** (EI): *m/z* calcd for $(C_{19}H_{11}F_5N_2\text{-}H)^+$ = 361.0764; observed = 361.0769

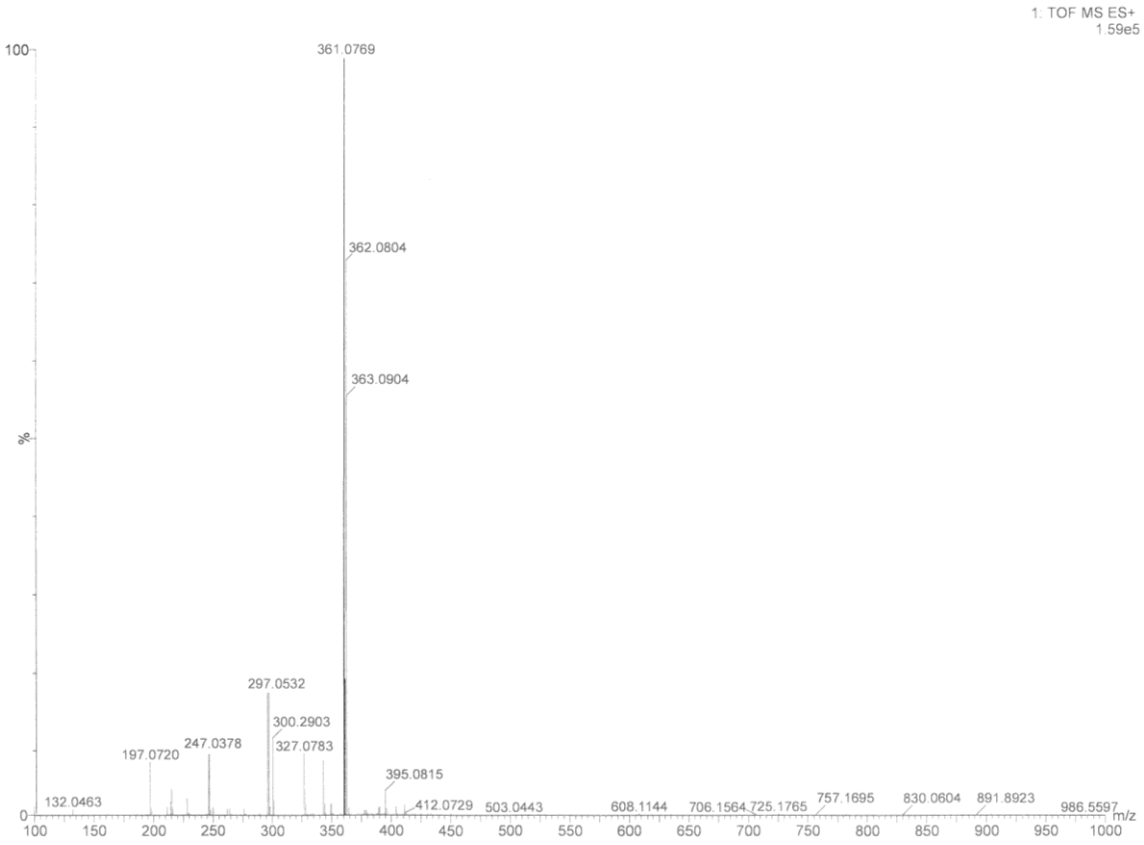

Figure IV.38: HR-ESI-TOF mass spectrum of **IV.5**.

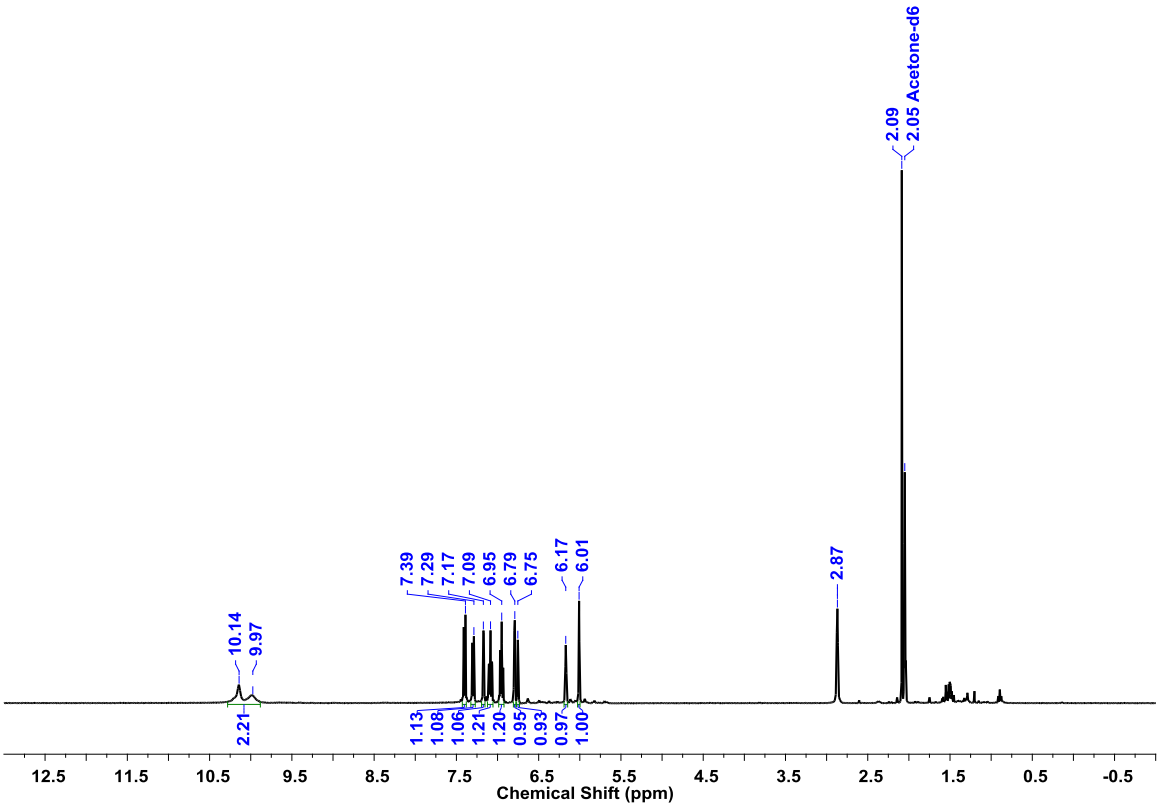

Figure IV.39: ^{1}H-NMR spectrum of **IV.5** in *Acetone-d_6* at 295K.

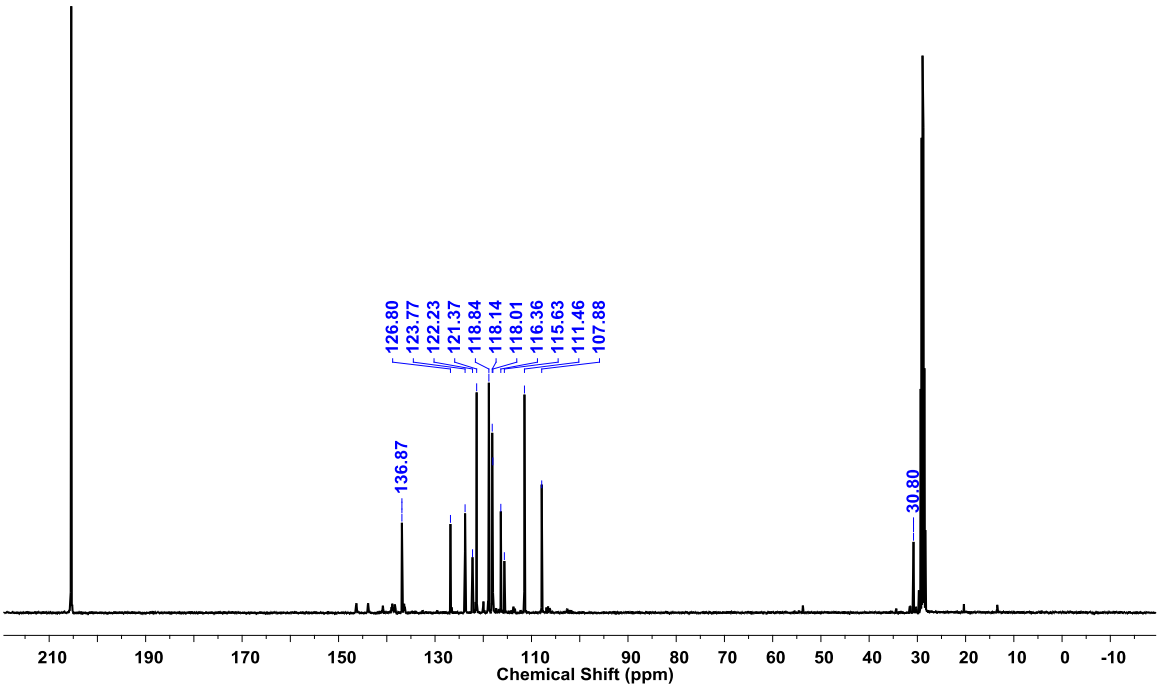

Figure IV.40: ^{13}C-NMR spectrum of **IV.5** in *Acetone-d_6* at 295K.

Procedure for Synthesis of IV.6:

The compound **IV.6** was synthesized by applying similar procedure as used for **IV.2a**. MBDNCDPM **IV.5** (700 mg, 1.9337 mmol, 1 equiv.) was oxidized to its dipyrrin using DDQ (966 mg, 4.2541 mmol, 2.2 equiv.) in 20 ml dry THF and further reaction with copper(II) acetate (348 mg, 1.9337 mmol, 1 equiv.) under goes oxidative cyclodimerization to compound **IV.6** (7 mg, Yield = 1%). **^{1}H NMR** (Dichloromethane-d_2, 400MHz, 295K): δ = 6.35(d, J = 8.0 Hz, 1H), 6.94(d, J = 4.0 Hz, 1H), 7.13(t, J = 8.0 Hz, 1H), 7.48(t, J = 8.0 Hz, 1H), 7.71(d, J = 8.0 Hz, 1H), 9.35(d, J = 4.0 Hz, 1H); **^{13}C NMR** (Dichloromethane-d_2, 400MHz, 295K)**:** δ = 114, 120, 121, 122, 123, 124, 125, 126, 128, 129, 152, 154 ppm; **^{19}F NMR** (Dichloromethane-d_2, 376MHz, 295K): -161.39(t, J = 18.80 Hz, 4F), -153.44(t, J = 18.80 Hz, 2F), -142.88(d, J = 18.80 Hz, 4F); **HRMS** (EI): *m/z* calcd. for $(C_{38}H_{12}N_4F_{10}+H)^+$ = 715.0981, Observed = 715.0965; **UV-Vis** (CH_2Cl_2): $\lambda_{max}(\varepsilon)$L $mol^{-1}cm^{-1}$ = 322 nm (17900), 388 nm (14420), 503 nm (7460), 540 nm (7960); **Crystal data:**$C_{38}H_{12}N_4F_{10}$(M_r = 714.52), triclinic, space group *P -1(No.2)*, *a* = 6.799(3), *b* = 8.219(3), *c* = 13.376(4)Å, *α* = 82.308(9), *β* = 75.542(7), *γ* = 83.754(10)°, V = 715.1(4)Å^3, Z = 1, ρ_{calcd} = 1.659 mg/m^3, *T* = 100K, R_{int} (all data) = 0.1119, R_1(all data) = 0.1656, R_W (all data) = 0.3393, GOF = 1.923

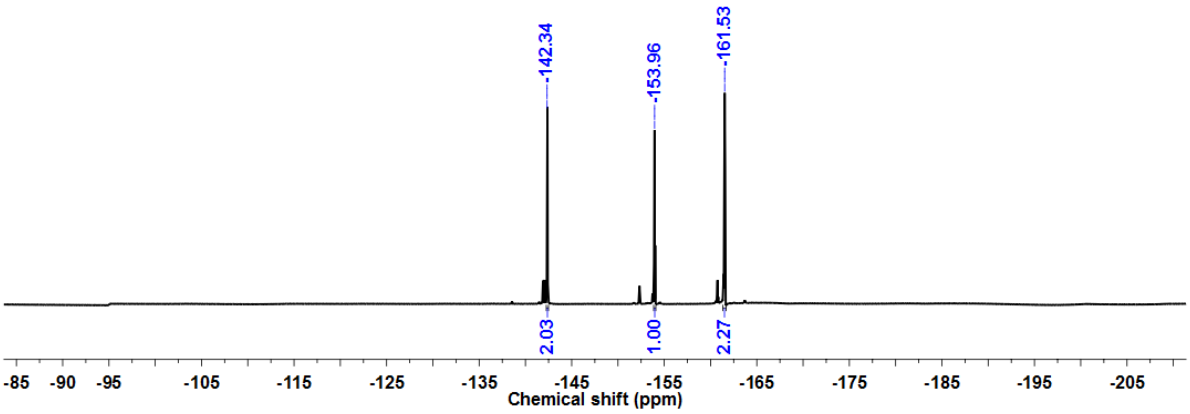

Figure IV.41: ^{19}F-NMR spectrum of **IV.6** in *Dichloromethane-d_2* at 295K.

Procedure for Synthesis of IV.7:

The Indole (2.34 gm, 20 mmol, 2 equiv.) was condensed with pentafluorobenzaldehyde (1.96 gm, 10 mmol, 1 equiv.) in 50 ml acetic acid by refluxing for 24 hours under inert N_2 atmosphere. Then the reaction mixture was evaporated and residue purified on silica gel (100-200 mesh). The colourless

compound DiBenzo Doubly N-Confused Dipyrromethane (DBDNCDPM) **IV.7** (4 gm, Yield = 97%) was obtained. **^{1}H NMR** (Acetone-d_6, 400MHz, 295K): δ = 6.37(s, 1H), 6.98(m, 2H), 7.14(m, 4H), 7.37(d, J = 8.0 Hz, 2H), 7.42(d, J = 8.0 Hz, 2H), 10.20(bs, 2H, exchangeable with D_2O); **^{13}C-NMR** (Acetone-d_6, 400MHz, 295K): δ = 29, 111, 114, 118, 119, 121, 124, 127, 137 ppm; **HRMS** (EI): *m/z* calcd for $(C_{23}H_{13}F_5N_2\text{-}H)^+$ = 411.0921; observed = 411.0923

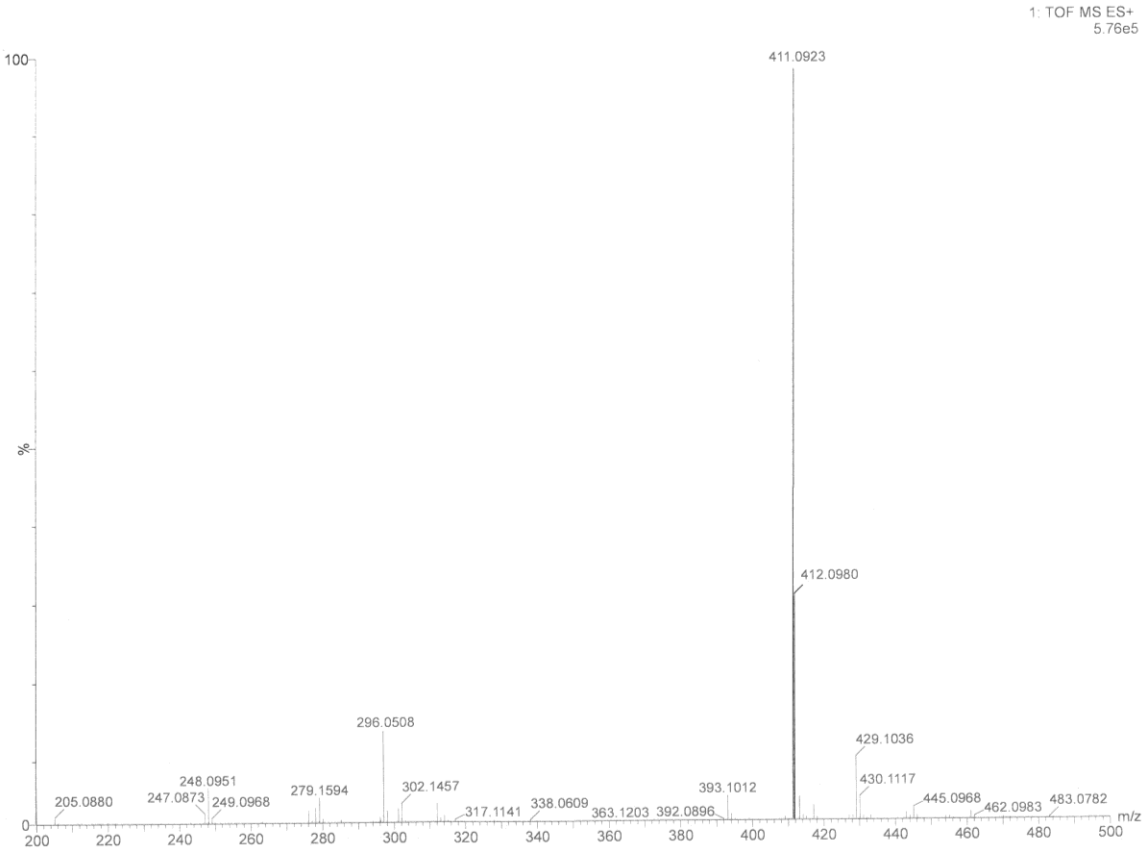

Figure IV.42: HR-ESI-TOF mass spectrum of **IV.7**.

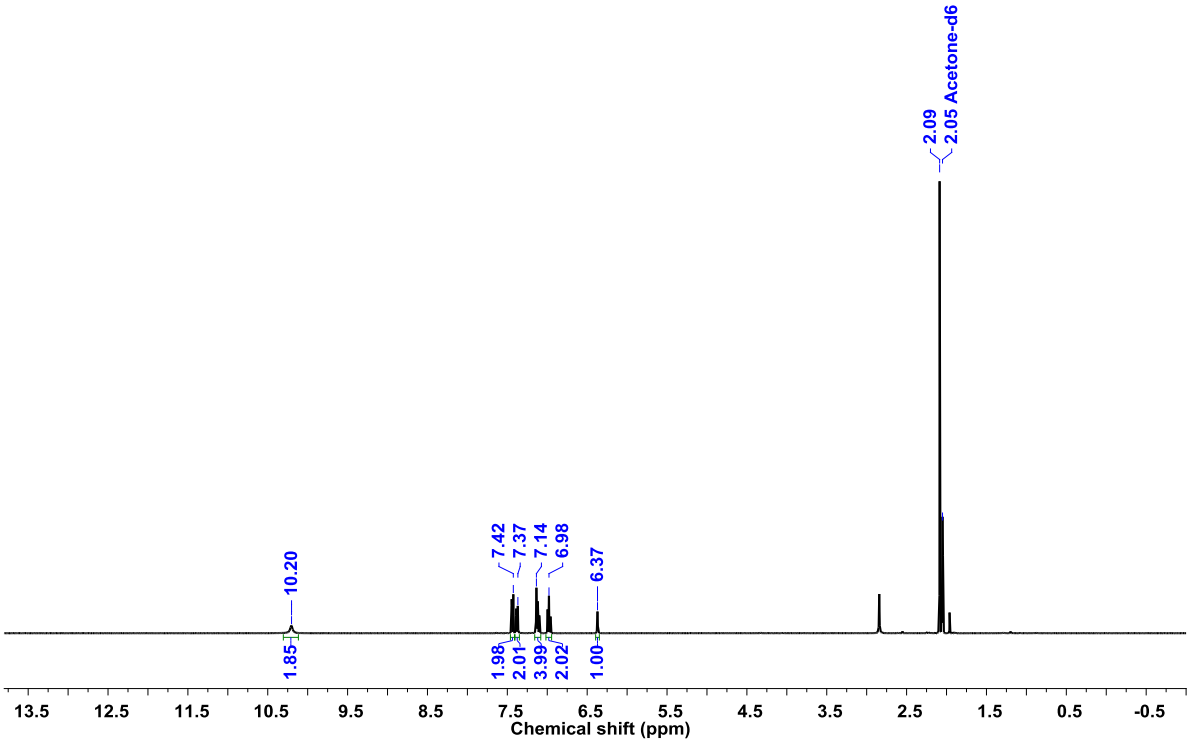

Figure IV.43: ^{1}H-NMR spectrum of **IV.7** in *Acetone-d_6* at 295K.

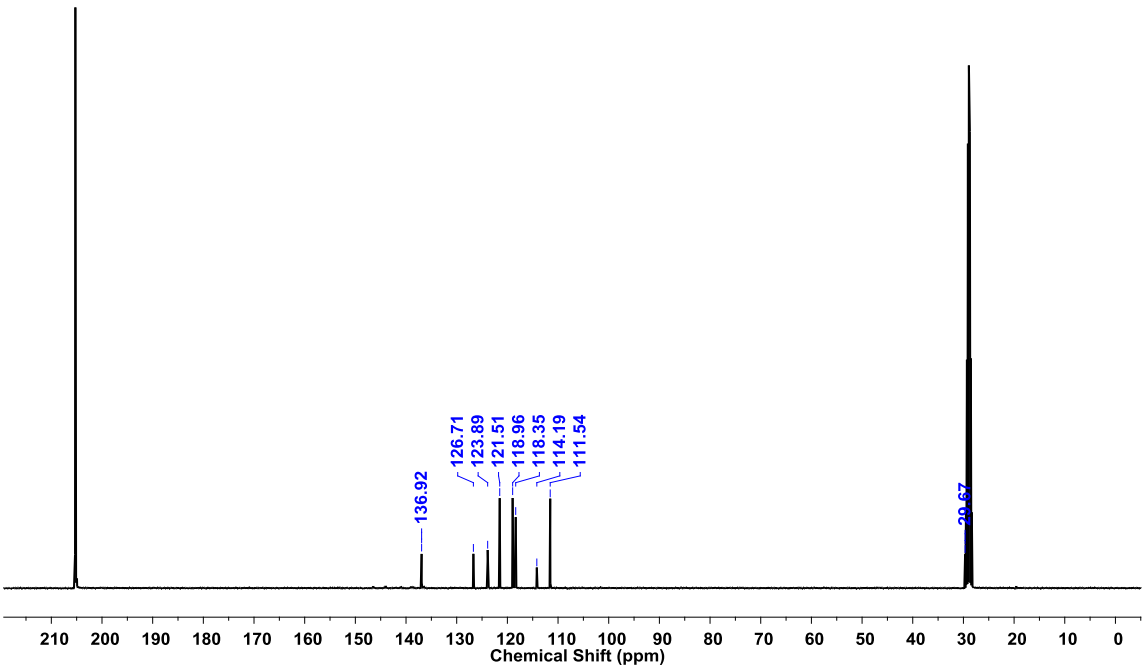

Figure IV.44: ^{13}C-NMR spectrum of **IV.7** in *Acetone-d_6* at 295K.

Procedure for Synthesis of IV.8:

In a 250 ml round bottom flask, under inert atmosphere DBDNCDPM **IV.7** (1.66 gm, 4.0291 mmol, 1 equiv.) was dissolved in 100ml dry THF and DDQ (2.01 gm, 8.8641 mmol, 2.2 equiv.) was added. After 1 hour, copper(II) acetate (725 mg, 4.0291 mmol, 1 equiv.) was added and reaction continued for overnight. Then brown colour compound **IV.8** (50 mg, 3%) was isolated by repetitive chromatographic purification. **^{1}H NMR** (Acetone-d_6, 400MHz, 295K): δ = 6.49(s, 1H), 6.62(d, J = 8.0 Hz, 1H), 6.76-6.82(m, 3H), 6.89(t, J = 8.0 Hz, 1H), 6.99(t, J = 8.0 Hz, 1H), 7.10-7.17(m, 2H), 7.26-7.35(m, 4H), 7.45-7.50(m, 2H), 7.60(d, J = 8.0 Hz, 1H), 8.26(d, J = 8.0 Hz, 1H), 11.81(bs, 1H, exchangeable with D_2O); **^{13}C NMR** (Acetone-d_6, 400MHz, 295K)**:** δ = 69, 108, 113, 114, 119, 121, 122, 125, 126, 128, 130, 131 ppm; **^{19}F NMR** (Acetone-d_6, 376MHz, 295K): -162.69(m, 3F), -159.37(t, J = 22.56 Hz, 1F), -155.28(t, J = 22.56 Hz, 1F), -153.05 (t, J = 22.56 Hz, 1F), -141.33 (d, J = 22.56 Hz, 1F), -140.89 (d, J = 22.56 Hz, 1F), -140.24 (d, J = 22.56 Hz, 1F), -136.88 (d, J = 22.56 Hz, 1F); **HRMS** (EI): *m/z* calcd. for $(C_{46}H_{18}N_4F_{10}+H)^+$= 817.1450, Observed = 817.1436; **UV-Vis** (CH_2Cl_2): $\lambda_{max}(\varepsilon)$L $mol^{-1}cm^{-1}$ = 283 nm (1436), 338 nm (755); **Crystal data:**$C_{46}H_{18}N_4F_{10}$(M_r = 816.64), monoclinic, space group *P 21/n (No.14)*, *a* = 10.144(2), *b* = 12.998(3), *c* = 25.579(5)Å, *α* = 90.00, *β* = 96.312(4), *γ* = 90.00°, V = 3352.2(12)Å^3, Z = 4, ρ_{calcd} = 1.618 mg/m^3, *T* = 100K, R_{int} (all data) = 0.0586, R_1(all data) = 0.1357, R_W (all data) = 0.1830, GOF = 0.972

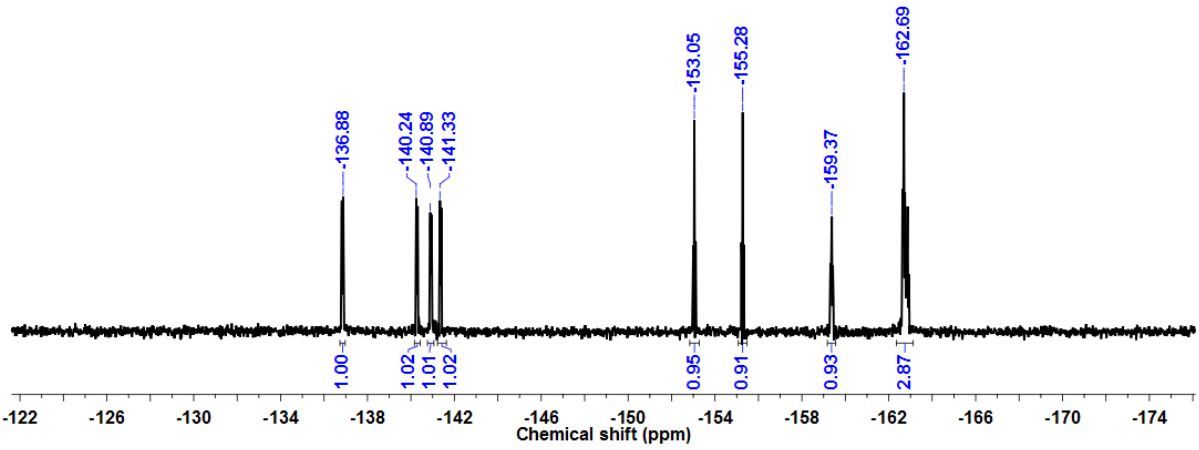

Figure IV.45: ^{19}F-NMR spectrum of **IV.8** in *Acetone-d_6* at 295K.

Summary of the Thesis

This thesis describes the synthesis and characterization of BODIPY derivatives, expanded norroles, aza-heptalenes and couple of unexpected dimers. 1,3-Bis**,** 1,4-Bis, 1,3,5-Tris and Tetra BODIPY derivatives were synthesized and their molecular structures were determined from single crystal X-ray analysis. All these fluorescent compounds exhibited strong intermolecular hydrogen bonding between donors -CH of the aromatic part (pyrrole or benzene) and -BF of the boron difluoride part hence act as a sythones for supramolecular architecture. Especially, 1,3,5-Tris BODIPY forms hydrogen bonded porous organic framework with the aid of strong intermolecular hydrogen bonding. Surprisingly, the molecular structure of Tetra-BODIPY displayed planar biphenyl unit along with delocalization of π-electron between two benzene rings. Tetra-BODIPY forms tetrameric structure with the help of intermolecular hydrogen bonds. Emission measurements indicated the decreased fluorescence in 1,4-Bis BODIPY as compared to the 1,3-Bis BODIPY due to free rotation between BODIPYs moieties and *meso*-phenyl ring. This was also supported by obtained molecular structures of 1,3-Bis BODIPY in locked conformation and 1,4-Bis BODIPY in comparatively open form. Tetra-BODIPY gives highest quantum yield and 1,3,5-Tris BODIPY has intermediate quantum yield amongst these BODIPY derivatives.

Employing N-confused dipyrrin and doubly N-confused dipyrrin as a chelating agent for various metal salts yielded the serendipitous expanded norroles and aza-heptalene respectively. In contrast to dipyrrin, N-confused dipyrrin undergoes intermolecular cyclomerization with metal salts to expanded norroles. The 24π anti-aromatic hexapyrrolic expanded norrole is the structural isomer of non-aromatic rosarin. Rosarin is known to take distorted conformation and recent report indicates the use of benzo substitution on bipyrrolic units to make rosarin into planar conformation. The hexapyrrolic expanded norrole displayed near planar conformation in solid state and this indicate the simplest way to synthesize hexaphyrin in a planar conformation instead of having benzo fusion. The 32π anti-aromatic octapyrrolic expanded norrole also exhibited planar conformation. In general, octaphyrins are known to adopt figure-of-eight conformation but octapyrrolic expanded norroles represent the first example of planar octaphyrin. Overall, the NMR studies are in agreement with the obtained molecular structures and indicate paratropic ring current effect. The computed NICS(0) value for hexapyrrolic and octapyrrolic macrocycles

are +4.5 and +1.5 and support the weak anti-aromatic nature. These expanded norroles are formed by head-to-tail interconnection of dipyrrin leading to form C-N linked bipyrrolic units. These molecules demonstrate the possibility of accommodating more than two neo-confused pyrrole moieties and represent a new class of stable, anti-aromatic expanded porphyrinoids with unusual π-conjugation. They have multiple C-N bonds along the conjugated pathway of the macrocyclic framework. The aza-heptalenes are confirmed by HRMS, NMR, SCXRD and UV-Visible spectroscopy. In contrast to dipyrrin, Doubly N-confused dipyrrin underwent intermolecular cyclodimerization with metal salts to aza-heptalene. Both the heptalenes displayed planar conformation in solid state and diatropic ring current effect in their ^{1}H-NMR spectrum hence aromatic in nature. As in expanded norroles, symmetrical heptalene **III.B.12** also adopted head-to-tail interconnection between two dipyrrin units. The unsymmetrical heptalene **III.B.13** has interconnection of two dipyrrin units and hence provided three different C_{α}-C_{α}, C_{α}-C_{β} and C_{α}-N linked bipyrrolic units. These molecules do not represent a macrocyclic core. The UV-Visible spectroscopy confirmed that these molecules represent heptalene characteristics rather than macrocyclic behaviour. The estimated NICS(0) support the aromatic nature of these molecules. Aza-heptalene **III.B.12 and III.B.13** are the structural isomer of each other which were obtained with copper(II) acetate and iron(III) acetylacetonoate respectively. They accommodate one and two neo-confused pyrrole rings hence contain one and two C-N bonds along the conjugated pathway of the molecular framework. This method of synthesis of expanded norroles and aza-heptalenes is simple and can be catalysed by a variety of metal ions.

The benzo fusion on confused pyrrole ring N-confused dipyrrin provided the 24π hexapyrrolic oxidized expanded norrole **IV.2a** and unusual dimer **IV.3**. The oxidized macrocycle **IV.2a** can be attributed to the high reactivity of the α-carbon of confused pyrrole rings facing the core of the macrocycle. On the other hand, the dimerized product **IV.3** was found to be chiral due to the unsymmetrical coupling between the two dipyrrin units. Another unexpected dimer **IV.8** derived from dibenzo doubly N-confused dipyrrin was also identified as an unsymmetrical chiral molecule. Also benzo fusion on one of the confused pyrrole ring of doubly N-confused dipyrrin has furnished another derivative of symmetrical aza-heptalene **IV.6**. This molecule has red shifted absorption than the unsubstituted aza-heptalene derivative and shows

strong π-π interactions with inter-planar distance of 3.307 Å. This molecule contains linear fusion of 6-5-7-7-5-6 membered aromatic rings and therefore represents a structure similar to hexacene.

In conclusion, this thesis discovers the few multi-BODIPY derivatives that display structural features good enough to act as synthons for supramolecular chemistry. It also discloses the attempts to metalate N-confused dipyrrin, doubly N-confused dipyrrin and their benzo derivatives which yielded novel molecules hitherto unknown so far.

References

[1] H. B. F. Dixon, A. Cornish-Bowden, C. Liebecq, K. L. Loening, G. P. Moss, J. Reedijk, S. F. Velick, P. Venetianer, J. F. G. Vliegenthart, *Pure Appl. Chem.* **1987**, *59*, 779-832.

[2] C. Bruckner, Y. Zhang, S. J. Rettig, D. Dolphin, *Inorg. Chim. Acta* **1997**, *263*, 279-286.

[3] A. Al-Sheikh-Ali, K. S. Cameron, T. S. Cameron, K. N. Robertson, A. Thompson, *Org. Lett.* **2005**, *7*, 4773-4775.

[4] S. M. Cohen, S. R. Halper, *Inorg. Chim. Acta* **2002**, *341*, 12-16.

[5] K. J. Brunings, A. H. Corwin, *J. Am. Chem. Soc.* **1942**, *64*, 593-600.

[6] A. J. Castro, J. P. Marsh, B. T. Nakata, *J. Org. Chem.* **1963**, *28*, 1943-1945.

[7] C. R. Porter, *J. Chem. Soc.* **1938**, 368-372.

[8] A. J. Castro, G. Tertzakian, B. T. Nakata, D. A. Brose, *Tetrahedron* **1967**, *23*, 4499-4507.

[9] L. H. Thoresen, H. Kim, M. B. Welch, A. Burghart, K. Burgess, *Synlett* **1998**, *1998*, 1276-1278.

[10] E. Vos de Wael, J. A. Pardoen, J. A. Van Koeveringe, J. Lugtenburg, *Recl. Trav. Chim. Pays-Bas* **1977**, *96*, 306-309.

[11] J. A. Van Koeveringe, J. Lugtenburg, *Recl. Trav. Chim. Pays-Bas* **1977**, *96*, 55-57.

[12] G. P. Arsenault, E. Bullock, S. F. MacDonald, *J. Am. Chem. Soc.* **1960**, *82*, 4384-4389.

[13] J. K. Laha, S. Dhanalekshmi, M. Taniguchi, A. Ambroise. J. S. Lindsey, *Org. Process Res. Dev.* **2003**, *7*, 799-812.

[14] C. Bruckner, V. Karunaratne, S. J. Rettig, D. Dolphin, *Can. J. Chem.* **1996**, *74*, 2182-2193.

[15] A. Treibs, F. H. Kreuzer, *Justus Liebigs Ann. Chem.* **1968**, *718*, 208-223.

[16] A. Loudet, K. Burgess, *Chem. Rev.* **2007**, *107*, 4891-4932.

[17] I. V. Sazanovich, C. Kirmaier, E. Hindin, L. Yu, D. F. Bocian, J. S. Lindsey, D. Holten, *J. Am. Chem. Soc.* **2004**, *126*, 2664-2665.

[18] S. A. Baudron, *Dalton Trans.* **2013**, *42*, 7498.

[19] C. Ikeda, S. Ueda, T. Nabeshima, *Chem. Commun.* **2009**, 2544-2546.

[20] S. Wang, *Coord. Chem. Rev.* **2001**, *215*, 79-98.

[21] N. Sakamoto, C. Ikeda, M. Yamamura, T. Nabeshima, *J. Am. Chem. Soc.* **2011**, *133*, 4726-4729.

[22] J. Kobayashi, T. Kushida, T. Kawashima, *J. Am. Chem. Soc.* **2009**, *131*, 10836-10837.

[23] V. S. Thoi, J. R. Stork, D. Magde, S. M. Cohen, *Inorg. Chem.* **2006**, *45*, 10688-10697.

[24] J. C. Marchon, R. Ramasseul, J. Ulrich, *J. Heterocycl. Chem.* **1987**, *24*, 1037-1039.

[25] G. Badger, R. Jones, R. Laslett, *Aust. J. Chem.* **1964**, *17*, 1028-1035.

[26] C. L. Hill, M. M. Williamson, *J. Chem. Soc., Chem. Commun.* **1985**, 1228-1229.

[27] J. A. S. Cavaleiro, M. d. F. P. N. Condesso, M. M. Olmstead, D. E. Oram, K. M. Snow, K. M. Smith, *J. Org. Chem.* **1988**, *53*, 5847-5849.

[28] T. E. Wood, A. Thompson, *Chem. Rev.* **2007**, *107*, 1831-1861.

[29] K. J. Brunings, A. H. Corwin, *J. Am. Chem. Soc.* **1944**, *66*, 337-342.

[30] S. R. Halper, M. R. Malachowski, H. M. Delaney, S. M. Cohen, *Inorg. Chem.* **2004**, *43*, 1242-1249.

[31] L. Do, S. R. Halper, S. M. Cohen, *Chem. Commun.* **2004**, 2662-2663.

[32] J. M. Sutton, E. Rogerson, C. J. Wilson, A. E. Sparke, S. J. Archibald, R. W. Boyle, *Chem. Commun.* **2004**, 1328-1329.

[33] S. R. Halper, S. M. Cohen, *Angew. Chem. Int. Ed.* **2004**, *43*, 2385-2388.

[34] a) T. Sakida, S. Yamaguchi, H. Shinokubo, *Angew. Chem. Int. Ed.* **2011**, *50*, 2280-2283; b) T. Ito, Y. Hayashi, S. Shimizu, J. Y. Shin, N. Kobayashi, H. Shinokubo, *Angew. Chem. Int. Ed.* **2012**, *51*, 8542-8545.

[35] a) S. Atilgan, T. Ozdemir, E. U. Akkaya, *Org. Lett.* **2008**, *10*, 4065-4067; b) Q. Zheng, G. Xu, P. N. Prasad, *Chem. Eur. J.* **2008**, *14*, 5812-5819; c) C. F. A. Gomez-Duran, I. Garcia-Moreno, A. Costela, V. Martin, R. Sastre, J. Banuelos, F. Lopez Arbeloa, I. Lopez Arbeloa, E. Pena-Cabrera, *Chem. Commun.* **2010**, *46*, 5103-5105; d) M. Mao, J. B. Wang, Z. F. Xiao, S. Y. Dai, Q. H. Song, *Dyes Pigments* **2012**, *94*, 224-232.

[36] a) M. Broring, F. Bregier, R. Kruger, C. Kleeberg, *Eur. J. Inorg. Chem.* **2008**, *2008*, 5505-5512; b) M. Broring, R. Kruger, S. Link, C. Kleeberg, S. Kohler, X. Xie, B. Ventura, L. Flamigni, *Chem. Eur. J.* **2008**, *14*, 2976-2983; c) B. Ventura, G. Marconi, M. Broring, R. Kruger, L. Flamigni, *New J. Chem.* **2009**, *33*, 428-438.

[37] S. Rihn, M. Erdem, A. De Nicola, P. Retailleau, R. Ziessel, *Org. Lett.* **2011**, *13*, 1916-1919.

[38] a) Y. Cakmak, S. Kolemen, S. Duman, Y. Dede, Y. Dolen, B. Kilic, Z. Kostereli, L. T. Yildirim, A. L. Dogan, D. Guc, E. U. Akkaya, *Angew. Chem. Int. Ed.* **2011**, *50*, 11937-11941; b) M. T. Whited, N. M. Patel, S. T. Roberts, K. Allen, P. I. Djurovich, S. E. Bradforth, M. E. Thompson, *Chem. Commun.* **2012**, *48*, 284-286.

[39] a) W. Pang, X.-F. Zhang, J. Zhou, C. Yu, E. Hao, L. Jiao, *Chem. Commun.* **2012**, *48*, 5437-5439; b) S. Kolemen, M. Işık, G. M. Kim, D. Kim, H. Geng, M. Buyuktemiz, T. Karatas, X. F. Zhang, Y. Dede, J. Yoon, E. U. Akkaya, *Angew. Chem. Int. Ed.* **2015**, *54*, 5340-5344.

[40] Y. Hayashi, S. Yamaguchi, W. Y. Cha, D. Kim, H. Shinokubo, *Org. Lett.* **2011**, *13*, 2992-2995.

[41] A. N. Kursunlu, *Tetrahedron Lett.* **2015**, *56*, 1873-1877.

[42] R. Takahashi, Y. Kobuke, *J. Org. Chem.* **2005**, *70*, 2745-2753.

[43] C.-H. Lee, J. S. Lindsey, *Tetrahedron* **1994**, *50*, 11427-11440.

[44] N. Kaur, J. G. Delcros, J. Imran, A. Khaled, M. Chehtane, N. Tschammer, B. Martin, O. Phanstiel, *J. Med. Chem.* **2008**, *51*, 1393-1401.

[45] O. A. Blackburn, B. J. Coe, M. Helliwell, J. Raftery, *Organometallics* **2012**, *31*, 5307-5320.

[46] a) P. J. Chmielewski, L. Latos-Grazynski, K. Rachlewicz, T. Glowiak, *Angew. Chem. Int. Ed. Engl.* **1994**, *33*, 779-781; b) H. Furuta, T. Asano, T. Ogawa, *J. Am. Chem. Soc.* **1994**, *116*, 767-768.

[47] K. Fujino, Y. Hirata, Y. Kawabe, T. Morimoto, A. Srinivasan, M. Toganoh, Y. Miseki, A. Kudo, H. Furuta, *Angew. Chem. Int. Ed.* **2011**, *50*, 6855-6859.

[48] H. Furuta, T. Ishizuka, A. Osuka, H. Dejima, H. Nakagawa, Y. Ishikawa, *J. Am. Chem. Soc.* **2001**, *123*, 6207-6208.

[49] M. Toganoh, Y. Kawabe, H. Furuta, *J. Org. Chem.* **2011**, *76*, 7618-7622.

[50] T. D. Lash, A. D. Lammer, G. M. Ferrence, *Angew. Chem. Int. Ed.* **2011**, *50*, 9718-9721.

[51] M. Toganoh, Y. Kawabe, H. Uno, H. Furuta, *Angew. Chem. Int. Ed.* **2012**, *51*, 8753-8756.

[52] H. Furuta, H. Maeda, A. Osuka, *J. Am. Chem. Soc.* **2000**, *122*, 803-807.

[53] S. C. Gadekar, B. K. Reddy, V. G. Anand, *Angew. Chem. Int. Ed.* **2013**, *52*, 7164-7167.

[54] M. Broring, S. Kohler, C. Kleeberg, *Angew. Chem. Int. Ed.* **2008**, *47*, 5658-5660.

[55] J. L. Sessler, S. J. Weghorn, T. Morishima, M. Rosingana, V. Lynch, V. Lee, *J. Am. Chem. Soc.* **1992**, *114*, 8306-8307.

[56] M. Ishida, S. J. Kim, C. Preihs, K. Ohkubo, J. M. Lim, B. S. Lee, J. S. Park, V. M. Lynch, V. V. Roznyatovskiy, T. Sarma, P. K. Panda, C. H. Lee, S. Fukuzumi, D. Kim, J. L. Sessler, *Nat. Chem.* **2012**, *5*, 15-20.

[57] a) S. Saito, A. Osuka, *Angew. Chem. Int. Ed.* **2011**, *50*, 4342-4373; b) M. Stepien, N. Sprutta, L. Latos-Grazynski, *Angew. Chem. Int. Ed.* **2011**, *50*, 4288-4340.

[58] These data can be obtained free of charge from The Cambridge Crystallographic Data Centre via www.ccdc.cam.ac.uk/data_request/cif.

[59] E. Vogel, M. Broring, J. Fink, D. Rosen, H. Schmickler, J. Lex, K. W. K. Chan, Y. D. Wu, D. A. Plattner, M. Nendel, K. N. Houk, *Angew. Chem. Int. Ed. Engl.* **1995**, *34*, 2511-2514.

[60] P. v. R. Schleyer, C. Maerker, A. Dransfeld, H. Jiao, N. J. R. v. E. Hommes, *J. Am. Chem. Soc.* **1996**, *118*, 6317-6318.

[61] Gaussian 09, Revision D.01, M. J. Frisch, G. W. Trucks, H. B. Schlegel, G. E. Scuseria, M. A. Robb, J. R. Cheeseman, G. Scalmani, V. Barone, B. Mennucci, G. A. Petersson, H. Nakatsuji, M. Caricato, X. Li, H. P. Hratchian, A. F. Izmaylov, J. Bloino, G. Zheng, J. L. Sonnenberg, M. Hada, M. Ehara, K. Toyota, R. Fukuda, J. Hasegawa, M. Ishida, T. Nakajima, Y. Honda, O. Kitao, H. Nakai, T. Vreven, J. A. Montgomery, Jr., J. E. Peralta, F. Ogliaro, M. Bearpark, J. J. Heyd, E. Brothers, K. N. Kudin, V. N. Staroverov, R. Kobayashi, J. Normand, K. Raghavachari, A. Rendell, J. C. Burant, S. S. Iyengar, J. Tomasi, M. Cossi, N. Rega, J. M. Millam, M. Klene, J. E. Knox, J. B. Cross, V. Bakken, C. Adamo, J. Jaramillo, R. Gomperts, R. E. Stratmann, O. Yazyev, A. J. Austin, R. Cammi, C. Pomelli, J. W. Ochterski, R. L. Martin, K. Morokuma, V. G. Zakrzewski, G. A. Voth, P. Salvador, J. J. Dannenberg, S. Dapprich, A. D. Daniels, Ö. Farkas, J. B. Foresman, J. V. Ortiz, J. Cioslowski, and D. J. Fox, Gaussian, Inc., Wallingford CT, 2009.

[62] M. Toganoh, S. Gokulnath, Y. Kawabe, H. Furuta, *Chem. Eur. J.* **2012**, *18*, 4380-4391.

[63] H. Furuta, H. Maeda, A. Osuka, *J. Am. Chem. Soc.* **2001**, *123*, 6435-6436.

[64] Y. Xie, P. Wei, X. Li, T. Hong, K. Zhang. H. Furuta, *J. Am. Chem. Soc.* **2013**, *135*, 19119-19122.

[65] Z. S. Yoon, D. G. Cho, K. S. Kim, J. L. Sessler, D. Kim, *J. Am. Chem. Soc.* **2008**, *130*, 6930-6931.

[66] P. Wei, K. Zhang, X. Li, D. Meng, H. Agren, Z. Ou, S. Ng, H. Furuta, Y. Xie, *Angew. Chem. Int. Ed. Engl.* **2014**, *53*, 14069-14073.

[67] S. C. Gadekar, B. K. Reddy, V. G. Anand, *Chem. Commun.* **2015**, *51*, 8342-8344.

[68] a) C. Jutz, E. Schweiger, *Angew. Chem. Int. Ed. Engl.* **1971**, *10*, 808-809; b) A. G. Anderson, A. A. MacDonald, A. F. Montana, *J. Am. Chem. Soc.* **1968**, *90*, 2993-2994.

[69] K. Hafner, H. U. Suss, *Angew. Chem. Int. Ed. Engl.* **1973**, *12*, 575-577.

[70] H. Hopf, *Angew. Chem. Int. Ed.* **2013**, *52*, 12224-12226.

[71] H. J. Dauben, D. J. Bertelli, *J. Am. Chem. Soc.* **1961**, *83*, 4659-4660.

[72] J. F. M. Oth, K. Mullen, H. Konigshofen, J. Wassen, E. Vogel, *Helv. Chim. Acta* **1974**, *57*, 2387-2398.

List of Publications

- **S. C. Gadekar**, B. K. Reddy, V. G. Anand, *Chem.Commun.* **2015**, *51*, 8342-8344. DOI: 10.1039/c5cc01367d. Metal Assisted Cyclodimerization of Doubly N-confused Dipyrrins into Planar Aza-Heptalenes.

- **S. C. Gadekar**, B. K. Reddy, V. G. Anand, *Angew. Chem. Int. Ed.* **2013**, *52*, 7164-7167. DOI: 10.1002/anie.201303184. Metal-Assisted Cyclomerization of N-Confused Dipyrrins into Expnaded Norroles.